QUANTITATIVE PHYTOLITH ANALYSIS: THE

KEY TO UNDERSTANDING BURIED SOILS AND

TO RECONSTRUCTING PALEOENVIRONMENTS

By

JOHN BYRON SUDBURY

Bachelor of Science in Chemistry
Oklahoma Christian College
Oklahoma City, Oklahoma
1973

Bachelor of Science in Biology
Oklahoma Christian College
Oklahoma City, Oklahoma
1973

Master of Science in Forensic Science/Criminalistics
University of Central Oklahoma
Edmond, Oklahoma
2001

Submitted to the Faculty of the
Graduate College of the
Oklahoma State University
in partial fulfillment of
the requirements for
the Degree of
DOCTOR OF PHILOSOPHY
May, 2010

QUANTITATIVE PHYTOLITH ANALYSIS: THE

KEY TO UNDERSTANDING BURIED SOILS AND

TO RECONSTRUCTING PALEOENVIRONMENTS

Dissertation Approved:

Dr. Brian J. Carter
_____
Dissertation Adviser

Dr. Alex Simms
_____

Dr. Hailin Zhang
_____

Dr. Leland C. Bement
_____

Dr. A. Gordon Emslie
_____
Dean of the Graduate College

ACKNOWLEDGMENTS

technical problem. Ted Martin (Conoco Oil Company) showed me the benefit of extreme

attention to detail, that seemingly intractable problems were actually opportunities

begging for a fresh multi-disciplinary analytical viewpoint, and that one should

communicate well enough up front in a project to understand a client's problem so the

result provided is what the customer actually needs to resolve the question at hand. Jeff

Meyers (Conoco Inc.)—with a great positive outlook on life—clearly demonstrates

boundless energy, inquisitiveness, the desire for constant improvement, and the value of

thinking outside of the box to solve problems. There have been many additional

individuals, unnamed, who have also had major positive impacts on my life and this

project. In the end, my children John and Laura make the ongoing journey worthwhile.

In spite of this noteworthy and phenomenal support, any factual or interpretive

errors that may have crept into this report are solely the author's responsibility.

TABLE OF CONTENTS

LIST OF TABLES

LIST OF FIGURES

CHAPTER I

INTRODUCTION

Project Research Objectives

The rapidly growing field of phytolith research is multidisciplinary in nature, with major advances being made by ethnobotanists, geographers, geomorphologists, geologists, botanists, archeologists, and researchers studying the development of agriculture. The direct input of soil scientists and chemists to the field has been relatively limited to date. The current research project has been tailored to have maximum impact on phytolith research from this vantage point of a chemist and soil scientist.

A career analytical chemist approaches laboratory tasks differently than those in a number of other disciplines. A true quantitative approach is second nature to an analytical chemist as compared to the more commonly used qualitative and semi-quantitative approaches frequently applied by practitioners in a number of other disciplines engaged in phytolith research. Thus, the excellent existing phytolith laboratory protocols in the literature (Piperno 2006, Pearsall 2000, Lentfer and Boyd 1998) will be slightly revamped to develop a quantitative phytolith recovery procedure (wt/wt % in soil). Although the additional work and time involved in quantitative

recovery may not be necessary for some field inquiries, some researchers may find this option useful for certain applications. Significantly, several potential weaknesses in the existing methodologies will be addressed, and other procedural options developed as alternatives.

The appreciable variation in phytolith signature at similar Great Plains prairie sites was noted (Fredlund and Tieszen 1994:330; Fredlund and Tieszen 1997a:203), so an extensive study of the horizontal soil phytolith variation across a small portion of one modern virgin Tallgrass Prairie site was conducted. The vertical phytolith distribution in the soil was also studied on this site and on alternate sites as well, and other components recovered in the biogenic silica fraction were also noted. The phytolith morphologic form count data and the resulting interpretation can be no better than the original soil sample that was processed. Thus, reference surface soil sampling variability is another point that is specifically addressed in this study. In addition to the overall soil phytolith signature, information was gleaned from the biogenic silica fraction record about soil development processes.

Soil phytolith/biogenic silica data was evaluated to determine what climatic information was presented in the buried Holocene A horizon phytolith samples. The climatic information in the phytolith data, based on the prior pioneering work of others studying the prairies of the Great Plains (Twiss, Suess, and Smith 1969; Fredlund and Tieszen (1994, 1997a)), will be presented. Modern control phytoliths were isolated from the major prairie grasses present in this study region; because of their informative nature,

these reference specimens—used to identify the major short cell phytolith forms recovered from soils—are photo-documented in this report.

The following three objectives are addressed in this dissertation research:

1. develop an efficient protocol for quantitative phytolith recovery, on weight basis, from soils improving on current established laboratory methodologies.

2. determine the horizontal and vertical distribution of phytoliths in modern prairie soil and buried A horizons, apply this information to soil sampling techniques, and use this biogenic silica data to develop a better understanding of pedogenesis.

3. interpret the soil biogenic silica signature of buried Holocene A horizons to determine what information is revealed about environmental conditions and paleoenvironments.

Silicon and Phytoliths

Silicon, an element comprising 27.7% by mass of the earth's crust, is ubiquitous in nature, second in frequency only to oxygen. Together, the elements oxygen and silicon comprise nearly 75% of the earth's crust (Tarbuck and Lutgens 1999:44). Much

of the silicon is present as silicate minerals (Tarbuck and Lutgens 1999:48); quartz is one major crystalline silicate (silica, SiO_2). Weathering of all minerals—including silicates—over geological time contributes to the mineral component of soils. Developed soil in turn enables rooted plant growth which supports much of multi-cellular terrestrial life as we know it. To complete the cycle, soil components may be gradually leached from the soil profile; soils are also exposed to erosional events, such as wind and water, which may entomb or remove them. Thus over time, soils are ultimately buried on land or re-deposited elsewhere, and the soil constituents are gradually assimilated into new geological formations.

In addition to the essential nutrients provided by weathered minerals, plants also require water. Water is the transport media that allows dissolved mineral nutrients to enter plants via uptake by the root system. Although sparingly soluble, silicon dissolved in the soil water enters plants via their roots in the form of monosilicic acid, $Si(OH)_4$ (Jones and Handrek 1967). Most researchers do not consider silicon to be an essential nutrient; silicon is, however, a beneficial nutrient (Matichenkov and Calvert 2002) and performs a number of important plant functions such as providing structural support, resistance to pathogenic fungi, and helping discourage herbivory (Piperno 2006:12-15).

In the plant, silicon forms deposits of hydrated silicon dioxide ($SiO_2 \cdot \eta H_2O$) which is variously referred to as opaline particles, opal-A, plant opal, and more recently phytoliths (Iler 1979:14; Piperno 1988:11; Drees, Wilding, Smeck, Senkayi 1989:957). The literal meaning of the term phytolith is "plant stone" (Piperno 1988:11). This solid

amorphous material may be deposited in interstitial spaces, within the cell wall, or inside of the cell wall (Piperno 1988:17). These later two forms often mirror plant cell shape. Although plants readily transport solubilized silicon in their vascular system, plants are unable to eliminate the resulting polymerized amorphous silicon solids (i.e., phytoliths) from their structures.

When the plant's organic material decomposes, either due to senescence or plant death, the relatively insoluble phytoliths are incorporated into the soil. These inorganic phytoliths may remain present as a stable soil mineral component for tens of thousands of years. Thus, soil phytoliths are trace microfossils representing the plants that initially formed them before depositing phytoliths from their aerial structures on the soil surface after which time they were incorporated into the soil (along with root phytoliths).

The slow development of increased soil depth by gradual addition of organic material (i.e., plant litter) and inorganic materials (such as wind-blown dust) enables the extant vegetation to maintain a stable plant community on the actively developing soil surface. This slow "developmental upbuilding" (Schaetzl and Anderson 2005:456) of the soil is commonly referred to as aggradation.

During geologic weathering events, well-developed surface soils supporting established plant communities may become buried. This may occur by a number of processes including being covered by extensive eolian (wind-borne) or by alluvial (water-borne) deposits. If an extensive deposit is superimposed suddenly enough, the extant soil

(and plant community) is encapsulated under the deposit becoming a buried soil—this process is referred to as "retardant upbuilding" (Schaetzl and Anderson 2005:456). Pedogenesis of the buried soil ceases, and with time, new soil horizons develop relative to the new ground surface, and a new plant community becomes established.

As different plants, plant communities, and plant associations thrive best under certain optimal climatic conditions (i.e., moisture and temperature), the newly established plant community that develops on the newly forming soil under new climatic conditions will not necessarily duplicate the previous plant community present on the now buried soil surface in the same location. The diagnostic phytolith forms from earlier plants are representative of the former climate regime (moisture and temperature) at the time the plant community thrived on a given established soil surface

In this study, the basic diagnostic phytolith morphologic signature present in soils under three different modern prairie types were studied as control samples: Tallgrass Prairie, Mixedgrass Prairie, and Shortgrass Prairie. The phytolith morphologic assemblages present in buried soils at three sites are determined and compared to the control prairie phytolith morphologic distributions, which serve as modern climate proxies. The vertical variation in phytolith distribution in these various prairie soils is used to help better understand soil genesis. Additionally, based on challenges encountered during this research, alternate laboratory procedures were developed that improve on the established methodology for phytolith recovery from soils resulting in a method optimized for efficient quantitative phytolith recovery.

Phytolith analysis has applications in many multidisciplinary fields, which is to say that phytolith data (recovery and identification, morphologic type frequency analysis, metrics, and/or concentration) can be used to address numerous research questions. Scarcely two decades ago—a century and a half after phytoliths were first observed and reported—Piperno (1988) authored the first phytolith book[1]. As of this date, the number of separate volumes—including conference proceedings---has increased by fifteen[2]. As the field has become more prominent and interdisciplinary applications developed, the number of researchers in many diverse fields utilizing and reporting phytolith data in journal articles has likewise increased during the same recent two-decade interval.

Numerous fields of investigation benefit from incorporating phytolith analysis and interpretation in their research design. For instance, studies related to botany, geology, paleontology, and the development of agriculture may utilize phytolith data. Important applications briefly discussed in Chapter 2 are agrostology, agronomy, forensic science, and health-related issues, as well as several pertinent climate-related topics. Several areas directly impacting this research project are addressed in more detail including prairies, soils, and paleoclimate.

---

[1] The seminal volume edited by Rovner (1986a) preceded Piperno's hardcover book, but was of limited distribution.

[2] Post-1988 phytolith volumes include Rapp and Mulholland (Eds.) 1992; Pearsall and Piperno (Eds.) 1993; Kondo, Childs, and Atkinson 1994; Pinilla, Juan-Tresserras, and Machado (Eds.) 1997; Bowdrey 1998; Piperno and Pearsall 1998a; Kealhofer and Piperno 1998; Runge 2000; Meunier and Colin (Eds.) 2001; Hart and Wallis (Eds.) 2003; Thorn 2004; Piperno 2006; Madella and Zurro (Eds.) 2007; Korstanje and Babot (Eds.) 2008; and Albert and Madella (Eds.) 2009. There are also several other significant volumes that could be included in this list (the Origins of Agriculture book (Piperno and Pearsall 1998b)) and Pearsall's paleoethnobotany volumes (1989 and 2000).

Phytolith data is used in the field of agrostology, which involves the taxonomic study of grasses and grasslands. In agrostology, phytoliths have been helpful in understanding the taxonomic relationships of the Poaceae.   Although this current study is targeted at grasses and grasslands, the major agricultural grain crops are grasses, so the phytolith research field is intertwined with multiple research applications.

The field of agronomy is the part of agriculture that is "concerned with the theory and practice of field-crop production and soil management" (Brady and Weil 2002:912). This field is indirectly addressed in the following discussion regarding the value of silicon to plants, of whether or not silicon is occasionally an essential (not just a beneficial) nutrient, and the fact that silicon appears to interact with the soil in a manner such as to make more soil phosphorous plant available thus increasing fertility (and also helping minimize manganese toxicity (see pages 20-21)). As silicon can be a valuable nutrient, the discussions regarding silicon solubility and soil water silicon concentrations are also in the domain of agronomy, as are plant soil interactions and the concept of soil-plant-atmosphere continuum. Soil Science is a part of agronomy, but as many interdisciplinary fields, soil science is also branching out to encompass many more applications. Soil science—including pedogenesis—is addressed in this review (pages 54-58), and will be a major emphasis in this research.

The potential application for phytolith analysis in the field of forensic science remains underutilized and essentially undeveloped. Although phytolith analysis was initially proposed by Marumo and Yanai (1986) as a means of forensic soil analysis, this

application has languished. Thus, phytolith analysis remains an untapped potential

source of trace evidence for the forensic community. To date, membership of

professional soil scientists in the American Forensic Science community is extremely

limited, with most of the soil work being performed by geologists, or others (Murray and

Tedrow 1992; Murray and Solebello 2002; Murray 2004; Pye 2007; Morgan and Bull

2007; Tibbet and Carter 2008).   As phytoliths often may make up 1% or more of the soil

and include morphologically distinctive specimens, they are another form of trace

evidence that could be utilized in criminal investigations. However, even the current

Forensic Botany text totally omits phytoliths (Coyle 2005). The potential sample types

involving soil are pretty much unlimited, but would include items such as

- Soil on clothing, shoes, under fingernails, on carpets

- Particulate in vehicle air filters (personal observation)

- Identification of burned plant residue

- Soil on tires, car bodies, wheel wells (Sudbury 2003; Schneck 2004:182)

- Soil around stolen (transplanted) plants

Phytolith analysis does not replace any other forensic techniques, but rather complements

other trace analyses and can become a tool in the forensic arsenal.

Medical issues related to phytoliths are also significant. In animal feed, high

phytolith concentration can be fatal in that silicon causes kidney stones; the preventive

treatment (besides being aware of the feed source) is to provide salt so water

consumption by livestock is increased (Iler 1979:70; 758). A common ailment in many

animals (sometimes called "fungal foot") may be initiated by high silica concentrations in

dead grasses—particularly the culms--in autumn injuring footpads enabling fungal infections (personal observation).

The first report of human health issues relating to biogenic silica was due to sponge spicules present in rich soil of dried ponds causing irritation and discomfort during corn cultivation (Virden 1886). More recently, phytoliths have been associated with cancer; an apparent correlation was demonstrated between esophageal cancer and high silica content foods (apparently due to silicified hair cells). The botanicals of interest in these studies were a food grain contaminant (*Phalaris* sp.) in northeast Iran (O'Neill et al. 1980; Newman and MacKay 1983; O'Neill, Jordan, Bhatt, and Newman 1986a); *Setaria italica* Beauv. (Foxtail Millet) northern China (O'Neill et al. 1982, Parry and Hodson 1982), and *Sonchus oleraceus* L. (Common Sowthistle) and *Bidens pilosa* (Hairy Beggarticks) in South Africa (Parry, Hodson, and Sangster 1984; Parry, O'Neill, and Hodson 1986).

Baker (1961) first reported the possible hazards of silica particle inhalation during wheat transfer at silos. Asbestiform fibers of biogenic silica have been reported from *Saccharum* sp. leaves (Newman 1986a:365):

> Following reports of mesotheliomas and lung cancers in sugar-cane workers, an examination of residues from sugar cane leaf has shown the presence of acicular biogenic silica, 0.85 μm in dia. and 10–300 μm long, which is within the carcinogenic size range for asbestos fibre.

Inhalation of silica is also known to cause silicosis (Iler 1979:754, 758, 769-783); although the form of silica is not always clearly stated in Iler's discussions, avoidance of breathing amorphous silica dust and fine particulate is prudent.

Although inhalation of finely divided silica and ingestion of fibrous silica have adverse human health effects, silicon is actually beneficial to human health. As amorphous silica is a relatively soluble form of silica, amorphous silica in the diet (i.e., phytoliths from botanical foodstuff) can actually be an important component of one's diet. Iler (1979:754) reports the blood concentration of silicon to be 8.3 ppm. A research group in the UK has compiled of the silicon content of 207 common foods and beverages (Powell et al. 2005). The apparent benefits of dietary silicon in bone and connective tissue development and cardiovascular health are also noted (Powell et al. 2005). In a dietary survey, grains were noted to provide an average of 30% of daily silicon intake (McNaughton, Bolton-Smith, Mishra, Jugdaohsingh, and Powell 2005). For the record, beer is referred to as a "saturated solution of silica" due to the silica in the grain (Iler 1979:744). The presence of silica in drinking water may serve to offset the effects of aluminum in potentially contributing to dementia (Rondeau et al. 2008); this is reminiscent of the protective benefit that plants appear to receive by the silica helping offset the effects of cation toxicity. For additional comments about silicon in common foodstuffs, see Appendix A.

Global climate change is currently a very hot political, scientific, and social topic. As demonstrated in numerous articles as well as this dissertation, phytoliths can provide a snap shot of past climate at the time of stable environments that resulted in episodes of soil formation. In addition to this interpretive function, phytoliths—which contain some carbon—have been proposed as an agent for stable carbon sequestration in soils (Parr and Sullivan 2005). For any given plant species, the higher the phytolith concentration,

carbon storage capability, and biomass, the greater the potential carbon sequestration capability of the species. Likewise, diatoms may also potentially provide a similar function.

In another climate-related issue, while evaluating satellite data from 1981-2006, a correlation has been observed between atmospheric dust and hurricane activity (Evan, Dunion, Foley, Heidinger, and Velden 2006). During periods of intense hurricane activity, it was noted that dust was relatively scarce in the atmosphere; conversely, in years when stronger dust storms occurred, fewer hurricanes swept through the Atlantic (Evan et al. 2006). Although a clear cause and effect was not demonstrated, an apparent linkage in the two occurrences was indicated. Along a similar vein, it is of interest that modeling studies about the 1930's Dust Bowl on the Great Plains have been interpreted to indicate that ocean surface temperatures may have contributed to that drought (Schubert, Suarez, Peglon, Koster, and Bacmeister 2004). The climatic effect of atmospheric dust is the subject of ongoing study (c.f. Thompson and Thompson 1981; Tegen 2003; Grousset and Biscaye 2005).

The first phytoliths reported were recovered by Darwin in a dust sample collected from the sails of the Beagle off of the coast of Africa (Darwin 1846). A representative NASA satellite image of a dust storm emanating from Africa is shown in Figure 1. Recalling that phytoliths are less dense than sand, as the particulate matter resulting from a dust storm settles out, phytoliths would tend to remain airborne longer than quartz-based particulate. This prolonged suspension time would be potentially exacerbated by

phytoliths non-spherical (i.e. tabular) shape. Thus, there is a potential severe weather

application for phytoliths to be pursued that is implied by the above correlation with

hurricanes. Similar dust storms are common in the study areas discussed in this

dissertation; a NASA satellite image of a recent dust storm in Texas is in Figure 2.

There are also a number of additional applications related to amorphous silica and

potentially to phytolith research. Amorphous silica is being used in nanotechnology
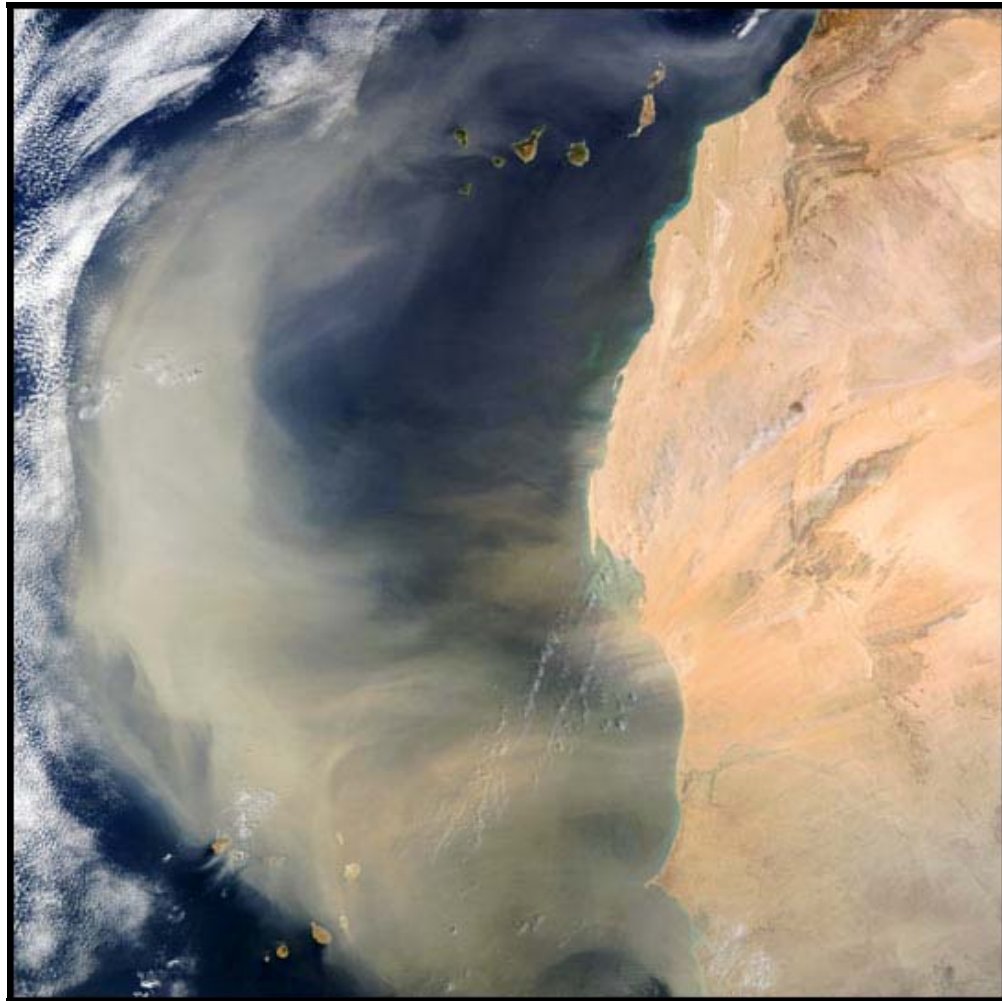
Figure 1. Dust storm off of the west coast of northern Africa.
(http://plantandsoil.unl.edu/croptechnology2005/UserFiles/Image/siteImages/AfricDustSt
ormNASA-LG.jpg (1-20-10).)
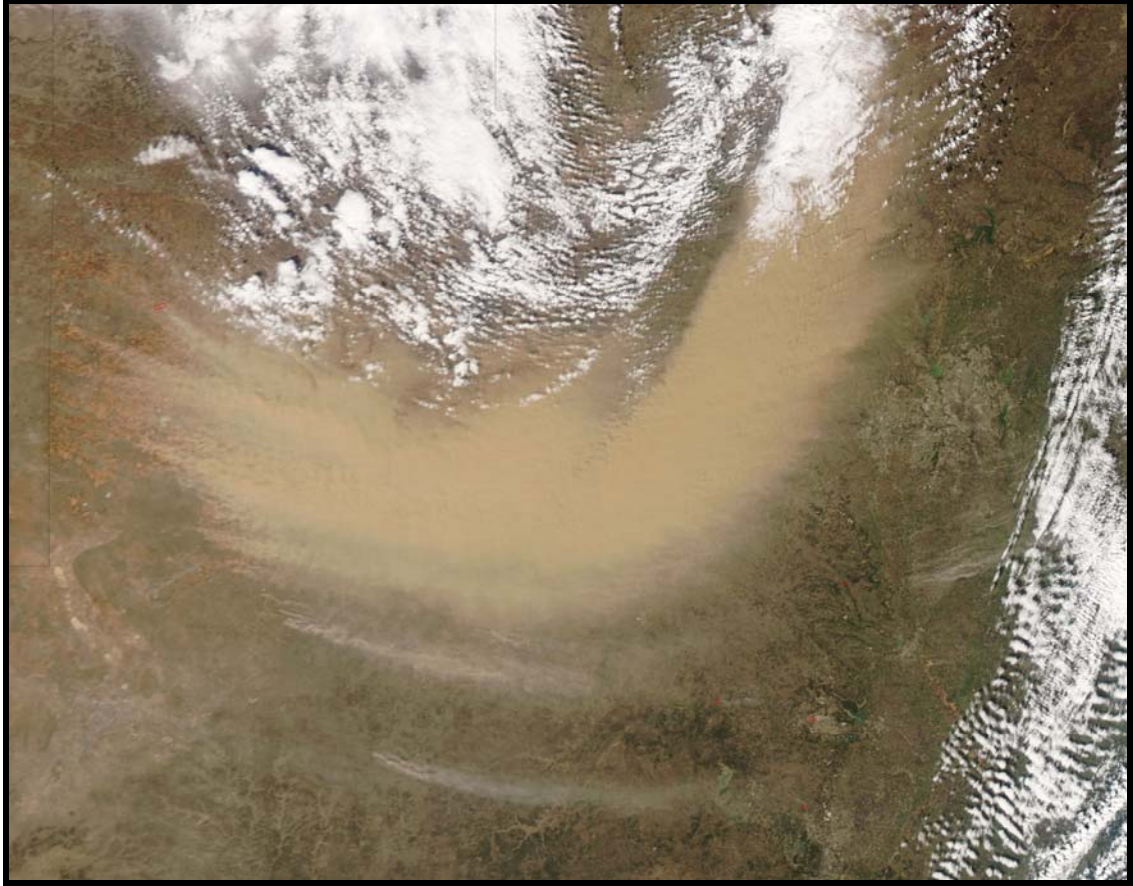
Figure 2. Dust storm (and small fires) in west Texas (NASA image taken February 24, 2007)[3].

(Neethirajan, Gordon, and Wang 2009), and amorphous silica (a-Si) is used in thin film

insulator and transistor production (Hiroshi and Masakiyo 1980; van Berkel 2003;

Shringarpure et al. 2008). Silicic acid is used in the production of silicon chips in the

computer industry (Yeh and Lee 1999). The addition of both silica fume and/or rice husk

ash [i.e., rice phytoliths] to concrete has been proposed as a means of disposing

of/recycling waste while improving concrete strength and conserving scarce resources

[3](http://images.google.com/imgres?imgurl=http://earthobservatory.nasa.gov/images/imagerecords/7000/7443/texas_amo_2007055_lrg.jpg&imgrefurl=http://earthobservatory.nasa.gov/IOTD/view.php%3Fid%3D7443&usg=__z6lxoNw8nbRtM8TZSlyoUdfWiC4=&h=2200&w=2800&sz=969&hl=en&start=17&sig2=XTXMN70XC4s8DXde11CB9w&um=1&itbs=1&tbnid=veWhUGDZNchIpM:&tbnh=118&tbnw=150&prev=/images%3Fq%3Dnasa%2Bdust%2Bstorm%2Btexas%26hl%3Den%26safe%3Doff%26rlz%3D1T4HPIA_enUS349US349%26sa%3DG%26um%3D1&ei=iFVXS_uVFI6MNvr_mcsE) (1-20-10)).

(Sakr 2006). Solubility and migration of opal A was used in evaluating the suitability of Yucca Mountain for long-term storage of radioactive waste (Neymark, Amelin, and Paces 2000; Stirling, Lee, Christensen, and Halliday 2000; Paces, Newark, Wooden, and Persing 2004). Beyond these brief highlights, numerous other fields are beginning to make use of phytolith data. Based on this introductory overview, it is apparent that phytolith analysis and research is a relevant, multidisciplinary, very viable, and rapidly growing discipline.

CHAPTER II

LITERATURE REVIEW

Phytoliths and Biogenic Silica

Phytoliths, meaning literally "plant stones," are a form of amorphous silica that occurs in plants (Piperno 2006); in the past, they have been called other names including amorphous silica gel, plant opal, grass opal, biogenic opal, Opal-A, opal phytoliths, opaline silica, biogenic silica, and biogenic silicon opal (Smithson 1956; Smithson 1958; Geis and Jones 1973; Kaufman et al. 1981; Drees et al. 1989). Biogenic silica means the form of silica that is produced by living organisms or biological processes, and that this silica is necessary for the maintenance of their life processes—such as frustules which are present as structural support in diatoms. Phytoliths are one form of biogenic silica.

In addition to phytoliths that occur in plants, three well-known groups of organisms that form biogenic silica for structural support are diatoms (frustules), radiolarians (scleracomas), and some sponge spicules (spicules of the glass sponges) (Jones 1956:21, 49, 85; Boardman et al. 1987; Clarke 2003). The spicules of most sponge species are actually composed of calcium carbonate; however, carbonate spicules (and carbonate phytoliths) were not encountered during this investigation and thus are not discussed in this literature review. Among the 180 species of freshwater sponges are a

number of species that make their structural framework of amorphous silica spicules, i.e., $SiO2 \cdot \eta H_2O$ (Schwandes and Collins 1994; Rigby 2003:18; Rigby 2004) and are frequently found in soils (Smithson 1959; Jones, McKenzie, and Beavers 1964; Wilkins, Delcourt, Delcourt, Harrison, and Turner 1991; Schwandes and Collins 1994; Dröscher and Waringer 2007). Spicules were reported as present in soil samples along with phytoliths and diatoms shortly after phytoliths were originally reported (Gregory 1855). The Chrysophyte cysts (stomatocysts or statospores of golden-brown algae), another sensitive paleoenvironmental indicator, are siliceous microfossils encountered in sediments of ponds, lakes, and coastal areas (Coleman 1969; Sandgren 1991a, 1991b; Duff, Zeeb, and Smol 1997; Lotter, Birks, Hofmann, and Marchetto 1997; Cohen 2003:99-100; Betts-Piper, Zeeb, and Smol 2004; Pla and Anderson 2005; García-Rodríguez 2006; Vanlandingham 2008). These stomatocysts, previously referred to as "siliceous cysts of the class Chrysophyta" (Cornell 1969), appear to be the "Chrysostomatacea shells" referred to by others (Jones, McKenzie, and Beavers 1964:421; Fredlund, Johnson, and Dort 1985:151; Drees et al. 1989:924) and are the statospores reported by Bozarth (1995:48). Together, these categories all have in common the same chemical compound—amorphous polymerized silica $SiO_2 \bullet \eta H_2O$ that the organisms synthesize. Although chemically identical, the final particle morphology of these biogenic silica sources is different so they are readily recognizable by category.

Various trace elements are present in phytoliths; however the basic chemical composition is the same: $SiO_2 \bullet \eta H_2O$. Variation in the amount of water incorporated in the amorphous silica matrix results in a very broad particle density range—for instance,

the particle density of phytoliths varies from 1.50 – 2.30 g/cm^3 with "model values from 2.10 to 2.15" (Jones and Beavers 1963:378). Several representative glass sponge spicule densities in the literature ((2.1 g /cm^3 (Muller, Jochum, Stoll, Wang 2008) and 2.25 g/cm^3 (Levi, Barton, Guillemet, Le Bras, and Lehuede 1989)) indicate that spicule densities are also variable although apparently within the phytolith density range. One study reports diatom density as 2.1 g/cm^3 (Leng et al. 2009). Various marine biogenic silica forms were reported as having a density ranging from 1.7 to 2.05 g/cm^3 (Drees et al. 1989:929-930).[4] Radiolia have been reported from soils formed from loess (Jones, Hay, and Beavers 1963:1222). Even though these biogenic forms all have the same chemical makeup, their density or specific gravity, varies according to the differences in framework, the amount of water present, lacunae, and occluded organic carbon (Drees et al. 1989:921, 926, 930). Occluded carbon in phytoliths (Jones and Beavers 1963) has been successfully used to obtain radiocarbon dates from phytoliths recovered from soil A Horizons (Wilding 1967; Wilding, Brown, and Holowaychuk 1967; Mulholland and Prior 1993). More recently, the carbon in phytoliths has been used to obtained delta 13 values for grassland reconstructions (Smith and Anderson 2001; Smith and White 2004; see also Krull et al. 2003). Nordt, von Fischer, and Tieszen (2007) developed a temperature correlation for the Great Plains during the Holocene based on delta 13 values obtained from buried soils. All biogenic silicas potentially contain useful environmental data in their silicon isotope and oxygen isotope information (Lotter, Birks, Hofmann, and Marchetto 1997; De La Rocha 2003; Pla and Anderson 2005; Hodson, Parker, Leng, and Sloane 2008; Leng and Sloane 2008; Swann and Leng 2009; and Leng et al. 2009).

---

[4] The density of the other various silica polymorphs is also given [opal-CT (2.20-2.38 g/cm^3), cristobalite (2.32 g/cm^3), and tridymite (2.26 g/cm^3) (Drees et al. 1989: 915, 929)].

Weathering gradually breaks down geological formations resulting in smaller particles and also dissolved constituents, one of which is silicon. Dissolved in the soil water, silicon occurs chemically as water soluble monosilicic acid ($Si(OH)_4$) (Jones and Handreck 1963). It has been noted that

> Some properties of water and silica are so similar that the transition between hydrated silicic acids and the aqueous matrix is a gradual one…Gelation of a silicic acid sol produces a heterogeneous system in which both the three-dimensional silicic acid polymer and the aqueous solution of low polymers of silicic acid form continuous interconnected systems… (Weyl and Marboe 1967:1480-1481).

This dissolved silicon in the soil water enters plants through their roots via active and/or passive uptake (Piperno 2006:5-6, 9). The relative importance and exact mechanism of these two pathways are the subjects of much debate, although both processes are known to occur (Piperno 2006:5-6, 9). Although water uptake by plants is complex and the mechanism varies by species and even due to specific environmental conditions, the general observation has been made that rapidly transpiring plants tend to take up water more by passive transport whereas plants that have low transpiration rates tend to take up water by active transport (Kramer and Boyer 1995:167). The concept of a soil-plant-atmosphere continuum (Slayter and Taylor 1960) regarding water balance and water movement through plants is one scenario by which to view plant water uptake via the roots and release to the atmosphere via transpiration from the leaves.

Once inside the plant, the dissolved silicon (i.e., monosilicic acid) accompanies the water throughout the plant via the vascular system. As water is transpired from the

leaves, additional water enters the leaf epidermal cells via the transport system. As the water exits the cell via evaporating into the atmosphere, the remaining supersaturated monosilicic acid polymerizes in the plant cell to form amorphous silica (i.e., becoming a phytolith). Thus, the resulting phytoliths that form in the plant cells may mirror the shape of the parent cells (Piperno 2006:24). Other amorphous silica deposits in plants that become phytoliths are made within the cell wall or interstitially (Piperno 2006:5). However, these other two forms tend to be less diagnostic than the cell cast type. The final concentration of silica in mature plants is highly variable depending on the species; the weight percent silica in the dry ash ranges from near zero in some species such as the 0.01% reported for honeylocust (*Gleditsia triacanthos* L.) (Geis 1973) to as high as 15% in rice (*Oryza sativa*) (Marshner 1995), and 26.5%-34% in the fruit pericarp of black bogrush (*Schoenus nigricans*) (Ernst, Vis, and Piccoli 1995). Even the silica content as percent of dry mass of different portions of a single plant varies widely; for instance, one research group reported silicon values for corn (*Zea mays*) including 0.9 % in the ear husk, 4.3% in the tassel, and 7.3% in the leaf blade—which was "about 2/3 of the ash" in the leaf (Lanning, Hopkins, and Loera 1980:550-551). Of the prairie grasses reported in the phytolith-related literature (Piperno 1988; 2006), Little Bluestem (*Schizachyrium scoparium* (Michx.) Nash [formerly named *Andropogan scoparius*]) and Indiangrass (*Sorghastrum nutans*) both have leaf silica concentrations over 9% (Table 1).

Silicon is not generally considered an essential element for plants—although in some cases silicon may actually be essential (Hagemeyer and Breckle 1996)[5]—but it is

---

[5] Taiz and Zeigler (2002:73) note that some "members of the family Equiseaceae… require silicon to complete their life cycle."

universally agreed that silicon is a beneficial nutrient. Silicon is beneficial because it

displaces phosphorous bound to the soil thus making the phosphorous plant available and

thereby increasing crop yields (Iler 199:746-747; Russell 1973:131-133, 635-639). Also,

aluminum influences silicon solubility and lowers the available silicon in soil solution

(Jones and Handreck 1965:80). In various grain crops, silicon content is important for

seed set and helps the plant tolerate high manganese concentrations; the presence of

phytoliths is important for cell strength, mechanical strength, and rigidity (Russell

1973:637; Iler 1979:742; Vlamis and Williams 1967). Reports indicate that rice plants

are not nearly as productive when silicon is inadequate, and that the silicon deficient rice

is more susceptible to fungal disease and insect predation (Okuda and Takahashi 1961;

Lanning 1963; Iler 1979:750-751; Kaufman et al. 1981; Kirk 2004:208) as are other food

crops. Iler (1979:744) indicates that the high silica content imparts a weather resistance

and helps prevent lodging. Also, "silicon can ameliorate the toxicity of many heavy

metals" (Taiz and Zeigler 2002:73). Regarding what he considers questionable

laboratory evaluations of plant growth, Epstein (1994:11) succinctly observed that

> omission of silicon from solution cultures may lead to distorted results in experiments on
> inorganic plant nutrition, growth and development, and responses to environmental stresses.

Higher silicon (i.e., phytolith) content has been cited as a protective mechanism

discouraging herbivory by mammals (Gali-Muhtasib, Smith, and Higgins 1992; Teaford,

Lucas, Ungar, and Glander 2006; Elger, Lemoine, Fenner, and Hanley 2009), insects

(Djamin and Pathak 1967; Massey, Ennos, and Hartley 2006; Massey and Hartley 2009),

and possibly even snails (Chevalier, Desbuquois, Le Lannic, and Charrier 2001).

Minimizing tooth wear appears to cause herbivores to preferentially select lower silicon

content browse when available (Maiorana 1978; Sanson 2006). In some cases, grazing induces an increase in silicon content in the target crop (McNaughton and Tarrants 1983; Brizuela, Detling, and Cid 1986; Myers and Bazely 1991). A higher plant silicon concentration is reported to make plants more difficult for ruminants to digest (Brazle, Harbers, and Owensby 1979; Hargers and Thouvenelle 1980; Harbers, Raiten, and Paulsen 1981).

When a plant dies, or the plant leaves fall due to senescence, the plant litter drops to the ground and decays. However, being inorganic, phytoliths are generally resistant to decay (except in cases of high pH soils (Piperno 2006); due to this inherent stability, phytoliths are gradually incorporated into the soil mineral fraction. Due to the physical size of the individual phytoliths, most of them become a part of the soil silt fraction (i.e., 2-50 microns in size). Once incorporated into the soil, phytoliths often remain as discrete identifiable particles for millennia.

The soil phytolith concentration has been reported up to 2.11% in dry Illinois soils (upper A horizon concentration reported range from 0.28 – 2.11% (Jones and Beavers 1964a), and 0.28-0.97% in a smaller A horizon sample set (Jones and Beavers 1964b)), with the concentration summarized as ranging up to 1-2% (Jones and Handreck 1967:144). A soil concentration of up to 3% was reported by Geis and Jones (1973). The soil phytolith concentrations reported by Yeck and Gray for four A and Ap horizons in Oklahoma ranged from 0.32-0.95 % (1972:641). In contrast to prairies, the phytolith concentration in forest soils has been recorded as low as 0.1% (Evett et al. 2006).

Historically, there has been considerable confusion within the phytolith community regarding the definition of the silt fraction. The basic published views are represented by Piperno (1988:121; 2006:91) who uses a silt fraction definition of 5-50 microns, and Pearsall (1989:365; 2000:430) who defines the silt fraction as 2-50 micron particles. As it turns out, both researchers are correct, albeit the situation remains confusing. Piperno's narrower silt size range is based on the engineering definition (AASHTO standards, American Association of State Highway and Transportation

Table 1
Silica Content in Grass (% Dry Wt) (Geis 1973; Lanning and Eleuterius 1987)

Genus Species	Common Name[6]	Silica (wt %)		Sample origin	Refer-ence
		Leaf	Culm		
Andropogon geradii	Big Bluestem	2.89	0.29	Konza Prairie	A[7]
Andropogon geradii	Big Bluestem	6.79	0.64	Illinois	B[8]
Andropogon scoparius[9]	Little Bluestem	9.25	1.05	Konza Prairie	A
Cenchrus longispinus	Sandbur	3.38		Mississippi	A
Echinochloa crusgalli	Barnyardgrass	3.65		Mississippi	A
Panicum virgatum	Switchgrass	5.04	1.03	Konza Prairie	A
Panicum virgatum	Switchgrass	5.00	0.96	Illinois	B
Paspalum urvillei	Vasey's Grass	4.84		Mississippi	A
Setaria geniculata	Marsh Bristlegrass	3.96		Mississippi	A
Sorghastrum nutans	Indiangrass	7.18	1.28	Konza Prairie	A
Sorghastrum nutans	Indiangrass	9.44	1.79	Illinois	B
Stipa spartea	Porcupine Grass	3.67	1.54	Konza Prairie	A
Stipa comata[10]	Needle and Thread	2.76	0.10	Colorado	A

---

[6] Common names from Tyrl, Bidwell, and Masters (2002) and http://www.plants usda.gov.

[7] Plant silica data from Lanning and Eleuterius (1987:364)

[8] Plant silica data taken from Geis (1978).

[9] Little Bluestem has since been renamed *Schizachyrium scoparium* (Michx.) Nash (Tyrl et al. 2002).

[10] Since renamed *Hesperostipa comata* (Trin. & Rupr.) Barkworth ssp. *Comata* (http://plants.usda.gov/java/profile?symbol=HECOC8).

Officials) applied to construction activities (Schoeneberger, Wysocki, Benham, and Broderson 2002:2-35), whereas the broader size range used by Pearsall represents that espoused by the soil science community (i.e., the USDA (Schoeneberger et al. 2002:2-35)).

Iler (1979:46) cites the solubility of hydrated amorphous silica as varying based on water content, from 18 ppm for $SiO_2 \cdot 2.5H_2O$ to 120 ppm for $SiO_2 \cdot 0.5H_2O$ in water. This solubility variation appears to suggest that individual phytolith particle density (i.e., specific gravity) affects relative dissolution rate in the soil profile; thus, selective phytolith dissolution occurs which may potentially skew distribution of recovered soil phytolith samples. Interestingly, based on this data, the densest phytoliths with the highest specific gravity are the most soluble phytoliths. Other phytolith preservation issues are noted by Piperno (2006:108-109). The reported values for the solubility of quartz ranges from 6-11 ppm (Iler 1979:31-34), indicating that on average biogenic silica in soil is significantly more soluble than quartz. The data cited by Weyl and Marboe (1962:1124) does indicate that quartz solubility varies several orders of magnitude based on particle size. Jones and Handreck (1967:108-109) reported a measured monosilicic acid concentration of 30-40 ppm in soil solution (calculated as SiO_2). In well-drained temperate soils, "annual losses of 15 kg/ha of silicon are common" although the soil silicic acid concentration remains constant (Russell 1973:635). Above pH 10.7, all amorphous silica dissolves (Iler 1979:47). Significantly, silica solubility is enhanced by the presence of salt in the solution (Iler 1979:74-75).

Phytoliths have a reported mean refractive index of 1.458 from one set of study specimens (range 1.410-1.465) (Jones and Beavers 1963:378) while Piperno (2006:92) suggests using a value of 1.42 for selecting microscope slide mounting media. These physical property values are important in the decisions that are made during laboratory processing of soils to isolate and visualize phytoliths.

Some of the earliest phytoliths described were recovered from wind-borne dust samples collected from the sails of the Beagle in the Atlantic Ocean in 1833 (Darwin 1846). During 1963-1967, the incidence of phytoliths in atmospheric dust on the Great Plains was documented as ranging from 2-35%, consisting primarily of grass phytoliths, and being most commonplace in the spring and summer (Twiss 1987). Botanists have long been aware of the presence and morphology of phytoliths in plants (e.g., Metcalfe 1960). As the number of scientific investigations and investigators studying phytoliths has grown during in the past half century, methods of recovering phytoliths from more complex matrices have been developed. For isolation of phytoliths from soil, the various detailed techniques share a common theme in that the separation from the soil matrix is achieved by flotation based on particle density difference. This basic laboratory technique was originally successfully applied in palynology (Frey 1955), and has seen numerous variations and refinements over the years. The early density separations involved a mixture of bromoform and acetone (Frey 1955). Subsequently, utilization of an aqueous zinc bromide solution with a density adjusted to 2.35 g/cm^3 was widely employed in many laboratories (Piperno 1988), although some have since recommended using a solution of the more expensive sodium polytungstate as a safer alternative

(Lentfer and Boyd 1997). Parr compared heavy liquid flotation with microwave digestion and found the microwave treatment advantageous (Parr 2002) although a quantitative phytolith recovery was not the target of that investigation.[11]

Burned Phytoliths

Although most phytoliths are optically clear via polarized light microscopy, darkened phytoliths—which display evidence of fire exposure—do occur. Initially, dark-colored phytoliths were reported to correlate with a lower particle density and thus the coloration was attributed to organic staining from the soil matrix (Jones and Beavers 1963:377). Subsequently recognized as evidence of burning, darkened phytoliths have since been used as a means to evaluate the environmental occurrence of fire. This concept was pioneered by Piperno who attributed phytoliths with carbon inclusions as being from burned plants, and thus one indicator of fire history (Piperno 1985a:17-18). Piperno later noted that "darker forms are related to higher quantities of organic carbon pigmentation occluded within or on the surface" (Piperno 1988:45), and that the incidence of burned phytoliths in soil samples was observed to increase with the initiation of agriculture (Piperno 1988:208). Parr (2006) provides a detailed discussion regarding means by which to distinguish burned versus soil stained phytoliths in order to enable use of phytolith color and appearance as a fire proxy.

---

[11] A microwave digestion apparatus was recently obtained, but too late for implementation in this current project.

In a forest environment, Kealhofer recognized three types of fire with increasing intensity: litter, under story, and extreme burns (Kealhofer 1996:236). Kealhofer counted burned specimens of all phytolith types in her soil samples, with a resulting burned specimen incidence ranging from 5-19 % (Kealhofer 1996:243). Kealhofer concluded that the data suggested that the entire landscape burned rather than selected patches, also noting that the presence of a minimal number of burned tree phytoliths suggested that intense extreme burns were rare (Kealhofer 1996:243). Although all taxa encountered were represented in the burned phytolith counts, relative phytolith morphological type frequency changes in different age soils suggested vegetative changes occurring on the landscape over time. Later, Kealhofer (2002) noted burned phytoliths had carbon inclusions and may also "appear blackened and sometimes even slightly 'melted'", subsequently noting that phytoliths often "show [evidence of] burning (through blackening and melting)" (Kealhofer 2003:80). Kealhofer and Penny (1998:90) note that burned phytoliths can provide information about the "seasonality… and intensity of the burn,… and indirectly, the role of anthropogenic agents". As of this date, the consensus seems to be that plant burning is indicated by "partial or total charring of the surface… [which may] serve as an index of the occurrence and intensity of prehistoric vegetation firing" (Piperno 2006:15).

Boyd (2002:478), who chose to use the elongate phytolith form in his study regarding burned phytoliths, indicated that the baseline incidence of burned ("blackened") phytoliths was about 8% in a modern control prairie soil sample with minimal major fire activity during the past century. Boyd pursued his "BPI" (Burnt

Phytolith Index) with examples of darkened elongate form phytoliths in a series of buried A horizons in his study area, finding one charcoal dense occupation layer with a BPI value of 73%. Although this large spike was documented, Boyd suggested using the change only as a relative fire indicator due to the many potential variables involved.[12]

Boyd's study was actually directed at determining the cause of prairie fires, using recovered charcoal and burned phytoliths as proxies. Based on recent historical records covering the study area, Boyd reported that lightning was a minor cause of prairie fires (Boyd 2002). Through historical ethnographic references, Boyd (2002) identified agriculture and helping control bison-herd movement as two reasons for anthropogenic generated fires. He also noted that more intensive land resource use (i.e., increased population density) during prehistoric times may have contributed to the observed increase in fire occurrence, with perhaps agriculture being a direct cause in late prehistoric times (Boyd 2002). Boyd also points out that although grasslands inherently imply relatively constant fire intensity, the variation in fuel load (i.e., total biomass, due to moisture changes) may vary the apparent change in proxy fire values even more so than climate change. Vankat (1979:164) stated that most prairie fires occur during the dry fall season when biomass loads are greatest, and that soil surface temperature normally remains under 100ºC during a prairie fire. The study of anthracology is actually a field unto itself (c.f. Teixeiraet al. 2002:819-830; Fiorentino and Magri 2008).

---

[12] In the same study, Boyd assumed that the recovered diatoms were probably eolian, although that possible transmission mechanism was apparently not considered for phytoliths. Jones, Hay and Beavers (1963:1223) reported sponge spicules up to 100 microns long were recovered from loess deposits. Thus, an eolian origin is presumed to be a possibility for a portion of all biogenic silica forms present in soils including those with evidence of burning.

For analysis of soil phytoliths, two different sample types are required. First, in order to properly interpret the total soil phytolith sample, specimens of representative local botanical specimens need to be collected, identified, and their phytolith composition studied and noted. The standard method is to digest (via treatment with acid or hydrogen peroxide) or to thermally ash the identified plant specimens, and then slide mount and study the phytoliths remaining following treatment. This effort can require a substantial amount of time and expertise, but modern control specimens are necessary to fully interpret the soil phytolith assemblage. At least one researcher has indicated that the time and expense involved in this extensive portion of the procedure may be one reason that phytolith studies are not used more frequently. Herbarium voucher specimens are an alternate method to obtain identified botanical species for phytolith recovery.

For modern prairie control soil samples, multiple samples are normally collected from a typical or representative area and pooled resulting in a composite soil sample characteristic of the modern surface A horizon. Individual researcher's procedures to collect composite modern day surface soil samples are variable as indicated in the literature: Pearsall (2000:407) recommends pinch sampling; in the example given, a composite surface soil sample is made from multiple small samples within a 10 x 10 meter area. Piperno (2006:87-88) also recommends the pinch sampling technique, with the further comment that 2 or 5 cm thick (i.e., deep) samples are appropriate; core and trowel sampling options are both mentioned; a transect collection variation is also noted.

Mulholland (1993:134-145) collected duplicate samples from each soil of interest as a check on variability. The surface soil sampling protocol used by Fredlund and Tieszen (1994:327) involved compositing four core samples collected from the corners of a 1 meter square at their study sites. In another report four 0.4 m^2 samples, each five cm thick, were pooled to obtain a surface prairie composite soil sample for analysis (Fernández Honaine, Osterrieth, and Zucol 2009:91). Kerns, Moore, and Hart (2001:479-480) created a composite soil sample from ten two centimeter deep core samples in a 40 meter circle in a wooded study setting to represent the modern soil surface.

Laboratory Methodology for Isolating Phytoliths:

Many variations of the laboratory procedures for the isolation of phytoliths have been detailed and compared in the literature (Piperno 1988, 2006; Pearsall 1989, 2000). Subsequently, other researchers have performed additional procedural evaluations. For the most part, all available procedures share the common thread of the separation of 1.50-2.30 g/cm^3 phytoliths from the slightly denser soil matrix (~2.65 g/cm^3) via flotation with a heavy liquid of intermediate density (~2.35 g/cm^3). A brief overview of the basic methodology condensed from the two 1980s sources (Piperno 1988; Pearsall 1989) is discussed in the following paragraphs along with information about new techniques and alternate procedures that have been developed since that time. Each step in the overall procedure has various options with benefits and proponents; however, the overall basic steps are common among most phytolith fraction isolation schemes evaluated. This

published methodology used to as the starting point for this current research project was gleaned from the Piperno (1988) and Pearsall (1989) and distilled into a laboratory protocol (Sudbury 2000:48-53 [reproduced in Appendix C]). The final laboratory procedure used at the conclusion of this project is presented in detail in the Materials and Methods Section.

In evaluating clay removal techniques, one study showed that centrifuging was a more effective means of clay removal than sieving through a fine mesh sieve; this data also compared favorably to the standard settling technique for clay removal (Lentfer and Boyd 1999). Clay removal is a critical step. Some finished slides for counting, prepared by other laboratories, have been observed to have large masses of clay remaining on the slides (personal observation); this clumped material includes phytoliths which may potentially skew the resulting counts if larger phytoliths happen to be preferentially released by incomplete clay removal.

The thermal option is good for quantitative recovery separations, but takes longer to process; ashing in a muffle furnace is not appropriate for quick and dirty preparations, or for separations where the particle dimensions will be measured. Jenkins (2009) reported that dry ashing tends to break up articulated phytoliths more than wet ashing. Another organic matter removal method in the literature involves adding ethanol to the samples and igniting the ethanol (Powers and Gilbertson 1987); a comparison of this method with heavy liquid flotation using other organic removal treatments led to the conclusion that flotation methods were superior (Lentfer and Boyd 1998).

Considerable effort has been devoted to searching for alternate procedures for organic material removal. In particular, Parr (with others) has been involved in efforts to study and improve on a number of the established laboratory methods. The use of pressurized microwave extraction was tested on sediments with good success—and included organic removal (Parr 2002; Parr, Dolic, Lancaster, and Boyd 2001). This procedure was also noted to be more effective at recovering starch from sediments than some other protocols (Parr 2002). Although much faster start to finish, the sample size via the microwave procedure is very limited (0.25 g), and the resulting slide mounted material is not as clean as material isolated via heavy liquid floatation. Thus, as with any developments, there are trade offs if one opts to utilize the pressurized microwave procedure which can process multiple samples simultaneously. The methods described in this and the preceding paragraphs are also appropriate for processing botanical reference specimens for use as phytolith standard materials (see Mulholland 1982 for other options).

The next basic step is separation of the phytoliths from the denser quartz-based silt matrix by heavy liquid flotation. Sulfuric acid was reported as ineffective when used to isolate pollen grains from a clay matrix (Faegri and Iverson 1950:61). Bromoform was originally used to float various microfossils, followed by a mixture of bromoform and acetone (Knox 1942; Frey 1955); bromoform remained in use for some flotation applications for decades (Gibson and Walker 1967). Sodium polytungstate has been in use for density separations since the 1980s; one effort was even made to speed up the separation by freezing different zones of the liquid (Morrow and Webster 1989). About

the same time, specifically for the solution density required for phytolith isolation,

mixtures of bromoform and nitrobenzene, tetrabromoethane and nitrobenzene,

tetrabromoethane and ethanol were also in use along with two heavy metal options: zinc

bromide in water and Piperno's preference which was a mixture of cadmium iodide and

potassium iodide (Piperno 1988:122).

As alternate heavy liquids have been implemented over the decades, some solvent

choices have gone by the wayside as improved options become available. Current

researchers use one of several effective heavy density liquids—each having its own

advantages and disadvantages (the decision is generally a trade-off between efficacy,

safety, and cost). One study compared four different heavy liquids on eight different test

soils to aid in the selection of the optimal heavy liquid solvent system and ended up

recommending zinc iodide or sodium polytungstate (Zhao and Pearsall 1998). Zinc

bromide was noted to give good results (Zhao and Pearsall 1998); the reaction observed

while using zinc bromide during their study was probably due to the hydrochloric acid

present in the reagent as was noted. Sodium polytungstate, a safer heavy liquid alterative

to the liquids containing heavy metals, has been demonstrated to be an effective flotation

media (Madella, Powers-Jones, and Jones 1998; Lentfer and Boyd 1998), and has been

adapted for use in a number of laboratories.

In this study, the heavy liquid flotation procedure was employed using zinc

bromide because zinc bromide produces excellent phytolith separations, zinc bromide is

less expensive than sodium polytungstate, the use of zinc bromide in water rather than

hydrochloric acid eliminated the carbonate reactions, the fact that the analyst was familiar with handling zinc bromide, and because the reagent was on hand and available for use (personal observation). As an aside, one of the phytolith laboratories that I visited had significant free iodine vapor present in their sample storage room. Iodine is corrosive and strong oxidizer; thus, this potential problem is mentioned as a caution when using Zinc Iodide and/or Cadmium Iodide. The analyst should make certain that the iodide reagent is totally removed from processed samples or neutralized prior to storage in order to minimize storage degradation (i.e., sample cartons, sacks, etc.) and more importantly the health risk to personnel. If the completed samples are not iodine free, ventilated storage (fume hood or vented cabinet) is recommended.

After flotation, the separated phytoliths and liquid are transferred to another container to which water is then added to lower the solution density so that the phytoliths sink (Piperno 2006). The phytoliths are then repeatedly rinsed with water to completely remove the heavy portion of the flotation solvent (which is later recycled); the phytoliths are transferred to vials or other suitable containers for storage. Some researchers store the phytoliths dry whereas others leave them in ethanol to minimize abrasion. A recent analysis indicates that stirring the isolated (suspended) phytoliths and not sampling from the top of the material is critical to obtaining a representative sample for analysis; the recommendation is made that dry samples are preferable for slide mounting (Strömberg 2007).

In the next step, after gently mixing, a small portion of the phytolith sample (~1-2 mg) is mounted on a clean microscope slide. The use of a variety of different mounting media in use have been reported in the phytolith literature including Canada Balsam (Andrejko 1982; Runge and Runge 1995), Benzyl Benzoate (Mulholland 1982, 1986a; Lentfer and Boyd 1998), silicon oil (Fredlund, Johnson, and Dort 1985 [Silicon oil mounting media was used in conjunction with phase contrast microscopy]), Permount (Mulholland 1982, 1986a), glycerin (Fredlund and Tieszen 1994), Dupex (Lentfer, Boyd and Gojak 1997), and water (Rovner 2004). Mounted slides can be examined by light microscopy and particle forms tabulated during scans; polarized light microscopy was used in this research to enable mineralogical evaluation of the particles being observed. Others have effectively used simple light microscopy and phase contrast microscopy; scanning electron microscopy is also an option although the specimen mounting procedures are different (McKee and Brown 1977:833-837).

Recently a detailed study about effective phytolith particle count size was published Strömberg (2009a; see also Alexandre and Brémond (2009), and Strömberg (2009b)]). As with many experimental variables, the appropriate count size is dependent on one's research design, objectives, and site specifics. However, for detailed studies, the target short cell count of 200 is recommended as an approximate good starting point although the number could be higher if conditions (i.e., if the relative frequency of particle forms of interest) warrant (Strömberg 2009a (also see Bodén 1991)). When a sufficient sample is available, this researcher always counts a minimum of 200 short cell

phytoliths, along with other identifiable forms present in the same fields of view that are scanned during counting.

In other analytical pursuits related to phytoliths, efforts to isolate plant DNA from soil phytoliths have been unsuccessful to date (Elbaum, Melamed-Bessudo, Tuross, Levy, and Weiner 2009).   Work is underway to standardize the nomenclature of the various phytolith morphologies (Pearsall and Dinan 1992; Bowdrey, Hart, Lentfer, and Wallis 2001; Madella, Alexandre, and Ball 2005).

Additionally, other matrices than soil and sediments are also analyzed, and have their own variations of prep methods. These include grinding implements (Fullagar and Field 1997; Tassara and Osterrieth 2008; Zucol and Bonomo 2008), edged flint tools (Anderson 1980; Kealhofer, Torrence, and Fullagar 1999; Piperno and Holst 1998), bone tools (d'Errico, Giacobini, Hather, Powers-Jones, and Radmilli 1995), and teeth (Armitage 1975; Ciochon, Piperno, and Thompson 1990; Middleton 1990; Middleton and Rovner 1994; Cummings and Magennis 1997; Cordova and Agenbroad 2009).

Based on particle size and density, other particle types are often included along with phytoliths in the isolated amorphous silica fraction which has a density

$$1.50 \text{ g/cm}^3 < x < 2.30 \text{ g/cm}^3.$$

In addition to phytoliths, other particle forms recovered from soil in the phytolith (i.e., biogenic silica) fraction may include glass sponge spicules (see Figure 104), diatoms,

chryophytes, radiolaria, charcoal fragments, calcium oxalate crystals from cacti and other

plants (Figure 3), and volcanic glass shards (Figure 4).
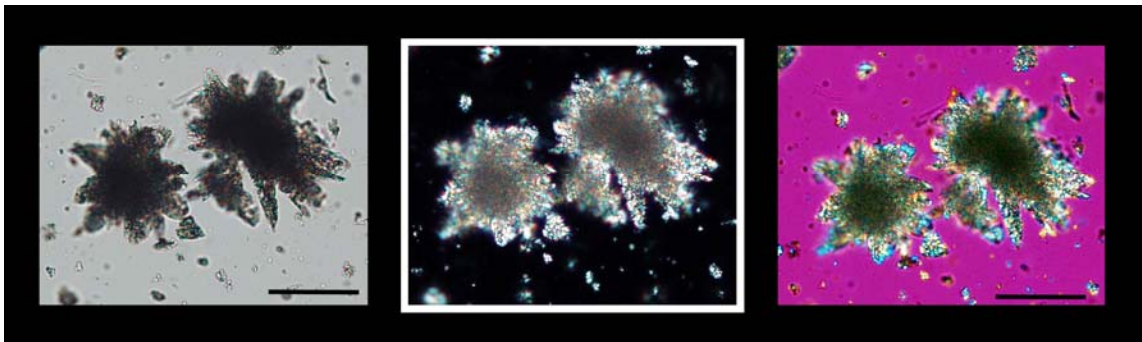
Figure 3.   Calcium oxalate rosettes isolated from a prickly pear cactus (Sudbury 2009a).
Left: polarized light, Center: crossed polars, Right: crossed polars with ¼ wave plate.
(Bar scales are 10 microns.)
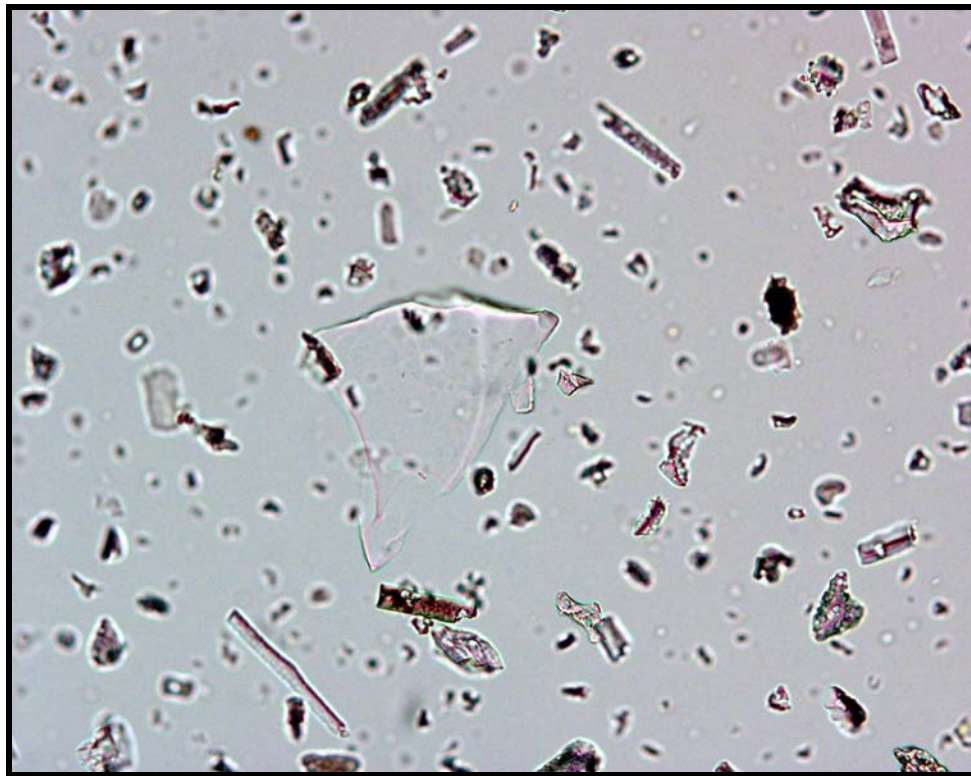
Figure 4. Example of possible volcanic ash recovered in some phytolith extracts of soils
(the larger clear shard in the center of this photograph of a phytolith isolate from Bull
Creek-28 (200x)). Although observed in various soil sample isolates, volcanic ash is not
addressed in this dissertation.

Grasses, more properly known as the botanical family Poaceae (formerly called Gramineae), include over 600 genera and 9000 species (Darke and Griffiths 1994:x) and are the third largest botanical family (Constable et al. 1985:19).   Perennial grasses make up about 95% of native grasslands, although annual grasses also occur (Constable et al. 1985:33). Grasses are much more than cosmetic; "of the fifteen major crops that stand between us and starvation, ten are grasses" (Brown 1979:1).   The grain crop data in Table 2[13] was obtained from the web site of FAOSTAT, the Statistics Division, Food and Agriculture Organization of the UN (FAOSTAT 2009). In addition to these grain crops, there are other members of Poaceae that are very significant in the world economy; several other notables are sugar cane (Gould 1968:2), bamboo (Gould 1968:40-45; Darke and Griffiths 1994:xix), and giant reed grass (Constable et al. 1985:19).

The data in Table 2 is a tabulation of the annual grain (cereal) yields for ten sequential years ending in 2007, and also includes representative crop yield data back to 1961which was the first year that the UN tabulated crop records.   The information tallied is for the ten major grains and two pseudograins (buckwheat and quinoa). The normalized relative percent column is based on the 12 specific crop yields listed for 2007. These world-wide production figures include grains for human consumption as well as for livestock feed.

---

[13] Data copied and compiled August 14, 2009 from http://faostat.fao.org/site/567/default.aspx#ancor, FAOSTAT, Statistics Division, Food and Agriculture Organization of the UN, and reproduced herein by permission.

Three crops (maize, rice, and wheat) accounted for 87.84% of the worldwide

produced grain tonnage in 2007, and world output for these three crops roughly tripled

from 1961 to 2007.   These three crops have long accounted for more than 50% of all

human calories consumed (Raven and Johnson 1995:28-12). Some of the other crops

show gradual increase over time; notably, the production of oats and rye has declined—

perhaps being replaced by other crops. The significant increase in maize production in

2007 is a response to government incentives to produce ethanol from corn which altered

the established market system balance; world-wide food grain shortages and price

increases resulted from this government intervention. Although there is an abundance of

available food in fertile productive America—enough to enable regular major grain

exports—the data for other parts of the world is much more sobering. In an excellent

news article, Gebisa Ejeta stated that in

> 1933, according to USDA ERS, Americans spent more than 25 percent of their
> income on food. By 1985, that had dropped to 11.7 percent and, in 2000, below
> 10 percent for the first time in history…. In contrast, the poorest nations spend
> 70 percent or more of their disposable income on feeding their families. (Laws
> 2009)

These important food grain crops have been the topic of considerable research

interest to the phytolith community; indeed, the early pioneering work regarding

development of maize agriculture in Ecuador (Pearsall 1978, 1979) marked the initiation

of significant active growth in the modern phytolith research field.

Prairies, which comprise nearly 25% of the land surface (Vankat 1979:158) or

32% of the vegetated land mass (Constable et al. 1985:22), are dominated by grasses. Of

prairies, it has been stated that

Table 2. Worldwide Production of Major Grain (10) and
Pseudograin (2) Crop Production (Millions of Tonnes/Year) (FAOSTAT 2009)

Crop	% 2007 Total	2007	2006	2005	2004	2003	2002	2001	2000	1999	1998	1988	1978	1968	1961
Maize	33.81%	791.8	706.2	714.9	729.4	645.1	605.7	615.5	592.5	607.5	615.8	403.1	393.6	255.6	205.0
Rice	28.16%	659.6	641.6	632.3	608.1	584.3	570.0	597.5	598.8	610.9	579.2	487.5	385.2	288.6	215.6
Wheat	25.87%	606.0	605.1	626.8	632.5	559.8	574.5	589.7	585.9	587.7	593.6	500.5	443.8	326.8	222.4
Barley	5.70%	133.4	139.6	138.6	153.8	142.6	136.7	144.0	133.1	128.4	137.7	163.4	174.9	113.5	72.4
Sorghum	2.71%	63.4	58.6	59.7	58.0	58.9	53.5	59.9	55.8	60.0	61.3	63.1	65.6	53.2	40.9
Millet	1.45%	33.9	31.8	30.9	29.7	34.8	23.9	29.1	27.7	27.3	29.0	30.7	28.5	26.8	25.7
Oats	1.06%	24.9	22.7	23.7	26.1	26.5	25.4	27.3	26.1	24.4	26.6	35.4	48.3	52.0	49.6
Rye	0.63%	14.7	12.6	15.1	17.7	14.6	20.9	23.3	20.1	20.2	21.1	31.0	30.9	33.0	35.1
Triticale	0.51%	12.0	10.7	13.3	13.9	11.0	11.4	10.8	9.1	8.3	8.8	2.9	0	0	0
Fonio	0.02%	0.4	0.4	0.4	0.3	0.3	0.3	0.3	0.3	0.3	0.2	0.2	0.2	0.2	0.2
Buckwheat	0.09%	2.0	2.0	2.1	2.3	2.6	1.8	2.6	3.8	2.8	3.1	3.1	3.7	3.0	2.5
Quinoa	0.00%	0.01	0.01	0.01	0.01	0.01	0.01	0	0.01	0.01	0	0	0	0	0

Data copied and compiled August 14, 2009 from http://faostat.fao.org/site/567/default.aspx#ancor, FAOSTAT, Statistics Division, Food and Agriculture Organization of the UN, and reproduced by permission. (http://faostat.fao.org/site/567/default.aspx#ancor. (accessed 8-14-09))

natural grassland ecosystems are fundamentally organized by three interactive processes: carbon assimilation and allocation, nitrogen assimilation and allocation, and rainfall-evapotranspiration. (McNaugton, Coughenour, and Wallace 1982:167)

Similar biomes on other continents are called the steppes (Russia), the pampas (South America), and the veld (Africa) (Vankat 1979:158). Prairies are also regulated by the "interrelated roles of fire, climate, and grazing animals" (Anderson 1982:297) with climate equating to temperature and moisture regime.

The major grassland or prairie region in the United States, known as the Great Plains, developed primarily over Mollisols (Brady and Weil 2002:104). Indeed, the very fertile Mollisols are associated with most of the world's major prairie ecosystems. In addition to the soils, other significant contributors to developing and maintaining prairies and specific plant associations are tempera-ture, precipitation, and fire. Grasslands are semiarid (Brady and Weil 2002:844) with "a low precipitation-evaporation ratio" with most rainfall occurring during the growing season (Vankat 1979:159). The growing season is roughly "120-200 days" (Vankat 1979:159) and is limited by summer drought and winter temperatures. Various grass species grow best in environmental/climatic conditions where they are most suited to thrive. Grasses have deep well-developed root systems that enable effective utilization of available water and help to minimize erosion. It has been stated that as much as 90 percent of the biomass of some grasses is in the roots (Brown 1979:6).

Fire is a critical component to maintaining grasslands, in part because frequent fires prevent trees from becoming established on the prairie; fires are thus important in

41

establishing and maintaining the grassland/forest boundary (Vankat 1979:167). A forest

has thick tree growth, whereas a "woodland vegetation is dominated by trees, but…most

of the crowns do not touch," and a savanna is "even more open; trees (or shrubs) have a

cover of less than 30 percent and the dense herbaceous layer is the best developed

stratum" (Vankat 1979:205). Summer droughts also enhance the action of fire to restrict

tree incursion (Anderson 1982:298-301). Grasses are able to survive fires because,

unlike most other plants that have apical meristems, the vegetative growth of grasses (via

bulbs, corms, or rhizomes) occurs at, or immediately below the ground surface (Vankat

1979:171-172). Grasses also have intercalary meristems throughout the culm (Gard,

personal communication). Thus, grass is able to resume growing after the aerial biomass

has burned. Many of the perennial grasses undergo vegetative growth by tillers and

stolons which also contain meristematic tissue enabling them to resume growth after a

heavy grazing or fire has removed the above ground biomass (Brown 1979:5).

In the Great Plains of North America, there are three main prairie types or plant

associations which are referred to as the Tallgrass Prairie, Mixedgrass Prairie, and

Shortgrass Prairie (Figure 5). The Shortgrass Prairie is bounded to the west southwest by

the Desert Grassland (which is not present in Oklahoma). These basic prairie types

mirror gradually decreasing water availability as one travels from east to west. Situated

between the Shortgrass and Tallgrass Prairies, the dominant plants of the Mixedgrass

Prairie association have intermediate moisture requirements between the two adjacent

extremes. Along with less moisture, overall soil depth, nutrients, and organic matter also

decreased (Bazzaz and Parish 1982:233). Even within these three basic prairie types, the
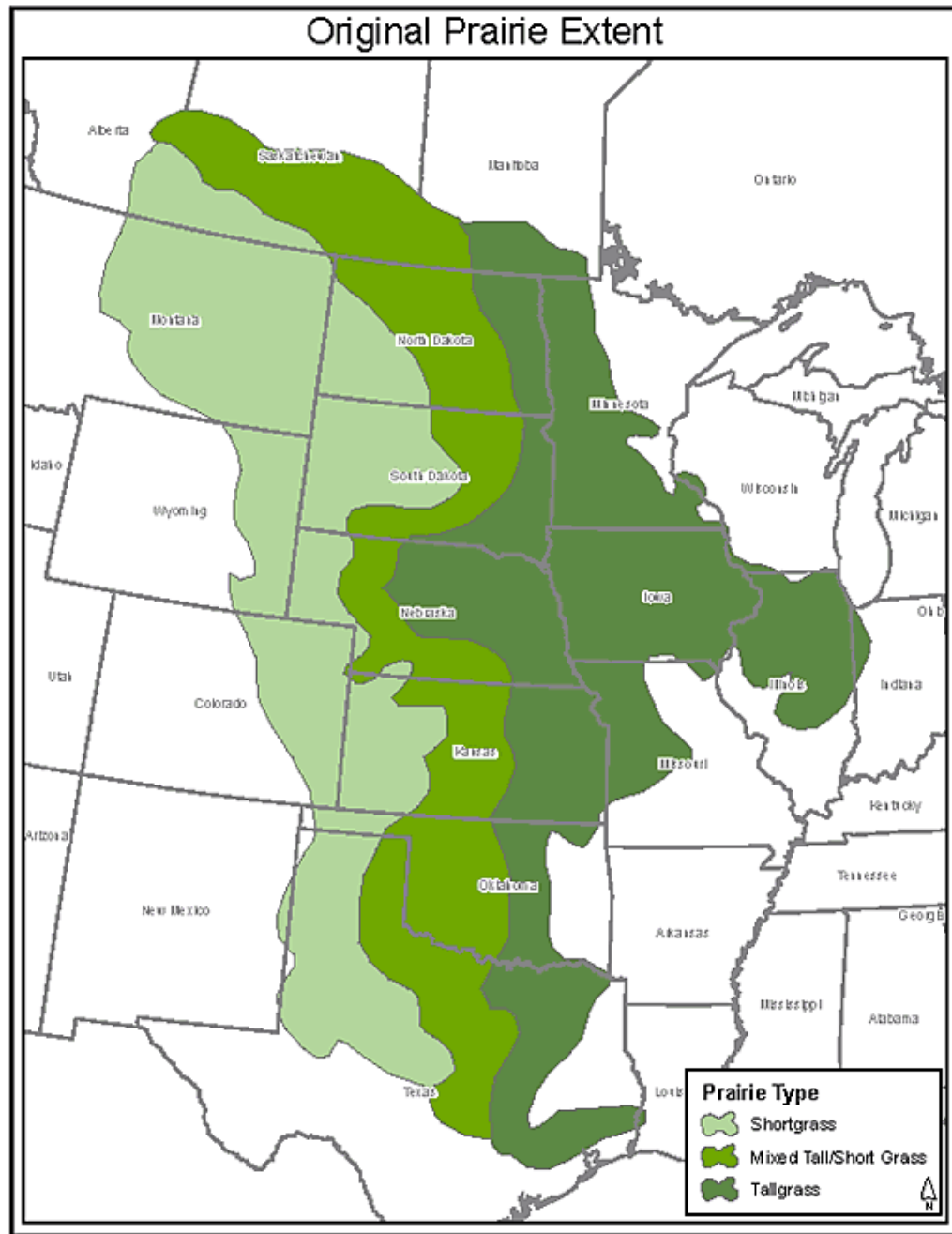
Figure 5. A depiction of the location of the three prairie types on the North American Great Plains during the early 19th Century exploration of the continent. (http://www.smscland.org/images/OriginalPrairieExtentMap.gif.)

plant community composition is not unchanging. Whereas the location of a given prairie

type may have 100 (or more) individual botanical species present, generally only 3-5

species at one given location make up 95% of the total annual biomass (Tyrl personal communication). The actual plant association composition or community making up a given prairie type varies by location due to specific local growing conditions (c.f. Fredlund and Tieszen 1994:323), and also includes forbs as well as grasses (Bazzaz and Parrish 1982:233; Tyrl, Bidwell and Masters 2002:17).

Of these three prairie types, it is generally the Mixedgrass Prairie boundaries that move most (Brown 1979:10) in response to variations in precipitation (Vankat 1979:167). Rather than actual physical movement of species across the boundary, the moisture variations over time generally result in various grass species that are already present becoming relatively more or less frequent in the particular prairie resulting in an apparent change or transition in the prairie type (Tyrl personal communication). In a contrarian view, Brown (1993) researched early explorer records and current field data and concluded that the eastern boundary of the Shortgrass Prairie has retreated significantly westward since the early nineteenth century, leading to his conclusion that dispersal may be a more significant cause of the Tallgrass Prairie invasion than climatic variation. It is possible that both of these mechanisms occur operating on vastly different time scales.

Prairie grasses have been the object of numerous phytolith studies once it was realized that morphologically distinctive and significant differences in the phytoliths were noted among basic botanical specimens. The original grass phytolith morphologic classes were first observed and reported by Twiss, Suess, and Smith (1969). Three basic groupings or clusters of forms were observed to be attributable predominantly (but not

exclusively) to the three grass subfamilies: the cool-season Pooideae (formerly referred to as the Festucoids.), the warm season (with some intermediate moisture requirement) Panicoideae, and the hot dry climate-adapted Chloridoideae (Twiss, Suess, and Smith 1969). Although some decades have passed since this initial proposal, this basic typologic clustering is still considered to be valid (Fredlund and Tieszen 1994:326; Pearsall 2000:363-368; Twiss 2001; Piperno 2006:28).

The reason for the morphologic differences observed primarily in the short cell phytoliths of species in these Poaceae subfamilies is due to metabolic differences between these families which in turn are due to their climatic preference; i.e., their metabolic rates in relation to their water regime and optimal growing temperature. The cool season Pooids are commonly referred to as "C3" plants, a specific reference to their metabolic pathway. All grasses take in carbon dioxide and utilize light energy from the sun via photosynthesis to generate their carbon fuel, and release oxygen. The so called C3 Pooids execute this via a 3 carbon chain-based metabolic pathway, incorporating the carbon from carbon dioxide (CO_2) into a larger non-volatile 3 carbon molecule via the Calvin cycle (Taiz and Zeigler 2002:146) which then ultimately undergoes further reaction to generate larger carbohydrate molecules. This particular process is very efficient at cooler temperatures, and becomes less energy efficient as the environmental temperature increases.

In a climatic adaptation, an alternate metabolic pathway—referred to as C4 metabolism—developed, and is used by the Panicoids and Chloridoids (both C4 type

plants) as a means of concentrating CO_2 and conserving plant water. Although the Calvin cycle is embedded as a sub-cycle in the overall C4 metabolic process, there are additional steps in the C4 process due to differences in plant cell architecture and layout. In short, in C4 plants the Calvin cycle biochemical machinery is located farther from the point of entry of the carbon dioxide into the plant (i.e., farther from the stoma, several cells removed). The ultimate reason for this architectural difference is that by moving the site of biochemical processing farther from the entrance (i.e., stomat), less water is lost during respiration. Upon entry into the plant in the mesophyll cell, the carbon from the CO_2 is fixed onto an existing C3 acid to form a C4 acid intermediate. This C4 molecule is then transported farther inside the plant to the bundle sheath cells where the CO_2 is released and enters the Calvin Cycle as described previously. The name of this overall C4 process is referred to as Kranz metabolism—being named after the bundle sheath cells. Both mesophyll and bundle sheath cell types have chloroplasts, but perform different biochemical processing steps. The biochemically different C4 process, based in part on physically different cell layout/architecture as compared to the C3 process, enables the plant to produce energy more efficiently in a drier climate at hotter temperatures; a major advantage of this process is minimizing the amount of water lost from the plant compared to the basic C3 metabolic pathway (Taiz and Zeigler 2002:156-160). C3 metabolism predominated in earlier geologic time, with C4 metabolism becoming more predominant in the late Miocene Epoch, about 7-8 million years ago (MacFadden 2000:49). Based on the difference in cell metabolism, the cell architecture is also different; in part, it is this physical manifestation of the morphologic difference

46

that is preserved, recovered, visualized, and evaluated via the short cell phytoliths recovered from soils.

An additional type of CO_2 concentration mechanism, not encountered in the field work during this current project, is referred to as Crassulacean Acid Metabolism (CAM) which improves water use efficiency even further. Although similar to C4 metabolism, in this variation, plant stomata only open at night when atmospheric CO_2 is collected and stored as a malate intermediate; then in the daytime, when the stomata are tightly closed, photosynthesis proceeds by metablolizing the malate and utilizing the internally released CO_2. This metabolic pathway, which occurs in cacti and some other plants, conserves as much as 90% the amount of water relative to the C3 and C4 processes (Taiz and Zeigler 2002:160-162). Another interesting observation is that cacti sometimes produce genus diagnostic phytoliths made of calcium oxalate rather than amorphous silica (Jones and Bryant 1992) (and calcium oxalate crystals occasionally occur in other species as well).

Based on phytolith evidence, grasses have been reported to have existed during the Miocene Epoch (Thomasson 1980; Thomasson, Nelson, and Zakrzewski 1986; Retallack, Dugas and Bestland 1990; Strömberg 2002). Strömberg also reports grass phytoliths from the late Oligocene (2002). Of particular interest is the report, based on coprolite evidence, that dinosaurs had actually grazed on grasses (Prasad, Strömberg, Alimonhammadian, and Sahni 2005; Piperno and Sues 2005). Although non-Poaceae specimens, even earlier phytoliths have been reported from the Devonian, Permian, and Triassic Periods (Carter 1999).

Grass phytoliths were first described by botanists looking at plant anatomy (c.f. Prat 1936; Metcalfe 1960). Via their roots, plants actually help to weather rocks and build soil (Iler 1979:747). The early soil phytolith work involving grasses determined soil phytolith concentrations, size variations, and also noted the presence of other biogenic silica (Beavers and Stephen 1958; Jones, Hay, and Beavers 1963; Jones and Beavers 1964a, 1964b; Jones, McKenzie, and Beavers 1964; Wilding and Drees 1968; Bonnett 1972). Other early work on grass phytoliths of the Great Plains also looked at concentration and size distribution in several Oklahoma soils (Yeck 1969; Yeck and Grey 1969, 1972). Since the firm basic morphologic foundation reported by Twiss et al. (1969) based on C3 and C4 metabolic differences, the study of grass phytoliths has continued to develop over the ensuing decades. Twiss continued to study grass phytoliths and their value as climatic indicators (1980; 1983; 1986; 1987; 1992; and 2001).

Brown studied and reported phytolith morphologic forms from a variety of voucher specimens; in addition to documenting forms, Brown also evaluated phytolith size relative to water availability (1984, 1986a, 1986b). Mulholland (Mulholland, Rapp, and Gifford 1982), who first studied phytoliths from Troy, later studied grass phytoliths on the northern Great Plains with particular interest in maize (Mulholland 1986c; Mulholland 1993; Mulholland, Rapp, and Ollendorf 1988), observed that the specific morphologic forms were encountered in multiple grass subfamilies (Mulholland 1989), and began to deal with trying to increase the availability of botanical reference standards

processed and studied (Mulholland and Rapp 1989), and to standardize morphologic

nomenclature (Mulholland and Rapp 1992b). The annotated bibliography by

Mulholland, Lawlor, and Rovner (1992) was also a significant contribution to the field.

Subsequent phytolith research on the Great Plains has studied climate change and

Paleoclimate as reflected in the Poaceae phytolith morphologic signature of soils. In a

survey of A horizon phytoliths across the Great Plains, Fredlund and Tiezen (1994,

1997a) developed a calibration formula to correlate the phytolith morphologic signature

to the temperature and tested it on buried soil phytolith signatures.   Other regional

research involves looking at riparian and alluvial settings on the plains (Johnson and

Martin 1987; Martin and Johnson 1987; Johnson and Logan 1990; Arbogast and Johnson

1994; Bozarth 1995; Baker, Fredlund, Mandel, and Bettis 2000). Cordova and Johnson

(2007) have initiated a study to look at the southern Great Plains during the Holocene,

and study the interaction of climate, fire, grazing and vegetation using paleobotanical

data (phytoliths, pollen, charcoal, and fungal spores).

Numerous reports regarding phytoliths in the extensive loess deposits covering

part of the plains have also been published (Fredlund 1986; Feng, Johnson, Sprowl, and

Lu 1994; Miao, Mason, Johnson, and Want 2007; Aleinkoff et al. 2008; Mason et al.

2008; Muhs et al. 2008). Sand dunes have been yet another active setting for phytolith

research (Goble, Mason, Loope, and Swinehart 2004; Boyd 2005; Cordova, Porter,

Lepper, Kalchguber, and Scott 2005), and playa features on the plains have also been

studied (Fredlund, Bousman and Boyd 1998; Holliday, Mayer, and Fredlund 2008).

Pursuit of radiocarbon dating and carbon isotope studies at Kansas prairie sites is ongoing; Martin and Johnson (1995) documented variations in radiocarbon dates obtained from three different soil organic matter factions (total, humic acid, and residue) while Johnson, Willey, and Macpherson (2007) studied the variation in carbon isotope ratio in soil profiles under a Tallgrass prairie. A phytolith study of a Colorado Shortgrass locale has been reported which involved five sites with Holocene buried soils formed in alluvium; periods of stability and instability were noted, along with changes in climatic conditions (Blecker, Yonker, Olson, and Kelly 1997). The vegetation history of the Prairie Peninsula of Illinois has been studied via phytolith signature (Wilding and Drees 1968), and the opal content of a prairie soil in Pennsylvania has also been documented (Waltman and Ciolkosz 1995).

Initial Great Plains phytolith work by this researcher was on soil from the Waugh Site during a one semester SEM course (Sudbury 2000); although instrument uptime was very limited, the conceptual groundwork for future studies was laid. At an early site on the northern plains, phytolith stability and preservation issues were encountered which resulted in the lack of phytoliths in the soil, presumably due to soil pH issues (Sudbury 2007). Working on samples from a late prehistoric archeological site in Oklahoma, maize agriculture was confirmed and site activity areas were evaluated (Sudbury 2006).

Although not true grasslands, studies involving mixed grassland-forest interfaces and intermingling are also significant to this current research. A number of studies looked at various established forest/grassland systems (Fisher, Jenkins, and Fisher 1986;

Reider, Huckleberry and Frison 1988; Bozarth 1993; McClenahen and Houston 1998; Kerns 2001; Kerns, Moore and Heart 2001). In soils under a *Sequoiadendron giganteum* forest in California, the absence of grass phytoliths was interpreted to indicate the historic absence or lack of grassland in the modern forest (Evett et al. 2006).

Outside of the Great Plains, numerous phytolith studies have been conducted involving grasses and grasslands. Coupled with pollen data and using core samples, Fearn (1995) studied the grassland history of the Southwestern Louisiana Prairie, and also used phytoliths recovered from sediment as an aid to identify the source of grass pollen (Fearn 1998). Lu and Liu (2003a, 2003b) studied a series of coastal grasses along the Gulf of Mexico documenting phytolith forms present in numerous reference specimens and taking important steps to associate various phytolith morphotypes with different coastal plant communities developed on loess deposits. The Pacific northwest has been the site of extensive research inquiries looking at modern phytolith assemblages and loess deposits to determine vegetation and climate change during the past 100,000 years (Blinnikov, Busacca, and Whitlock 2001, 2002; Sweeney, Busacca, Richardson, Blinnikov, and McDonald 2004; Blinnikov 2005). Several early Canadian range grass studies are of note; Johnston, Bezeau, and Smoliak (1967) looked at the variation in silica content of range grasses over time, whereas Blackman (1971) reported the phytolith forms present in a variety of reference specimens. Three important studies out of the Missouri Botanical Garden deal with the relative age of several grasslands, the development of grasslands, and the phylogeny of the Poaceae (Leopold and Denton 1987; Jacobs, Kingston, and Jacobs 1999; GPWG 2001).

In South America, following a very early report by Fontana (1954) about silica deposition in *Panicum maxicum* leaves, a series of studies about grasses from the Brazilian Cerrados began appearing in the 1960s (Sendulsky and Labouriau 1966; de Campos and Labouriau 1969; Teixeira and Labouriau 1970; Songdahl and Labouriau 1970; Figueiredo and Handro 1971) as well as one study about Amazonian grasses (Cavalcante 1968). In the past 15 years, the resurgence in published South American grassland studies has come from Argentina (Zucol 1996, 1998; Gallego and Distel 2004; Gallego, Distel, Camina, and Rodrígues Iglesias 2004; Fernández Honaine, Laborde, and Zucol 2008; Fernández Honaine, Osterrieth, and Zucol 2009; Fernández, Gil, and Distel 2009; Osterrieth, Madella, Zurro, and Alvarez 2009).

Other major contributions to grassland phytolith studies come from Africa. Palmer (1976) suggested using phytoliths to help identify grasses represented by the pollen in lake core samples. Subsequently, the Smithsonian Institution Press has published a series of volumes documenting the epidermis of African grasses (Palmer and Tucker 1981, 1983; Palmer, Gerbeth-Jones, and Hutchinson 1985; Palmer and Gerbeth-Jones 1986, 1988 [Also, Smithsonian Contributions to Botany phytolith volumes have issued for the tropical American grasses (Piperno and Pearsall 1998a), and for Southeast Asia (Kealhofer and Piperno 1998)]). Again, the early African studies looked at morphology (Stewart 1965). Alexandre studied silicon cycling and weathering (Alexandre, Meunier, Colin, and Koud 1997) and also late Holocene grasslands (Alexandre, Meunier, Lézine, Vincens, and Schwartz 1997). Beyond the African phytolith volume (Runge 2000), soil phytoliths and paleoenvironmental reconstructions

were also addressed (Runge and Runge 1995, 1997). Bremond, Alexandre, Peyron, and Guiot (2005a) looked at the correlation between water stress and grass types as reflected in the phytolith record as it relates to evapotranspiration, and developed effective humidity-aridity and water stress indices. The timing of the development and expansion of C4 African grasses in geologic time was studied (Ségalen, Lee-Thorp, and Cerling 2007). In several related studies, grass subfamilies in mountains were studied to develop a phytolith index to correlate with the C3/C4 grass composition and tree cover density (Bremond, Alexandre, Wooller, Hély, Williamson, Schäfer, Majule, and Guiot 2008), and also looking at the leaf area index—as well as the same grass composition and tree density factors—in Cameroon (Bremond, Alexandre, Hely, and Guiot 2005b).

Although prairie grasses were prominent in early phytolith studies, the body of phytolith literature is not restricted to the Great Plains of North America, nor to prairies. The field is international in scope with many different lines of investigation. In particular, much research (including the early seminal work by Pearsall (1978, 1979, 1987) and Piperno (1984, 1985c, 2001)) has been directed to the development of agriculture in the tropics—concentrating on maize (also see Pearsall and Piperno (1990), Piperno and Pearsall (1998b), and Staller, Tykot and Benz (2006)). Other agricultural-related research has involved the early development of wheat (Hodson and Sangster 1988; Tubb, Hodson, and Hodson 1993; Ball, Brotherson, and Gardener 1993; Ball, Gardner, and Anderson 1999) including examining the effects of irrigation on phytolith size (Rosen and Weiner 1994). Also significant activity has been expended studying the development of rice agriculture in Asia (Akai 1939; Lanning 1963; Kido and Yanatori

1964; Watanabe 1968; Chaffey 1983; Kealhofer and Piperno 1994; Kealhofer and Penny 1998; Jiang 1995; Pearsall et al. 1995; Houyuan, Naiqin, and Baozhu 1997; Zhao 1998).

Soils and Buried Soils

The primary soil horizon of interest in this current research is the A horizon which is "the topmost mineral soil horizon, usually showing signs of organic matter accumulation [i.e., darkening]" (Schaetlz and Anderson 2005:741). This organic-rich layer, in common vernacular often referred to as topsoil, supports active plant growth— including the visible modern prairies that were studied during this project. A very detailed and useful system of soil taxonomy has been developed (Soil Survey Staff 1999; Schaetlz and Anderson 2005:106-163; Buol, Southard, Graham, and McDaniel 2003: 193-213). Soil is critical to survival; by one estimate, soil is ultimately responsible for producing 97% of the calories consumed by humans (Bouyoucos 2009).

If the rate of alluviation on an A horizon is greater than 3 mm per year, then well-developed soils cannot form and distinct stratified sediments accumulate (Alexandrovskiy, Glasko, Krenke, and Chichagova 2004). Soil development may not occur at sediment accumulation rates as low as 1 mm per year; well developed soils can develop when accumulation is less than 1 mm/year (Alexandrovskiy et al. 2004). When an A horizon is buried by an alluvial, eolian, fluvial, or another event, it becomes referred to as a buried soil, or Ab horizon. The Soil Survey Staff (1992:1) defines a buried soil as

covered

with a surface mantle of new soil material that is either 50 cm or more thick, or is 30 to 50 cm thick and has a thickness that equals at least half the total thickness of the name diagnostic horizons that are preserved in the buried soil.

However, Schaetzl and Anderson (2005:53) argue that a buried soil is one that is simply unrelated to the overlaying mantle—regardless of mantle thickness—meaning that the previously active soil forming processes stopped at the time of burial (Schaetzl and Anderson 2005:587). The buried soil actually represents a former geomorphic surface (Schaetzl and Anderson 2005:619) and thus contains discrete historical information—unraveling this story at the time of burial is a major objective of this dissertation.

With time the new surface material will undergo pedogenesis to form a new A horizon in this location. Buried deeply enough, the newly designated Ab horizon no longer is actively involved in pedogenic processes. When this process occurs repeatedly in one location, the series of stacked buried A horizons are numbered sequentially from the top down (i.e., Ab, Ab2, Ab3, etc.). On some occasions, a process known as soil welding combines overlaying A horizons (Ruhe and Olson 1980); soil welding occurs when extensive melanization in a stable upper A horizon causes distinct A horizons below it to become incorporated into the upper melanized unit as the upper unit continues to develop downward through the lower A horizons. Recent investigations indicate that variations in clay mineralogy in such polygenic soils can help identify instances of soil welding (Presley, Hartley, and Ransom 2010).

One unresolved question regarding thick buried A horizons is whether they form by addition of mineral components to an A horizon thus resulting in a cumulic A horizon, or whether it is possible that these soils may sometimes develop solely by the process of melanization. The tendency in the archeological literature seems to be to assume that thick well-developed A horizons must be cumulic in order to become so thick; however, melanization should also be considered as a soil formation option (Ferring 1992).

In geological formations, paleosols—or fossil soils (i.e., buried soils)—can generally be identified by three features: soil horizons, soil structure, and root traces (Retallack 2001:13). Retallack (2001:187)—whose interest includes paleosols within the geological record—also defines five stages of paleosol development. Buried soils, sometimes also referred to as buried paleosols, are actually one of three classes of paleosols (Waters 1996:57-60). The other two types of paleosols are relict paleosols and exhumed paleosols (Ruhe 1965). A relic paleosol has never been buried, thus remains at the modern surface, yet it formed under "previous and presumably different paleoenvironmental conditions" (Schaetzl and Anderson 2005:621-622). Exhumed paleosols were once buried, and then have been subsequently re-exposed by removal of the overburden and thus are again the modern surface (Schaetzl and Anderson 2001:621-622). To avoid possible confusion, the term buried soil is used in the remainder of this dissertation; all buried soils are considered to be paleosols, but not all paleosols are buried soils. Another term sometimes used interchangeably with paleosols and buried soils is geosol (Waters 1992:75); however, Holliday states that the term geosol does not simplify the lexicon and suggest that the word soil is equally appropriate (Holliday

2004:76-77). More recently, the The North American Stratigraphic Code clearly

recognizes and defines identifes a geosol as

> … a laterally traceable, mappable, geologic weathering profile that has a consistent stratigraphic position. The term is adopted and redefined here as the fundamental and only unit in formal pedostratigraphic classification… (AAPG 2005:1560)

and also clearly states that

> (1) a geosol may be in any part of the geologic column, whereas a pedoderm is a surficial soil;
> (2) a geosol is a buried soil, whereas a pedoderm may be a buried, relict, or exhumed soil;
> (3) the boundaries and stratigraphic position of a geosol are defined and delineated by criteria that differ from those for a pedoderm; and
> (4) a geosol may be either all or only a part of a buried soil, whereas a pedoderm is the entire soil. (AAPG 2005:1559).

Pedology is the study of soils; Schaetzl and Anderson (2005:774) define peology

as

> The branch of soil science that addresses soils, their properties, origins, distribution and occurrence on the landscape, as well as their evolution through time. The study of soils as a naturally occurring phenomena taking into account their composition, distribution and method of formation.

Easterbrook (1999:49) notes that paleosols, which represent a stable soil surface that

underwent pedeogenesis long enough for A horizon development, are actually an

unconformity in the soil sequence. Paleopedology, a growing field, is "the study of

paleosols and the environments in which they formed" (Schaetzl and Anderson

2005:773); volumes devoted to Paleopedology are available (c.f., Retallack 2001;

Constantini, Makeev, and Sauer 2009).

Geoarchaeologists, who frequently study buried soils, do so because past stable

soil surfaces are often associated with human occupations; thus, the detail that the soil

matrix contains provides information about the site setting and climate at the time of site

occupation (Valentine and Dalrymple 1976; McCarty and Schwandes 2006:472). The presence of buried soils has long been recognized in Oklahoma (Harper and Hollopeter 1931; Harper 1932, 1933; Sears and Couch 1934; Hall 1968; Goss, Ross, Allen, and Haney 1972). During the Holocene, the Great Plains—and indeed all of North America—is known to have been subject to considerable climatic variation. Between any and perhaps all of the intervals of climatic fluctuation during the Holocene, periods of relative climatic stability would be expected to have been conducive to landscape stability and thus periods of soil formation that supported relatively stable plant growth that would be potentially be recorded as A horizons in the soil record. Conversely, during periods of intense climatic activity, erosion might remove existing soil whereas during intervals of fluvial, colluvial, or eolian deposition, sediments would cover an existing stable surface A horizon resulting in the creation of a buried soil (Rapp and Hill 2006:43).

Climate and Paleoclimate

Based on North American pollen data and radiocarbon dates Wendland (1978) and Wendland and Bryson (1974) identified the following "Holocene episodes" (dates given are radiocarbon dates BP[14]; descriptive comments taken from Wendland 1978). The so-called Late Glacial period lasted until ca. 10,030 BP, and was followed by the Pre-Boreal (ca. 10,030-9,300 BP) during which time the grasslands shifted eastward.

---

[14] The development of an accurate correlation between calendar years and radiocarbon years is ongoing (Broecker 2006; Bement and Carter 2008).

During the Boreal ca. (9,300-8,490 BP) the grasslands continued to expand eastward and the vegetation border moved northward. During the Atlantic (ca. 8,490- 5,060 BP) the "Great Plains were drier and/or warmer than today, particularly from ca. 7,000 BP to 5,500 BP" and the "northern limit of the conifer-hardwood forest had about reached its modern position" (Wendland 1978:278-279). The Atlantic, also often referred to as the Altithermal or Hypsithermal, was a period of "maximum warmth and dryness" (Vehik 2001:146-148).

The Altithermal was followed by the Sub-Boreal interval (ca. 5,060-2,760 BP) when moisture distribution on the Great Plains appears to have been uneven; this was followed by the somewhat moister Sub-Atlantic which began ca. 2,760 BP, and was next followed by the warmer Scandic which occurred from about 1,680-1,260 BP (Wendland 1978:280-281). The next interval was the somewhat moister Neo-Atlantic (ca. 1,260-850 BP), followed by the somewhat drier Pacific interval during ca. 850-400 BP, and the cooler Neo-Boreal period from ca. 400 -100 BP (Wendland 1978:280-281). The Neo-Atlantic interval is also known as the Medieval Warming period (Vehik 2001:146) while the Neo-Boreal period is frequently referred to as the Little Ice Age (Vehik 2001:146; Wendland 1978:281).

The current interstadial, referred to as the Holocene Epoch, includes three distinct cooler periods. The first and most severe, known as the Younger-Dryas, occurred early in the Holocene, lasted about 1,300 years (Kennett et al. 2009), and saw the temperatures rapidly cool ~5ºC for a period of time (Fredlund and Tieszen 1997a). The so-called

8,200 BP cool event (von Grafenstein, Erlenkeuser, Müller, Jouzel, and Johnsen 1998;

Dean, Forester, and Bradbury 2002) was a shorter less intense cooling interval, whereas

the final reported distinct Holocene cooling event is commonly referred to as the Little

Ice Age.

In the latter half of the Holocene, there was increased eolian activity which

resulted in sand dune formation on the north side of drainage basins in Oklahoma as well

as other parts of the Plains and southwest (Arbogast 1996; Arbogast and Johnson 1998;

Lepper and Scott 2002; Cordova, Porter, Lepper, Kalchgruber, and Scott 2005; Boyd

2005; Forman et al. 2006). The fluctuating regional weather during later parts of the

Holocene was such that periods of valley cutting and filling occurred (c.f. Holliday 1995;

Arbogast and Johnson 1994).

CHAPTER III

MATERIALS AND METHODS

Background

The laboratory methodology used in this current study is based extensively on the

method outline presented by Piperno (1988) and Pearsall (2000) as summarized

previously (Sudbury 2000). Relying on past analytical chemistry experience and the

specific needs of this current project, some simplifications and improvements of the

established procedure were implemented during the course of this research. The resulting

phytolith isolation method used in this project is presented in this section. Not all soil

samples were processed identically during the course of this study. A discussion of the

different methods employed and reason for alterations in the method is presented in

Appendix D. The equipment, materials, and supplies used during this research are listed

in Appendix E.

Methodology – Collecting Soil Samples (Modern Prairie Control Soils)

Three major prairie types occur in Oklahoma (Tallgrass, Mixedgrass, and Shortgrass

Prairies (Figures 5-7)). Modern surface soil samples (0-5 cm) were collected from
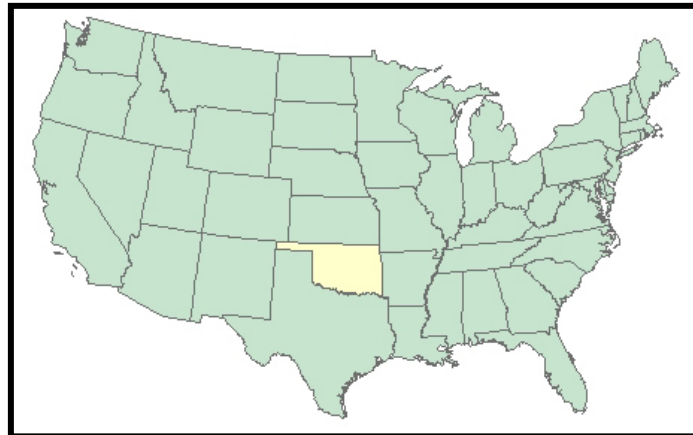
Figure 6. Map of the state of Oklahoma in the United States of America
(http://www.cleanairworld.org/images/statesrevOK.jpg (1-3-10)).
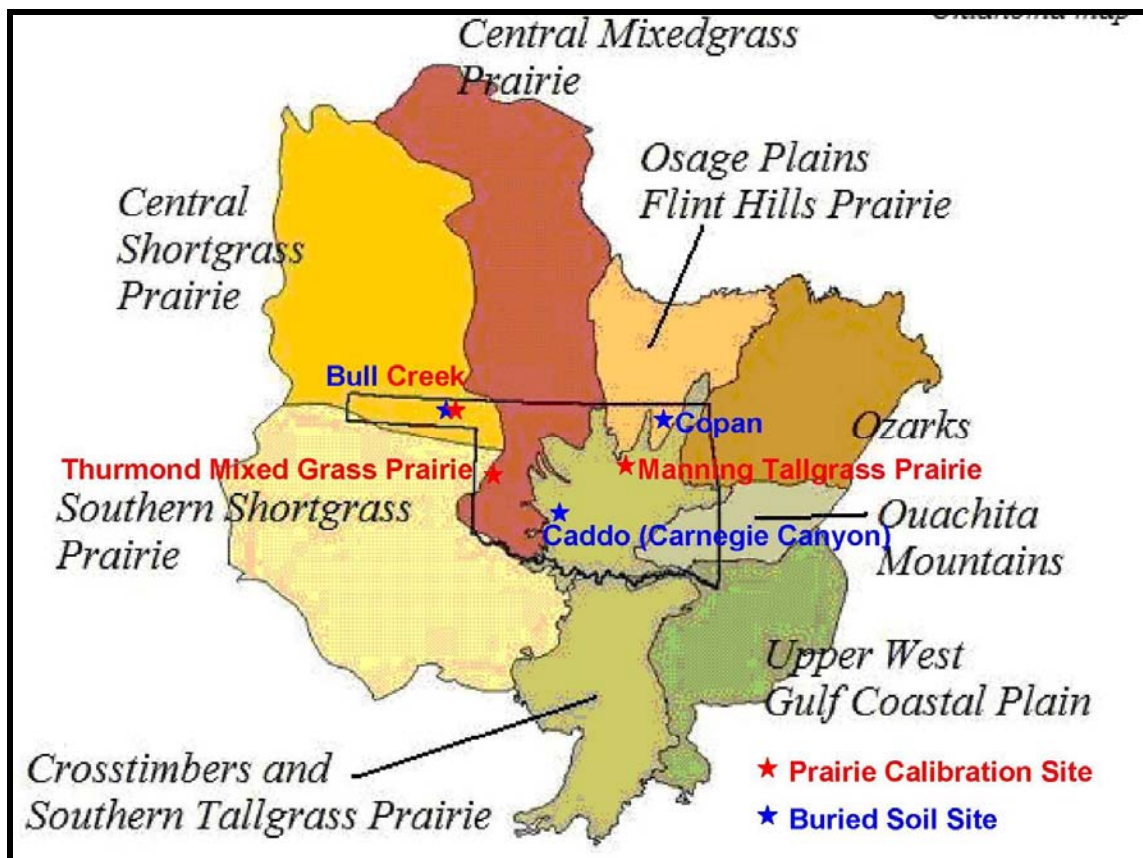
Figure 7. Oklahoma ecoregions map showing prairie types, prairie reference soil
(calibration) sampling sites, and buried soil sampling sites. [Original base map from
http://www.nature.org/wherewework/northamerica/states/oklahoma/images/places_eco.jpg.]

examples of each of these major vegetation units. These soil samples were used as controls from which to extract reference soil phytoliths from known modern prairie types. The control site surface soil sample locations are denoted by the red stars in Figure 7. Initial sampling of the modern Shortgrass Prairie occurred during sampling a series of buried soils in an exposed profile at the Bull Creek Site (Bement et al. 2007). The Bull Creek surface sample consisted of a single 10 cm depth sample. As field work progressed to other prairie control sample locations, a more extensive sampling protocol was developed. A twenty-meter diameter circle was laid out over the area to be sampled, and twenty soil samples were collected at spaced intervals within the circle (the numbered sampling locations are identified in Figure 8).

The soil probe was fitted with an adjustable stop to control depth of soil penetration. This was done by affixing a piece of Tygon® tubing to the soil probe and holding it in place with a hose clamp to act as a stop. A wooden block was perforated to
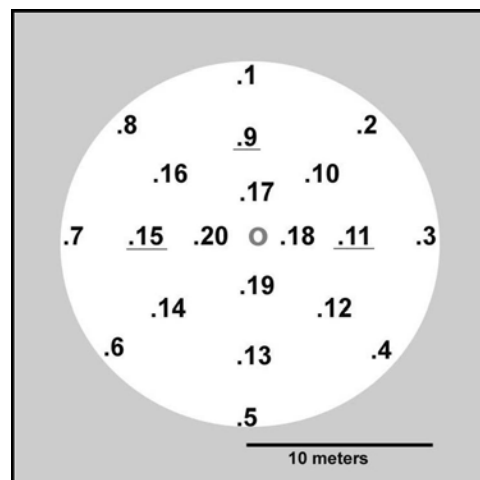
Figure 8. Twenty-meter sampling area showing individual sample locations. The singleton samples were collected at the center of the circle, the three underlined sample locations were pooled for the n=3 sample, and samples from the twenty numbered sample locations were pooled to become the n=20 composite sample.

accommodate the probe. The tubing/clamp placement on the probe was adjusted so that 5 cm of the probe tip extended below the block in order to collect the initial 5 cm deep soil sample (Figure 9). This enabled collection of replicate soil samples of a known constant cross-sectional area and depth from various locations at the prairie soil of interest.

An individual soil sample (n=1) was collected from the center of the sampling area (to obtain enough soil for extraction from the central n=1 location, three replicate samples were taken from immediately adjacent to each other in the center of the sampling circle and combined into a single sample). Single soil samples were taken from the remaining twenty numbered sample locations and pooled in pre-weighed sample jars (n = 1 [x=3; single soil core samples from sample locations 9, 11, and 15 were pooled for this n=1 sample], and n=1 [x=20]; separate cores at the previous three locations (i.e., 9, 11, and 15) were included in the n=1 [x=20] sample which consisted of one sample from each of the 20 individual sample locations). Once sampling was completed, the tubing/wood block stop was moved up the probe in 5-centimeter increments, and each hole re-sampled for the next 5-centimeter soil increment. In this manner, nine sequential composite soil samples were collected in repeatable 5-centimeter increments from each sampling hole up to the effective depth of the soil probe (0-45 centimeters).

This controlled circular pooled sampling protocol was first employed on a Mixedgrass Prairie site located in the Dempsey Divide region of western Oklahoma (Figure 10). Engineering flags were used to mark the individual sample locations   in the

sampling template. After core sampling in the center of the circle, a soil profile block

was removed from the central sampling location and returned to the laboratory for study.

The back dirt from the shovel hole made to enable collection of the soil block clearly

shows the presence of carbonate (Figure 11).

The Dempsey Divide region is actually interfingered grasslands, with Shortgrass

Prairie on the uplands, and Mixedgrass Prairie on the side slopes (Figure 12). Sampling

of the adjacent Dempsey Shortgrass Prairie by this same sampling protocol was initiated,

but not completed (Figure 13). The severe drought and extremely hard dry soil resulted

in both available soil probes being rendered unusable (twisted into S-shapes) after the

first 10 cm of sample depth, so sampling this Shortgrass Prairie location was abandoned.

Figure 9. Soil sampling probe with depth stop set for 5 cm sampling depth. Photograph
taken at Dempsey Divide Mixedgrass Prairie.

Figure 10. Dempsey Divide Mixedgrass Prairie sampling location (circle #1) and intended Dempsey Divide Shortgrass Prairie sampling location (circle #2) on the Thurmond Ranch along Brokenleg Creek.. Soil types on this USDA/NRCS aerial photograph with mapped soil designations are QwE (Quinlan-Woodward Complex, 5-12% slopes), SaB (St. Paul Silt Loam, 1-3% slopes), WoD Woodward Loam (5-8% slopes), and Rb (Quinlan-Rock Outcrop Complex, 12-45% slopes). (Aerial photo from USDA/NRCS Soils Web Site).

Figure 11. Dempsey Divide Mixedgrass Prairie site sampling template location "o". The dense vegetation is predominantly little bluestem (with some western ragweed and side-oats grama visible); soil carbonates are clearly visible in the back dirt.

Figure 12. Upland Shortgrass Prairie interfingered with Mixedgrass Prairie on the adjacent side slope at Dempsey Divide, Roger Mills County, Oklahoma.

Figure 13. Shortgrass Prairie upland sampling location at Dempsey Divide. The flags mark soil sampling locations.

The same twenty-meter circular sampling protocol was successfully used on a virgin Tallgrass Prairie site northeast of Cushing Oklahoma, referred to as Manning Tallgrass Prairie or Manning Prairie (Figures 14 and 15). Two Manning Prairie locations were selected on which to perform three different soil phytolith investigations:

1. Determine the total phytolith concentration relative to soil depth in five centimeter increments to a depth of 45 cm (n=1, n=1 [x=3], and n=1 [x=20]).

2. Evaluate the composite soil samples (n=x [x=20]) for phytolith morphologic type distribution relative to soil depth.

3. Conduct a singleton study of 21 separate replicate samples to evaluate sampling reproducibility and homogeneity of soil components and phytoliths in the top 5 centimeters of soil (n=21).

The two locations experimentally sampled at Manning Prairie are identified as white circles in Figure 14. Investigation numbers 1 and 2 (above) were conducted at location 1 and investigation number 3 was conducted at location 2 (Figure 15). Composite sampling in 5 cm depth intervals was conducted at 20 locations in one 20 meter diameter circle in investigations 1 and 2, and at 21 locations in investigation 3 (20 sampling points plus central origin). The numbered sampling locations on the 20 meter diameter sample template (Figure 8) are used to denote specific sample numbers in the following description, data sets, and ensuing discussion. The USDA/NRCS aerial photo also includes information about soil types present at Manning Prairie (Figure 14). Nearly

Figure 14. Manning Tallgrass Prairie site showing the two sample template locations in this study locatead in Coyle Loam. USDA soil series reported in this marked aerial photograph are: CoyB (Coyle Loam, 1-3% slopes), 12 (Agra Silt Loam, 1-3% slopes), 13 (Agra Silt Loam, 3-5% slopes), FSLE (Foraker-Shidler-Lucien Complex, 1-12% slopes, "very rocky"), MulC (Mulhall Loam, 3-5% slopes), and StDD (Stephenville-Darnell Complex, 3-8% slopes, "rocky"). (Aerial photograph with soil designations obtained from NRCS/USDA web site http://websoilsurvey.nrcs.usda.gov/app/HomePage.htm).

Figure 15. One Manning Tallgrass Prairie sample template location. The two five gallon buckets are stacked in the center of the 20 meter circle; some sample location flags are visible (view to the northeast).

all samples were successfully completed to full 45-centimeter depth (the target of x=20 in

investigations 1 and 2 was reduced for the 5 cm sample increments below 20 cm (see

Table 10) due to rock encountered in the lower part of the profile in some sample

locations.).

Methodology – Collecting Soil Samples (Buried Soils)

At the Bull Creek site, the entire profile was sampled in fixed ten-centimeter

increments (Bement et al. 2007), and then selected soil samples were analyzed for their

phytolith signature. At the Carnegie Canyon and Lizard Sites, the profiles were sampled

by individual soil units (Carter et al. 2009). When these soil horizons were too thick, the

individual units were subdivided into smaller sections. Phytolith content (weight percent

of soil, and morphologic type distribution) were obtained for the entire vertical sequence

of soil samples at these later two sites. The buried soils investigated and discussed in this

dissertation are on the Great Plains of North America and primarily date to Holocene

Epoch (i.e., the past ~11,000 years); the research sites are located in Oklahoma (Figure

6).

Methodology – Laboratory Soil Sample Processing and Phytolith Analysis[15]

During the course of this investigation, a number of sample preparative

techniques were employed in an effort to identify the most effective and reproducible

procedure for quantitative recovery of phytoliths from soil. The final optimized method

used to process the Manning Tallgrass and Dempsey Divide Mixedgrass Prairie reference

soil samples (and part of the Lizard Site soil sample sequence) is described on the

following pages. Additional comments and observations regarding some of the other

laboratory methods employed are presented and discussed in Appendix D. The reagents,

supplies, and equipment used in this project are listed in Appendix E.

<u>*Soil Processing and Quantitative Silt Fraction Isolation*</u> - The soil samples are

first passed through a 10 mesh (2 mm) sieve to remove large particles (both mineral and

organic matter) and thoroughly mixed to homogenize the samples. Next, the portion of

each soil sample to be analyzed is oven-dried at 105°C in pre-weighed glass sample

containers, cooled in a desiccator, and reweighed to determine initial parent soil sample

---

[15] In addition to the phytolith extraction and recovery, samples were also prepared for carbon isotope (Delta 13) analysis (see a description of the prep method developed in Appendix F).

weights that are processed. Diagnostic phytoliths from most soils, including prairie environments, occur predominantly in the silt fraction of the soil (2-50 microns ["μ"] particle size). Thus, the first series of steps in recovering soil phytoliths is to isolate the silt fraction of the soil.

The USDA (Schoeneberger et al. 2002:2-35) defines fine silt as 2-20 microns, and coarse silt as 20-50 microns. Piperno (1985b:263; 1988:121; 2006:91) reported the fine fraction as 5-20 microns and coarse fraction as 20-50 microns, whereas in a phytolith method summary, Pearsall (1989:365, 2000:430) corrected the fine silt fraction definition to 2-20 microns with coarse silt remaining 20-50 microns.

Based on past confusion in the literature, this researcher recommends that the Canadian Society of Soil Science silt size designations—which splits the smaller particle size silt fraction in question into fine (2-5 microns) and medium (5-20 microns) (Sheldrick and Wang 1993:500)—be adopted by the phytolith research community in order to help minimize terminology confusion in future literature. This size difference is significant as there are very small phytoliths (c.f. Table 7, page 135), and there is a drastic difference in settling time between 2 and 5 micron particles [for instance for 2.30 g/cm^3 particle to settle 10 cm at 20ºC, the calculated times are 588.9 minutes for a 2 micron particle and 94.3 minutes for a 5 micron particle]. Under this current proposal, the coarse silt fraction definition remains unchanged (20-50 microns). These three proposed silt size definitions are used throughout the remainder of this dissertation.

The particle settling times used were calculated based on Stokes Law (Scott 2000:46-49). Representative calculated settling times in minutes for various sized idealized spherical particles of four different particle densities at three representative temperatures are listed in Table 4.

As can be seen from these sample times, temperature makes a difference in settling time, but by far the biggest variable is particle size followed by another large discrepancy based on particle density. Tabular particles of a given dimension will actually settle more slowly than the calculated times for spherical particles, so conservative settling times were used in this project to separate silt and clay (i.e., clay is < 2 microns) and for the sand removal (sand is > 50 microns). When performing particle separations via timed sedimentation, the settling times presented in Table 4 should be considered. If one performs the timed separation at 20ºC for 2 micron particles for 588.93 minutes, any lower density biogenic silica particles present (of the same dimension) will be decanted and lost with the clay fraction. Regardless of the settling time selected, reproducibility is a key ingredient to having internally consistent results. The shorter settling time gives a cleaner fraction, but it also potentially provides income-plete fraction recovery as it is missing any lower density biogenic silica component that is present in the original sample. (When working with pollen, measuring the terminal settling velocity for one's particle and then using the observed settling time as the settling time for the same non-spherical particles in future sedimentations is recommended (Brush and Brush 1994:36-38). With the large diversity of shapes and densities in a phytolith assemblage, this would not seem to be a viable option for phytoliths.)

Table 3. Fine Earth Fraction Definitions of Various Particle Size Classification Systems[16]

Particle Class	Size Designation	USDA	CSSC	ISSS	AASHTO	FAA	USCS	ASTM (UNIFIED)
Sand (mm)		0.05-2.0	0.05-2.0	0.02-2.0	0.074-2.0	0.05-2.0	0.075-5.0	0.074-2.0
	Very Coarse	1.0-2.0	1.00-2.0					
	Coarse	0.50-1.0	0.50-1.0	0.20-2.0	0.25-2.0	0.20-2.0	2.0-5.0	0.25-2.0
	Medium	0.25-0.50	0.25-0.50				0.42-2.0	
	Fine	0.10-0.25	0.10-0.25	0.02-0.20	0.074-0.25	0.05-0.20	0.075-0.42	0.074-0.25
	Very Fine	0.05-0.10	0.05-0.10					
Silt (μ)		2-50	2-50	2-20	5-74	5-50	5-75	
	Coarse	20-50	20-50					
	Medium		5-20					
	Fine	2-20	2-5					
Clay (μ)		<2.0	<2.0	<2.0	<5.0	<5.0	<5.0	
	Coarse		0.2-2					
	Fine		<0.2					
	Colloids				<1.0			
Silt or clay (μ)								<0.074

---

[16] Various agencies with established soil particle size definitions: USDA (U.S. Department of Agriculture), CSSS (Canada Soil Survey Committee), ISSS (International Society of Soil Science), AASHTO (American Association of State Highway and Transportation Officials), FAA (Federal Aviation Agency System), USC/USCS (Unified Soil Classification System), and ASTM/UNIFIED (American Society of Testing Materials/Unifed Soil Classification System). In addition to these soil systems, geologists use the Phi and modified Wentworth scales.

Each soil sample is suspended in water containing a detergent solution (5%

Calgon® or hexametaphosphate solution) and shaken vigorously for 24 hours to

deflocculate the clays so the soil particles are disaggregated. In the initial sample

series[17], the samples were passed through a 270 mesh (53 micron) sieve which retained

the sand fraction by washing the silt and clay through the sieve leaving the silt and clay

components together for further processing. The following step is ordinarily to remove

the smaller clay particles (< 2 microns) from the silt fraction (2-50 microns). This is

performed by taking the clay/silt mixture that passed through the sieve, suspending it in

water, allowing the larger silt particles to settle out for a predetermined time, and then

decanting or pipetting off the suspended clay particles. Repetitive decant steps are

required for an effective clay removal step leaving a clean silt fraction.

The final separation method developed during this project involved first

repetitively decanting the clay fraction from the soil based on the maximum settling time

(1.50 g/cm^3). This timed decant is repeated 20-30 times for each sample—each time

pouring off about 80% of the liquid phase including the suspended clay particles—until

the decant from above the settled silt/sand fraction is clear. The decanted clays are

retained until the entire phytolith isolation and analysis procedure is completed. Once the

repeated clay decants were clear, the silt fraction was repetitively decanted into fresh

containers leaving the sand behind in the quart jars (Figure 16 shows the initial clay

decanting step).

---

[17] The initial samples were processed via the routine method described in the literature (see Appendix C).

The density of phytoliths (maximum of 2.30 g/cm^3) is less than the density of sand (2.65 g/cm^3). Thus, if one decants the clay and silt fractions away from the sand, any larger sand-sized phytoliths in the sand fraction (such as cucurbits, bulliforms, elongates, and phytolith aggregates) and also sponge spicules are generally retained with the decanted fractions (in the previous method, these larger particles would potentially be removed by the standard established procedure of sieving out the sand fraction and thus separated from the finer silt and clay factions). This novel approach was developed to expedite removal of the clay fraction and to retain the maximum amount of phytolith residue possible with the silt fraction—including large biogenic silica particles. Some very small clay-size phytolith fragments were not retained; however, the soils in each sample series were all processed identically within the series enabling comparison of the

Figure 16. Soil sample series during the clay fraction decanting step. At a calculated time interval after mixing, the suspended soil fractions were transferred to and pooled in the individual labeled 2-liter bottles visible in the back row. The buried soil of interest in this particular sample series begins with the darker solutions 2/3s of the way down the row of sequential samples. In this illustration, the clay is being decanted from the sand and silt fractions; in subsequent sample series both the clay and silt were simultaneously decanted from the sand; later the clay fraction was decanted away from the silt fraction with a settling time calculated on 1.50 g/cm^3 density.

recovered phytolith content of the samples. An added benefit of processing in this

manner is that the sand fraction separated in this manner does not ordinarily need to be

examined for larger phytoliths or other particles of interest. The sand fraction isolate by

all permutations were oven dried, weighed, and then transferred to vials for storage.

The sequential decants containing the silt fraction (including the phytoliths) for

each sample are collected and pooled for further processing.   Each sample's silt fraction

(2-50 microns) was processed as illustrated in Figures 17-32. These pooled decants were

first allowed to sit undisturbed for three days so most of the particulate settled (Figure 17)

(based on the bottle height, this is the time required for 1.50 g/cm^3 particles to settle).

The majority of the settled silt fraction for each sample is present in the first decant bottle

(normally one sample's silt decants filled at least five two-liter bottles, to be filtered

later). The relatively clear liquor from the initial decant liquid receiving bottle was

transferred to another bottle leaving the bulk of the silt fraction behind in the first

bottle (Figures 18-20). The silt remaining in the original decant bottle (Figure 20) is

transferred directly to a 100 ml crucible (Figures 21-22); filtering this portion of the silt

(estimated to be > 95% of the silt in the sample) is not required. The bottle is next rinsed

with pure water to effect quantitative transfer of the bulk of the remaining residue from

the bottle to the crucible (Figure 23). To complete rinsing and transfer, a small amount of

ultra pure water is added to the bottle, the lid put in place, and the bottle is vigorously

shaken to effectively rinse the walls. This rinse is repeated until the rinse water is clear

(Figure 24). The entire settled silt fraction and all of the bottle rinses of the bulk silt can

be achieved in less than 100 milliliters (Figure 25). The last remaining trace

silt residue on the bottle walls in the previous step is easiest to remove and transfer if the

particulate has never been allowed to dry out in the bottle. If required (i.e., if drying has

occurred), ultrasonication can be used as needed to facilitate particulate removal.

This process of pre-settling the sediment in two-liter bottles and in the crucible

enables the remaining relatively clear liquid to be vacuum-filtered for phytolith and silt

Table 4
Calculated Settling Times for
Phytoliths of Different Size and Particle Density[18]

T (°C)	Particle Density (gm/cm^3)	Minutes for Particle to Fall 10 cm			
		2 microns	5 microns	20 microns	50 microns
20	1.60	1272.26	204.00	12.74	2.04
"	2.00	764.53	122.46	7.66	1.22
"	2.30	588.93	94.27	5.89	0.94
"	2.65	464.25	74.27	4.64	0.74
22	1.60	1216.55	194.02	12.13	1.94
"	2.00	727.80	116.55	7.29	1.17
"	2.30	561.17	89.70	5.61	0.90
"	2.65	442.09	70.01	4.42	0.71
25	1.60	1126.13	180.77	11.30	1.81
"	2.00	680.27	1.8.65	6.79	1.09
"	2.30	522.47	83.67	5.23	0.84
"	2.65	412.54	65.93	4.12	0.66

---

[18] Minutes to fall calculated for a 10 cm distance. Times for three representative densities of phytoliths are provided (1.60, 2.00, and 2.30 g/cm^3 (sand density is 2.65 g/cm^3)).

Figure 17. Decanted silt fraction after settling for several days. FDA approved 2-liter bottles are used in lieu of ten to fifteen 1 liter beakers per sample as an effective cost- and space-saving alternative. Most of the particulate matter that was originally suspended in solution has settled. The volume of the liquor is poured off into another bottle (fitted with funnel in photograph) and the majority of the sediment is left behind in the original settling bottle. The retained liquid is later vacuum filtered to recover remaining suspended silt and phytoliths. Sampling of the haze present suspended in the bottle indicated it was predominantly clay-size particles.

Figure 18. Decanting supernate from initial sample silt decant container. A paperclip between the funnel and the receiving bottle mouth prevents bumping as air escapes from the receiving bottle. Although there some solution cloudiness is visible, most of the settled silt remains in the original bottle.

Figure 19. Transfer of decanted solution above silt is nearly complete.

Figure 20. Solution transfer complete; the bottle shape helps to retain the majority of the settled silt fraction. Also, the bottle lip design effectively minimizes sample or liquid drippage.

Figure 21. After decanting the relatively clear upper liquid, the silt on the bottom of the original decant bottle is transferred to a 100 ml porcelain crucible. Other clarified sample solutions are visible in the background, as well as the quart jars containing the sand fraction from which the suspended silt fraction was decanted (center, top).

Figure 22. The settled silt in the bottom of the settling bottle is poured into a 100 ml porcelain crucible. Prior to initiating sample transfer, the crucible is placed in a Pyrex® Petri dish in order to minimize the possibility of loss through spillage or overflow. Glass countertops help minimize sample loss and ease of recovery or clean up.

recovery in about ¼ of the time (6-8 hours vs. 24+ hours for the entire silt fraction). This entire protocol is felt to be advantageous for quantitative phytolith recovery as fine silt-size lower density phytoliths (perhaps as low as 1.5 g/cm³) will take much longer to settle than the same size silt particle with the density of sand (2.65 g/cm³).[19]

---

[19] For instance, at 20°C in water and assuming spherical particles, a 2 μ sand particle will settle 10 cm in 464 minutes, where the following settling rates would occur for various density phytoliths:

2.30 g/cm³ phytoliths settle 10 cm in 589 minutes (9.82 hours),
2.00 g/cm³ phytoliths would settle 10 cm in 764 minutes (12.73 hours, and
1.50 g/cm³ phytoliths settle 10 cm in 1529 minutes (25.48 hours).

The height of the water column in the two liter bottles is 27 cm, so three days settling time before filtration is adequate to allow most of the suspended low density silt particles to settle. Since the remaining decanted liquid is later filtered, no significant quantity of phytoliths is lost. Allowing most of the suspended solids to settle out of the solution prior to filtration results in much faster solution and sample processing.

Figure 23. The final sediment residue on the bottom and on the sides of the settling bottle is rinsed into the same crucible using Milli-Q water.

Next, the suspended silt in the decanted liquid from one sample is vacuum filtered through ashless filter paper in the reverse sequence to the order in which the bottles had been decanted to recover the fine suspended particulate (Figures 26-28). By using the larger pore size filter on top of the finer one, one effectively installs a prefilter in front of their operational filter which retards filter plugging. As soon as any particulate material hits and is retained by the first filter, the effective top filter paper pore size rapidly decreases—thus one is literally using the sample silt particles as a filter bed on the top filter. Consequently, even though the filter manufacturer's guaranteed pore size is larger than one might initially select to filter fine silt-sized phytoliths, the stacked filter papers

Figure 24. The bottle is then rinsed with additional small water aliquots until no sediment remains. The screw cap and constricted bottle neck make vigorous mixing in this manner very effective.

Figure 25. The final clear rinses are added to the crucible. The crucible is allowed to sit one day enabling most of the sediment to settle. The clear liquid in the crucible is then filtered with the rest of the clear silt sample supernate that was retained in the 2-liter bottles (Figures 18-21).

effectively remove nearly all silt size particles—including diagnostic phytoliths—from suspension. That is the reason that the two filter papers specified in the materials list are different diameters (Appendix E); the smaller filter always goes on top (i.e., Whatman ashless filter paper 40 goes on top of Whatman ashless filter paper 41). Using two 41 filters below the 40 enhances the efficiency even further in cases where samples contain more fine size particles. In the rare event some cloudiness occurs in the filtrate, additional number 41 paper can be added to the bottom of the stack and the solution re-filtered if necessary. Examination of the cloudy material with a polarizing microscope can help one determine if any amorphous silica is present in the material that passes through the filter pack. Multiple filter packs are normally required to filter one silt sample (10+ liters of decanted solution). If desired the filtrate can be isolated for each sample and retained to check for filtration efficiency.

Figure 26. Ashless Filter paper is used to filter the "clear" decanted liquid from the silt settling bottles using a Millipore vacuum ultra-filtration unit.

Figure 27. Even though the settled decanted solution appeared to be clear, sediment is visible on the filter in this image. The walls of the filter funnel need to be rinsed before the filters are removed from the holder.

Figure 28. After the 2-liter bottles are empty, they are rinsed to effect 100% transfer of all particulate matter to the funnel. The bottle can be capped and shaken if necessary to obtain an efficient rinse (see Figure 24). Working in a clean catch basin allows sample retention and recovery should a loss or equipment failure occur.

After completion of the filtration step, the filter papers are added to the sample crucible containing the bulk of the settled silt, a lid installed, and the crucible and contents oven-dried overnight at 105°C to remove the water. The samples are then transferred to a muffle furnace to remove organic matter from the isolated silt fraction via ashing.

There are several different ways to remove organic matter; these include removal using an industrial hydrogen peroxide solution, via digestion with nitric acid, via digestion with nitric acid with perchlorate added, and dry or thermal ashing (i.e., via muffle furnace). All four methods were utilized during the course of this project in the order presented. During this research project, it was concluded that thermal ashing was best although all four treatment methods work well with each technique having its specific benefits and drawbacks.

The muffle furnace treatment must be used carefully. Heating via furnace at 550ºC to remove organic matter changes the phytolith refractive index, water content, surface area, and trace element composition (Jones and Milne 1963:217). Phytolith density may increase closer to 2.30 g/cm^3 by muffle furnace ashing up to 550ºC (Jones and Milne 1963:213). Although some amorphous silica was converted to cristobalite at these low temperatures, most of the amorphous silica was converted to cristobalite by ashing at 700ºC and to the tridymite form at 900ºC (Jones and Handreck 1967:125). The temperature selected to use in this current project was 530ºC, and was achieved via a gradual stepped temperature ramp so no temperature overshot would. The samples are

heated for four hours at 110°C, ramped up to 325°C for three to six hours, and then slowly to 530°C for a minimum of six hours.

After ashing and cooling, the ashless filter paper is effectively gone although the silt layered on the paper has retained form of the paper (Figure 29). At this point, 10% hydrochloric acid can be added to the crucible to react with any carbonates that are present (Figure 30). If effervescence is noted (Figure 31), additional hydrochloric acid can be added to the sample until no reaction is observed. The silt and acid are gradually quantitatively transferred to pre-weighed 50 milliliter test tubes (Figure 32). If more acid needs to be used than the tube will hold, the partially filled test tube can be centrifuged, the clear liquid removed via pipette before sample additions continue, and more acid can be added to the sample and the transfer repeated until no further reaction is observed.

Figure 29. The sample crucible containing the silt fraction after ashing in the muffle furnace to remove the organic material. The thin layers of silt that coated the filter papers are visible on the top of the bulk transferred sediment deposit.

Figure 30. Hydrochloric acid is added to the ashed silt sample to react with any carbonates that are present.

Figure 31. Effervescence is visible in this image from reaction of carbonates with the hydrochloric acid. After acid addition, the crucible is covered, and the neutralization reaction allowed to continue; the crucible resides in a glass Petri dish during this reaction.

Figure 32. After the initial aliquot of hydrochloric acid has been neutralized, the silt and acid solution is transferred to a 50 ml centrifuge tube. Additional acid is used to rinse the crucible to effect 100% transfer of the sediment to the tube. The acidified ashed silt fraction is then centrifuged and the clear liquid removed via Pasteur pipette. Additional acid is added to the tube, and the mixture stirred on the Vortex Genie®. Repeated acid addition, mixing, centrifuging, and removal of clear liquid continues until the sample carbonates have completely reacted. The silt pellet is then rinsed 5-7 times with pure water, centrifuging between rinses, and finally dried in a 40°C oven. At this point the silt fraction has been isolated, the carbonates removed, and the dry soil silt fraction is ready for phytolith flotation and recovery.

90

Generally, the crucible walls need to be scraped with a spatula so the remainder of the moist sample residue can be dislodged and transferred to the centrifuge tube. If the reaction is ongoing after completion of transfer to the tube, more acid can be added to the centrifuge tube after each clear liquid removal.

Once the reaction is completed, the silt in the centrifuge tube should be rinsed five or more times with ASTM Type A water which effectively dilutes the acid; pH strips can be used to test solution pH if needed. The centrifuge tube containing the recovered neutralized silt is then dried in a 40°C oven; once dry, the tube is reweighed to determine the amount of silt recovered from the original sample. Knowing the silt and sand weights, one knows the soil sample texture. The quantitative phytolith content of the sample can be calculated as weight percent soil or weight percent silt.

Quantitative Phytolith Recovery Procedure - This quantitative recovery method involves exhaustive extractions in an effort to recover all phytoliths present in the isolated silt fraction (nominally, larger than 2 microns). Recovery improves with each repetition of the phytolith flotation and subsequent cleanup step. The first step is that the phytoliths need to be released from the silt fraction if the silt fraction has been thermally processed (either by organic removal in the muffle furnace, or oven drying to remove the water in order to obtain the recovered silt weight). Simple passage of time (i.e., weeks) sitting in the zinc bromide solution will gradually loosen up the matrix and release the phytoliths. This procedure can be accelerated somewhat by occasional agitation using a Vortex Genie, or placing the tube in an ultrasonic bath for a few minutes; either of these

procedures enhances wetting, particle separation, and phytolith release. The actual time required depends on the tightness of the specific sample matrix. If one does not disaggregate the silt fraction, no phytoliths will be recovered. The time required is definitely longer than if no thermal treatment was used and the silt was never dried out since the original 24 hour sample disaggregation in Calgon® solution. The original treatment was primarily aimed at the clay component contributing to the parent soil sample structure; in this current step, concern has shifted to the dried silt fraction, usually compacted by centrifugation before drying.

Zinc bromide solution (density of 2.35 g/cm³) is added to the dried silt fractions in 50 ml centrifuge tubes. Once released from the silt matrix, the phytoliths (density ≤ 2.3 g/cm³) float on this dense aqueous solution whereas quartz-based minerals that comprise most of the remaining soil matrix (density of ~2.65 g/cm³) sink—thereby separating the trace phytolith component from the bulk of the denser sand-based silt matrix. Once the phytoliths are released, the silt fraction/zinc bromide solution mixtures are centrifuged and the upper liquid phases decanted into clean labeled centrifuge tubes; this procedure is repeated a minimum of four more times—adding fresh zinc bromide, mixing, centrifuging, and pooling the sequential decants of light fraction for each sample. It is best to float the silt residue two times after the final phytoliths were visually observed during the previous transfer to make certain that the remaining trace amount is recovered. The separated phytolith solutions are then capped, remixed on the Vortex Genie®, and centrifuged to release any heavier minerals that may have carried over in the original light particle fraction decants. If any heavy mineral contamination is observed, the upper

phytolith solution is decanted to a clean tube, rinsed as needed, and the separation and fraction cleanliness confirmation process repeated until a pure isolate is obtained.

Once phytolith fraction purity is verified, water is added to the tubes containing the pure phytoliths in zinc bromide in order to lower the liquid density below 1.50 g/cm^3. These tubes containing the diluted zinc bromide/phytolith mixture are centrifuged which results in the purified phytoliths forming a pellet at the bottom of each tube. The phytolith pellets are next rinsed with pure water, mixed, and centrifuged seven times to remove zinc bromide residue from the phytoliths. The clean phytoliths are transferred to pre-weighed labeled vials, oven-dried, desiccator-cooled, and weighed to determine the quantity of phytoliths (also including other forms of biogenic silica) recovered. Any time sample vials or tubes are weighed for determination of quantitative analyte recovery, a similarly labeled blank vial or tube also needs to be simultaneously carried through the identical analytical procedure. Then the resulting sample weights can be blank corrected. When multiple samples are being processed, it is always a good idea to label the lids as well as the containers. This quantitative phytolith extraction and recovery enables determination of the phytolith concentration as weight percent phytoliths in the parent soil sample and in the silt fraction. An effort was made to identically process all of the samples in a given sample series, using the same processing time, and with the same solutions and other parameters, so the data within a given set of samples would be comparable.

Following sample processing, the diluted zinc bromide solutions collected during sample processing are filtered, and the water removed by evaporation in order to recover and recycle the zinc bromide. Once the phytolith analysis is complete, the silt samples are also water extracted to recover the zinc bromide for reuse. The filtered concentrated reagent density can be checked, the density adjusted as necessary, and then stored for later use. Recycled zinc bromide solution is kept separate from fresh (virgin or first use) zinc bromide as soluble species from the soil are present in the recovered solvent. New zinc bromide solutions are reserved for instances when phytolith samples need to be isolated for radiometric dating in order to help minimize the possibility of sample contamination.

Preparing Microscope Slides for Scans and Particle Counting – Each dry phytolith isolate is gently mixed (Figure 33), and a ~1-2 milligram sample of phytoliths is transferred to a clean microscope slide (Figures 34-36). For this current study, the recommendation to use Canada Balsam (Deborah Pearsall, personal communication) was followed which allows particle rolling and thus enables three dimensional particle examination to confirm particle morphology (see Figure 41). The initial slide mounts in this current project were made using Norland Optical adhesive; this was discontinued once the need for and value of particle rolling was realized.

Separate clean spatulas are used for each step; extreme caution must be used to never contaminate the Canada Balsam reagent. For this reason, a small amount of Canada Balsam is transferred [poured into] to a one-half ounce glass bottle to use for

phytolith sample mounting. A drop of Canada Balsam is placed on top of the phytoliths (Figure 36), and the mixture is then gently stirred (Figure 37). Next, a cover slip is placed on the sample on the slide. The completed slides are placed on the hot plate used to warm the Canada Balsam for 1-2 minutes to help spread and level the Canada Balsam. After the mounting media spreads and levels (Figure 38), the slide is stored in a Boekel incubator (35°C) for 1-2 weeks to accelerate curing until the balsam seals along the edge

Figure 33. Dry phytolith fraction being gently mixed prior to sampling.

Figure 34. A small phytolith sample being transferred with stainless steel micro-spatula.

Figure 35. Phytoliths after being placed on the microscope slide.

Figure 36. A drop of Canada Balsam being placed on top of the phytoliths on the slide.

Figure 37. Canada Balsam and phytoliths being mixed prior to installing the cover slip to seal the slide.
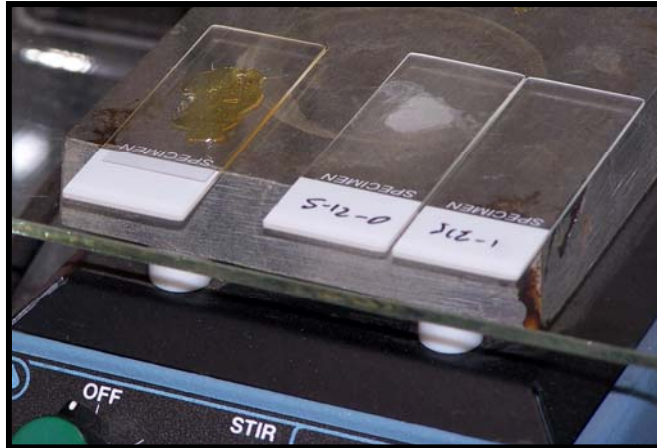
Figure 38. Slide (left) mounted with Canada Balsam on low temperature hot plate for several minutes to help level and spread the Canada Balsam and sample mixture under the coverslip. The other two slides were part of an evaluation to look at particle size of materials passing through the filter pack during vacuum filtration (the particles observed were micron size or smaller). The sheet of tempered glass on the hot plate helps to minimize temperature fluctuations and eliminate hot spots.

of the cover slip. Cover slip size is determined by the amount of Canada Balsam placed on the slide; a variety of sizes ranging from 18 x 18 mm through 24 x 60 mm is kept on hand and used as appropriate.

After curing, the slides are microscopically scanned while observing for phytoliths at 500x. While scanning, a count is taken of the standard phytolith morphologic forms observed during the scan (example tabulation sheet shown in Figure 39; debris, fragments, and odd forms are not normally tabulated). Photographs of representative phytoliths are taken during the sample scans via a digital camera on the PLM (Figure 40). After the formal particle count is complete, the entire slide is examined for any other significant particle forms present that may not have been observed during the particle count; any additional observed particles of interest are photographed.

JSE Phytolith Count Form

Lab Sample ID PC- ___ Site _Manning Prairie, n=___ Spl Depth ___ cm Date Prepped/Mounted _~1/09_ ___ Sample Origin ___

Mounting Media _Canada Balsam_ ___ Vernier Y-Axis location where count started (left slide edge) ___ mm Page ___ of ___

Field # | Total | 1 | 2 | 3 | 4 | 5 | 6 | 7 | 8 | 9 | 10 | 11 | 12 | 13 | 14 | 15 | 16 | 17 | 18 | 19 | 20 | 21 | 22 | 23 | 24 | 25

Row labels (top to bottom):
- Keeled
- Conical
- Pyramidal
- Crenate
- Saddle, squat
- Saddle, tall
- Stipa
- Lobate, Simple
- Lobate, Panicoid
- Lobate, Pan'd(cmpd)
- Cross, Panicoid (<10 um)
- Cross, Panicoid (>10 um)
- Maize Rondel
- Rondel (bipoint)
- Rondel, other
- Dicot, knobby
- Spiny spheroid
- Schlerid
- Sponge spicule
- Trichome, Hair Cells
- Bulliform, square
- Bulliform, rectangular
- Bulliform, keystone
- Bulliform, Y-shaped
- Bulliform, other
- Elongate, smooth
- Elongate, sinuous
- Elongate, castillate
- Elongate, spiny
- Sedge
- Charcoal
- Diatom (Pinnularia Borealis E.)
- Diatom, other

Analyst ___ Date ___ Comments ___

Figure 39. Sample count form for recording phytolith particle count frequency for Manning Tallgrass Prairie samples (original size 8.5 x 11 inches).

Figure 40. Microscopy work station showing the petrographic microscope (right) used to count phytoliths in sample slides; camera system includes a monitor that shows the center of the field of view.

Use of Canada Balsam as the mounting media enables particle rolling so that a three dimensional examination of the sample phytoliths can be performed during microscopy (Pearsall, personal communication). An example of a short cell phytolith before and after rolling is shown in Figure 41.
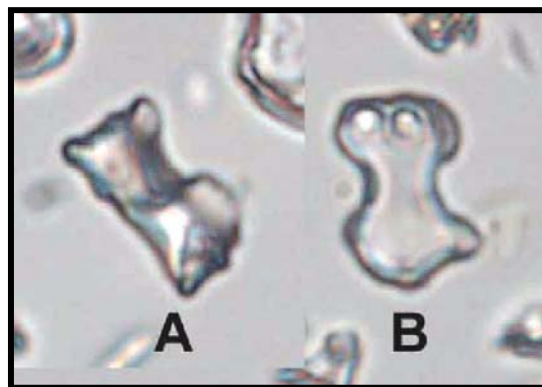
Figure 41. Example of the benefit of particle rolling. Phytolith as originally observed on the slide (A) and after particle rolling (B). (Phytolith is 12 microns long).

CHAPTER IV

RESULTS AND DISCUSSION

Reference Botanical Specimen Phytoliths

The initial step in any phytolith analysis is to obtain reference phytolith specimens

from representative botanical species in the study area. The basic grass phytolith

morphologic short cell forms were defined by Twiss et al. (1969) and later illustrated by

Fredlund and Tieszen (1994). The individual grass species selected from which to

prepare spodograms are listed in Table 5; phytolith reference data are used to evaluate

modern soil phytoliths from the three modern control prairie sites and also from the

buried soils. The grass species selected are from three of the twelve subfamilies of the

Poaceae: Pooideae, Panicoideae, and Chloridoideae. Additionally, due to peculiarities in

the soil phytoliths encountered at one of the research sites (see the discussion at the end

of the Manning Tallgrass Prairie results and discussion section) two members of the

subfamily Arundinoideae were added to the original botanical reference specimen

inventory.

Identified botanical specimens collected in the field at the research sites, and from

the OSU/Ag Herbarium, were used to prepare reference phytolith specimens. These

fourteen samples (predominantly leaves) were water rinsed to dislodge any contaminants

that were present, dried, cut into small sections, placed in a covered crucible, and ashed

in the muffle furnace in the same manner as the silt fractions described previously. After

ashing, the samples were treated with 10% hydrochloric acid, repeatedly water-rinsed to

neutralize the pH, centrifuged, transferred to labeled 4-dram glass storage vials, and

dried.   Representative portions were mounted on microscope slides in Canada Balsam in

the same manner as the field phytolith samples as shown in the previous illustrations.

The soil sample phytolith types observed, tabulated, and analyzed during this

research project are based on the established literature morphologic phytolith types

(Twiss et al. 1969) as illustrated by these actual reference botanical specimen phytoliths

(Figures 42-56). Representative images these isolated reference Poaceae leaf phytoliths

are shown in the following fifteen plates; the range of short cell forms observed in these

reference preparations is illustrated in these figures. When possible, *in situ* phytoliths

(i.e., articulated silica cell skeletons taken from the epidermal layer of botanical specimen

leaves) are shown. These images illustrate the extensive variation and diverse

appearance of various short cell phytolith forms in one small section of one leaf. A

familiarity of the morphologic variation within any single short cell category is very

helpful when actually classifying and counting specimens during scans of soil phytoliths

on microscope slides.

The crenate short cell form is observed in Prairie Junegrass (Figure 42). For the

most part, these crenate phytoliths are generally rectangular with gently rounded corners

Table 5

Prairie Poaceae Species Used to Generate Known Origin Phytolith Specimens

Poaceae Subfamily / Metabolic Type	Genus species	Common Name[20]
Pooideae / C3	*Koeleria macrantha* (Ledeb.) Schult.	Prairie Junegrass
Pooideae / C3	*Elymus smithii* (Rydb.) Gould	Western Wheatgrass
Pooideae / C3	*Elymus canadensis* L.	Canada Wildrye
Pooideae / C3	*Hordeum jubatum* L.	Foxtail Barley
Pooideae / C3	*Phalaris arundinacea* L.	Reed Canarygrass
Pooideae / C3	*Poa pratensis* L.	Kentucky Bluegrass[21]
Pooideae / C3	*Hesperostipa comata* (Trin. & Rupr) Barkworth	Needle-and-Thread Grass
Pooideae / C3	*Oryzopsis hymenoides* (Roem. & Schult.) Ricker[22]	Indian Ricegrass
Arundinoideae / C4	*Aristida longiseta*	Red Threeawn
Arundinoideae / C4	*Aristida purpurea* Nutt.	Purple Threeawn
Panicoideae / C4	*Andropogon gerardii* Vitman	Big Bluestem
Panicoideae / C4	*Schizachyrium scoparium* (Michx.) Nash	Little Bluestem
Panicoideae / C4	*Sorghastrum nutans* (L.) Nash	Indiangrass
Chloridoideae / C4	*Buchloe dactyloides* (Nutt.) Engelm.	Buffalograss

and weakly developed crenate edge profiles. In contrast, the crenate phytoliths in

Western Wheatgrass have considerable more edge contour detail, and vary substantially

from the general rectangular form noted previously (Figures 43 B-D, F, and G). Western

Wheatgrass also contains keeled short cell phytoliths (Figures 43 A and G). Canada

Wildrye was observed to have two primary short cell phytolith forms: a less developed

---

[20] Common names based on Tyrl et al. (2002). Species not listed in Tyrl's book were researched on the USDA Plants web site (http://plants.usda.gov/).

[21] Kentucky Bluegrass, the only non-native species listed in Table 5, was processed in order to obtain good examples of pyramidal phytoliths which were not readily apparent in the other C3 species examined.

[22] The USDA name is *Achnatherum hymenoides* (Roem. & Schult.) Barkworth (http://plants.usda.gov/java/nameSearch?keywordquery=indian+ricegrass&mode=comname&submit.x=18 &submit.y=7 (6-26-09)).

rectangular crenate phytolith with more closely spaced edge contours (Figure 44B) and a round disc-shaped form referred to as a disc-shape (Figures 44 A, C, and E). Some phytoliths were also noted that may possibly be an intermediate form between these two cell types (Figure 44D).

Foxtail Barley was noted to have an abundance of fairly weakly developed crenate forms (Figures 45 A, B, D, and E) as well as some smaller rondels and a few keeled phytolith short cells (Figure 45C).

Reed Canarygrass contains an abundance of keeled phytoliths (Figures 46 A-E and H); there are also weakly developed crenate short cell phytoliths (Figures 46 I and K). The crenate phytoliths occur with keeled short cell forms (Figure 46 K) as well as some much shorter crenate forms (Figure 46 I). Generally, adjusting the microscope to focus through crenate phytoliths, a faint purple band is visible along the long axis of the cell (Figures 42 F, 44 B, and 45 B); the presence of this band in some shorter near-round forms (disc or rondel?) (Figure 46 I) suggests that these may be another crenate variant or related form even though there is no edge development. However, not all of these apparent rondels have the purple band (Figures 46 F and 45 C), so the proper identification of these plain disks—which were only observed in Pooideae species in this study, remains uncertain. These rondels may represent a distinct short cell phytolith form, a large conical variant, or perhaps an intermediate morphologic type between conical and crenate forms.
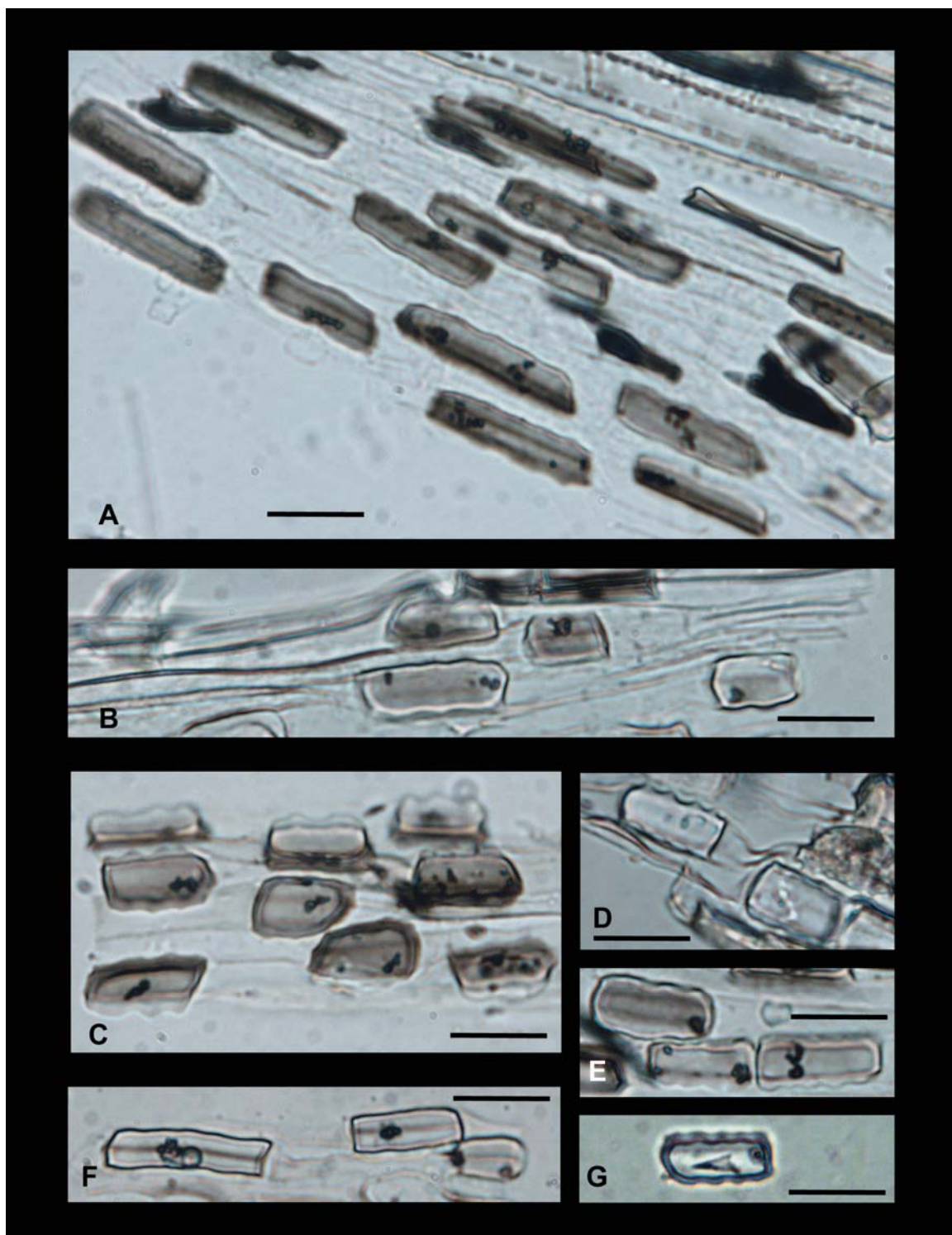
Figure 42. Phytoliths prepared from Prairie Junegrass (*Koeleria macrantha* (Ledeb.) Schult.). The predominant diagnostic phytoliths present are the crenate form. Bar scales are 20 microns.
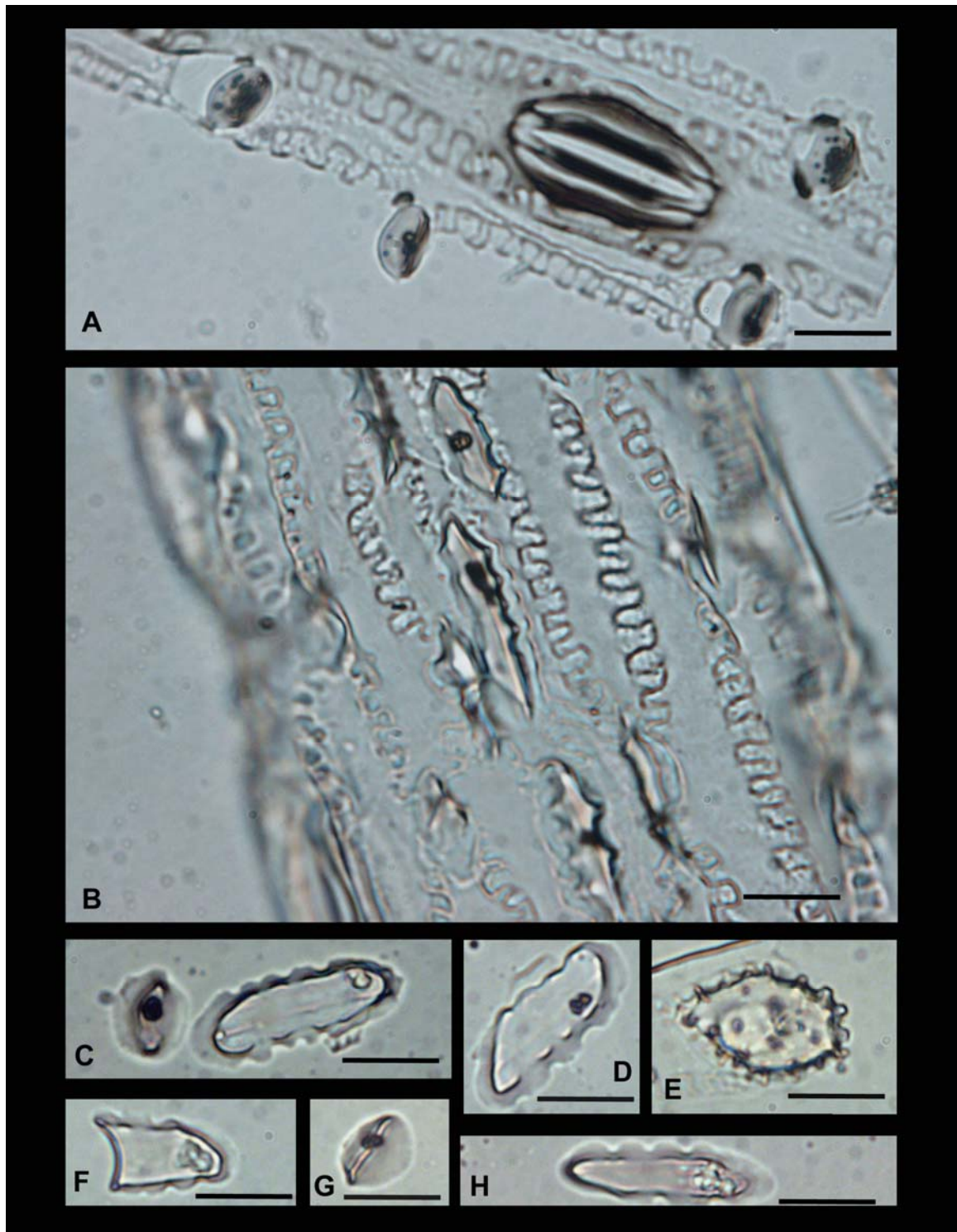
Figure 43. Phytoliths prepared from Western Wheatgrass (*Elymus smithii* (Rydb.) Gould) showing predominantly crenate (B-D, F and H) and keeled (A, C, D) short cell phytoliths. Bar scales are 20 microns.
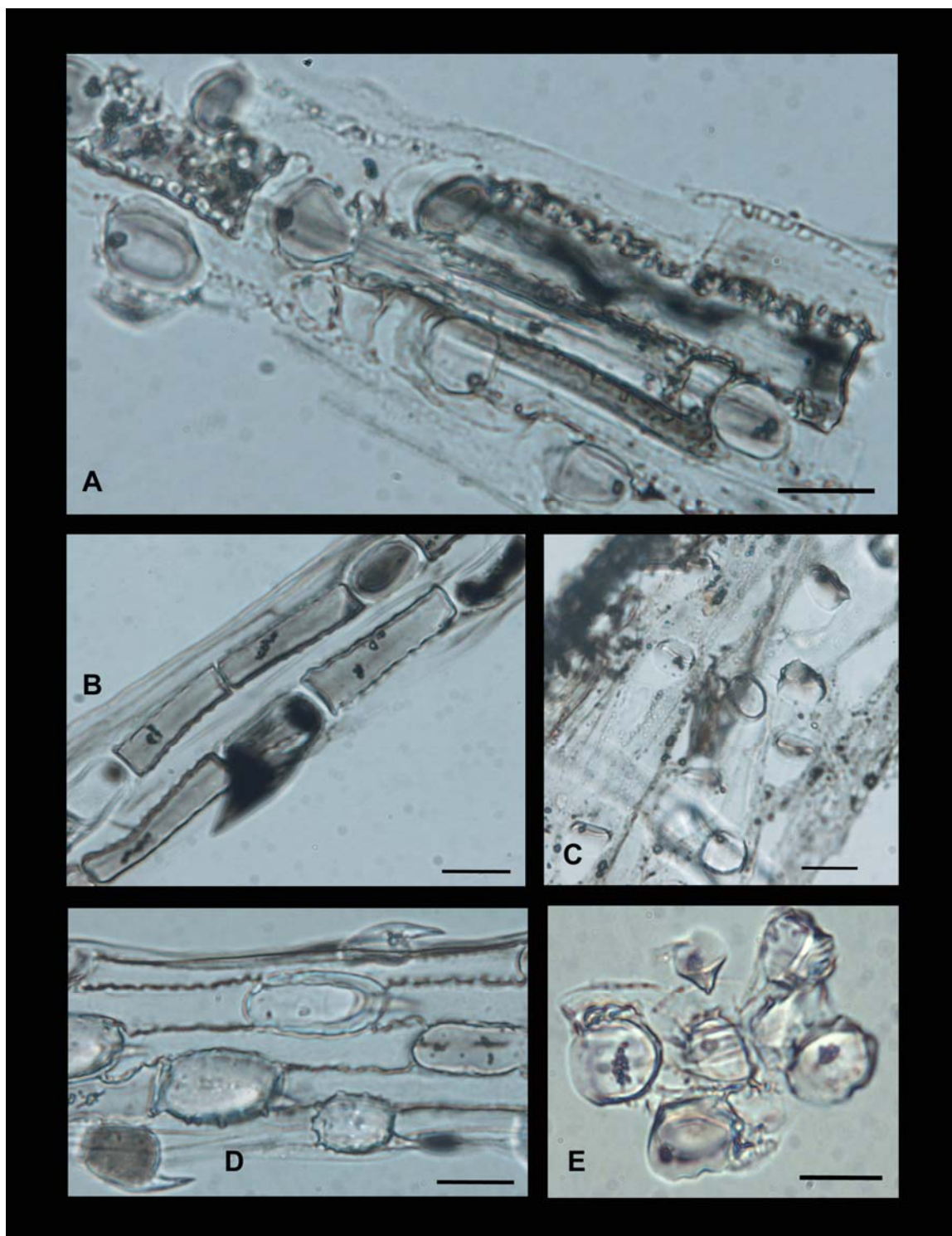
Figure 44. Phytoliths prepared from Canada Wildrye (*Elymus canadensis* L.) showing predominantly crenate (B) and round disc-shaped (A, C, and E) short cell phytoliths. Bar scales are 20 microns.
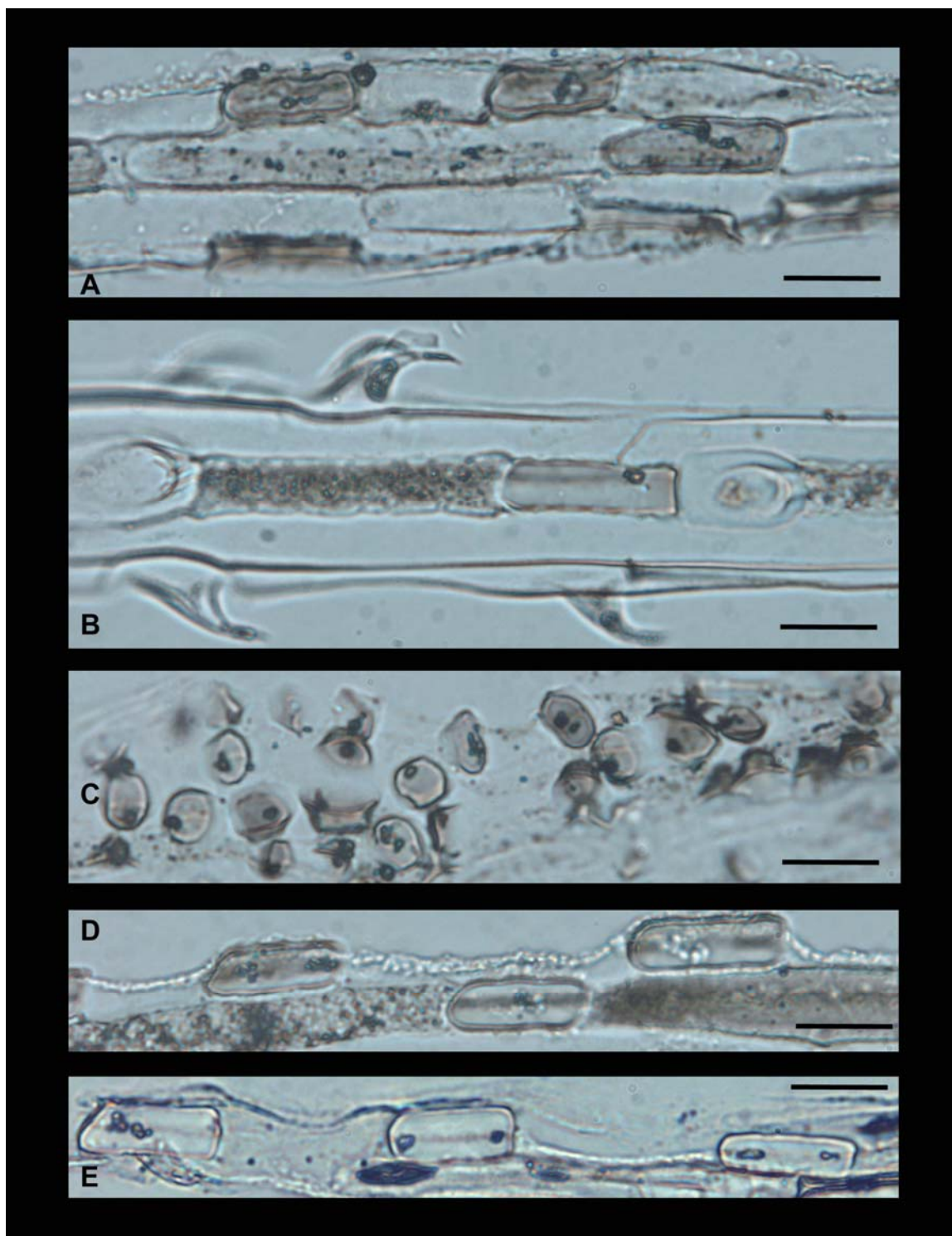
Figure 45. Phytoliths prepared from Foxtail Barley (*Hordeum jubatum* L.) showing predominantly crenate short cell phytoliths (A-B and D-E). Bar scales are 20 microns.

Kentucky Bluegrass, a non-native species, contains well-developed crenate short cell phytoliths with deep edge convolutions (Figures 47 H-I). Keeled phytolith short cells are also present (Figure 47 E) as well as pyramidal phytoliths (Figure 47 D) and mixtures of keeled and pyramidal phytoliths (Figure 47 F). Most interesting is the gradational series of phytoliths in Figure 47 A which shows the range of forms from keeled through pyramidal short cells in one small epidermal area. These various short cell forms in such close proximity suggest that these different distinctive short cell morphologic types established and described in the literature may actually be a family or series of related particle types. In the specimens examined, all of these short cell forms are in the Pooideae subfamily as previously reported by other researchers (c.f. Twiss et al. 1969, Fredlund and Tieszen 1994).

The next two specimens in Table 5, Needle-and-Thread Grass and Indian Ricegrass, are both members of the Stipeae tribe of the Pooideae subfamily. Although stipa short cell phytoliths were expected from the Needle-and-Thread Grass specimen, none were observed in the scanned slides. The Needle-and-Thread Grass specimen did show a number of keeled short cell phytoliths (Figure 48 A) and mixtures of keeled and conical short cell forms (Figure 48 C) as well as weakly formed crenate cells (Figure 48 E). The epidermal section in Figure 48 B includes weak "lined" crenates and rounder unlined specimens or rondels, as well as keeled, conical, and pyramidal short cell forms. A concentration of the rounder forms is in Figure 48 D. The phytoliths in Figure 48 F are another ("true") form of rondel. On the other hand, Indian Ricegrass showed less short cell variety, primarily consisting of the stipa short cell form (Figures 49 B and C) and
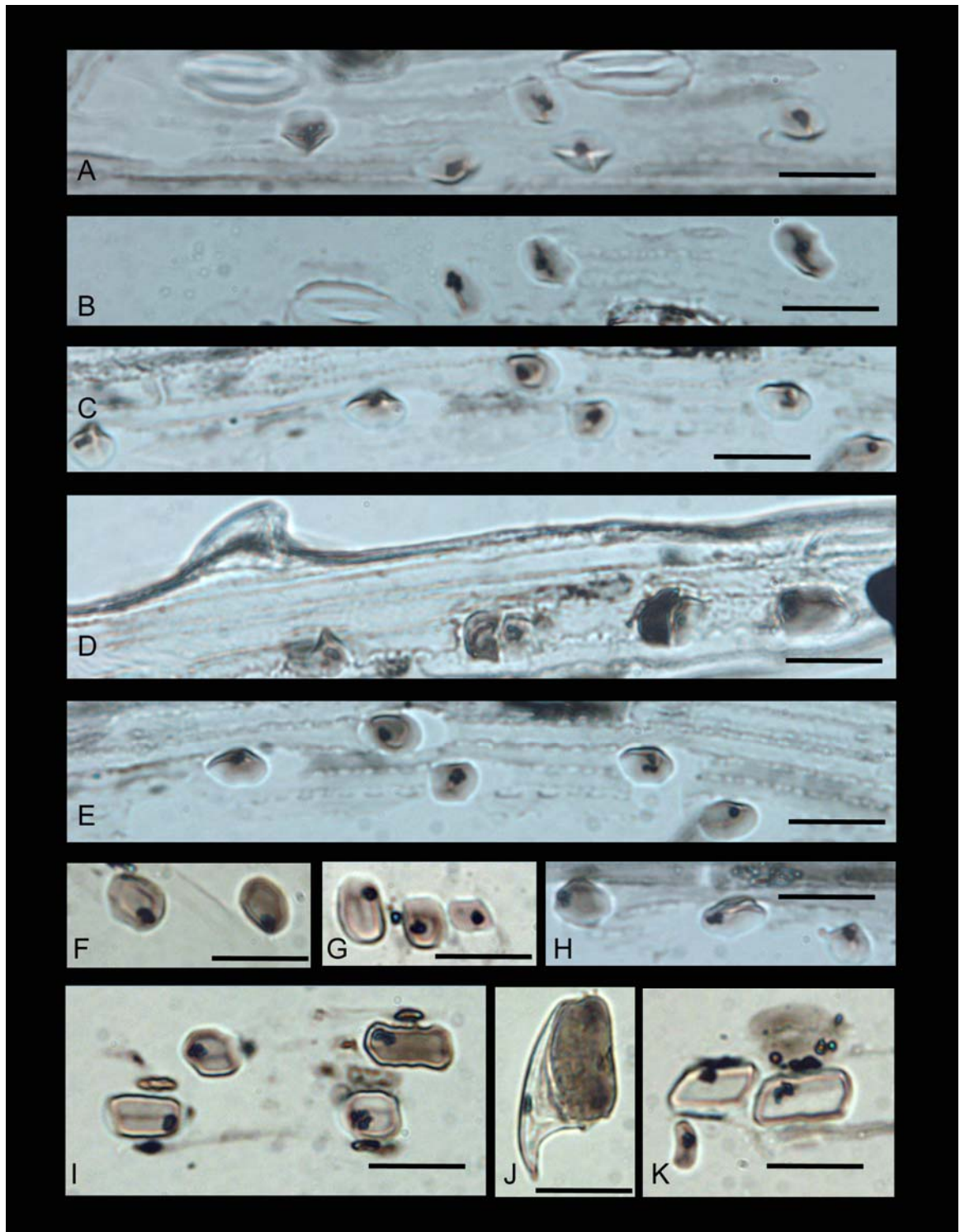
Figure 46. Phytoliths prepared from Reed Canarygrass (*Phalaris arundinacea* L.) showing predominantly keeled (A-E and H) and crenate (I and K) short cell phytoliths. Bar scales are 20 microns.
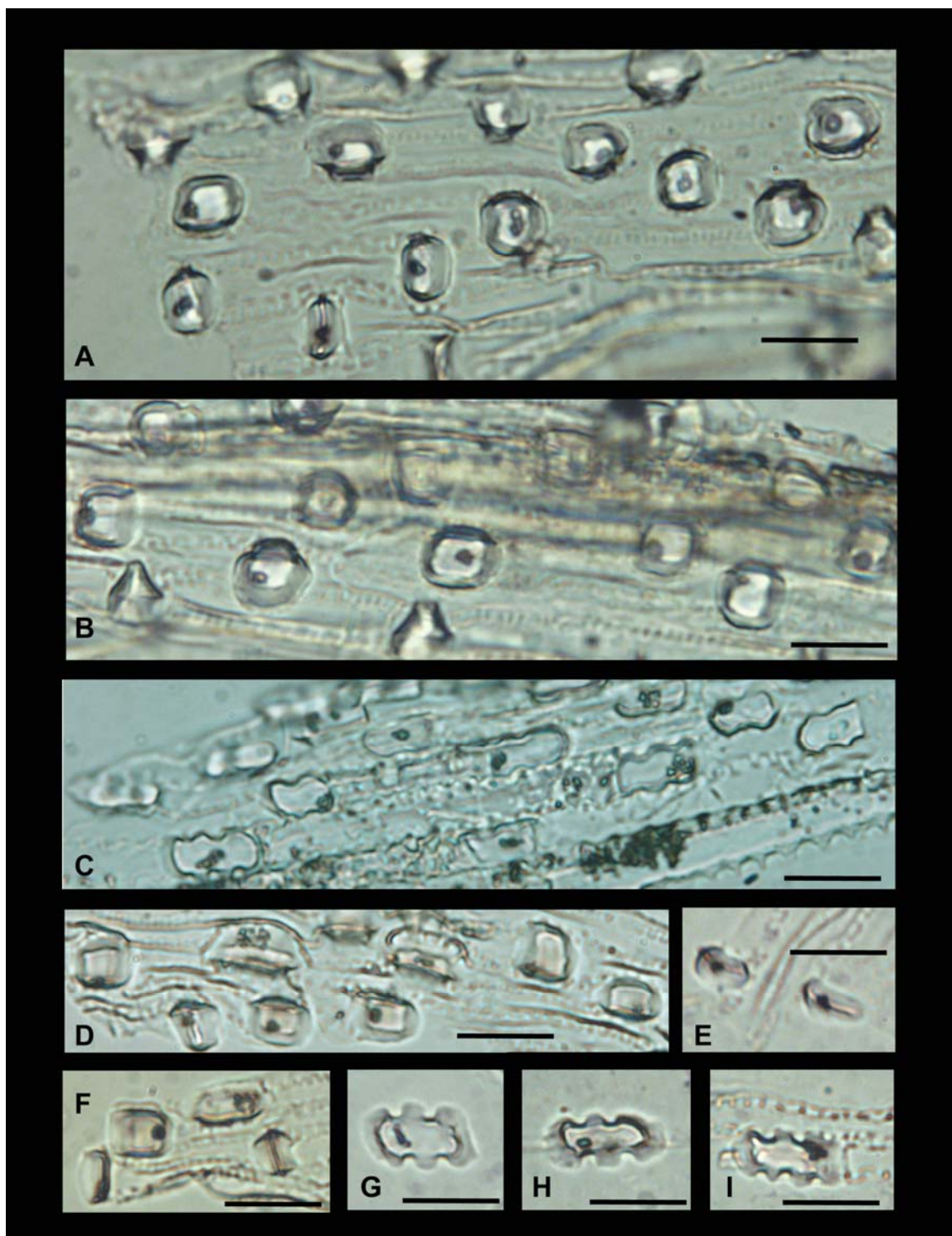
Figure 47. Phytoliths prepared from Kentucky Bluegrass (*Poa pratensis* L.) showing keeled, conical and pyramidal forms (A, D, and F) and crenate (C and G-I) short cell phytoliths. Bar scales are 20 microns.

also including a few keeled specimens (Figures 49 A and D). The third through fifth

stipa cells on the bottom row (Figure 49 D) have a pale purple line down the middle, and

the third specimen actually has two indentations on the upper side which might make it

more correctly identified as a crenate form rather than true stipa. This variation may be

another indication that the short cell phytolith forms within individual species of the

Pooideae subfamily are actually a continuum with inter-morphological type gradations

present between the clearly defined and established morphological types in the literature.

Next, two species of subfamily Arundinoideae were evaluated (Red Threeawn

and Purple Threeawn). These and the remaining specimens discussed in the following

paragraphs are C4 metabolic species whereas the specimens previously discussed were

all C3 plants (Pooideae). In moving to the C4 species, a marked change in short cell

phytolith form is observed with both Threeawn species being predominantly bilobate

forms (Figures 50-51). Considerable variation in the size and relative width and length of

the shaft connecting the lobes is present. The polylobate form was also observed in a

very limited quantity (Figure 51 E).

Phytoliths were isolated from three specimens of the Panicoideae subfamily: Big

Bluestem (Figures 52-53), Little Bluestem (Figure 54) and Indiangrass (Figure 55). In

Big Bluestem, we see the Panicoid lobate form (Figure 52 B), varieties of the so-called

crosses (Figure 52 C), as well as several polylobate forms (Figures 53 D-E) (also some

specimens in Figures 52 A, B, 53 B, and C). Little Bluestem also demonstrated Panicoid

lobate, polylobate, and crosses (Figure 54) as well as one specimen of an odd untyped
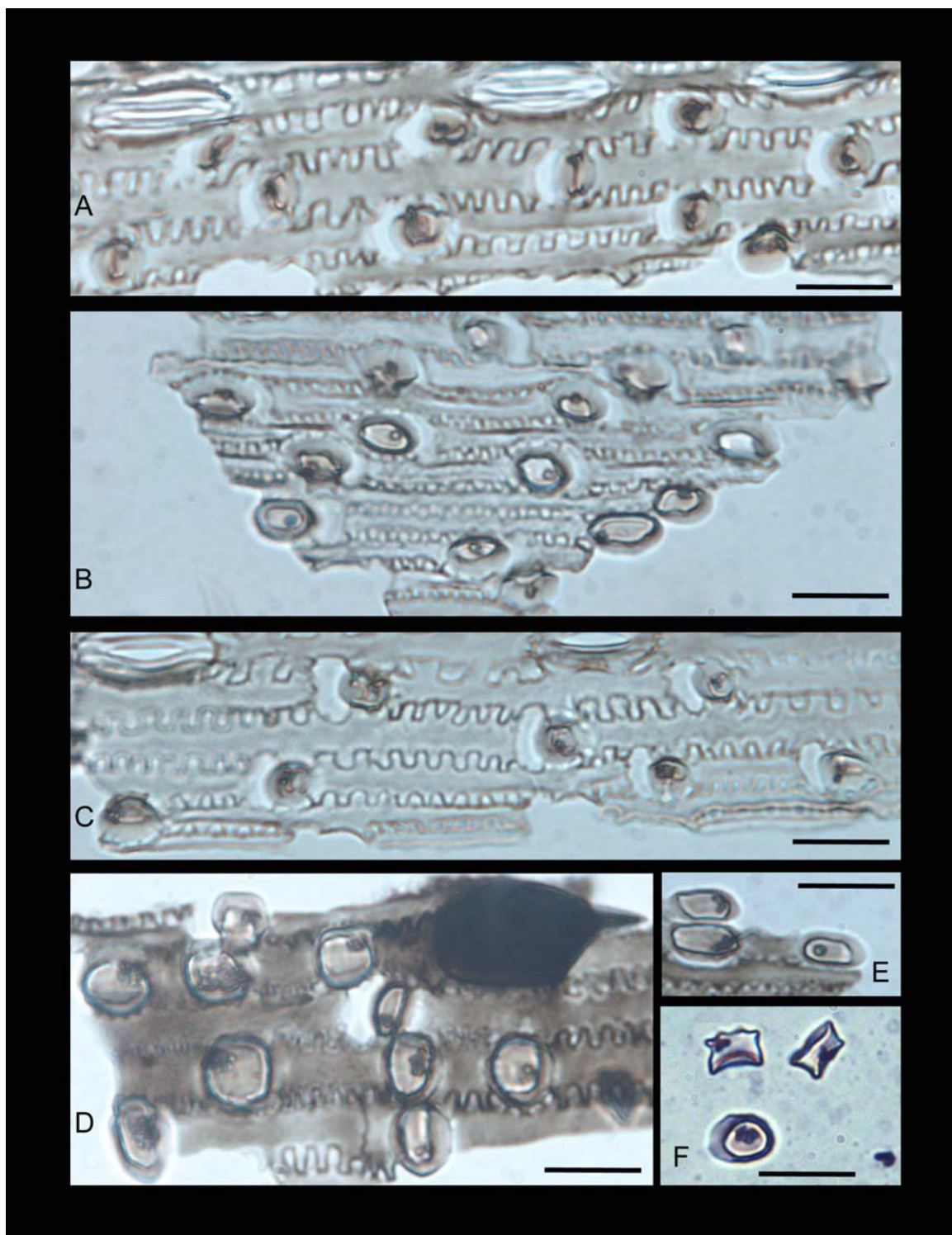
Figure 48. Phytoliths prepared from Needle-and-Thread (*Hesperostipa comata* (Trin. & Rupr) Barkworth). Bar scales are 20 microns.
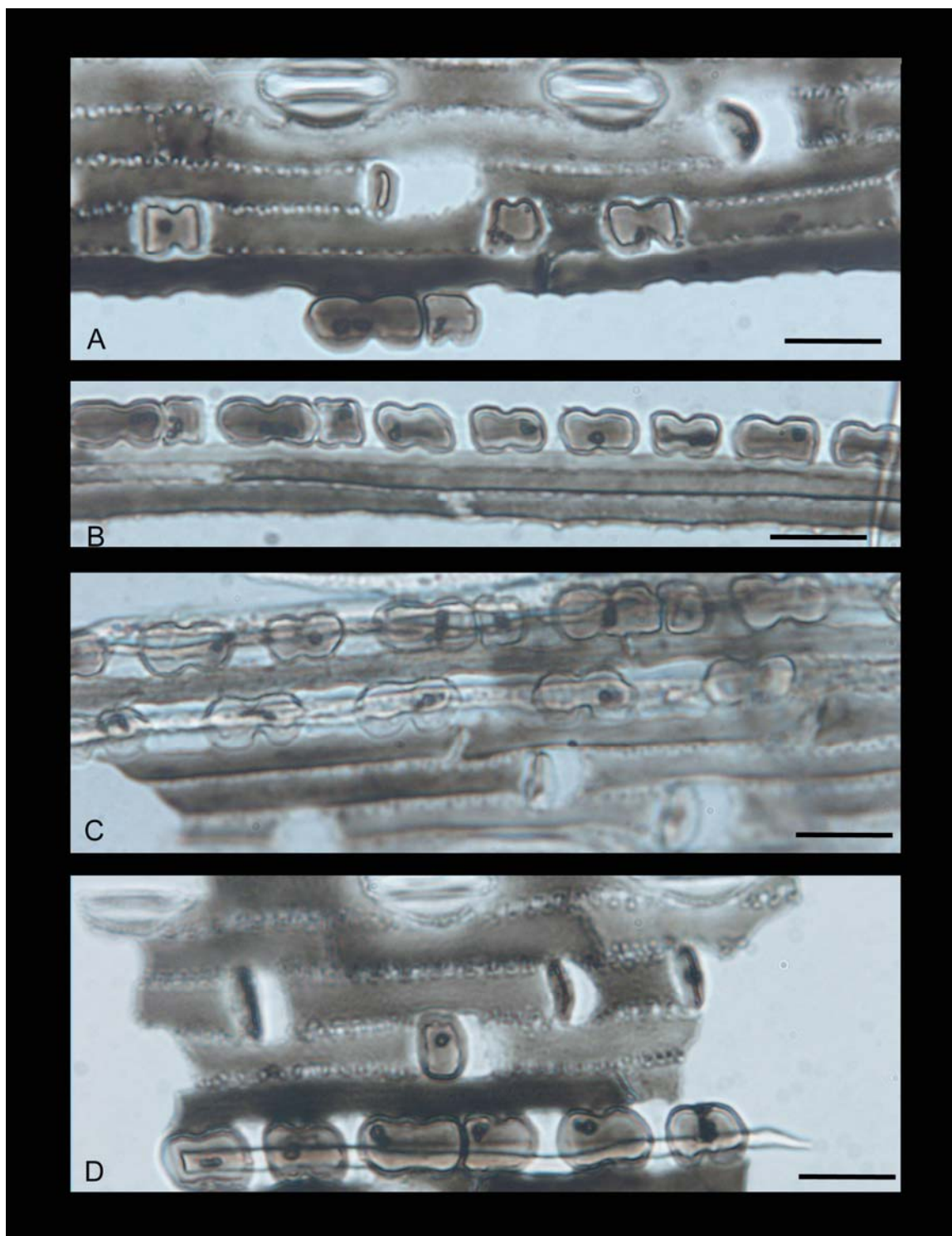
Figure 49. Phytoliths prepared from Indian Ricegrass (*Oryzopsis hymenoides* (Roem. & Schult.) Ricker). Bar scales are 20 microns.

variant (Figure 54 F). Indiangrass likewise showed the same three basic Panicoid

phytolith short cell forms although fewer polylobates were observed (Figure 55).

The final botanical reference specimen, Buffalograss, is from the subfamily

Chloridoideae--plants that are adapted to thrive in a hot dry climate. The predominant

short cell phytolith form in these plants is referred to as "saddles" (Figure 56).

Isolation of these phytolith short cells from known botanical specimens enables the

microscopist to become proficient at identifying the various morphologic types so that

accurate tabulations can be made from unknown samples. Overall, the basic typology,

originally defined by Twiss et al. (1967) and illustrated by others (Fredlund and Tieszen

1994) was used for identifications in this current research. The cool season C3 grasses of

the Pooideae contain one or more of certain short cell types (referred to as keeled,

conical, rondel, crenate, and pyramidal); in addition, some members of the C3 Stipeae

tribe have what is designated as the "stipa" form. The phytolith short cell "saddle" form

appears to be unique to the Chloridoideae subfamily of grasses which is adapted to very

hot dry climatic conditions. The so-called Panicoid forms (Panicoid lobates, crosses, and

polylobates) occur in specimens of the Panicoideae subfamily of Poaceae, which are the

hot season grasses with higher water requirements than the Chloridoideae specimens (i.e.,

Panicoideae thrive in a hot moist climate). For convenience, in the remainder of this

study, these forms will be referred to as the Pooid, Panicoid, and Chloridoid forms. The

different cellular architecture of these three grass subfamilies as evidenced in these

distinctive short cell phytolith forms is a reflection of their metabolism and the climate in

which they have adapted to thrive. Thus, when preserved as a soil phytolith record,

114
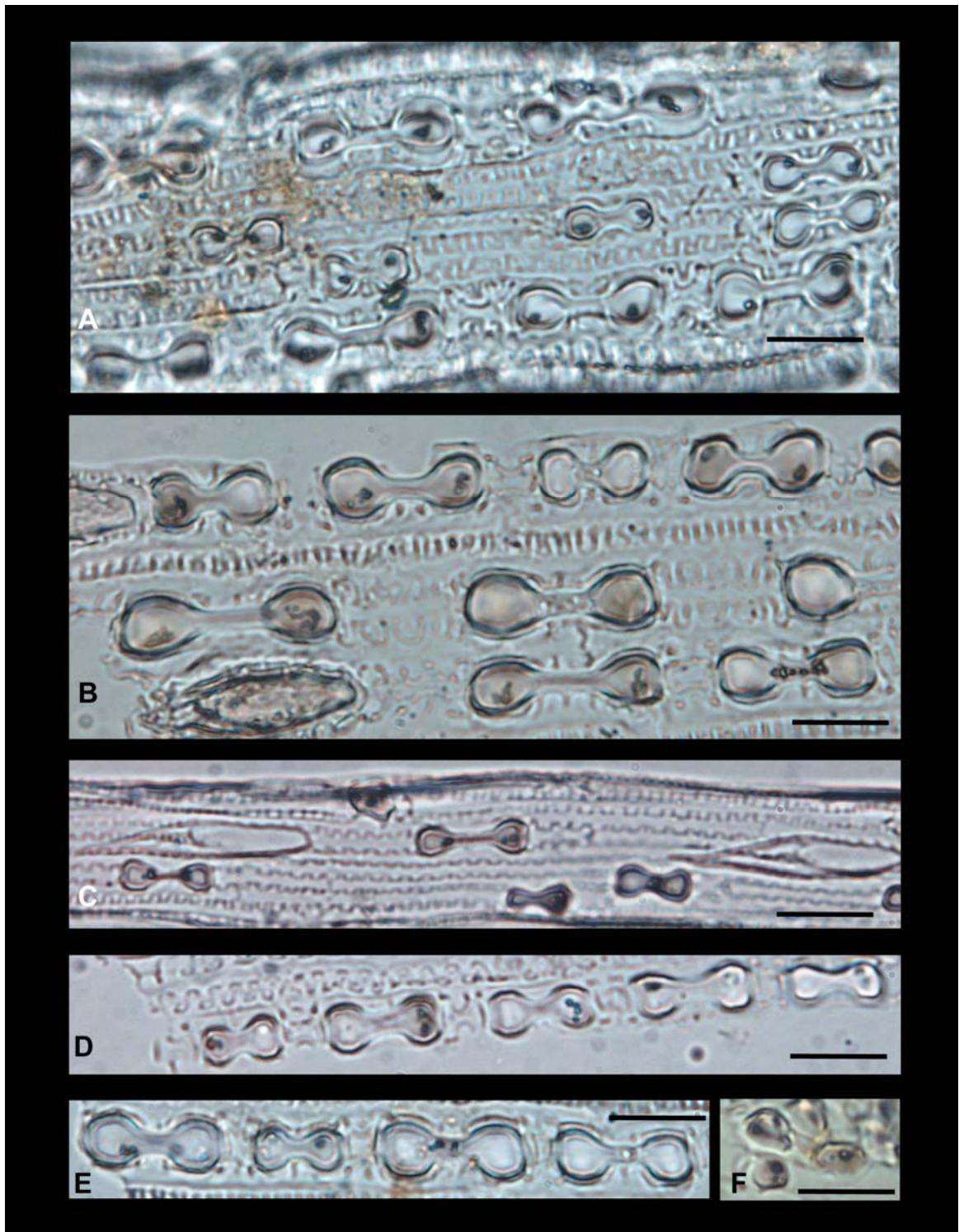
Figure 50. Phytoliths prepared from Red Threeawn (*Aristida longiseta*) showing a considerable variation of predominantly dumbbell form phytoliths (A-E). Bar scales are 20 microns.
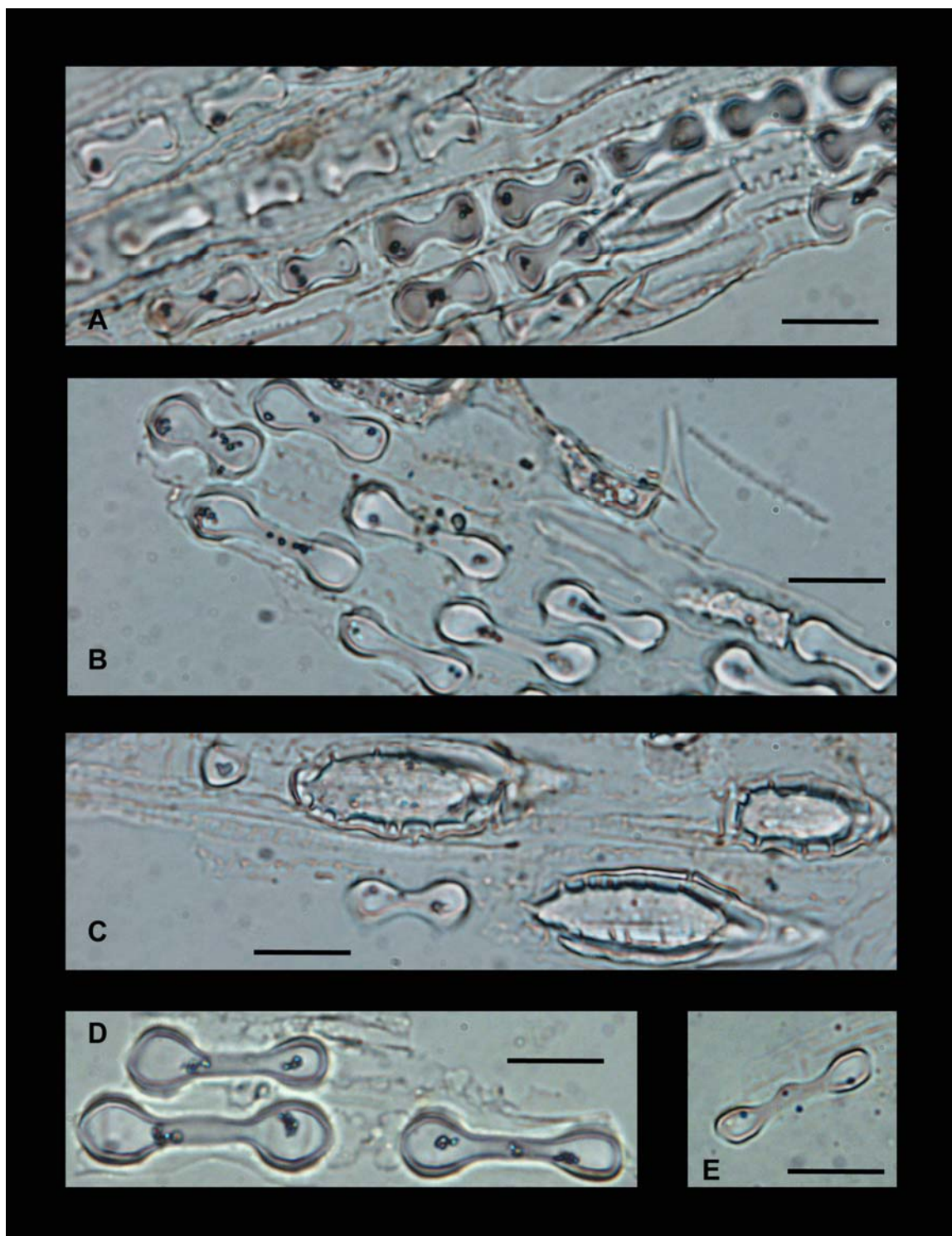
Figure 51. Phytoliths prepared from Purple Threeawn (*Aristida purpurea* Nutt.). Bar scales are 20 microns.
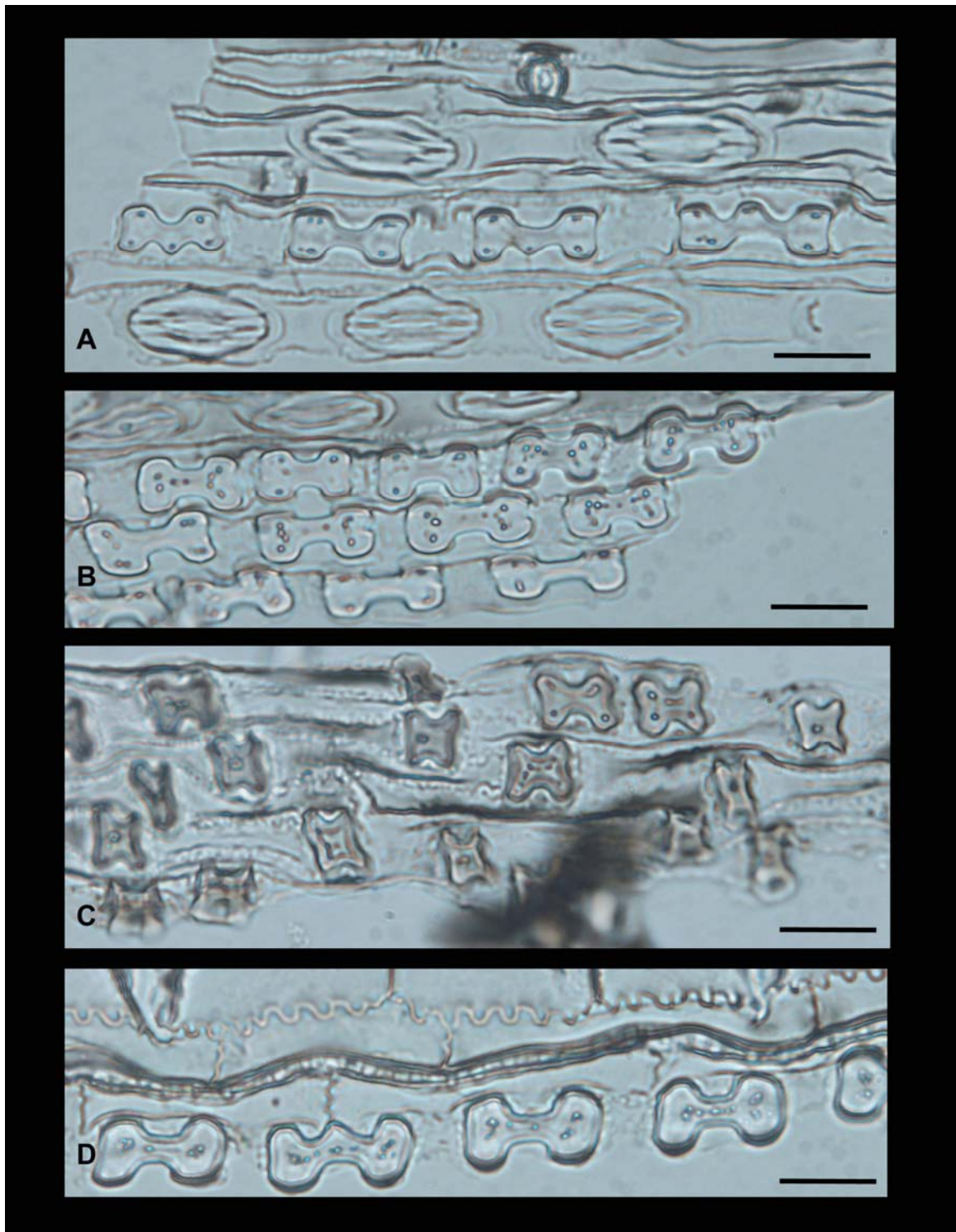
Figure 52. Phytoliths prepared from Big Bluestem (*Andropogon gerardii* Vitman) showing crosses (C), panicoid lobate (B), and polylobate (A and D (second from left) short cell forms. Bar scales are 20 microns.
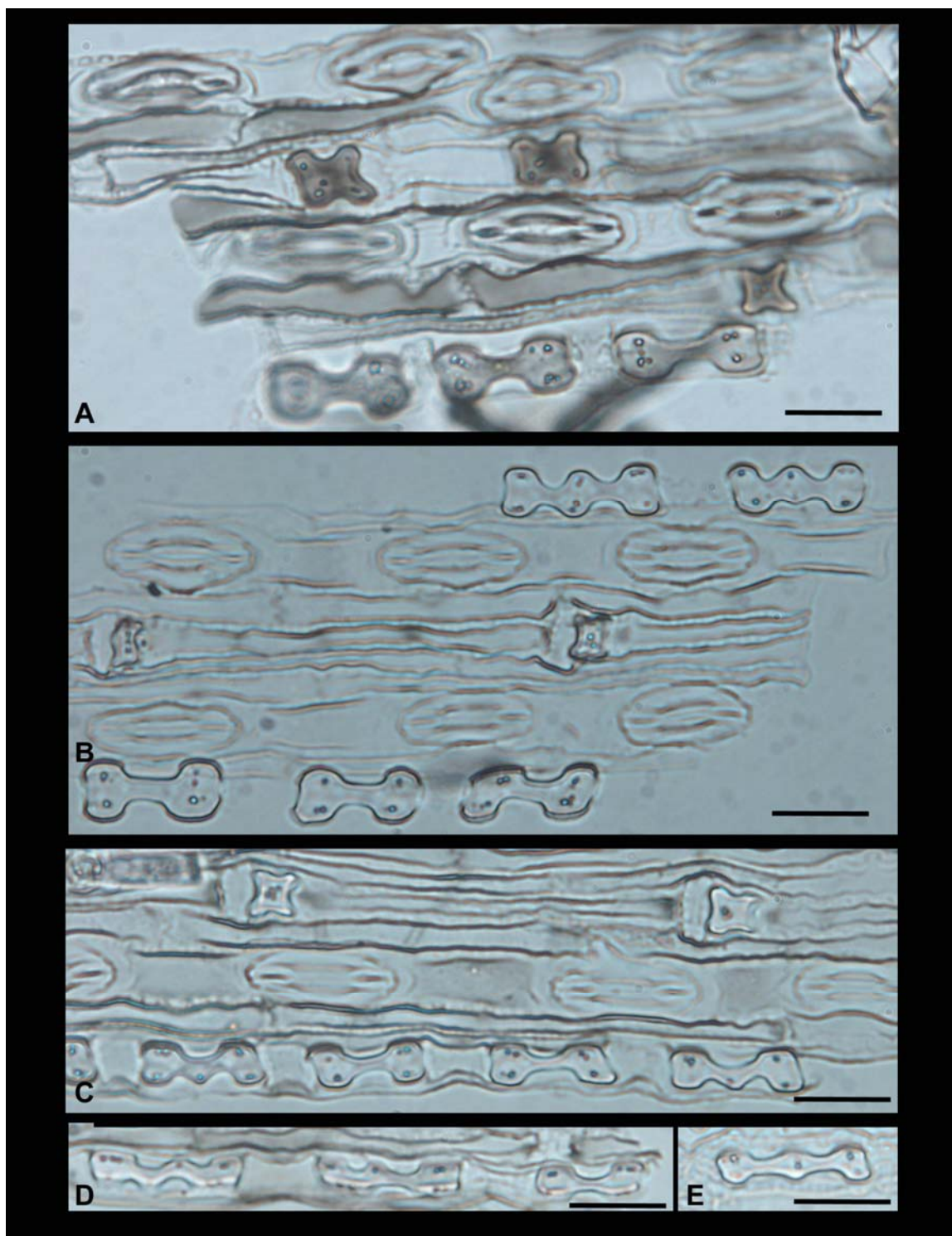
Figure 53. Phytoliths prepared from Big Bluestem (*Andropogon gerardii* Vitman) showing cross, lobate, and polylobate (E) short cell phytolith forms. Bar scales are 20 microns.
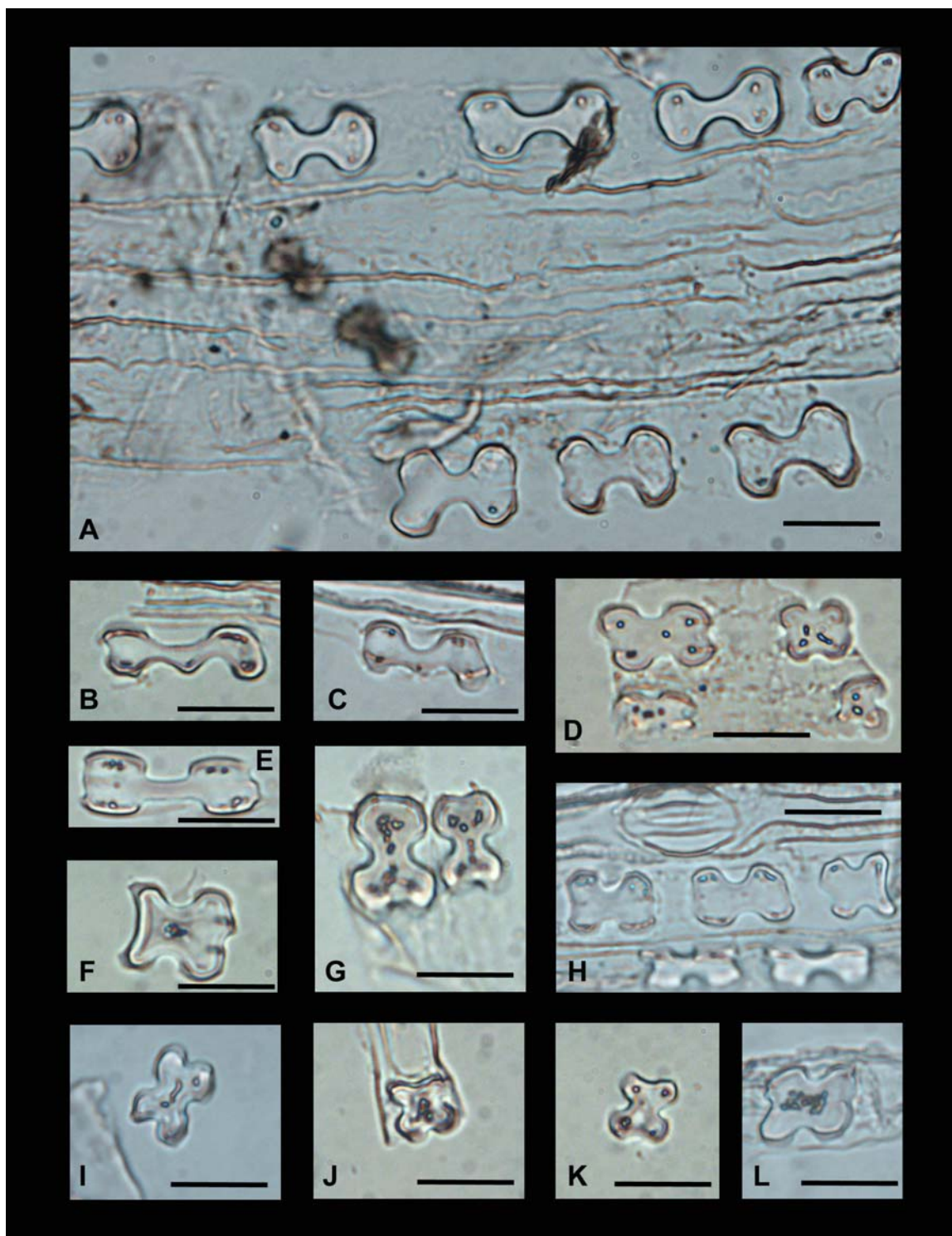
Figure 54. Phytoliths prepared from Little Bluestem (*Schizachyrium scoparium* (Michx.) Nash) showing panicoid lobate, polylobate (B-C), and cross-shaped (D and I-L) short cell phytoliths. Bar scales are 20 microns.

119
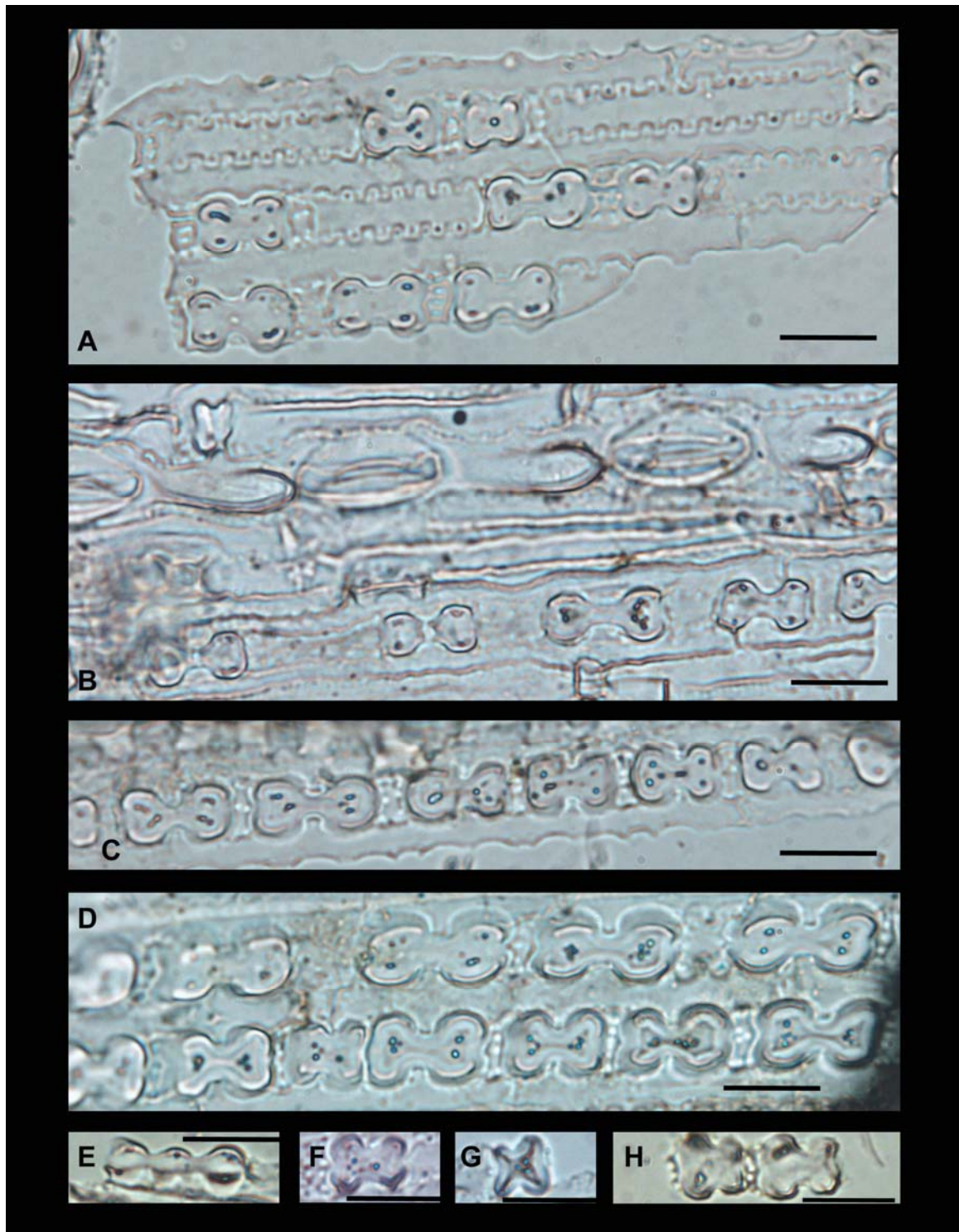
Figure 55. Phytoliths prepared from Indiangrass (*Sorghastrum nutans* (L.) Nash) showing panicoid lobate (B-D), polylobate (E), and cross-shaped (F-H)short cell phytoliths. Bar scales are 20 microns.
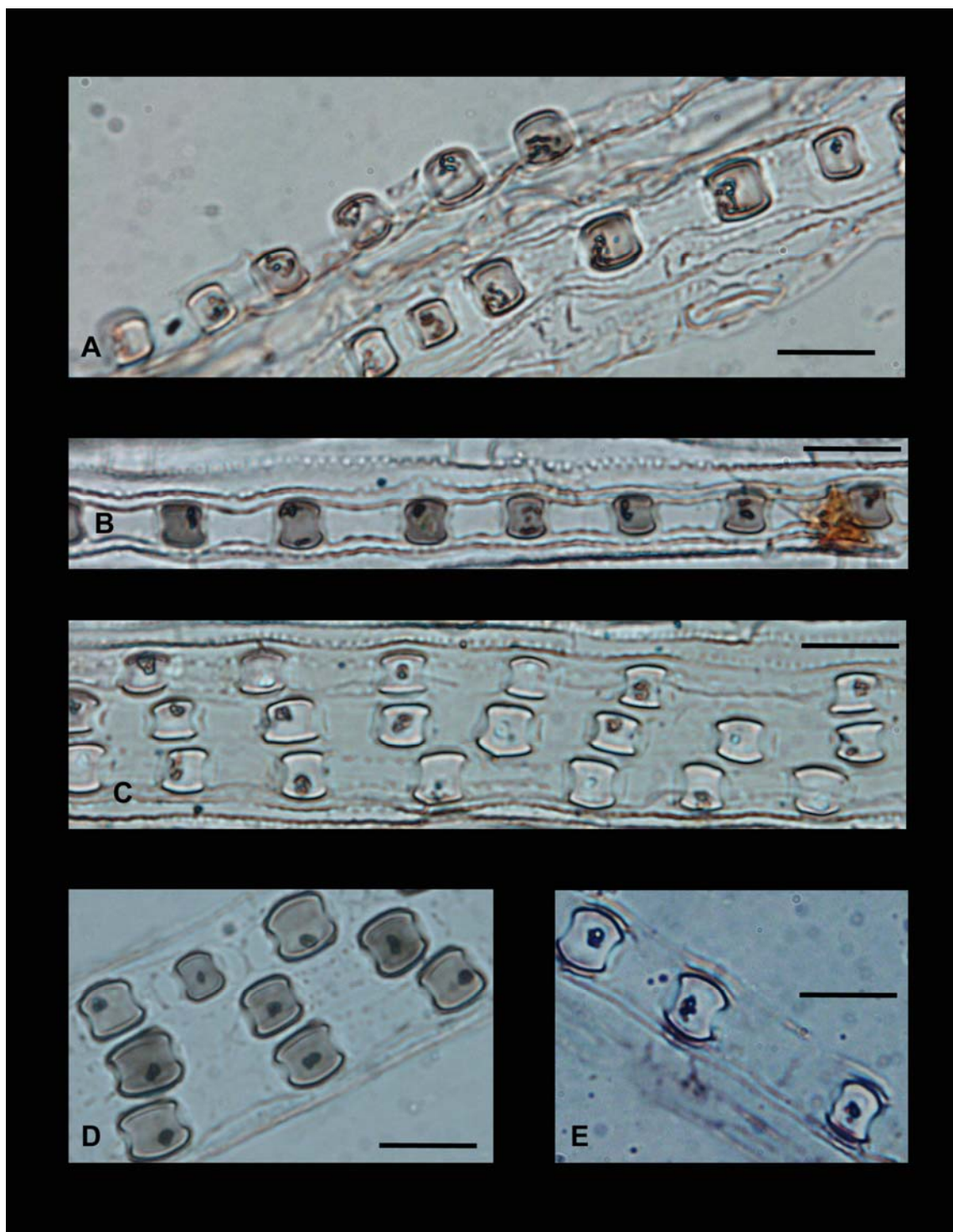
Figure 56. Phytoliths prepared from Buffalograss (*Buchloe dactyloides* (Nutt.) Engelm.) showing saddle-shaped short cell phytoliths. Bar scales are 20 microns.

the relative frequency of these various short cell forms can be used to interpret the prevailing climatic condition (temperature and moisture) that was present when the vegetation was actively growing.

Panicoid and Saddle Phytolith Imposters

One problem was encountered in examining and tabulating phytoliths during scans of the Manning Tallgrass Prairie slides that deserves special mention. There is a phytolith form present at the Manning Tallgrass Prairie site that initially superficially appears to a Panicoid lobate form (Figure 57). These phytoliths are narrower, and often have a significantly longer shank than regular Panicoid lobate phytoliths (see Figures 57 A and B). Mulholland (1989:506) suggested that these long-shank forms are found in *Aristida*. Due to this different morphology, these bilobate forms are clearly discernable from Panicoid lobate phytoliths once one is aware of the need to look for them. The potential problem in phytolith counting enters the picture when these long shank phytoliths are broken (Figures 58 and 59).

As these long-shanked lobate phytoliths appear to be relatively fragile, they often appear in slide preps in fragmentary condition. It is generally recommended that each partial lobate specimen be counted as ½ particle in the tabulation. Thus, the fragmentary *Aristida* lobate forms such as those shown in Figure 58 would potentially often be counted with lobate type C4 phytoliths. The longer shank fragments on these particular

specimens are an indicator that these phytoliths are distinct from normal Panicoid lobates

as defined by Twiss et al. (1969) and reiterated Fredlund and Tieszen (1994). The real

potential problem occurs when the shank is nearly or completely broken off (Figure 59).

In these cases, one could potentially misidentify the fragmentary lobate particle as a

saddle form (i.e., Chloridoid phytolith) which could significantly skew the resulting

phytolith climatic data. Awareness of the presence of potential imposter forms, being

aware of asymmetry in the particle and presence of a small shank portions, and particle

rolling to examine the 3-D shape of the particle in question are all effective means to help

avoid fragmentary phytolith misidentifications. This potential for misidentification is the

reason why Canada Balsam was used as the slide mounting media in this study (Figure

41).

The variety of morphologic forms shown in these three figures (57-59) indicates

that many species may be represented in these illustrations, so an identification of

specific plant origin for all of these specimens is not being claimed. However, the need

to be aware of the possibility of confusing these lobate fragments with saddle

(Chloridoid) forms should be kept in mind when assessing prairie phytolith morphology.

All phytoliths illustrated in Figures 57-59 are from the 0-5 cm surface soil samples at

Manning Tallgrass Prairie. Cummings (1996) likewise recommended caution when

examining and categorizing bilobate form phytoliths. On the other end of the "confuser"

or "imposter" phytolith spectrum, a bilobate form has been reported from *Danthonia*

spicata which is a Pooid (Brown 1984:Figure 1:VI:23C)—again indicating that the

boundaries between phytolith morphology are not always clear-cut between the various

Poaceae subfamilies (i.e., redundancy is an ongoing issue).

Figure 57. Panicoid imposter forms, Manning Tallgrass Prairie (0-5 cm surface soil samples). True panicoid lobate forms are on the left in Figures A and B, with the probable *Aristida* forms on the right. The other images are all non-Panicoid forms. (Bar scales are 20 microns.)
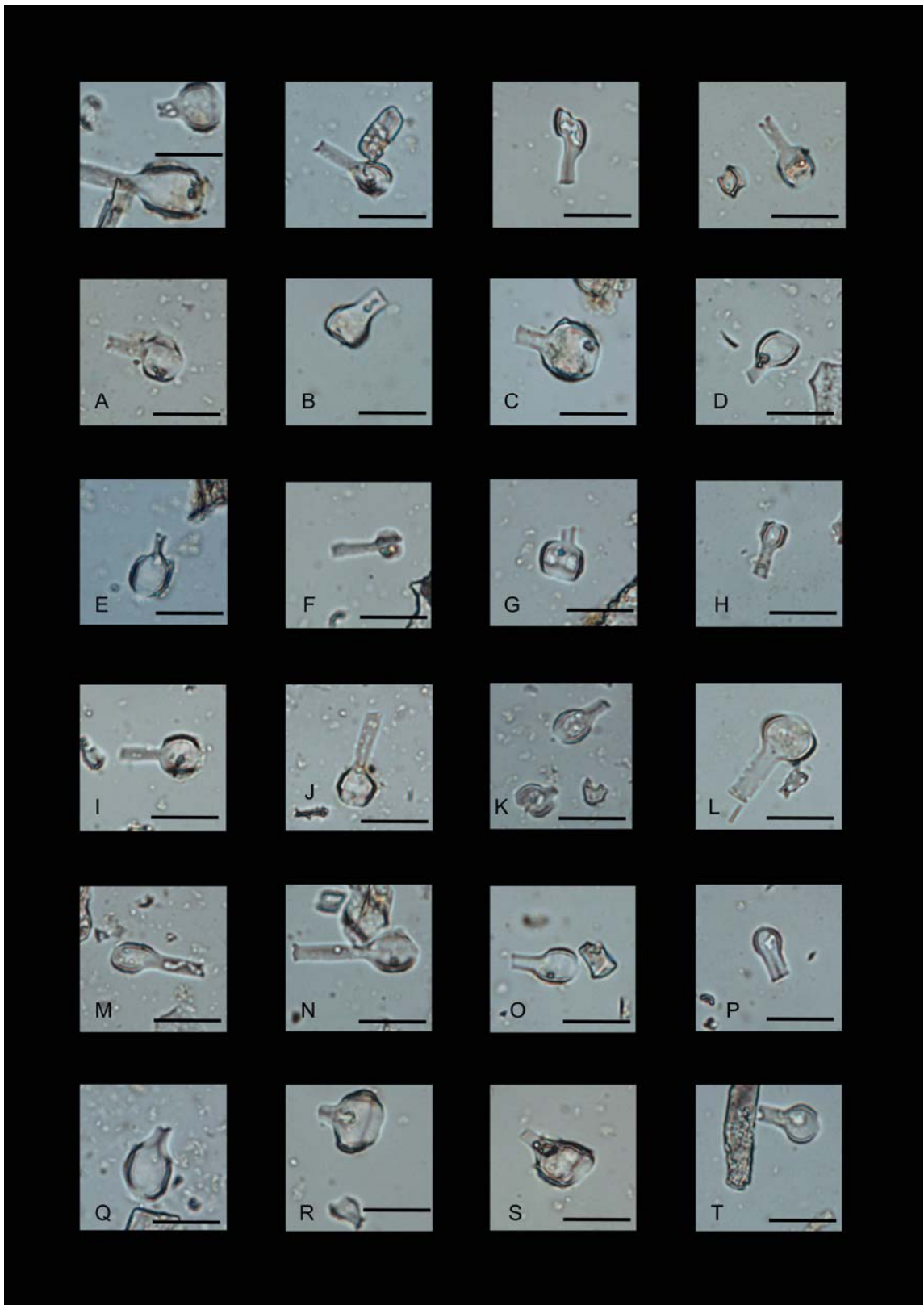
Figure 58. Various apparent long shank lobate forms, broken with partial shank remaining. (Bar scales are 20 microns.)
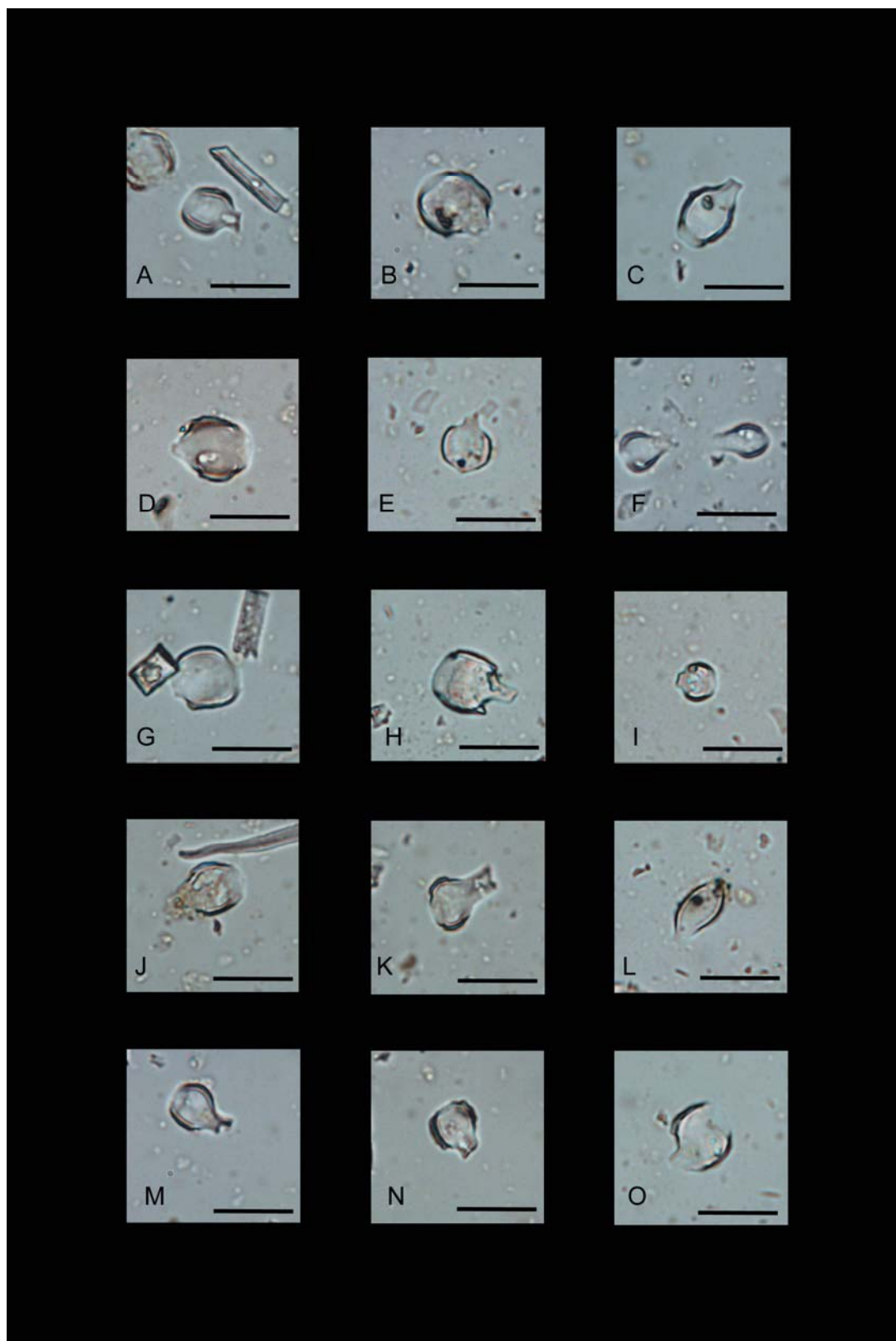
Figure 59. Various broken apparent lobate forms that at times superficially look more like saddles. (Bar scales are 20 microns.)

The laboratory method detailed in the previous chapter included a number of modifications and recommended changes from established protocols. This method is felt to be an optimized quantitative phytolith recovery procedure for a number of reasons.

This method as presented enables retention and recovery of larger particles that are part of the phytolith/biogenic silica fraction that would otherwise be removed via initially sieving the soil sample with a 270 mesh sieve (i.e., > 50 micron particles). In addition to sand, sieving removes larger biogenic silica particles of interest (such as large phytoliths, articulated phytolith skeletons, and longer sponge spicules). By leaving the biogenic silica fraction intact, the sand fraction does not need to later be separately evaluated or processed for phytolith recovery. The lower particle density (relative to sand) and non-spherical shape of the larger phytoliths helps them to remain suspended longer while the sand particles settle when using the preceding technique of decanting the silt and clay fractions away from the sand fraction before isolating the silt fraction.

The vacuum filtration using stacked ashless filter paper was implemented to speed up the overall silt recovery process. The total volume of suspended silt solution (about 10+ liters per sample [depending on initial soil sample size]) remaining after decanting from could be filtered much more rapidly than trying to filter the entire suspended silt effluent. Allowing the silt to pre-settle minimized the amount of particulate processed by filtration.

Thermal treatment of the isolated silt fraction does allow use of the preceding filtration step as the ashless paper is removed by the muffle furnace treatment.   However, thermal treatment for organic removal—very advantageous in the procedure as presented here—may not be appropriate for studies involving phytolith micrometrics as some distortion of phytoliths reportedly may occur.

The thermal treatment of the silt fraction does necessitate the need to disaggregate the silt fraction in order to be able to extract the phytoliths (either mechanically, or by allowing time to loosen up in the flotation solvent); this added step cannot be circumvented when using this procedure. This is the primary draw back of this new method (in addition to the required longer settling times).

Zinc bromide was selected for use as the heavy density liquid in this study as it provides excellent quality phytolith preparations. Use of reagent grade zinc bromide in aqueous solution was effective. The only reason to use zinc bromide in hydrochloric acid may be that the acid may better dissolve the other calcium salt contaminant impurities when using technical grade reagents. When using reagent grade zinc bromide, there is no apparent benefit to adding HCl. Due to toxicity issues, use of zinc bromide solution may be inadvisable due to safety concerns when the analyst only possesses rudimentary chemical laboratory skills. Use of recycled zinc bromide solution is inadvisable when processing phytolith samples to use for radiometric dating although new reagent grade zinc bromide should be readily useable in sample preparations destined for dating purposes.

The silt fraction should be dried prior to adding the heavy liquid for phytolith

flotation. Otherwise, depending on the ratio of sample size (i.e., total residual water

content in the sample) to volume of heavy liquid used for flotation, the water in the

sample may dilute the heavy liquid to the point that the densest phytoliths (2.30 g/cm^3)

may not be recovered. Using excess heavy liquid for the flotation would minimize if not

eliminate this dilution problem; however, the expense of the heavy liquid is such that

most analysts tend to be quite frugal with their reagents[23].

To demonstrate this density problem, a simple experiment was conducted. Using

2.348 g/cm^3 density zinc bromide solution, a series of volumetric dilutions were made

with ultrapure water to simulate the effect of residual soil water on the effective density

of the zinc bromide solution when mixed with a soil or silt sample in order to recover

phytoliths. The experiment was conducted using 10 ml volumetric flasks, a volumetric

pipette for the water, a transfer pipette for the zinc bromide, and a four place balance.

Although the soil samples used in this dissertation ranged from 25 to 100 grams, a more

common sample size reported in the phytolith research literature seems to be 5 grams.

Thus, a 5 gram sample weight was used for these experimental calculations. Although

the volume of zinc bromide added tends to vary in normal sample processing (i.e. enough

to wet everything and have room to float phytoliths free of the matrix, but not so much

solvent as to be excessive or wasteful), a total liquid volume (zinc bromide stock solution

plus simulated soil water) was set at 10.0 ml and held constant for the purposes of this

experiment. The water volume used and the sample weights are in Table 6. As can be

---

[23] The cost of 2.35 g/cm^3 density reagent grade zinc bromide solution is more than $1.00 per milliliter. This reagent expense encourages solvent recycling.

seen in the resulting density data (Figure 60) the dry soil sample maintained an effective

zinc bromide solution density of 2.348 g/cm^3. However, as little as 0.5 ml of water

present in the sample matrix (i.e., 10% soil moisture in a 5 gram soil or silt sample) is

enough to lower the zinc bromide below 2.30 g/cm^3, and the drop off continues in a linear

fashion (Figure 60). Of course, things are never as simple as they seem; for one thing,

soluble soil minerals may serve to help mitigate this impact by increasing flotation

solution density and offsetting at least part of this effect.

In practice, there are several simple ways to help mitigate the negative impact of

potential low phytolith recovery due to this solution density issue, including:

- to use more flotation solution (i.e., add enough high density liquid to the
  sample dilute out the soil water at the time of extraction thus raising the
  total solution density to more than 2.30 g/cm^3),
- to use a higher initial density of zinc bromide solution so the sample's
  inherent water does not dilute the mixture below 2.30 g/cm^3 (being careful
  not to approach too closely to the density of sand (2.65 g/cm^3)), or
- to use sequential additions of the heavy liquid to the soil sample so that the
  resulting solution density of the pooled decanted solution is greater than
  2.30 g/cm^3.

Table 6

Experimental Data from Simulating the Effect of Soil Water on Zinc Bromide Density

Sample No.	Empty 10 ml Volumetric Flask plus Stopper Weight (g)[24]	ml of Water placed in 10 ml Volumetric Flask	Wt. Flask + Water Aliquot made to 10.0 ml with $ZnBr_2$ solution (g)	Density of Resulting 10.0 ml Mixture (g/cm^3)	Equivalent Soil Moisture Concentration in this 5.0 g Sample (Wt %)
0	43.4607	0	66.9424	2.348	0%
1	43.5994	1.00	65.7809	2.218	20%
2	43.9702	2.00	64.8564	2.089	40%
3	42.9374	3.00	62.4875	1.955	60%
4	43.3919	4.00	61.7201	1.833	80%
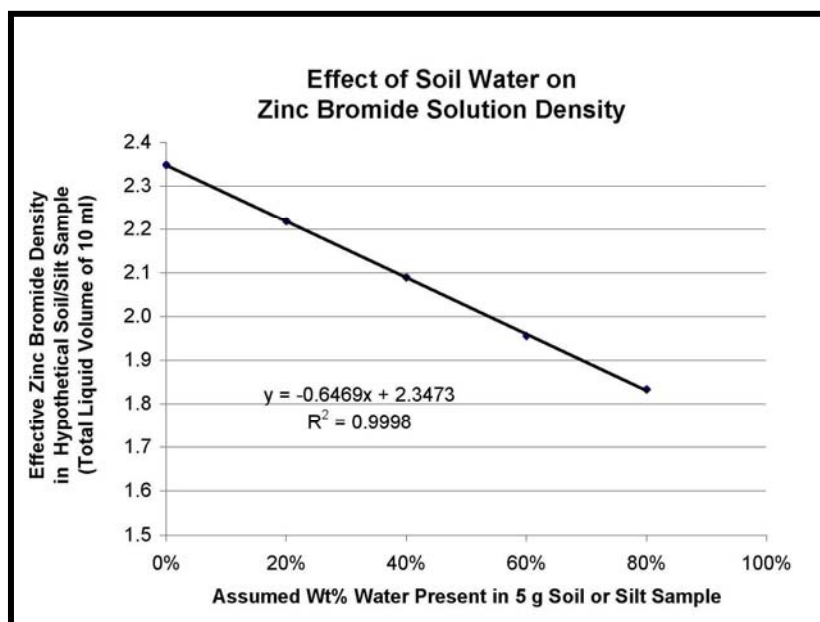
Figure 60. Effect of soil water on zinc bromide flotation solution density (weight water/weight dry soil).

Considering the expense of the zinc bromide solution, the possible dissolution of

other soil minerals, and the existence of intermediate density particles (i.e., 2.30 g/cm^3 <

other particles < 2.65 g/cm^3), and the fact that thermal removal of the organic matter can

---

[24] Each flask was weighed in a labeled 50 ml beaker (the beakers served as containment in case of spillage, and stabilized the flasks to prevent them from tipping over).

increase phytolith density from 2.02 to 2.26 (Jones and Milne 1963:213), I concluded it was appropriate for purposes of quantitative recovery to isolate phytoliths from an oven dried silt matrix (i.e., 0% water). In part, this decision was supported by the fact that following carbonate removal before flotation—the samples were wet [i.e., saturated at the very least] in the centrifuge tubes. The down side of this decision to remove one variable from the processing procedure is that additional time is required for the sample to "loosen up" and disaggregate in the zinc bromide solution following oven drying. An upside is that a dry organic-free silt fraction sample weight is obtained. When thermal ashing is used to remove organic material, making certain the soil water does not dilute the heavy liquid is even more important to help maximize phytolith recovery.

This probable procedural error (potentially not recovering denser phytoliths when floating wet samples) is pointed out in some detail so other researchers can make an informed decision regarding sample soil/silt water content and phytolith recovery. The analyst can oven dry a duplicate sample at this step in their procedure and determine what adjustments, if any, are needed in the flotation protocol. To my knowledge, this laboratory error potentially affecting recovery of the densest phytoliths has not been previously addressed in the literature.

Use of ASTM Type A water helps to minimize ionic contamination in recycled zinc bromide (recycling involves filtering the dilute zinc bromide solution and then evaporating the excess water until the target density is achieved).

Although there are many assumptions involved with Stoke's law (the primary assumption relative to phytolith research is the assumption of sphericity; many phytoliths are more tabular than spherical), the established phytolith isolation methodology in the literature bases the heavy liquid separation on the density differences of particles (i.e., phytolith vs. sand), then proceeds to use the sand density to calculate the needed settling times to obtain various size fractions. If the phytoliths of specific interest in one's research project are large, this would not cause a problem. However, if dealing with smaller reference phytolith specimens—particularly towards the lower end of the particle density spread—this can cause potentially major difficulties and poor diagnostic specimen recovery. If one lengthens the time of clay settling the small phytolith recovery will be enhanced. Then, by filtering all of the silt fraction decants (which may include excess clay if prolonged clay settling is allowed), all phytoliths included with the silt fraction are recovered while the actual clay particles pass through the ashless filter pack. The filtrate passing through the filter can be examined for recovery information, and refiltered if necessary. This change thus potentially results in much better phytolith recoveries in various research situations. One should be aware of idealized phytolith particle settling times when using the laboratory protocol outlined in this dissertation.

The phytolith literature varies in defining the silt fraction as 5-50 microns (the engineering definition) and 2-50 microns (the soil science definition). Given the potential to lose small lower density phytoliths in the separation process, universal adaptation of the conservative 2-50 micron silt fraction definition would seem to be prudent. Again, if one's research is studying bulliform phytoliths, this issue is not

relevant. However, if one is looking at phytoliths in the lower size range of the silt

fraction size range (~2-5 microns), one should be aware of the potential to not be

completely recovering the smaller phytoliths by current established published methods.

As a convenient example, Jones and Beavers (1964a and 1964b) reported particle

size distribution of phytoliths in specimens of Big Bluestem and Reed Canary Grass

prepped by thermal ashing. Their data is reproduced in Table 7, with the values for 2-5

micron amorphous silica being calculated from their data and included in the table.

Clearly, in some cases, there is a significant amount of amorphous silica in the fine (2-5

μ) fraction—while more than half of the soil total amorphous silica may be in the clay

fraction. Although the clay fraction is predominantly small nondescript fragments, the

fine silt fraction does contain some diagnostic biogenic silica specimens. While is it

most important to always routinely process one's samples in an identical manner, it is

also important to not accidentally and unknowingly skew the data by missing very small

(or very large) specimens of interest.

The use of cheap, readily available, and potentially disposable 2-liter plastic

(soda) bottles for settling containers and other processing steps is a major opportunity to

Table 7
Weight % Amorphous Silica in Two Grasses
by Size Fraction (Jones and Beavers 1964a:414)

	> 50 microns	20-50 microns	5-20 microns	2-5 microns	< 2 microns
Big Bluestem	19.8%	13.5%	29.2%	13.6%	23.9%
Reed Canary Grass	19.8%	7.3%	18.8%	3.0%	51.1%

not only minimize costs but to also make saving various fractions until the project is completed more palatable—especially when using larger size soil samples. The 2-liter bottles pour easily with no drip, the shoulder helps retain solids during decanting, they are easy to seal and shake (or store), they do not break when dropped, they are readily storable, and they can be discarded or recycled when appropriate. (In this researcher's laboratory, bottles are not reused between projects, between sites, and seldom if ever between samples—and bottles are never reused if samples have dried in them.)

Likewise the use of quart jars for multiple steps (from settling and decanting containers to bottles to oven dry to obtain sample or fraction weights) without ever having to transfer the samples provides a number of time-saving and cost-saving benefits as well as minimizing the number of sample transfers.

The use of the ashless filter pack (i.e., a stacked ashless filter paper series of different porosity) enables faster processing and better recovery of residual fine silt fraction still suspended in water—which consists of the finer particles and/or lower density particles.

These laboratory procedures result in cleaner phytolith fractions than I have observed in most other laboratories where I have been able to observe phytolith processing results. The extensive photographs were included to help document and transfer this new protocol information.

Although not included in the preceding chapter, during the course of this research an improved procedure for preparing soil samples for delta 13 analysis was developed (Sudbury 2007:29-32). For convenience, this basic information is included as Appendix F at the end of this dissertation.

The stop gauge added to the soil probe for field sampling is a very convenient and affordable means of obtaining a constant cross-sectional area, depth, and volume soil samples. Although a spoon works for collecting samples, a known volume probe sample offers the potential of better reproducibility, control, and permits all of the soil sub-samples to uniformly contribute to the final composite soil sample.

Quantitative phytolith recovery takes much longer than semi-quantitative or qualitative recovery. Although the steps described here to execute quantitative recovery take longer (calendar time) than alternative procedures, they actually require less hands on analytical time per sample than established methods if applied for quantitative phytolith recovery from soil samples. It is for these reasons—improved data quality and efficiency—that these method alterations were developed during this project, and are presented here (additional method comments are included in Appendix D).

Discussion of Laboratory Procedure and Sampling Enhancements - The suggested improvements made in the laboratory phytolith isolation protocols were designed to result in efficient quantitative phytolith recovery from relatively large soil

samples (25-100 g)[25]. Depending on phytolith preservation at any given site, this larger

soil sample size enables recovery of an adequate quantity of phytoliths for radiocarbon

dating as well as climatic interpretation based on Poaceae phytoliths. Data from other

particle forms (including diatoms, sponge spicules, and charcoal) is also present in the

same isolate and contributes to the interpretable environmental data. Several serious

discrepancies in the phytolith literature were observed during the course of this

research—and recommended method improvements developed—including:

- the silt particle size definition was inconsistent (the recommended change is to recognize three size fractions: fine (2-5 microns), medium (5-20 microns) and coarse (20-50 microns) (pages 23-24)),

- the apparent historical tendency to base phytolith settling times on sand density (representative calculated values are shown of the settling times for different size and density particles [Table 4, page 77][26] ; although consistent times are the key to reproducibility within any given study, other laboratory protocols potentially lose smaller and/or less dense biogenic silica from their phytolith isolates; conservative settling times are recommended. A revised order of serial fraction decants followed by filtration to recover the total silt fraction is the method recommended to overcome these potential losses),

---

[25] Enough sample is needed to adequately address the research topic at hand. It is particularly beneficial to process larger size samples in high sand content soils.

[26] Base the settling time determined by Stoke's Law on the correct minimum target particle size and the correct particle density range. Use target phytolith density rather than sand density in the calculation.

- adding heavy density liquid to wet soil samples potentially dilutes the heavy liquid below the effective upper phytolith density range (i.e., if the sample contains 10% water, 2.35 g/cm^3 zinc bromide would possibly be diluted to less than the 2.30 g/cm^3 density target (pages 129-132))[27]. Several potential techniques to circumvent this problem were noted; for this current research, floating phytoliths from totally dry silt fractions was selected as the method of choice. This technique is somewhat slower in that the silt must disaggregated again before phytolith flotation; however, this procedure resulted in cleaner and more complete silt-size phytolith fraction recovery), and

- performing phytolith morphologic counts on non-pure phytolith isolates (i.e., prepared sample fractions with significant non-biogenic silica content)[28] leads to incorrect recovery information (phytolith wt% concentration in soil) and contamination interferences during counting. In order to circumvent this problem, multiple flotations, multiple rinses of the isolate, using large enough starting sample size, minimizing losses, repetitive separations, and completely disaggregating the sample are can be utilized.

---

[27] The original phytolith density information provided by Kanno and Arimura (1958) and Jones and Beavers (1963) was obtained by analysis of coarse silt fraction phytoliths (20-50 μ), yet most climatic/environmental interpretations are based on short cell phytoliths which populate the medium silt fraction (5-20 μ). Although the phytolith density from these different phytolith types and sizes (i.e., from cells with different functions in the parent plant) may be the same, to simply assume the density is uniform is risky at best. A conservative separation method (i.e., making certain that the *effective* flotation solution density remains above 2.30 g/cm^3 [see discussion involving Table 6 and Figure 60]) is one way to help minimize potential phytolith loss until the actual short cell phytolith density range is determined.

[28] Phytolith isolates previously observed in some reports and communications by other researchers include significant clumps of clay containing phytoliths and other particles that potentially may obscure smaller phytoliths thus skewing the resulting particle count results.

The laboratory techniques section in the Literature Review chapter (pages 30-37) and in the Materials and Methods chapter regarding laboratory methods used in this study (pages 71-99) clearly discuss and illustrate the laboratory methods used during this research. A number of the basic improvements to the standard method protocol developed during this study include:

- processing larger soil samples, oven dried,

- retaining the larger biogenic silica particles with the silt fraction by repeatedly decanting the clay and silt away from the sand rather than sieving out the sand fraction,

- using conservative settling times (based on 1.50 g/cm^3 density phytoliths) to decant the clay from the silt, and allowing the decanted liquid to settle in order to recover the entire silt fraction,

- vacuum filtering the large volume of decanted silt solution to improve the speed of the silt particulate fraction recovery,

- removing organic material (including the ashless filter paper) by thermal ashing,

- using flotation to separate phytoliths from dry silt in order to keep the solvent density at the effective 2.35 g/cm^3 target rather than diluting it with soil water (additional disaggregation is necessary due to this procedural modification).

- Quart canning jars and 2-liter plastic soda bottles were readily incorporated into the laboratory processing protocols, and provide a significant cost savings in operating supplies in addition to making quantitative processing and recovery simpler while helping to minimize transfer losses. Use of reagent grade reagents

is also highly recommended.

The resulting final laboratory method yielded quantitative phytolith recoveries that were effective for performing the detailed phytolith studies on the control prairie and buried soil site A horizons analyzed and discussed in this dissertation. Depending on one's research objectives, quantitative recovery is a viable option, and these various method improvements can be readily implemented by other laboratories.

An improved processing method for carbonate removal prior to δ-13 analysis was also developed. All processing for one sample was performed in a single sample container which minimizes potential sample transfer losses [Appendix F].

In addition to these enhancements in laboratory protocol, a very simple sample probe modification that enables repetitive controlled depth/volume soil sampling of surface prairie soil samples was implemented (pages 63-65). This tool was also used to collect individual samples and to prepare composite soil samples. Soil sample reproducibility and homogeneity are both important.

Careful sample collection, preparation, and skillful execution of the laboratory procedure are the key first steps to obtaining quality data in any application. As the resulting data cannot be any better than the sample or sample fraction, so one should not allow the field sampling technique or the laboratory methodology to become the limiting quality factor in the overall analysis.

Three different botanical sites serve as modern prairie controls in this phytolith study. These sites are representative of the three main prairie types found in Oklahoma:

- Tallgrass Prairie (Manning Tallgrass Prairie, Payne County),

- Dempsey Mixedgrass Prairie (located on the Thurmond Ranch in the Dempsey Divide area, Roger Mills County), and

- Shortgrass Prairie (the Bull Creek Site locale in Beaver County).

The location of these three sites is shown in Figure 61. These three sites are comprised of typical indigenous prairie vegetation which differ from each other due to their local temperature and moisture regimes (Table 8) resulting in the three different prairie types (Figures 5 and 7) . The reference prairie sites will be discussed in the above order, with the most extensive investigative work having been conducted at Manning Prairie near the end of this project.
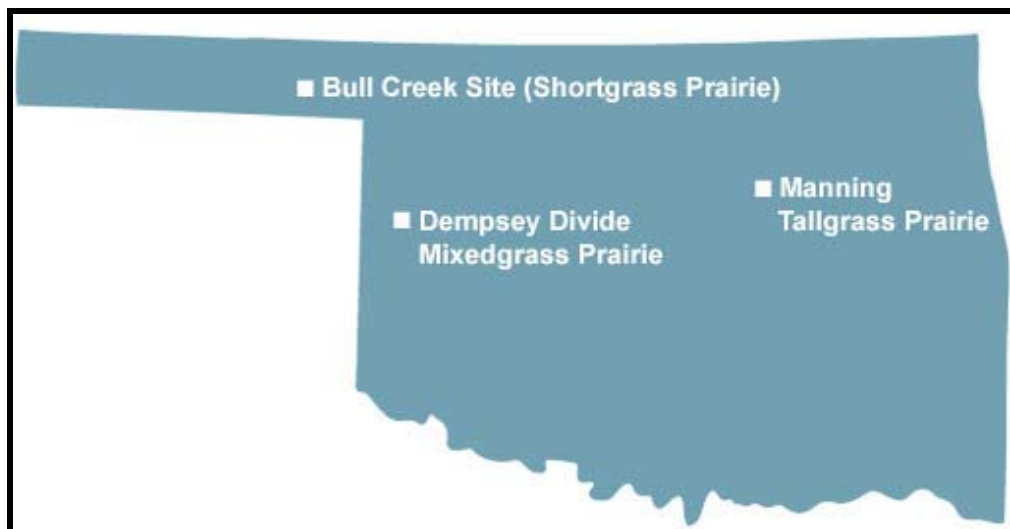
Figure 61. Oklahoma map indicating the location of the prairie control reference sites discussed in this report. (Base map from http://www.okhistory.org/outreach/map.jpg.)

As far as site ecogeography, the following average modern data for geomorphic province, annual number of frost free days, annual normal precipitation, and precipitation effectiveness were gleaned from Tyrl, Bidwell, and Masters (2002:7-12) for the five sites studied in this project (Table 8).

Reference botanical specimens were collected from Manning Tallgrass Prairie and the Dempsey Mixedgrass Prairie at Thurmond Ranch. Phytoliths were quantitatively isolated and recovered from surface A horizon soil samples collected at all three prairie

Table 8
Study and Control Site Ecogeography (Tyrl, Bidwell, Masters, and Jansen 2002)

Site Name	Geomorphic Province	Annual No. Frost Free Days	Normal Precipi-tation (cm)[29]	Precipita-tion Effective-ness[30]	Prairie Control Site[31]	Buried Soil Site
Bull Creek	High Plains	182-189	51-56	< 32 %	SG	X
Dempsey Divide	Western Redbed Plains	196-203	56-61	32-48 % [~34]	MG	
Carnegie Canyon	Western Sandstone Hills	203-210	71-76	32-48 % [~44]		X
Manning Prairie	Northern Limestone Cuesta Plains	203-210	86-91	48-64 % [~55]	TG	
Lizard Site	Claremore Cuesta Plains	189-196	91-97"	48-64 % [~60]		X

---

[29] Average regional rainfall for the interval 1961-1990 originally reported in inches (in ascending order: 20-22", 22-24", 28-30". 34-36", and 36-38" [data presented in the table is rounded to the nearest cm]) (Tyrl et al. 2002:9).

[30] Defined as the ratio of precipitation to evaporation in a 24 hour period (Tyrl et al. 2002:7, 10).

[31] SG = Shortgrass Prairie, MG = Mixedgrass Prairie, and TG = Tallgrass Prairie.

reference sites. Short cell phytoliths from these surface soil samples were tabulated as described in the materials and methods section in order to evaluate climatic indicators present in these modern prairie soil environments.

Manning Tallgrass Prairie – The small relict Tallgrass Prairie remnant known as Manning Prairie is located east-northeast of Cushing, in Payne County, Oklahoma. This 13.4 hectare native pasture (Figure 14) currently serves as a hay meadow which is regularly cut except in times of drought. This site is known to be a virgin (i.e., never plowed) Tallgrass Prairie. The sandstone outcrops present on the eastern end of the site may indicate one reason that the acreage remains unplowed. The west end of the site was selected for reference sampling in this study as the soil column was deeper before sandstone fragments were encountered (20-45 cm deep). Three separate visits to Manning Prairie were conducted to identify botanical species present at the site; the results from those surveys are presented in Table 9.

In a photograph of sampling template location 1 (Figure 14), the center of the sampling area is marked by a white bucket and some of the orange flags at the 20 sampling locations are visible (Figure 11). Due to the ongoing drought when the initial soil samples were collected, prairie hay at Manning Prairie was not cut in 2006. The two sample locations were selected along the top of the gently convex ridge to help minimize potential effects on the phytolith data from being down-slope and potentially subject to

Table 9
Species Identified at Manning Tallgrass Prairie (2006-2009) (page 1 of 3)

Genus species	Common Name	Date[32]
Achillea millefolium L.	Yarrow	1
Aegilops cylindrica L.	Jointed Goatgrass	3
Agrostis hyemalis (Walter) Britton, Sterns & Poggenb.	Winter Bentgrass	2
Allium canadense L.	Meadow Garlic	1, 2
Ambrosia psilostachya DC.	Wester Ragweed	3
Amorpha canescens Pursh	Leadplant	1, 3
Andropogon gerardii ssp.gerardii	Big Bluestem	3
Andropogon ternarius Michx.	Splitbeard Bluestem	3
Andropogon virginicus L.	Broomsedge Bluestem	3
Antennaria neglecta Greene	Field Pussytoes	1
Apocynum cannabinum L.	Indianhemp	2.3
Aristida oligantha Michx.	Annual Threeawn	3
Aristida purpurea Nutt.	Perennial Threeawn	3
Asclepias stenophylla A. Gray	Slimleaf Milkweed	2
Asclepias viridis Walter	Antelope-horn Milkweed	2
Aster ericoides L.	Heather Aster	3
Baptisia australis (L.) R.Br.	Blue Wild Indigo	1
Baptisia spp.	Wild Indigo	3
Baptisia x bushii Small (pro sp.) [bracteata × sphaerocarpa]		1
Baptisia x variicolor M. Kosnik, G. Diggs, P. Redshaw & B. Lipscomb [australis × sphaerocarpa]		1
Bothriochloa laguroides ssp. torreyana	Silver Bluestem	3
Bouteloua curtipendula (Michx.) Tort.	Sideoats Grama	3
Bouteloua gracilis (Willd. Ex Kunth) Lag. ex Griffiths	Blue Grama	3
Bouteloua hirsuta Lag.	Hairy Grama	3
Callirhoe alcaeoides (Michx.) A. Gray	Light Poppymallow	2
Callirhoe involucrata (Torr. & A. Gray) A. Gray	Purple Poppymallow	1
Camassia scilloides (Raf.) Cory	Atlantic Camas	2
Carex meadii Dewey	Mead's Sedge	1
Carex sp. (x3)	Sedge	1
Carya sp.	Hickory	3
Castilleja indivisa Engelm.	Indian Paintbrush	1
Coelorachis cylindrica (Michx.) Nash	Rattail Grass	2
*Coreopsis grandiflora*Hogg ex Sweet	Largeflower Tickseed	2
Coreopsis tinctora Nutt.	Plains Tickseed	1
Dalea purpurea Vent.	Purple Prairie Clover	3

---

[32] Botanical survey inventory dates: 1 = April 22, 2009, 2 = May 23, 2009, and 3 = November 2, 2006.

Genus species	Common Name	Date
Delphinium carolinianum Walter	Carolina Larkspur	2
Desmodium sp.	Trefoil	3
Dichanthelium oligosanthes (Schult.) Gould var.scribnerianum (Nash) Gould	Scribner's Panicum	2, 3
Dichanthelium sphaerocarpon (Elliot) Gould	Roundseed Panicgrass	2
Diospyros virginiana L.	Persimmon	3
Echinacea pallida (Nutt.) Nutt.	Pale Purple Coneflower	2
Eleocharis compressa Sull.		2
Eleocharis sp.	Spikerush	1
Elymus canadensis L.	Canada Wildrye	3
Elymus virginicus L.	Virginia Wildrye	3
Eragrostis spectabilis (Pursh) Steud.	Purple Lovegrass	3
Euthamia gymnospermoides Greene	Texas Goldentop	3
Festuca paradoxa Desv.	Clustered Fescue	2
Helianthus annuus (L.)	Annual Sunflower	3
Helianthus mollis Lam.	Ashy Sunflower	3
Hypoxis hirsuta (L.) Coville	Common Goldstar	1
Juncus acuminatus Michx.	Tapertip Rush	2
Juncus interior Wiegand	Inland Rush	3
Juncus secundus P. Beauv. ex Poir.	Lopsided Rush	2
Juncus torreyi Coville	Torrey's Rush	3
Juniperus virginiana L.	Eastern Redcedar	3
Lepidium densiflorum Schrad.	Common Pepperweed	2
Leptoloma cognatum (Schult.) Chase	Fall Witchgrass	3
Lespedeza capitata Michx.	Roundhead Lespedeza	3
Lespedeza virginica (L.) Britton	Slender Lespedeza	3
Liatris punctata Hook.	Dotted Gayfeather (Blazing Star)	3
Linaria canadensis (L.) Chaz.	Canada Toadflax	2
Marselia vestita Hook. & Grev.	Hairy Waterclover	2
Marshallia caespitosa Nutt. ex DC.	Puffballs	2
Mimosa quadririvalis L. Var. Nuttallii (DC.) Barneby	Catclaw Sensitivebriar	2, 3
Muhlenbergia sp.	Muhly	3
Nemastylis geminiflora Nutt.	Prairie Pleatleaf	1. 3
Nothoscordum bivalve (L.) Britton	Crowpoison	1
Oenothera linifolia Nutt.	Threadleaf Evening Primrose	2
Oenothera speciosa Nutt.	Pinkladies	2
Opuntia macrorhiza Engelm.	Prickly Pear	1, 3
Oxalis violacea L.	Violet Wood Sorrel	1

Genus species	Common Name	Date
Packera glabella (Poir.) C. Jeffrey	Butterweed	2
Packera tampicana (DC.) C. Jeffrey	Great Plains Ragwort	1
Penstemon cobaea Nutt.	Cobaea Beardtongue	2
Penstemon oklahomensis Pennell	Oklahoma Beardtongue	2
Petalostemon purpureus Vent. var. purpurea	Purple Prairie Clover	3
Phalaris caroliniana Walter	Carolina Canarygrass	2
Polytaenia nuttallii DC.	Nuttall's Prairie Parsley	1
Populus deltoides Marshall	Easter Cottonwood	3
Psoralidium tenuifolium (Pursh) Rydb.	Scurfpea (Prairie Turnip)	1
Quercus marilandica Muenchh.	Blackjack Oak	3
Quercus stellata Wangenh.	Post Oak	3
Rhus copallinum L.	Winged Sumac	2, 3
Rubus sp.	Blackberry	2, 3
Salvia azurea Michx. Ex Lam.	Blue Sage (Pitcher Sage)	3
Schedonorus pratensis (Huds.) P. Beauv.	Meadow Fescue	2
Schizachyrium scoparium (Michx.) Nash	Little Bluestem	3
Scirpus sp.		3
Silphinium laciniatum L.	Compass Plant	2, 3
Sisyrinchium angustifolium Mill.	Narrowleaf Blue-eyed Grass	1
Sisyrinchium campestre E.P. Bicknell	Prairie Blue-eyed Grass	1
Solidago missouriensis Nutt.	Missouri Goldenrod	3
Sorghastrum nutans (L.) Nash	Indiangrass	3
Spermolepis inermis (Nutt. ex DC.) Mathias & Constance	Red River Scaleseed	2
Sphenopolis obtusata (Michx.) Scribn.	Prairie Wedgescale	2
Sporobolus asper (Michx.) Kunth	Tall Dropseed	3
Sporobolus compositus (Poir.) Merr.	Composite Dropseed	2
Tradescantia ohiensis Raf.	Bluejacket	2
Tridens flavus (L.) Hitchc.	Purpletop	3
Tridens strictus (Nutt.) Nash	Longspike Tridens	3
Triodanis perfoliata (L.) Nieuwl. var. biflora (Ruiz & Pav.) Bradley	Small Venus' Looking-glass	1
Ulmus americana L.	American Elm	3
Valerianella radiata (L.) Dufr.	Beaked Cornsalad	2
Vulpia octoflora (Walter) Rydb.	Sixweeks Fescue	2

the influence of run off (i.e., erosion or deposition) or from a different soil type. No specific or unusual surface features were visible due to uncut prairie growth.

Soil in the center of sample location 1 was removed with a 4 inch hand auger at position "o" [origin, or center of sampling template] to a depth of 107 cm. The top 35 cm from the side of the auger hole wall was removed by shovel and photographed showing the A and BA horizons (Figure 62). The study area was selected in Coyle Loam which is a fine-loamy, siliceous, active, thermic udic argiustolls (Web Soil Survey). The soil profile description of the soil encountered at sample location "o" is in Table 10. The soil pH values are in Table 10.

Individual soil samples for phytolith analysis were collected at each black numbered location in the circle (Figure 8) and pooled resulting in the n=1 [x=20] composite sample. Additional soil samples taken at the locations of the three underlined numbers were pooled to yield the n=1 [x=3] composite sample. The n=1 [x=1] sample was taken at the center of the template (location "o") where the soil profile sample was taken.

Manning Prairie Data Set 1: Phytolith concentration change with soil depth - The phytolith concentration of the soil samples is presented as the percent of the weight of phytoliths/weight of dry soil [or weight of phytoliths/weight of dry silt] (wt/wt %) in Table 11.   The phytolith/soil wt/wt % data from Table 11 are plotted in Figure 63 for all three samples (n=1 [x=1, 3, and 20]).

Although there is some variation in the data, overall there is good agreement in the three different soil samples analyzed (n=1 and composite samples n=1 [x=3], and n=1 [x=20]). The increased phytolith concentration deviations in the n=1 [x=20] profile (10-15 cm, 25-30 cm, and 30-35 cm in Figure 63) are attributed to be the result of several soft spots or voids (suspected rodent runs and/or nests) encountered in the southeast quadrant of the sampling area. These questionable sample aliquots were pooled with the others as planned in an effort to retain the total target number of subsamples comprising the

Figure 62. Top 35 cm of soil showing A and BA horizons at Manning Tallgrass Prairie sampling site number 1.

Table 10. Soil Description at Manning Prairie Sampling Site 1, Payne County, Oklahoma (page 1 of 2)

Horizon	Depth (cm)	Color	Texture	Structure	Consistency	Special Features
A	0-15	10YR3/2	L	3fGR	vfr	many fine roots
BA	15-30	10YR4/3	L	2mGR	vfr	common fine roots
	30-45	10YR4/3	L	2mGR	vfr	few fine roots
Bt1	45-61	10YR5/4	CL	2mSBK	vfr	ss frag 23" few fine roots. common fine redox concentrations (5YR5/8). Size and abundance of concentrations increase with depth to amount reported below
	61-69	10YR5/4	CL	2mSBK	fr	common med redox concentrations (5YR5/8) few coarse Fe/Mn concentrations along ped faces/- weathered ss fractures
Bt2	69-76	10YR5/4	SCL	1cSBK	fr	few med redox depletions (2.5 YR7/1) many fine redox concentrations 7.5YR5/8 many coarse/very coarse Fe/Mn concentrations along ped faces/weathered sandstone fractions and inside of ss many fine-coarse ss gravels, ss color 7.5YR5/8
	76-84	10YR5/4	SCL	1cSBK	fr	common med redox concentrations (7.5YR5/8) many fine-coarse ss gravels (7.5YR5.8) Fe/Mn prevalent within ss gravels and on surface very few fine redox depletions (7.5Yr7/1)
	84-90	10YR5/4	SCL	1cSBK	fr	many fine-coarse redox concentrations (7.5YR5/8) many fine-coarse Fe/Mn concentrations common fine redox depletions (7.5YR7/1) many fine-coarse ss gravels

149

Table 10. Soil Description at Manning Prairie Sampling Site 1, Payne County, Oklahoma (page 2 of 2)

Horizon	Depth (cm)	Color	Texture	Structure	Consistency	Special Features
Cr	90-99	10YR5/8	s and			many fine-coarse ss gravels (5YR5/8 and 10YR5/8) center of gravels are red (5YR5/8), weathered to yellow (10YR5/8) few redox depletions (7.5YR7/1) many fine-coarse Fe/Mn concentrations many medium masses (10YR5/3)
	99-107	10YR5/8	predominantly degraded ss			many medium-coarse masses (10YR5/3) many fine-coarse ss gravels (5YR5/8 and 10YR5.8) many med redox depletions (7.5YR7/1) many fine-coarse Fe/Mn concentrations

Table 11

Manning Tallgrass Prairie Soil pH and n=1 [x=20] Replicate Information

Sample Depth (cm)	Soil pH	No. of Replicates in n=20 Composite Sample
0-5	5.67	20
5-10	4.61	20
10-15	4.63	20
15-20	4.65	20
20-25	4.75	19
25-30	4.91	18
30-35	5.22	17
35-40	5.59	15
40-45	5.88	13

composite sample. However, in retrospect, the suspect subsamples should have been discarded and omitted from the study. The presumed rodent disturbances were not encountered in the n=1 and n=3 samples. The substantial variation that can actually occur between individual samples is addressed later in Manning Experiment ("Data Set") 3.

Overall the exponential phytolith data concentration profile as relative to soil depth (Figure 63) is interpreted as indicative of stable long-term soil development, with probable contributions to soil building by gradual accumulation of wind-borne sediment and accumulation of inorganic portions of decaying vegetation. The stats for the three sets of data (Table 12 and Figure 63) are in Table 13.

Table 12
Manning Tallgrass Prairie
Experiment 1 - Phytolith Weight in Coyle Loam
Soil Profile in 5 cm Depth Intervals through 45 cm

Depth (cm)	Composite Sample Size (n=1 [x=_])	Phytoliths (g)	Phytoliths/Soil (wt/wt %)	Phytoliths/Silt (wt/wt %)
0-5	1	0.1726	0.69%	1.86%
5-10	1	0.1345	0.53%	1.28%
10-15	1	0.1096	0.43%	1.07%
15-20	1	0.0913	0.36%	0.91%
20-25	1	0.0767	0.30%	0.79%
25-30	1	0.0618	0.25%	0.67%
30-35	1	0.0574	0.23%	0.71%
35-40	1	0.0382	0.15%	0.51%
40-45	1	0.0341	0.13%	0.43%
0-5	3	0.1385	0.55%	1.52%
5-10	3	0.1185	0.47%	1.24%
10-15	3	0.0936	0.37%	1.10%
15-20	3	0.0825	0.33%	1.03%
20-25	3	0.0825	0.33%	1.01%
25-30	3	0.0610	0.24%	0.79%
30-35	3	0.0517	0.21%	0.72%
35-40	3	0.0369	0.15%	0.52%
40-45	3	0.0233	0.09%	0.34%
0-5	20	0.1577	0.63%	1.61%
5-10	20	0.1244	0.49%	1.31%
10-15	20	0.1163	0.46%	1.30%
15-20	20	0.0935	0.36%	1.03%
20-25	19	0.0728	0.29%	0.92%
25-30	18	0.0894	0.35%	1.18%
30-35	17	0.0703	0.28%	0.99%
35-40	15	0.0416	0.17%	0.58%
40-45	13	0.0362	0.14%	0.53%
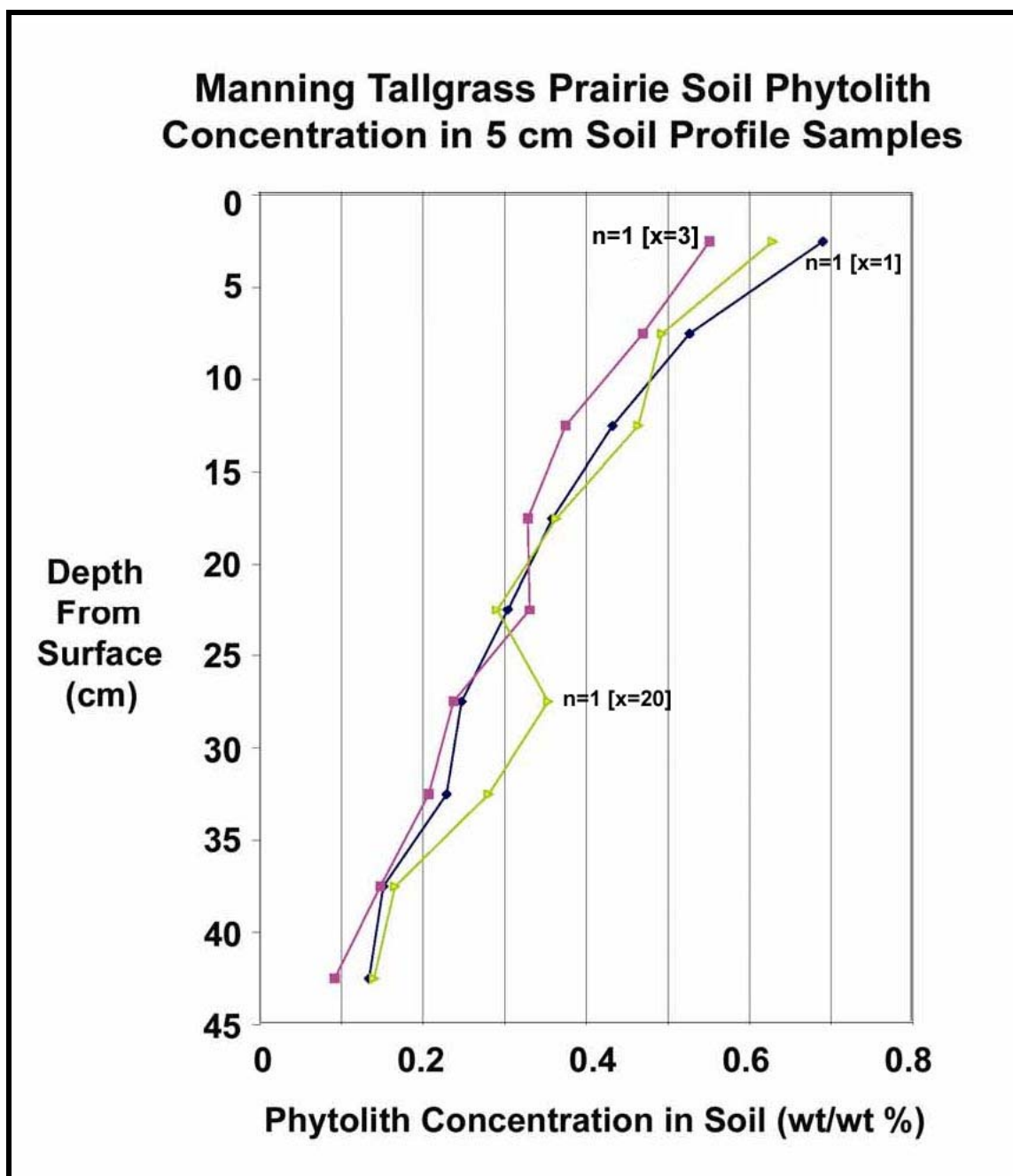
Figure 63. Soil Phytolith concentration plotted versus sample depth (soil samples collected in 5 cm increments). [Actual n = 1 [x = 20] sample sizes for each depth are in Table 11.]

Table 13
Manning Tallgrass Prairie Experiment 1
Phytolith Concentration Mean and Standard Deviation in Soil (wt/wt %)

Sample depth (cm)	n=1 [x=1]	n=1 [x=3]	n=1 [x=20]	Mean (n=3)	Std Dev (n=3)
0-5	0.69%	0.55%	0.63%	0.62%	0.070
5-10	0.53%	0.47%	0.49%	0.50%	0.031
10-15	0.43%	0.37%	0.46%	0.42%	0.046
15-20	0.36%	0.33%	0.36%	0.35%	0.017
20-25	0.30%	0.33%	0.29%	0.31%	0.021
25-30	0.25%	0.24%	0.35%	0.28%	0.061
30-35	0.23%	0.21%	0.28%	0.24%	0.036
35-40	0.15%	0.15%	0.17%	0.16%	0.012
40-45	0.13%	0.09%	0.14%	0.12%	0.026

Manning Prairie Data Set 2: Phytolith Distribution as Climatic Indicators – The

phytoliths recovered during Manning Tallgrass Prairie Experiment 1 were analyzed

further. A representative portion recovered from each soil phytolith sample (n=1 [x=20])

was mounted on microscope slides for evaluation. The observed morphologic forms

observed were tabulated (Table 14). The concentration of the major short cell phytolith

forms in the composite soil samples (n=1 [x=20]) was determined by summing the

individual counts for those short cell types, and normalizing their values (Table 15). In

these twelve categories, there are cool season morphologies (Pooid forms: keeled,

conical, pyramidal, and crenate), hot/dry climate season morphologies (Chloridoid forms:

tall saddles and squat saddles), and hot moist climate morphologies (the five Panicoid

forms designated as lobate and cross). The Stipa category actually has plants in both the

cool and warm moist season categories—in the following data processing, the Stipa are

included in the hot moist climatic category. The values for the members of these three

metabolic/climatic groups are summed in Table 16, and presented as normalized values

in Table 17. The additional phytolith forms listed in Table 14 are not short cells,

although their frequency was tabulated when scanning the slides to count short cell

phytoliths.

The climatic categories represented in the different phytolith short cell forms

indicate the environment where these specific species (and plant communities or

associations) of plants best thrive. These plant adaptations to climate are reflected in

their cell metabolism, specifically their ability to efficiently utilized carbon at various

temperatures and their need for and ability to utilize (and sequester) water (Taiz and

Zeiger 2002). The Pooids are the cool wet season phytoliths which have C3 metabolism.

The Chloridoids are the hot dry season phytoliths and best thrive under those conditions

with their C4 metabolism which are adapted to conserving plant water. The hot moist

season plants are the Panicoids which do well in warm weather and also have C4

metabolism—but have a higher water requirement than the Chloridoids. With both C3

and C4 members, the Stipa straddle these two metabolic groups. The contribution by the

so-called Stipa form is a relatively minor component of these phytolith counts; the other

three Poaceae subfamilies are the predominant climatic short cell phytolith indicator

groupings.

A plot of the data in Table 16 is presented in Figure 64. Modern day climate is

assumed to be represented by sample 1. Relative to sample 1, the interval represented by

sample 2 appears to have been a wetter period, while the interval represented in sample 3 (10-15 cm deep) appears to have been more similar to the modern climate. The interval shown by intervals 4-7 was relatively stable, although there was a slight cooling after interval 4. In intervals 8 and 9, significant long term continuous cooling is reflected in the phytolith data. (As discussed later in this chapter, the climatic interpretation of non-A horizons based on phytolith composition is not nearly as straightforward as for A horizons because A horizons had stable long-term established plant communities present during pedogenesis.) There are no radiocarbon dates available for this profile. The 5 cm sampling interval makes each individual sample a time composite representing many years (perhaps hundreds if not thousands of years). Thus, climatic events of short duration are not discernible in this record. What is often identifiable in the phytolith data are times of stability marked by stable soil surfaces, major changes, and/or long term events.

Several other particle types recovered with the phytoliths were tabulated with the original data when scanning microscope slides of phytoliths (Table 14). These other specimen counts were summed; in order to provide a more useful frequency of occurrence value, these forms were ratioed to the total diagnostic short cell count in the same fields of view (from Table 16); these ratios are tabulated in Table 18.

The sponge spicules were very uncommon in the scanned microscope slide fields, but were present in small numbers on each slide. In this upland setting, the spicules are presumably a result of eolian contribution (Wilding and Drees 1971) and/or from animal

Table 14
Manning Tallgrass Prairie Experiment 2
Counts by Phytolith Morphology in Representative
5 cm Interval Soil Profile Samples (n=1 [x=20])

Sample Depth, 5 cm increments	0-5	5-10	10-15	15-20	20-25	25-30	30-35	35-40	40-45
Keeled	26	32	21	15	11	17	28	12	14
Conical	49	116	58	66	40	56	96	104	72
Pyramidal	9	12	4	2	4	2	6	16	14
Crenate	12	15	23	15	23	27	50	56	13
Saddle, Squat	36	69	34	41	34	46	80	43	11
Saddle, Tall	47	65	48	66	41	49	90	76	31
Stipa	3	8	3	5	1	3	4	11	9
Lobate, Simple	7.5	10	16	10	18	19	37	24	6
Lobate, Panicoid	71	173.5	62	84	46	61	107	95	23.5
Lobate, Panicoid (compound)	0	4	4	8	12	20	32	1	0
Cross, Panicoid (<10 µ)	9.5	11	7	3	1	2	3	3	8
Cross, Panicoid (>10 µ)	2	2	2	3	3	2	5	0	2
Spiny spheroid	0	0	0	0	0	0	0	7	0
Sponge spicule	0	1	0	0	0	0	0	4	0
Trichome, Hair Cells	4	6	1	3	4	0	4	5	2
Bulliform, square	5	7	10	8	5	6	11	55	2
Bulliform, rectangular	18	35	21	15	9	15	24	62	2
Bulliform, keystone	5	8	16	10	3	6	9	29	4
Bulliform, Y-shaped	1	1	7	0	0	0	0	4	1
Bulliform, other	3	16	12	3	2	8	10	29	3
Elongate, smooth	7	21	11	2	4	1	5	12	6
Elongate, sinuous	3	3	7	1	1	1	2	3	2
Elongate, castillate	3	6	5	0	0	2	2	5	0
Elongate, spiny	0	0	0	0	0	2	2	1	0
Sedge	1	8	2	2.5	4	6.5	10.5	2.5	1
Charcoal	12	25	5	29	12	18	30	105	176
Diatoms and fragments	64	65	27	19	19	13	32	18	16
Burned Panicoid lobates	9	14.5	10.5	9	4	9	13	28.5	9

Table 15
Manning Tallgrass Prairie Experiment 2
Normalized % Phytolith Counts (n=1 [x=20])
Composite Soil Samples in 5 cm Depth Intervals through 45 cm

Phytolith Short Cell Morphology	0-5 cm	-10 cm	-15 cm	-20 cm	-25 cm	-30 cm	-35 cm	-40 cm	-45 cm
Keeled	9.6	6.2	7.6	4.8	5.0	6.0	5.5	2.7	6.9
Conical	18.0	22.4	20.9	21.3	18.0	19.7	19.0	23.6	35.4
Pyramidal	3.3	2.3	1.4	0.6	1.8	0.7	1.2	3.6	6.9
Crenate	4.4	2.9	8.3	4.8	10.4	9.5	9.9	12.7	6.4
Saddle, Squat	13.2	13.3	12.2	13.2	15.3	16.2	15.8	9.8	5.4
Saddle, Tall	17.3	12.6	17.3	21.3	18.5	17.3	17.8	17.2	15.2
Stipa	1.1	1.5	1.1	1.6	0.5	1.1	0.8	2.5	4.4
Lobate, Simple	2.8	1.9	5.8	3.2	8.1	6.7	7.3	5.4	2.9
Lobate, Panicoid	26.1	33.5	22.3	27.1	20.7	21.5	21.1	21.5	11.5
Lobate, Panicoid (compound)	0.0	0.8	1.4	2.6	5.4	7.0	6.3	0.2	0.0
Cross (>10 μ)	3.5	2.1	2.5	1.0	0.5	0.7	0.6	0.7	3.9
Cross (>10 μ)	0.7	0.4	0.7	1.0	1.4	0.7	1.0	0.0	1.0

Table 16
Manning Tallgrass Prairie Experiment 2
Total Short Cell Phytoliths Grouped by Climatic Indicators
(n=1 [x=20]) Composite Soil Samples in 5 cm Depth Intervals through 45 cm)

	0-5 cm	-10 cm	-15 cm	-20 cm	-25 cm	-30 cm	-35 cm	-40 cm	-45 cm
Pooids (Cool Wet Phytoliths)	96	175	106	98	78	102	180	188	113
Chloridoids (Hot Dry Phytoliths)	83	134	82	107	75	95	170	119	42
Panicoids (Hot Moist Phytoliths)	93	208.5	94	113	81	107	188	134	48.5
Total Short Cell Phytoliths	272	517.5	282	318	234	304	538	441	203.5

Table 17
Manning Tallgrass Prairie Experiment 2
Normalized % Short Cell Phytoliths Grouped by Climatic Indicators
(n=1 [x=20]) Composite Soil Samples in 5 cm Depth Intervals through 45 cm)

	0-5 cm	-10 cm	-15 cm	-20 cm	-25 cm	-30 cm	-35 cm	-40 cm	-45 cm
Cool Wet Phytoliths	35.3	33.8	38.1	31.6	35.1	35.9	35.6	42.6	55.5
Hot Dry Phytoliths	30.5	25.9	29.5	34.5	33.8	33.5	33.6	27.0	20.6
Hot Moist Phytoliths	34.2	40.3	32.4	33.9	31.1	30.6	30.8	30.4	23.8
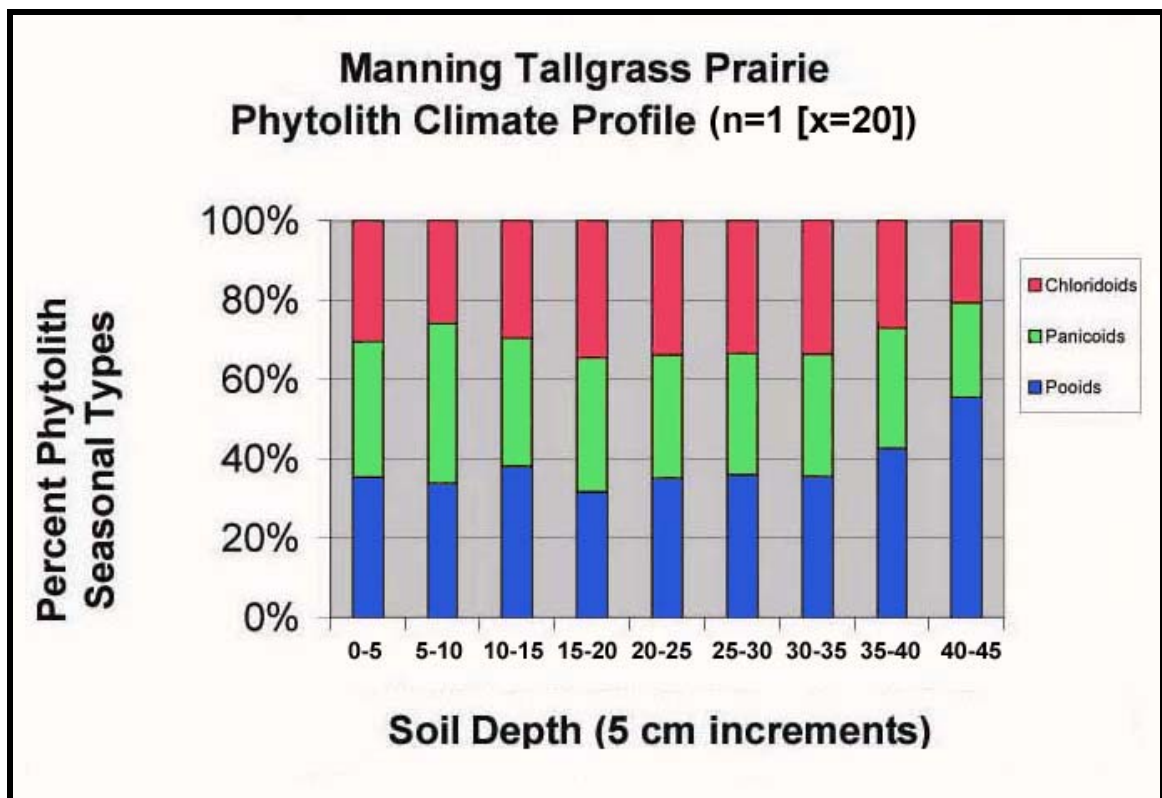
Figure 64. Graph of data from Table 16 illustrating representative contribution of each seasonal phytolith short cell category to the total phytolith count.

Table 18
Manning Tallgrass Prairie Experiment 2
Incidence of Other Particles Recovered in the Phytolith Fraction
Relative to Phytolith Short Cell Forms Counted (Soil Composites, n=1 [x=20])

Sample Depth (cm)	Charcoal	Burned Panicoids	Diatoms	Sedge Phytoliths	Sponge Spicules
0-5	4.41%	1.40%	23.53%	0.37%	0.00%
05-10	4.83%	5.36%	12.56%	1.55%	0.00%
10-15	1.80%	3.70%	9.71%	0.72%	0.00%
15-20	9.35%	2.90%	6.13%	0.81%	0.00%
20-25	5.41%	1.80%	8.56%	1.80%	0.00%
25-30	6.34%	3.17%	4.58%	2.29%	0.00%
30-35	5.93%	2.57%	6.32%	2.08%	0.00%
35-40	23.81%	6.46%	4.08%	0.57%	0.91%
40-45	86.49%	4.42%	7.86%	0.49%	0.00%

droppings. The other four categories in Table 18 were present in all counted sample

tabulations. Sedges are present at this dry upland site in modern times, so their presence

in the phytolith record is not unexpected. The observed diatoms may be indigenous soil

diatoms (Sylvia, Fuhrmann, Hartel, Zuberer 1999:98). Many diatoms at Manning

Tallgrass Prairie were small (suggesting they may be soil diatoms (Sylvia et. al.

1999:98)), and very faint or "wispy". This later observation and their very high surface

area may indicate that their decreasing count with soil depth is due to gradual dissolution

by soil water. The exponential decrease of the relative soil diatom content (Table 18)

mirrors that previously noted for phytoliths (Figure 63) albeit at a lower overall

concentration.

     Two other tabulated forms of note are the burned Panicoid phytoliths (which were

also counted as various Panicoid forms, but these were noted to be discolored by having

been exposed to fire), and the charcoal fragments (Table 18). Although a few burned Chloridoid and Pooid phytoliths were observed, the vast majority of burned phytoliths were Panicoid forms. If fire is present, this burned Panicoid prevalence would be expected as the bulk of the Tallgrass prairie biomass is present as Panicoid species. This occasional burning may have been caused by spring fires (such as occurs during modern thunderstorms from lightning strikes) when the dry biomass from the preceding year was still standing. Several large aggregates of charred phytoliths were observed, implying based on particle size that at least some of the prairie fires were definitely local rather than all of the burned phytoliths being introduced by eolian processes.

The other major particle type of interest is another fire indicator—charcoal. However, the charcoal concentration data does not seem to correlate with the burned Panicoid data. There is a small charcoal spike in sample 4, and a huge spike in samples 8 and 9. The sample 4 spike correlates with a period of warmer climate, but with roughly the same moisture level as indicated by the 31.1-33.9 % Panicoid range (Table 17 and Figure 64). However, the charcoal fragment concentration increase in samples 8 and 9 (35-45 cm) is different because it correlates with a strong prolonged cooler, wetter period (Table 17 and Figure 64). Sample 8 also had a significant increase in burned Panicoid phytolith concentrations. One way to explain this combination of parameters would be some cataclysmic incident such as a volcanic eruption or an asteroid-related event. The time interval represented by samples 8 and 9 is currently unknown. Unfortunately, it is not possible to determine if charcoal deposition at a particular site is due to water or aerial transport as charcoal is simply an environmental variable (Williams, Dunkerley,

De Deckker, Kershaw, and Chappell 2003:201-203).
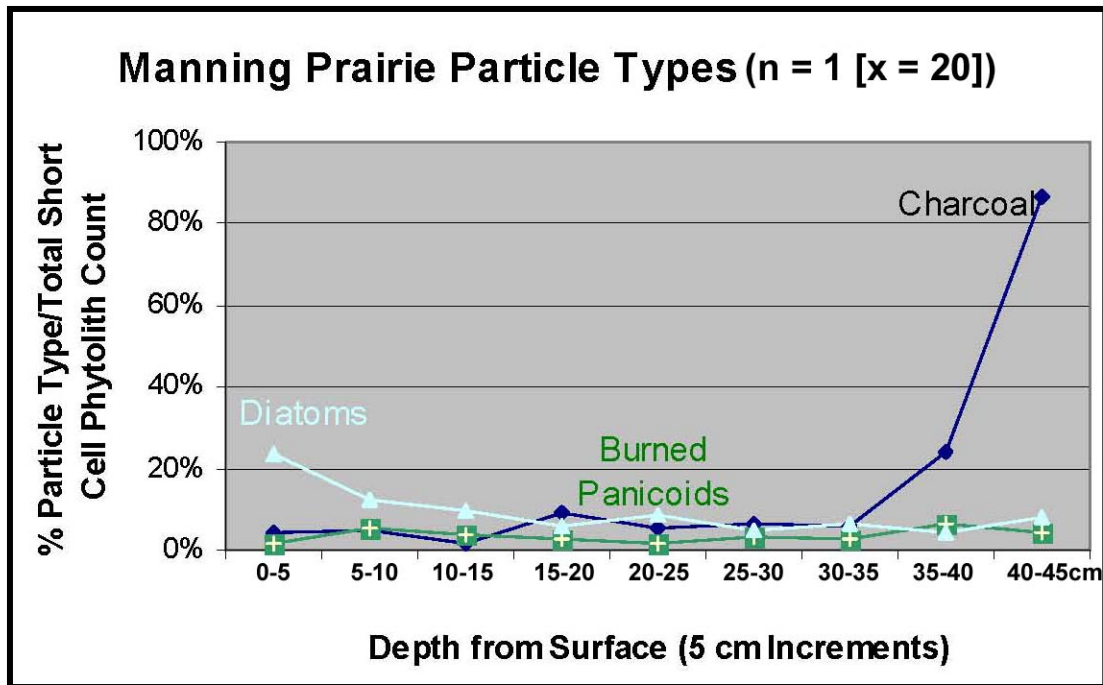
Figure 65. Incidence of diatoms, burned Panicoid phytoliths, and charcoal relative to total short counts in the same microscopic fields.

Manning Prairie Data Set 3: Study of 5 cm replicate surface soil samples to evaluate sampling reproducibility and homogeneity of soil components and phytoliths (n=21) – In this final experiment at Manning Prairie, the same circular sampling design was used (Figure 8) at location 2 (Figure 14). The center of the circle was designated as sample 0, so a total of 21 samples were collected. Four sequential 5 cm sample sets were collected with increasing depth; however, only the top 5 cm set of 21 soil samples were analyzed. These samples were collected with the soil probe stop set at 5 cm intervals, and immediately transferred to preweighed labeled sample jars from the probe. The discrete samples were then oven dried and weighed to determine soil sample weight in

each soil sample pulled. The remaining steps in sample processing were identical to those described previously. Phytoliths were extracted from each intact soil sample.

The resulting total soil sample weight (corrected weight after organic material in the sand and silt fraction was back calculated out), sand weight, silt weight, and weight of phytoliths recovered from all 21 samples are shown in Table 19. The same data ranked by relative soil phytolith concentration is presented in Table 20. The average values for n=21 are shown at the bottom of this table.

The next step of this evaluation was to count phytolith forms on microscope slides for each of the 21 samples; the resulting sample counts are presented in Tables 22 and 23. The normalized short cell phytolith values for these 21 five cm surface soil samples are presented in Tables 24 and 25. The average value and relevant statistics for these 12 short cell form categories are presented in Table 26.

The same data, ranked by highest to lowest normalized % relative to short cell phytolith count is shown in Table 27. As would be expected if the data was reasonable, the highest concentration of phytoliths has the lowest percent standard deviation. The lower concentration particles have very high percent standard deviations; this is due to their relative paucity in the samples. This phenomenon is also in part due to the non-uniform distribution of plants on the prairie, and that most of the plant litter containing phytoliths is incorporated into the soil follows a vertical drop to the soil as the individual plants die and decay or undergo senescence.

Table 19. Manning Prairie Surface Soil (0-5 cm) Sample Reproducibility Test, Sample Values Ranked by Sample Numerical Order

Sample	Corrected Sample Wt (g, no OM)	Initial Sand Wt (g)	Sand after OM removal (g)	OM Loss from Sand (g)	Silt Wt (g, no OM)	Clay by Difference	% Sand	% Silt	% Clay	phytolith wt (g)
Manning 0	9.6007	5.2755	5.0362	0.2393	3.6132	0.9513	52.5%	37.6%	9.9%	0.0753
Manning 1	11.2742	6.4659	5.9001	0.5658	4.2654	1.1087	52.3%	37.8%	9.8%	0.1093
Manning 2	11.0900	6.0928	5.7728	0.3200	4.3563	0.9609	52.1%	39.3%	8.7%	0.1140
Manning 3	10.9175	5.4831	5.3206	0.1625	4.4269	1.1700	48.7%	40.5%	10.7%	0.0961
Manning 4	12.4471	6.3850	6.1221	0.2629	4.7347	1.5903	49.2%	38.0%	12.8%	0.1087
Manning 5	13.7457	7.6667	7.4124	0.2543	4.9297	1.4036	53.9%	35.9%	10.2%	0.1237
Manning 6	9.7228	5.4704	5.1632	0.3072	3.5086	1.0510	53.1%	36.1%	10.8%	0.1130
Manning 7	12.2336	6.5332	6.3468	0.1864	4.4989	1.3879	51.9%	36.8%	11.3%	0.1023
Manning 8	13.2876	7.1961	6.9637	0.2324	4.9502	1.3737	52.4%	37.3%	10.3%	0.1084
Manning 9	12.8533	6.6297	6.3730	0.2567	4.9868	1.4935	49.6%	38.8%	11.6%	0.1172
Manning 10	13.5109	7.4437	7.1646	0.2791	5.1905	1.1558	53.0%	38.4%	8.6%	0.1264
Manning 11	12.6947	6.8171	6.6018	0.2153	4.8900	1.2029	52.0%	38.5%	9.5%	0.1528
Manning 12	12.3168	6.1879	5.9847	0.2032	4.9092	1.4229	48.6%	39.9%	11.6%	0.1252
Manning 13	15.1965	8.1874	8.0239	0.1635	5.6478	1.5248	52.8%	37.2%	10.0%	0.1169
Manning 14	12.8275	7.0557	6.8032	0.2525	4.6797	1.3446	53.0%	36.5%	10.5%	0.1040
Manning 15	14.1343	7.9512	7.6555	0.2957	5.1284	1.3504	54.2%	36.3%	9.6%	0.1184
Manning 16	11.3837	6.3348	6.0785	0.2563	4.0876	1.2176	53.4%	35.9%	10.7%	0.1079
Manning 17	15.0764	7.8490	7.6054	0.2436	5.8288	1.6422	50.4%	38.7%	10.9%	0.1456
Manning 18	11.8499	6.0436	5.8335	0.2101	4.6757	1.3407	49.2%	39.5%	11.3%	0.1162
Manning 19	14.0073	7.5588	7.3361	0.2227	5.1291	1.5421	52.4%	36.6%	11.0%	0.1304
Manning 20	14.1552	7.5250	7.3102	0.2148	5.2948	1.5502	51.6%	37.4%	11.0%	0.1281

164

Table 20. Manning Prairie Surface (0-5 cm) Sample Reproducibility Test, Samples Ranked by Phytolith Concentration/Unit Soil

Manning Surface Sample	Corrected Sample Wt (g)	Initial Sand Wt (g)	Sand (g) (no OM)	Silt (g) (no OM)	Clay (g)	Sand (%)	Silt (%)	Clay (%)	phytolith wt (g)	phytolith/ soil (wt/wt %)	phytolith/ silt (wt/wt %)
13	15.1965	8.1874	8.0239	5.6478	1.5248	52.8%	37.2%	10.0%	0.1169	0.77%	2.07%
0	9.6007	5.2755	5.0362	3.6132	0.9513	52.5%	37.6%	9.9%	0.0753	0.78%	2.08%
14	12.8275	7.0557	6.8032	4.6797	1.3446	53.0%	36.5%	10.5%	0.1040	0.81%	2.22%
8	13.2876	7.1961	6.9637	4.9502	1.3737	52.4%	37.3%	10.3%	0.1084	0.82%	2.19%
7	12.2336	6.5332	6.3468	4.4989	1.3879	51.9%	36.8%	11.3%	0.1023	0.84%	2.27%
15	14.1343	7.9512	7.6555	5.1284	1.3504	54.2%	36.3%	9.6%	0.1184	0.84%	2.31%
4	12.4471	6.3850	6.1221	4.7347	1.5903	49.2%	38.0%	12.8%	0.1087	0.87%	2.30%
3	10.9175	5.4831	5.3206	4.4269	1.1700	48.7%	40.5%	10.7%	0.0961	0.88%	2.17%
5	13.7457	7.6667	7.4124	4.9297	1.4036	53.9%	35.9%	10.2%	0.1237	0.90%	2.51%
20	14.1552	7.5250	7.3102	5.2948	1.5502	51.6%	37.4%	11.0%	0.1281	0.90%	2.42%
9	12.8533	6.6297	6.3730	4.9868	1.4935	49.6%	38.8%	11.6%	0.1172	0.91%	2.35%
19	14.0073	7.5588	7.3361	5.1291	1.5421	52.4%	36.6%	11.0%	0.1304	0.93%	2.54%
10	13.5109	7.4437	7.1646	5.1905	1.1558	53.0%	38.4%	8.6%	0.1264	0.94%	2.44%
16	11.3837	6.3348	6.0785	4.0876	1.2176	53.4%	35.9%	10.7%	0.1079	0.95%	2.64%
17	15.0764	7.8490	7.6054	5.8288	1.6422	50.4%	38.7%	10.9%	0.1456	0.97%	2.50%
1	11.2742	6.4659	5.9001	4.2654	1.1087	52.3%	37.8%	9.8%	0.1093	0.97%	2.56%
18	11.8499	6.0436	5.8335	4.6757	1.3407	49.2%	39.5%	11.3%	0.1162	0.98%	2.49%
12	12.3168	6.1879	5.9847	4.9092	1.4229	48.6%	39.9%	11.6%	0.1252	1.02%	2.55%
2	11.0900	6.0928	5.7728	4.3563	0.9609	52.1%	39.3%	8.7%	0.1140	1.03%	2.62%
6	9.7228	5.4704	5.1632	3.5086	1.0510	53.1%	36.1%	10.8%	0.1130	1.16%	3.22%
11	12.6947	6.8171	6.6018	4.8900	1.2029	52.0%	38.5%	9.5%	0.1528	1.20%	3.12%
Average:											
(n=21)	12.5869	6.7692	6.5147	4.7492	1.3231	51.7%	37.8%	10.5%	0.1162	0.93%	2.45%

Table 21. Manning Prairie Surface Soil (0-5 cm) Sample Reproducibility Test; Comparison of n=17 and n=21 data

n=		Corrected Sample Wt (g) (no OM)	Sand (g) (no OM)	Silt (g) (no OM)	Clay (g)	Sand %	Silt %	Clay %	phytolith wt (g)	Phytolith/ soil (wt/wt %)	Phytolith/ silt (wt/wt %)
21	Average	12.5869	6.5147	4.7492	1.3231	51.7%	37.8%	10.5%	0.1162	0.93%	2.45%
21	Std Dev	1.5618	0.8689	0.5814	0.2042	0.0173	0.0136	0.0100	0.0165	0.0011	0.0058
21	Avg Dev	1.2412	0.7362	0.4423	0.1682	0.0140	0.0113	0.0077	0.0117	0.0008	0.0020
21	% Std Dev	12.41%	13.34%	12.24%	15.43%	3.34%	3.60%	9.50%	14.22%	12.08%	23.83%

Table 22. Manning Prairie 0-5 cm Surface Soil Sample Raw Phytolith Counts (Sample Locations 0-10)

Soil Sample Location	0	1	2	3	4	5	6	7	8	9	10
Phytolith morphology											
Keeled	32	29	30	23	19	19	16	15	10	18	23
Conical	67	76	79	44	73	70	88	78	71	88	83
Pyramidal	13	15	9	5	9	14	15	11	10	11	9
Crenate	9	10	20	12	15	15	7	14	5	11	10
Saddle, squat	32	38	33	27	37	44	27	28	15	35	24
Saddle, tall	59	65	72	41	53	66	60	59	71	57	82
Stipa	2	8	8	9	5	6	6	4	7	3	6
Lobate, Simple	25	11	6	5	12	3	9.5	16	5	5	16
Lobate, Panicoid	92.5	102.5	129	82.5	87	101.5	135	77	94	89	104
Lobate, Panicoid (compound)	0	6	1	1	3	1	7	3	0	0	7
Cross, Panicoid (<10 um)	7.5	6	9	7	8	9	14	22.5	18	8	11
Cross, Panicoid (>10 um)	2	1	1	2	3	4	2	3	0	3	2
Maize Rondel	0	0	0	0	0	1	0	0	0	0	0
Spiny spheroid	0	0	2	0	1	1	0	1	0	1	0
Sponge spicule	0	0	2	1	0	1	0	1	0	0	0
Trichome, Hair Cells	1	5	0	2	3	7	6	7	4	0	5
Bulliform, square	11	6	10	19	17	17	7	16	12	8	10
Bulliform, rectangular	22	16	10	19	25	17	18	10	31	14	10
Bulliform, keystone	18	11	10	6	25	14	9	8	15	11	10
Bulliform, Y-shaped	1	0	0	0	0	2	1	1	1	2	1
Bulliform, other	15	6	7	12	19	7	7	17	26	28	28
Elongate, smooth	5	3	2	5	4	9	11	9	14	13	4
Elongate, sinuous	2	0	0	0	0	1	1	2	0	4	1
Elongate, castillate	1	0	1	5	3	1	2	4	1	4	3
Elongate, spiny	0	1	0	0	1	0	2	1	1	2	0
Sedge	4.5	0.5	5	3.5	6.5	5	1.5	1.5	5	2	1
Charcoal Fragments	10	13	14	10	23	4	13	8	20	6	9
Diatoms and fragments	95	97	76	93	52	75	99	89	76	88	118

Table 23. Manning Prairie 0-5 cm Surface Soil Sample Raw Phytolith Counts (Sample Locations 11-20)

Soil Sample Location	11	12	13	14	15	16	17	18	19	20
Phytolith morphology										
Keeled	30	11	33	12	12	18	21	18	12	23
Conical	61	72	59	45	66	43	76	47	42	56
Pyramidal	9	9	7	11	14	15	15	5	10	13
Crenate	9	8	10	9	10	10	20	12	7	12
Saddle, squat	26	22	25	11	18	17	27	28	21	20
Saddle, tall	40	52	42	44	31	33	72	37	26	31
Stipa	5	3	1	2	2	5	8	9	5	3
Lobate, Simple	16	12	12	5	7	10	13	13	3	11.5
Lobate, Panicoid	66.5	81.5	73	54.5	69	73	106	73.5	87.5	84
Lobate, Panicoid (compound)	1	0	2	0	3	2	1	2	2	1
Cross, Panicoid (<10 um)	15	6.5	3.5	6	8	13	13	11	6	12
Cross, Panicoid (>10 um)	4	2.5	3	2	2	9	6	3	2	5
Maize Rondel	0	0	0	0	0	0	0	0	0	0
Spiny spheroid	0	0	0	0	0	0	0	0	0	0
Sponge spicule	0	0	0	0	0	0	0	0	0	0
Trichome, Hair Cells	2	6	0	11	7	1	5	3	12	2
Bulliform, square	6	8	6	14	11	4	8	7	6	18
Bulliform, rectangular	10	17	8	23	20	6	22	16	22	13
Bulliform, keystone	5	6	10	35	15	4	15	13	15	10
Bulliform, Y-shaped	0	0	1	0	0	0	0	0	0	0
Bulliform, other	7	13	5	15	28	8	18	7	14	10
Elongate, smooth	3	12	3	2	5	7	14	5	2	8
Elongate, sinuous	0	4	0	1	1	1	2	1	0	2
Elongate, castillate	4	3	0	1	3	1	5	2	1	0
Elongate, spiny	0	0	4	0	2	1	0	2	3	0
Sedge	1	2	0	4	5	2	4	1	1	4
Charcoal Fragments	9	6	14	13	17	11	8	9	15	15
Diatoms and fragments	112	72	72	79	53	110	122	45	70	69

168

Table 24. Manning Prairie 0-5 cm Surface Soil Sample Normalized Short Cell Phytolith Counts (Sample Locations 0-10)

Soil Sample Location	0	1	2	3	4	5	6	7	8	9	10
Phytolith morphology											
Keeled	9.38%	7.89%	7.56%	8.90%	5.86%	5.39%	4.14%	4.54%	3.27%	5.49%	6.10%
Conical	19.65%	20.68%	19.90%	17.02%	22.53%	19.86%	22.77%	23.60%	23.20%	26.83%	22.02%
Pyramidal	3.81%	4.08%	2.27%	1.93%	2.78%	3.97%	3.88%	3.33%	3.27%	3.35%	2.39%
Crenate	2.64%	2.72%	5.04%	4.64%	4.63%	4.26%	1.81%	4.24%	1.63%	3.35%	2.65%
Saddle, squat	9.38%	10.34%	8.31%	10.44%	11.42%	12.48%	6.99%	8.47%	4.90%	10.67%	6.37%
Saddle, tall	17.30%	17.69%	18.14%	15.86%	16.36%	18.72%	15.52%	17.85%	23.20%	17.38%	21.75%
Stipa	0.59%	2.18%	2.02%	3.48%	1.54%	1.70%	1.55%	1.21%	2.29%	0.91%	1.59%
Lobate, Simple	7.33%	2.99%	1.51%	1.93%	3.70%	0.85%	2.46%	4.84%	1.63%	1.52%	4.24%
Lobate, Panicoid	27.13%	27.89%	32.49%	31.91%	26.85%	28.79%	34.93%	23.30%	30.72%	27.13%	27.59%
Lobate, Pan'd(cmpd)	0.00%	1.63%	0.25%	0.39%	0.93%	0.28%	1.81%	0.91%	0.00%	0.00%	1.86%
Cross, Pan'd (<10 um)	2.20%	1.63%	2.27%	2.71%	2.47%	2.55%	3.62%	6.81%	5.88%	2.44%	2.92%
Cross, Pan'd (>10 um)	0.59%	0.27%	0.25%	0.77%	0.93%	1.13%	0.52%	0.91%	0.00%	0.91%	0.53%

Table 25. Manning Prairie 0-5 cm Surface Soil Sample Normalized Short Cell Phytolith Counts (Sample Locations 11-20)

	11	12	13	14	15	16	17	18	19	20
Keeled	10.62%	3.94%	12.20%	5.96%	4.96%	7.26%	5.56%	6.96%	5.37%	8.47%
Conical	21.59%	25.76%	21.81%	22.33%	27.27%	17.34%	20.11%	18.18%	18.79%	20.63%
Pyramidal	3.19%	3.22%	2.59%	5.46%	5.79%	6.05%	3.97%	1.93%	4.47%	4.79%
Crenate	3.19%	2.86%	3.70%	4.47%	4.13%	4.03%	5.29%	4.64%	3.13%	4.42%
Saddle, squat	9.20%	7.87%	9.24%	5.46%	7.44%	6.85%	7.14%	10.83%	9.40%	7.37%
Saddle, tall	14.16%	18.60%	15.53%	21.84%	12.81%	13.31%	19.05%	14.31%	11.63%	11.42%
Stipa	1.77%	1.07%	0.37%	0.99%	0.83%	2.02%	2.12%	3.48%	2.24%	1.10%
Lobate, Simple	5.66%	4.29%	4.44%	2.48%	2.89%	4.03%	3.44%	5.03%	1.34%	4.24%
Lobate, Panicoid	23.54%	29.16%	26.99%	27.05%	28.51%	29.44%	28.04%	28.43%	39.15%	30.94%
Lobate, Pan'd(empd)	0.35%	0.00%	0.74%	0.00%	1.24%	0.81%	0.26%	0.77%	0.89%	0.37%
Cross, Pan'd (<10 um)	5.31%	2.33%	1.29%	2.98%	3.31%	5.24%	3.44%	4.26%	2.68%	4.42%
Cross, Pan'd (>10 um)	1.42%	0.89%	1.11%	0.99%	0.83%	3.63%	1.59%	1.16%	0.89%	1.84%

The comparable statistical values for a smaller data set, half of these samples were calculated to generate comparable data to that shown in Tables 26 and 27. Tables 28 and 29 resulted from using the sample data from Table 25 (n=10). As would be predicted the percent standard deviations of the higher concentration particles went up and the percent standard deviations of the lowest concentrations went down. However, in this ranking, only the relative positions of pyramidal and crenate reversed between Tables 27 (n=21) and 29 (n=10). To enable ease of comparison, both sets of these values are placed side by side in Table 30.

This initial data suggests that the number of replicates needed depends on the particle types of interest. For the common/high concentration particles, a smaller number of composited sub-samples is probably acceptable. However, for the low concentration

Table 26
Manning Tallgrass Prairie 5 cm Surface Soil Test
Average Normalized Values by Phytolith Short Cell Type (n=21)

Phytolith Short Cell Type	Average	Standard Deviation	95% Confidence Interval	% Standard Deviation
Keeled	**6.66%**	**0.0228947**	**0.0097920**	**34.39%**
Conical	**21.52%**	**0.0281694**	**0.0120480**	**13.09%**
Pyramidal	**3.64%**	**0.0118427**	**0.0050651**	**32.50%**
Crenate	**3.69%**	**0.0103398**	**0.0044223**	**28.03%**
Saddle, Squat	**8.60%**	**0.0200694**	**0.0085837**	**23.34%**
Saddle, Tall	**16.78%**	**0.0322803**	**0.0138063**	**19.23%**
Stipa	**1.67%**	**0.0082163**	**0.0035141**	**49.23%**
Lobate, Simple	**3.37%**	**0.0164790**	**0.0070481**	**48.83%**
Lobate, Panicoid	**29.05%**	**0.0355179**	**0.0151910**	**12.23%**
Lobate, Panicoid (cmpd)	**0.64%**	**0.0059820**	**0.0025585**	**93.07%**
Cross, Panicoid (<10 um)	**3.37%**	**0.0144870**	**0.0061961**	**43.00%**
Cross, Panicoid (>10 um)	**1.01%**	**0.0074267**	**0.0031764**	**73.68%**

particles (trace components of the phytolith assemblage), larger sample composites are clearly more beneficial to the study.

Summing the short cell values into the three climatic groupings (Pooids, Chloridoids, and Panicoids) was performed and the values normalized. The results of this final step for n=21 are shown in Tables 31 and 32. The summary data for n=21 is presented in Table 33. The same calculation performed for the previously discussed n=10 data set is shown in Table 34.

Table 27
Manning Tallgrass Prairie 5 cm Surface Soil Test
Average Normalized Values Ranked by Phytolith Short Cell Type Concentration (n=21)

Phytolith Short Cell Type	Normalized % of Short Cell Phytolith Count	% Standard Deviation
Lobate, Panicoid	29.05%	12.23%
Conical	21.52%	13.09%
Saddle, tall	16.78%	19.23%
Saddle, squat	8.60%	23.34%
Keeled	6.66%	34.39%
Crenate	3.69%	28.03%
Pyramidal	3.64%	32.50%
Lobate, Simple	3.37%	48.83%
Cross, Panicoid (<10 um)	3.37%	43.00%
Stipa	1.67%	49.23%
Cross, Panicoid (>10 um)	1.01%	73.68%
Lobate, Panicoid (compound)	0.64%	93.07%

Table 28
Manning Tallgrass Prairie 5 cm Surface Soil Test
Average Phytolith Values by Short Cell Type (n=10)

Phytolith Short Cell Type	Average	Standard Deviation	95% Confidence Interval	% Standard Deviation
Keeled	7.13%	0.026162	0.016215	36.70%
Conical	21.38%	0.031711	0.019654	14.83%
Pyramidal	4.15%	0.014016	0.008687	33.81%
Crenate	3.99%	0.007668	0.004753	19.24%
Saddle, Squat	8.08%	0.015681	0.009719	19.41%
Saddle, Tall	15.27%	0.034752	0.021539	22.76%
Stipa	1.60%	0.009079	0.005627	56.79%
Lobate, Simple	3.78%	0.012739	0.007896	33.66%
Lobate, Panicoid	29.12%	0.040276	0.024963	13.83%
Lobate, Panicoid(compound)	0.54%	0.004088	0.002534	75.13%
Cross, Panicoid (<10 um)	3.53%	0.012886	0.007987	36.55%
Cross, Panicoid (>10 um)	1.44%	0.008389	0.005200	58.45%

Table 29
Manning Tallgrass Prairie 5 cm Surface Soil Test
Average Phytolith Values Ranked by Short Cell Type Concentration (n=10)

Phytolith Short Cell Type	Normalized % of Short Cell Phytolith Count	% Standard Deviation
Lobate, Panicoid	29.12%	13.83%
Conical	21.38%	14.83%
Saddle, tall	15.27%	22.76%
Saddle, squat	8.08%	19.41%
Keeled	7.13%	36.70%
Pyramidal	4.15%	33.81%
Crenate	3.99%	19.24%
Lobate, Simple	3.78%	33.66%
Cross, Panicoid (<10 um)	3.53%	36.55%
Stipa	1.60%	56.79%
Cross, Panicoid (>10 um)	1.44%	58.45%
Lobate, Panicoid (compound)	0.54%	75.13%

Table 30

Manning Tallgrass Prairie 5 cm Surface Soil Test Comparing Average
Normalized Values Ranked by Phytolith Short Cell Type Concentration (n=21 vs. n=10)

Phytolith Short Cell Type	Normalized % of Short Cell Count (n=21)	Normalized % of Short Cell Count (n=10)	% Standard Deviation (n=21)	% Standard Deviation (n=10)
Lobate, Panicoid	29.05%	29.12%	12.23%	13.83%
Conical	21.52%	21.38%	13.09%	14.83%
Saddle, tall	16.78%	15.27%	19.23%	22.76%
Saddle, squat	8.60%	8.08%	23.34%	19.41%
Keeled	6.66%	7.13%	34.39%	36.70%
Crenate	3.69%	3.99%	28.03%	19.24%
Pyramidal	3.64%	4.15%	32.50%	33.81%
Lobate, Simple	3.37%	3.78%	48.83%	33.66%
Cross, Panicoid (<10 um)	3.37%	3.53%	43.00%	36.55%
Stipa	1.67%	1.60%	49.23%	56.79%
Cross, Panicoid (>10 um)	1.01%	1.44%	73.68%	58.45%
Lobate, Panicoid (compound)	0.64%	0.54%	93.07%	75.13%

The data from the Tables 33-34 is summarized in Table 35. The n=21 stats are clearly the best and provide greater reliability than n=10.

This final set of sample counts in this project also provided the opportunity to compare frequency of burned Panicoid, Chloridoid, and Pooid phytoliths in these 21 replicate samples. These values, as well as those for charcoal, diatoms, sedges, and sponge spicules, are presented in Table 36. This data gives an idea of the average value that would be obtained for these various forms had these 21 sample portions been pooled into one composite sample for analysis. As expected, the individual standard deviations

Table 31. Manning Prairie Surface Soil Sample Short Cell Phytolith Summed by Climatic Indicators (Sample Locations 0-10)

Soil Sample Location	0	1	2	3	4	5	6	7	8	9	10
Pooids (Cool Wet Climate)	121	130	138	84	116	118	126	118	96	128	125
Chloridoids (Hot Dry Climate)	91	103	105	68	90	110	87	87	86	92	106
Panicoids (Hot Wet Climate)	129	134.5	154	106.5	118	124.5	173.5	125.5	124	108	146
Total Diagnostic Short Cell Phytoliths	341	367.5	397	258.5	324	352.5	386.5	330.5	306	328	377
Normalized % Cool Wet Climate Phytoliths	35.48%	35.37%	34.76%	32.50%	35.80%	33.48%	32.60%	35.70%	31.37%	39.02%	33.16%
Normalized % Hot Dry Climate Phytoliths	26.69%	28.03%	26.45%	26.31%	27.78%	31.21%	22.51%	26.32%	28.10%	28.05%	28.12%
Normalized % Hot Wet Climate Phytoliths	37.83%	36.60%	38.79%	41.20%	36.42%	35.32%	44.89%	37.97%	40.52%	32.93%	38.73%

Table 32. Manning Prairie Surface Soil Sample Short Cell Phytolith Summed by Climatic Indicators (Sample Locations 11-20)

Soil Sample Location	11	12	13	14	15	16	17	18	19	20
Pooids (Cool Wet Climate)	109	100	109	77	102	86	132	82	71	104
Chloridoids (Hot Dry Climate)	66	74	67	55	49	50	99	65	47	51
Panicoids (Hot Wet Climate)	107.5	105.5	94.5	69.5	91	112	147	111.5	105.5	116.5
Total Diagnostic Short Cell Phytoliths	282.5	279.5	270.5	201.5	242	248	378	258.5	223.5	271.5
Normalized % Cool Wet Climate Phytoliths	38.58%	35.78%	40.30%	38.21%	42.15%	34.68%	34.92%	31.72%	31.77%	38.31%
Normalized % Hot Dry Climate Phytoliths	23.36%	26.48%	24.77%	27.30%	20.25%	20.16%	26.19%	25.15%	21.03%	18.78%
Normalized % Hot Wet Climate Phytoliths	38.05%	37.75%	34.94%	34.49%	37.60%	45.16%	38.89%	43.13%	47.20%	42.91%

Table 33
Manning Tallgrass Prairie 5 cm Surface Soil Test
Average Phytolith Values Grouped by Climatic Type (n=21)

Phytolith Short Cell Climatic Type	Average Normalized Short Cell %	Standard Deviation	95% Confidence Interval	% Standard Deviation
Pooids (Cool Wet Climate Phytolith Types)	**35.51%**	**0.0298690**	**0.0127750**	**8.41%**
Chloridoids (Hot Dry Climate Phytolith Types)	**25.38%**	**0.0322174**	**0.0137793**	**12.69%**
Panicoids (Hot Moist Climate Phytolith Types)	**39.11%**	**0.0378090**	**0.0161709**	**9.67%**

Table 34
Manning Tallgrass Prairie 5 cm Surface Soil Test
Average Phytolith Values Grouped by Climatic Type (n=10)

Phytolith Short Cell Climatic Type	Average Normalized Short Cell %	Standard Deviation	95% Confidence Interval	% Standard Deviation
Pooids (Cool Wet Climate Phytolith Types	**36.64%**	**0.034677**	**0.021493**	**9.46%**
Chloridoids (Hot Dry Climate Phytolith Types)	**23.35%**	**0.030670**	**0.019009**	**13.14%**
Panicoids (Hot Moist Climate Phytolith Types)	**40.01%**	**0.043290**	**0.026831**	**10.82%**

for these minor particle forms are high. The charcoal value for this sampling site compares well to that of 4.41% obtained for the n=20 actual composite sample analyzed from Sampling Area 1 (Table 18). This suggests that charcoal particles are fairly uniformly distributed across the site. The normalized diatom concentrations are also in reasonably good agreement (27.91% vs. 23.53%). The other minor particle types show

Table 35
Comparison of Manning Tallgrass Prairie 5 cm Surface Soil Test
Average Phytolith Normalized % Grouped by Climatic Type (n=10 and n=21)

Phytolith Short Cell Climatic Type	Average Short Cell %		% Standard Deviation	
	(n=21)	(n=10)	(n=21)	(n=10)
Pooids (Cool Wet Climate Phytolith Types)	**35.51**	**36.64**	**8.41**	**9.46**
Chloridoids (Hot Dry Climate Phytolith Types)	**25.38**	**23.35**	**12.69**	**13.14**
Panicoids (Hot Moist Climate Phytolith Types)	**39.11**	**40.01**	**9.67**	**10.82**

more variability between these two data sets which may be due to differences in specific plant location and moisture regime relative to individual sampling location.

There are a number of important points that are clearly demonstrated by this final experiment on Manning Tallgrass Prairie soil samples. First, the reproducibility of counting the individual short cell phytolith morphologic forms is relatively poor—especially the minor forms (see Table 30). However, summing the same phytolith data into three climatic categories provides much more reproducible results (Tables 33-35) than any of the individual twelve short cell phytolith forms considered. Second, the smaller subsample (n=10) yields a climatic value different than n=21 and has a somewhat worse standard deviations than n=21 for the climatic version of this consolidated data set (Table 35). This confirms that larger composite sample from more multiple small samples does indeed produce better data as previously indicated by others (see discussion pages 29-30, and Strömberg's (2009a) comments about relative particle frequencies).

Table 36
Manning Tallgrass Prairie Experiment 3
Ratio of Other Particle Forms to Total Phytolith Short Cell Count, Top 5 cm Soil (n=21)

Sample Location	Burned Panicoids	Burned Chloridoids	Burned Pooids	Charcoal	Diatoms	Sedges	Sponge Spicules
0	3.08%	0.88%	0	2.93%	27.86%	1.32%	0
1	2.18%	0	0.27%	3.54%	26.39%	0.14%	0
2	3.27%	1.26%	0.25%	3.53%	19.14%	1.26%	0.50%
3	4.64%	0.77%	0	3.87%	35.98%	1.35%	0.39%
4	3.09%	0.62%	0.62%	7.10%	16.05%	2.01%	0
5	3.69%	0.28%	0.85%	1.13%	21.28%	1.42%	0.28%
6	2.72%	0.00%	0.52%	3.36%	25.61%	0.39%	0
7	4.54%	0.30%	0.61%	2.42%	26.93%	0.45%	0.30%
8	4.58%	0.33%	0	6.54%	24.84%	1.63%	0
9	3.51%	0.91%	0.30%	1.83%	26.83%	0.61%	0
10	3.85%	0	1.59%	2.39%	31.30%	0.27%	0
11	1.59%	0.35%	0	3.19%	39.65%	0.35%	0
12	1.25%	0.72%	1.43%	2.15%	25.76%	0.72%	0
13	2.77%	0	0	5.18%	26.62%	0	0
14	4.47%	0.50%	0	6.45%	39.21%	1.99%	0
15	3.72%	0.41%	0	7.02%	21.90%	4.13%	0
16	2.42%	0.40%	0	4.44%	44.35%	0.81%	0
17	2.38%	0.79%	0	2.12%	32.28%	1.06%	0
18	3.09%	0.39%	0	3.48%	17.41%	0.39%	0
19	2.24%	0	0.45%	6.71%	31.32%	0.45%	0
20	4.79%	0.37%	0.74%	5.52%	25.41%	1.47%	0
average	3.23%	0.44%	0.36%	4.04%	27.91%	1.06%	0.07%
% Std Dev	31.7%	79.6%	131.0%	46.4%	26.4%	87.6%	218.3%

The exponential Manning Tallgrass Prairie phytolith concentration curve with depth through 45 cm suggests long term stable soil development in this upland setting. The individual phytolith categories show considerable variation in distribution, but when the relevant short cell phytolith totals are summed to evaluate the three major botanical climatic indicators—based on cellular metabolic type--the phytolith data clearly show past environmental fluctuations (i.e., temperature and moisture). Burned particles (phytoliths and charcoal) indicate occurrence of occasional fires as would be expected to

maintain the prairie environment. The increased charcoal concentration down profile

suggests the possibility that some massive past fire event did occur that directly affected

the site and/or made an eolian contribution to site debris that was concurrent with

considerable climatic cooling.

Discussion of Manning Tallgrass Prairie Phytolith Data – Of the three prairie

reference sites studied during this research project, the Manning Tallgrass Prairie

provided by far the most complete data set. The Manning data provided information

about soil sampling reproducibility and the distribution of the various phytolith

morphologic forms. The percent standard deviation for the normalized soil content of

twelve individual short cell phytolith forms varied from 12.23-93.07 % (n=21, Table 27).

However, by grouping these twelve short cell forms into their three Poaceae subfamily

"climatic groupings", the statistics for the same sample data's percent standard deviation

improved to 8.41-12.69 % for the three categories (Table 33) indicating the benefit of

using the summed short cell data as climatic indicators (i.e., the representing the overall

temperature and moisture regime of the specific study area rather than individual short

cell forms). The values and reproducibility of the n=21 data set were better than those

achieved by the n=10 data subset (Tables 30, 33, 34). Smaller composite samples may be

useful for developing a general climatic signature of the particular soil being investigated;

however, phytoliths with a low incidence of occurrence at a given site are more likely to

be recovered in the larger pooled samples due to their limited representation. Thus, the

size of the composite sample collected (i.e., number of individual soil aliquots added to

make up the composite soil sample) may be altered depending on one's specific research objectives.

Actual constant soil volume sampling proved to be a reliable sampling technique. The percent standard deviation of the soil sample weight collected (12.41%, n=21, Table 21) was much larger that that obtained for the percents of sand indicating that the soil textural components are uniformly distributed. The larger variation in soil sample size is primarily due to air voids in the soil sample and bioturbation (i.e., bulk density) which do not affect the overall average textural composition of the soil itself.

The three phytolith concentration curves relative to soil depth of the different samples (n=1 [x=1, 3, and 20]) tend to mirror each other reasonably well (Figure 63). The most concentration variation is near the surface; this is presumably due to variations in distribution of plant litter across the soil surface. At the time of the April 2009 botanical inventory to the site, the ground cover was estimated to be about ~30-50%, so there is definite variability in plant density and location. The large variation from the general phytolith concentration curve profile at a depth of 25-35 cm (n=20, Figure 63) is felt to be due to the presence of rodent burrows encountered and included in the n=20 composite soil sample. The higher phytolith values in these particular samples are most likely due to accumulated vegetation stored in the burrows (or silt transported into the burrows by weathering activities) skewing the phytolith concentration.

The plots of phytoliths/silt and phytoliths/soil (wt/wt %) for the Manning

Tallgrass Prairie are shown in Figure 66 (n=20). Both data sets were fitted with an

exponential curve (equations shown). Although the presumed rodent-induced phytolith

concentration aberration is still visible in the phytolith/soil plot, it has significantly less

effect on the correlation coefficient as silt is only one soil component. The benefit of

grouping the short cell phytolith forms into Pooids, Panicoids, and Chloridoids noted in

the surface singleton study would apply equally well down profile.
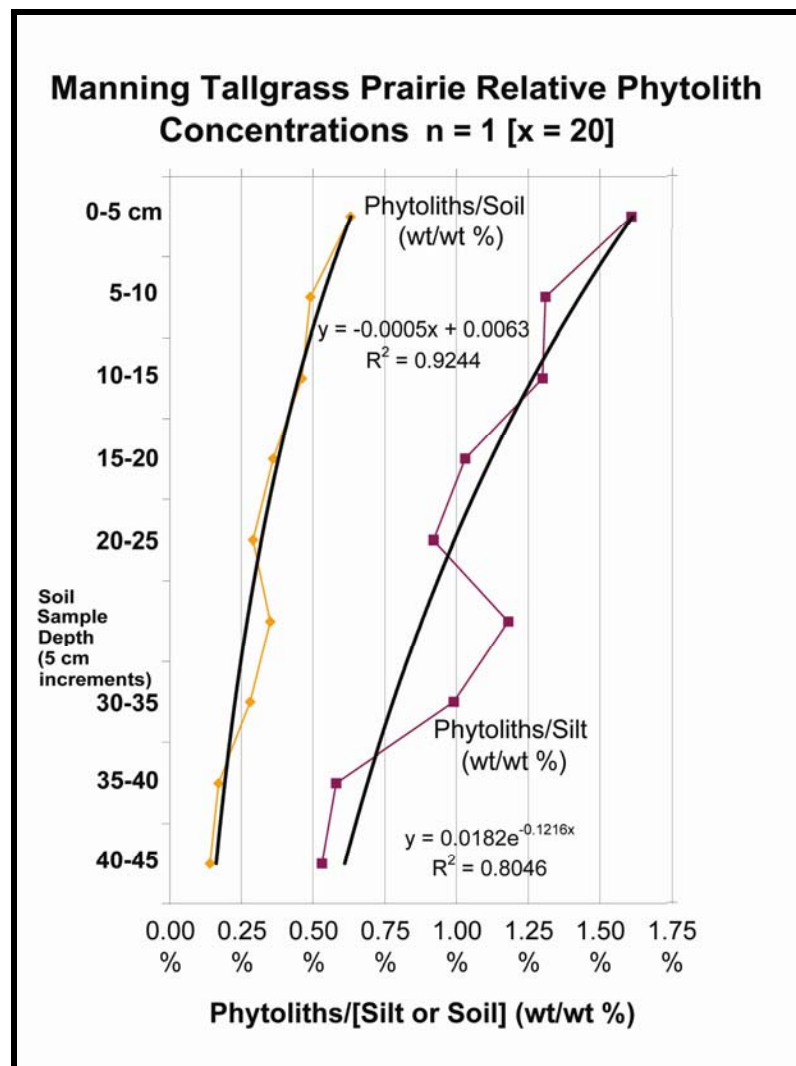
Figure 66. Plot of relative phytolith concentration versus depth, Manning Tallgrass
Prairie (n = 1 [x = 20]).
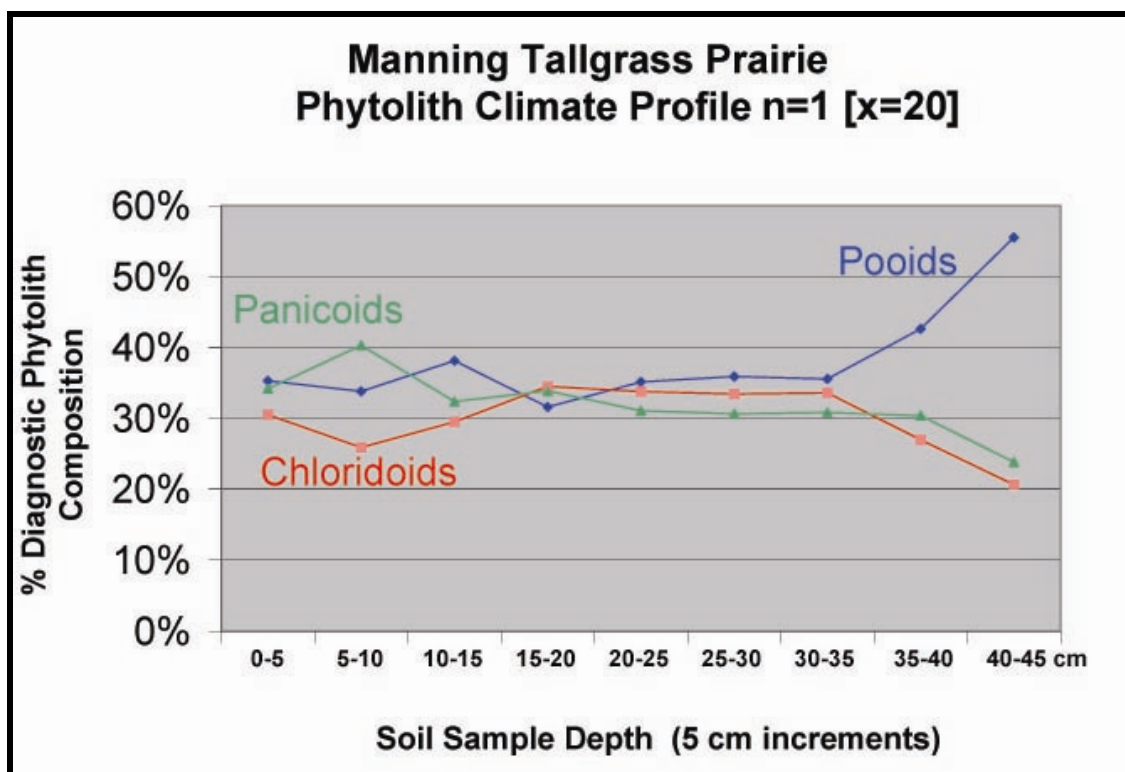
Figure 67. Plot of Manning Tallgrass Prairie soil phytolith concentrations when grouped by three Poaceae subfamilies used as climatic indicators.

The n=1 [x=20] data set for the three climatic groupings is shown in Figure 67. Interval 2 is cooler than interval 1 with more summer-time moisture. In contrast to interval 2, interval 3 appears to have less summer moisture with a temperature similar to modern day, and an expanded cool C3 growing season. Although the warmer temperature returns in soil interval 4 with a much less productive C3 component the Panicoid fraction also increases slightly perhaps indicating a longer warm growing season. Intervals 5-7 were essentially constant indicating a period of climatic stability. However, the big change indicated by this climatic indicator is a very strong prolonged cooling trend in intervals 8 and 9 (again, these are non-A horizon samples). Other particle data showed an increased in charcoal particle concentration in the same two soil intervals (35-45 cm) in the profile (Figure 65). Simultaneous cooling and increase in fire

183

activity suggest the occurrence of some major environmental perturbation. With no radiocarbon dates available, the rate of soil formation at this locale is uncertain; thus, the time period represented by this cooling interval is not known. Obtaining radiocarbon dates for this soil profile is an obvious next step in order to better assess the information provided by this soil phytolith data.

Dempsey Divide Mixedgrass Prairie – The Mixedgrass Prairie sampled in this study is located on the Thurmond Ranch in Roger Mills County, Oklahoma. This prairie is named the Dempsey Divide Mixedgrass Prairie; the location name refers to the "uplands between the Washita and North Fork of the Red rivers in western Oklahoma" (Thurmond 1990, Thurmond et al. 2002:10). This Mixedgrass Prairie area is adjacent to a Shortgrass Prairie, and located on Woodward Loam (Figure 10). Woodward loam is a coarse-silty, mixed, superactive, thermic typic haplustept.

An extensive botanical survey was conducted in the Dempsey Divide region in 2001 (Thurmond et al. 2002). The species noted in the specific Mixedgrass Prairie area sampled during this 2006 phytolith study are listed in Table 37.

The 20 meter diameter circle from which soil samples were collected was predominantly little bluestem (Figure 68). The n=1 [x=20] composite soil samples were processed to recover the phytoliths; phytolith concentrations recovered versus soil weight and silt weight are given in Table 38. No appreciable phytoliths were recovered below

184

25 cm in this particular sampling location, and the soil pH was found to be slightly alkaline (Table 39). Basic soil conditions are known to result in poor phytolith preservation (Piperno 2006). The soil at the center of the sampling template shows an abundance of carbonate at the lower levels (Figure 11); no phytoliths were recovered from depth. A soil profile taken from the wall of the hole at the center of the sampling template is shown in Figure 69.

Soil pH may affect phytolith survival by increasing rate of phytolith dissolution into the ground water, although this phenomenon is normally reported under more basic soil conditions (Piperno 2006, Sudbury 2007). As an illustration of relative phytolith weathering at Dempsey Divide, a series of bulliform phytolith images is shown in Figure 70. Although all soil sample levels had some bulliform phytoliths present in good condition, overall phytolith preservation deteriorated as one moved down profile. The observed variation in phytolith preservation at any given depth and soil pH may be an indicator of the plant origin and the actual specific gravity of the bulliform phytolith (i.e., how much water is present in the amorphous silica matrix) at any given depth. Although phytolith dissolution rates have been compared for different plant types (Wilding and Drees 1974, Bartoli and Wilding 1980), the actual density and solubilization rate of different phytolith morphologic forms from the same plant have not been determined.

As bulliform phytoliths are larger than short cell phytoliths and have a lower surface area relative to volume, they may well be more durable in a given soil pH environment than the smaller short cell forms with a higher surface area to volume ratio.

185

Evaluated by the preservation scale presented by Fredlund and Tieszen (1997a:211), the

Dempsey bulliform phytoliths range from 0-6 (none to excellent, with many in the poor

and extremely poor preservation category).   Thus, the low soil phytolith concentrations

compared to other sites, such as Manning Tallgrass Prairie (Figure 63) may be due to

poor preservation due to issues such as soil pH. Soil solution silica concentration (and

thus potentially phytolith solubility) is affected by the presence of metal ions and salts

(Iler 1979:747, 74).   It is also possible that in this young soil, less total phytolith

deposition has had time to occur.

Table 37
Botanical Species Identified at Dempsey Divide Mixedgrass Prairie (September 2006)

Genus Species	Common Name
Ambrosia psilostachya DC.	Western Ragweed
Bouteloua curtipendula (Michx.)	Side-oats Grama
Buchloe dactyloides (Nutt.)	Buffalograss
Bouteloua hirsuta v hirsuta	Hairy Grama
Croton texensis	Texas Croton (Texas Doveweed)
Cirsium sp.	Thistle
Eriogonum lachnogynum Torr. ex Benth.	Woollycup Buckwheat
Helenium amarum	Bitterweed (Bitter Sneezeweed)
Heterotheca stenophylla	Stiffleaf False Goldenaster
Liatris punctata	Dotted Gayfeather (Blazing Star)
Lygodesmia juncea	Rush Skeletonplant
Paronychia jamesii	James' Nailwort
Plantago sp.	Platain
Schizachyrium scoparium (Michx.) Nash	Little Bluestem
Stenosiphon sp.	Stenosiphon

Figure 68. Dempsey Divide Mixedgrass Prairie site sampling template adjacent to a Shortgrass Prairie (foreground) which is predominantly Buffalograss; the interfingered Mixedgrass Prairie is predominantly Little Bluestem. Five orange engineering flags are visible between the two white spots; most of the entire template (18 of 21 flags) is present in this photograph. The center of this sampling template is shown in Figure 11.

Table 38
Dempsey Divide Mixedgrass Prairie Phytolith Weight in
Woodward Loam Profile in 5 cm Depth Intervals through 45 cm (n=1 [x=20])

Depth (cm)	Soil Sample Weight (g)	Silt Weight (g)	Phytoliths Weight (g)	Phytoliths/Soil (wt/wt %)	Phytoliths/Silt (wt/wt %)
0-5	25.16	7.2566	0.0344	0.14%	0.47%
05-10	25.41	7.4800	0.0285	0.11%	0.38%
10-15	25.17	7.5472	0.0221	0.09%	0.29%
15-20	25.71	7.5839	0.0158	0.06%	0.21%
20-25	25.47	7.2995	0.0075	0.03%	0.10%
25-30	25.37	7.5900	0.0000	0	0
30-35	25.62	8.4172	0.0000	0	0
35-40	25.32	8.8288	0.0000	0	0
40-45	25.55	8.9387	0.0000	0	0

Table 39
Dempsey Divide Mixedgrass Prairie Soil pH

Sample Depth (cm)	Soil pH
0-5	7.01
5-10	7.22
10-15	7.19
15-20	7.19
20-25	7.46
25-30	7.48
30-35	7.45
35-40	7.42
40-45	7.49

The phytolith counts for these n=1 [x=20] samples are recorded in Table 40, and the normalized values for the short cell forms are presented in Table 41. The same data summed by short cell climatic form is given in Table 42, and the normalized (relative to total short cell count) climatic values are in Table 43 with a bar graph illustrating the data in Figure 71. Some of the other particle types observed in these samples are presented in Table 44; the values presented are a ratio of the particle count (Table 40) to the total short cell phytolith count (Table 42). A plot of the other soil particle data is shown in Figure 72.

Three soil intervals (1, 4, and 5) appear to reflect similar climatic conditions (Figure 71) with the two deeper zones being slightly moister and cooler than modern day. The interesting climatic changes in this profile show a dramatically warmer period represented in interval 2 (5-10 cm) preceded by an intermediate warming period in interval 3 (10-15 cm) as reflected by the soil short cell phytolith record.

Figure 69. Woodward Loam profile from the wall of the excavation shown in Figure 69 showing the A, Bw, and BCk horizons. The board in the figure is ¾ inch thick. (The backdirt from the hole generating this soil profile sample is visible in Figure 11.)
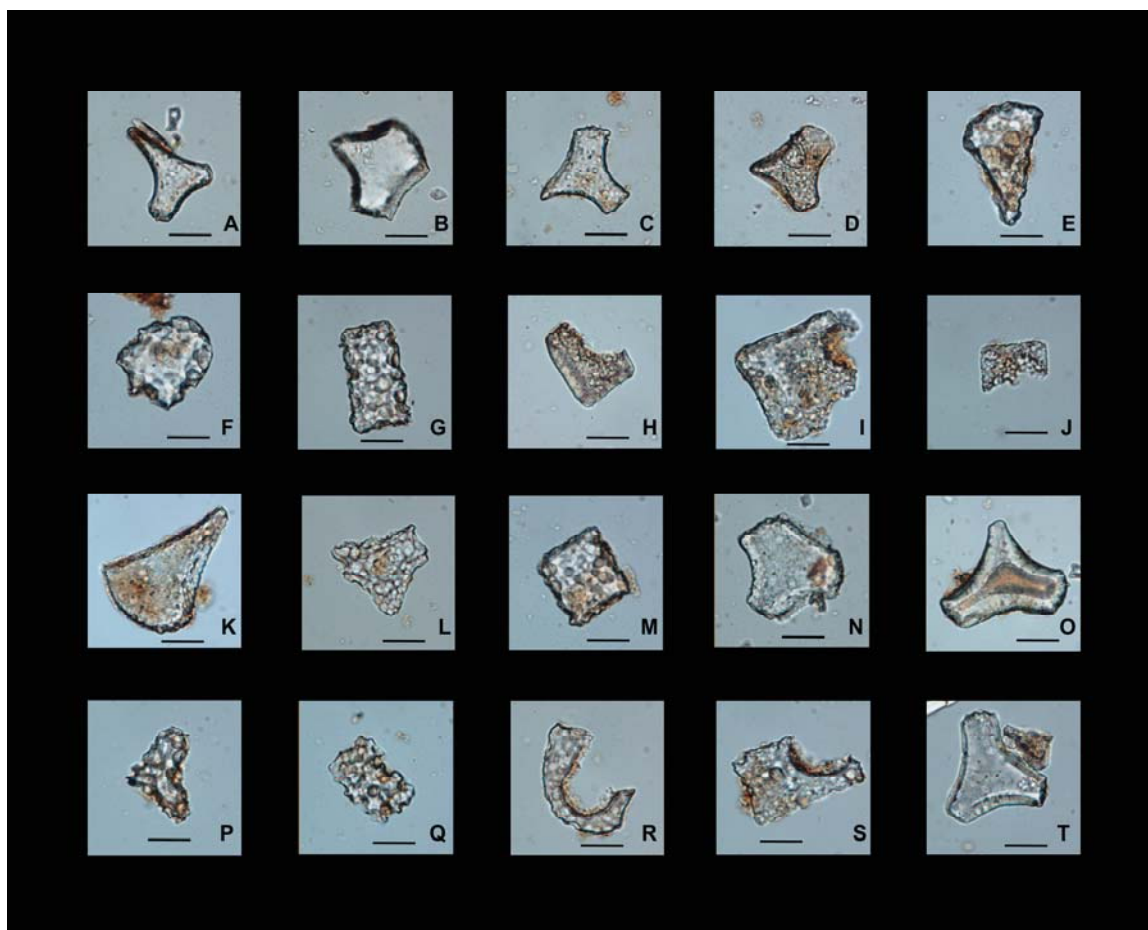
Figure 70. Dempsey Divide Mixedgrass Prairie soil sample bulliform phytoliths showing variation in phytolith preservation (i.e., weathering and dissolution). A-B: 0-5 cm, C-D: 5-10 cm, E-J: 10-15 cm, K-O: 15-20 cm, and P-T: 20-25 cm.

As for the other particle types (Figure 72), there is a small spike in charcoal concentration that correlates with the warmest period (interval 2, 5-10 cm) and a large charcoal spike in interval 5 (20-25 cm soil depth) which actually correlates with the coolest interval in this sample series. Unfortunately, the soil phytolith record at this location is not complete to 45 cm--apparently due to phytolith preservation issues. There was also a charcoal spike noted at the deepest levels of Manning Tallgrass Prairie (Figure 65). Again, the actual age of these particular soil increments remains to be determined, so a positive inter-site

Table 40

Dempsey Divide Mixedgrass Prairie Phytolith Counts with Depth (n=1 [x=20])

Sample Depth, 5 cm Increments	0-5	-10	-15	-20	-25	-30	-35	-40	-45
Keeled	**42**	**15**	**31**	**17**	**13**	**0**	**0**	**0**	**0**
Conical	**60**	**28**	**61**	**53**	**34**	**0**	**0**	**0**	**0**
Pyramidal	**4**	**1**	**1**	**4**	**1**	**0**	**0**	**0**	**0**
Crenate	**5**	**4**	**6**	**5**	**8**	**0**	**0**	**0**	**0**
Saddle, Squat	**87**	**64**	**89**	**50**	**33**	**0**	**0**	**0**	**0**
Saddle, Tall	**189**	**113**	**195**	**128**	**86**	**0**	**0**	**0**	**0**
Stipa	**3**	**0**	**1**	**2**	**1**	**0**	**0**	**0**	**0**
Lobate, Simple	**7.5**	**3**	**8**	**6.5**	**4.5**	**0**	**0**	**0**	**0**
Lobate, Panicoid	**14**	**5.5**	**5.5**	**8**	**5.5**	**0**	**0**	**0**	**0**
Lobate, Panicoid (cmpd)	**0**	**0**	**0**	**0**	**0**	**0**	**0**	**0**	**0**
Cross, Panicoid (<10 um)	**1**	**0**	**1**	**0**	**0**	**0**	**0**	**0**	**0**
Cross, Panicoid (>10 um)	**1**	**0**	**0**	**0**	**0**	**0**	**0**	**0**	**0**
Spiny spheroid	0	1	0	1	3	0	0	0	0
Sponge spicule	1	1	0	0	2	0	0	0	0
Trichome, Hair Cells	11	3	2	9	12	0	0	0	0
Bulliform, square	12	11	8	32	52	0	0	0	0
Bulliform, rectangular	18	14	16	36	65	0	0	0	0
Bulliform, keystone	9	10	12	29	53	0	0	0	0
Bulliform, Y-shaped	0	0	0	3	2	0	0	0	0
Bulliform, other	6	10	10	16	9	0	0	0	0
Elongate, smooth	2	3	0	3	3	0	0	0	0
Elongate, sinuous	1	0	3	1	1	0	0	0	0
Elongate, castillate	1	1	3	1	7	0	0	0	0
Elongate, spiny	0	0	0	0	0	0	0	0	0
Sedge	2	0.5	2.5	0.5	0	0	0	0	0
Charcoal	8	7	3	4	21	0	0	0	0
Diatoms and fragments	8	4	5	5	2	0	0	0	0
Burned Panicoid lobates	0	0	0	0	0	0	0	0	0

Table 41
Dempsey Divide Mixedgrass Prairie Normalized % Phytolith
Counts in Composite Soil Samples in 5 cm Depth Intervals through 45 cm (n=1 [x=20])

	0-5 cm	-10 cm	-15 cm	-20 cm	-25 cm	-30 cm	-35 cm	-40 cm	-45 cm
Keeled	10.2%	6.4%	7.8%	6.2%	7.0%	0	0	0	0
Conical	14.5%	12.0%	15.3%	19.4%	18.3%	0	0	0	0
Pyramidal	1.0%	0.4%	0.3%	1.5%	0.5%	0	0	0	0
Crenate	1.2%	1.7%	1.5%	1.8%	4.3%	0	0	0	0
Saddle, Squat	21.0%	27.4%	22.3%	18.3%	17.7%	0	0	0	0
Saddle, Tall	45.7%	48.4%	48.9%	46.8%	46.2%	0	0	0	0
Stipa	0.7%	0.0%	0.3%	0.7%	0.5%	0	0	0	0
Lobate, Simple	1.8%	1.3%	2.0%	2.4%	2.4%	0	0	0	0
Lobate, Panicoid	3.4%	2.4%	1.4%	2.9%	3.0%	0	0	0	0
Lobate, Panicoid (compound)	0.0%	0.0%	0.0%	0.0%	0.0%	0	0	0	0
Cross (>10 μ)	0.2%	0.0%	0.3%	0.0%	0.0%	0	0	0	0
Cross (>10 μ)	0.2%	0.0%	0.0%	0.0%	0.0%	0	0	0	0

Table 42
Dempsey Divide Mixedgrass Prairie
Total Short Cell Phytoliths Grouped by Climatic Indicators
(Composite Soil Samples in 5 cm Depth Intervals through 45 cm (n=1 [x=20])

	0-5 cm	-10 cm	-15 cm	-20 cm	-25 cm	-30 cm	-35 cm	-40 cm	-45 cm
Cool Wet Phytoliths	111	48	99	79	56	0	0	0	0
Hot Dry Phytoliths	276	177	284	178	119	0	0	0	0
Hot Moist Phytoliths	26.5	8.5	15.5	16.5	11	0	0	0	0
Total Short Cell Phytoliths	413.5	233.5	398.5	273.5	186	0	0	0	0

Table 43
Dempsey Divide Mixedgrass Prairie
Normalized Short Cell Phytoliths Grouped by Climatic Indicators
(Composite Soil Samples in 5 cm Depth Intervals through 45 cm (n=1 [x=20]))

	0-5 cm	-10 cm	-15 cm	-20 cm	-25 cm	-30 cm	-35 cm	-40 cm	-45 cm
Cool Wet Phytoliths	26.8%	20.6%	24.8%	28.9%	30.1%	0	0	0	0
Hot Dry Phytoliths	66.7%	75.8%	71.3%	65.1%	64.0%	0	0	0	0
Hot Moist Phytoliths	6.4%	3.6%	3.9%	6.0%	5.9%	0	0	0	0
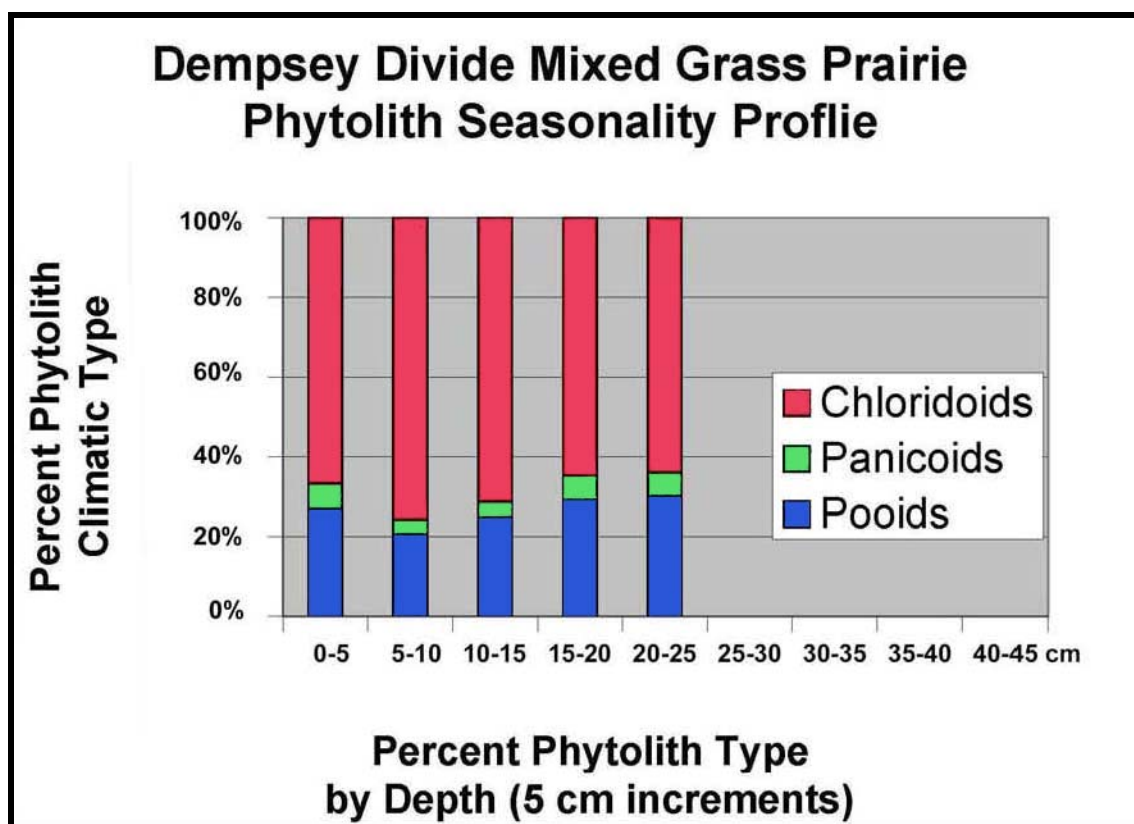
Figure 71. Dempsey Divide Mixedgrass Prairie seasonality profile (plot of data in Table 42).

Table 44
Dempsey Divide Mixedgrass Prairie
Incidence of Other Particle Types Recovered in the Phytolith Fraction
Relative to Tabulated Phytolith Short Cell Forms (Soil Composite Sample (n=1 [x=20]))

Sample Depth (cm)	Charcoal	Burned Panicoids	Diatoms	Sedge Phytoliths	Sponge Spicules
0-5	1.93%	0	1.93%	0.48%	0.24%
05-10	3.00%	0	1.71%	0.72%	0.43%
10-15	0.75%	0	1.25%	0.63%	0
15-20	1.46%	0	6.13%	0.18%	0
20-25	11.29%	0	1.08%	0	1.08%
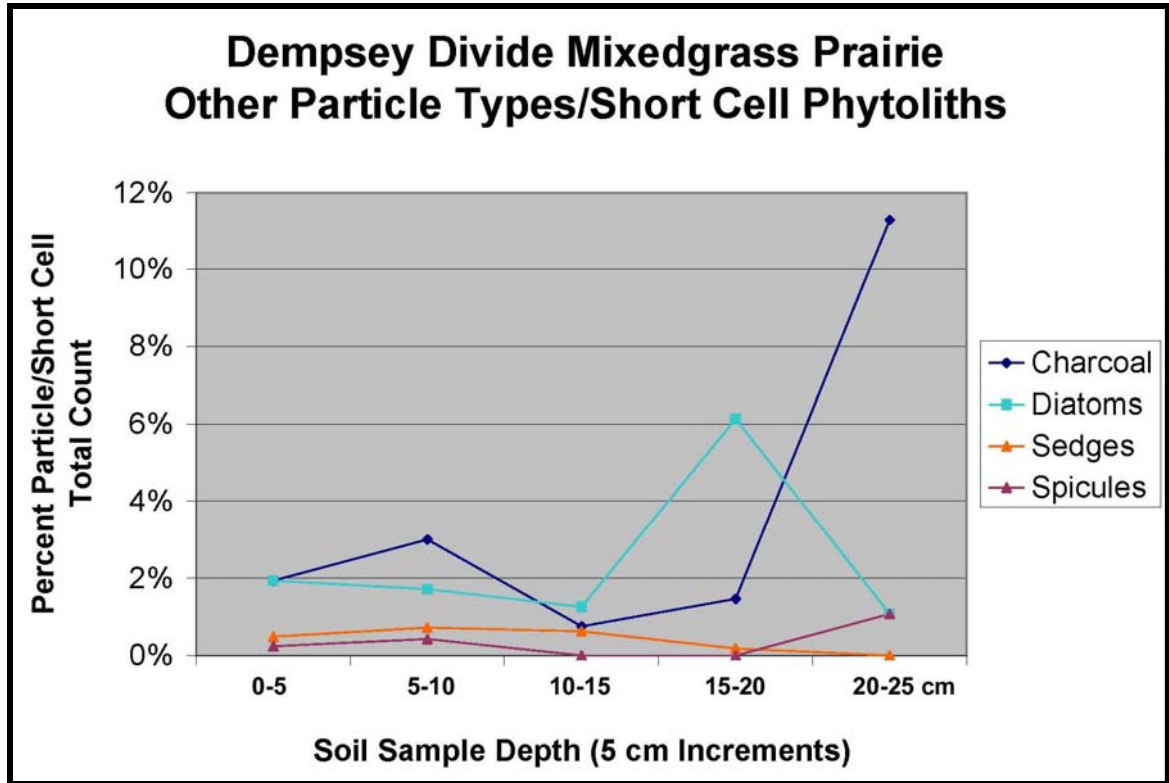
Figure 72. Dempsey Divide soil particles relative to total short cell phytolith count (plot of data in Table 43).

correlation has not been established. Concurrent environmental cooling and an increase

activity (i.e., interval 5, 20-25 cm at Dempsey Mixedgrass Prairie) may be a marker for a

serious environmental event. A spike in the interval 4 diatom concentration was also

observed; the significance of this fluctuation is unknown.

Discussion of Dempsey Mixedgrass Prairie Phytolith Data – Although soil dates

are again unknown, the Dempsey Divide Mixedgrass Prairie data also shows a warming

trend in soil depth interval 2 (5-10 cm, Figure 73). The other particle data also shows a

strong spike in charcoal concentration in the lowest soil interval reported (Table 18). If

the Manning and Dempsey prairie charcoal spikes are from the same event, the relative

soil depths would suggest that soil building and development occurred somewhat more

slowly at the Dempsey Divide Mixedgrass Prairie than at Manning Tallgrass Prairie.

Unfortunately, the apparent dissolution of phytoliths
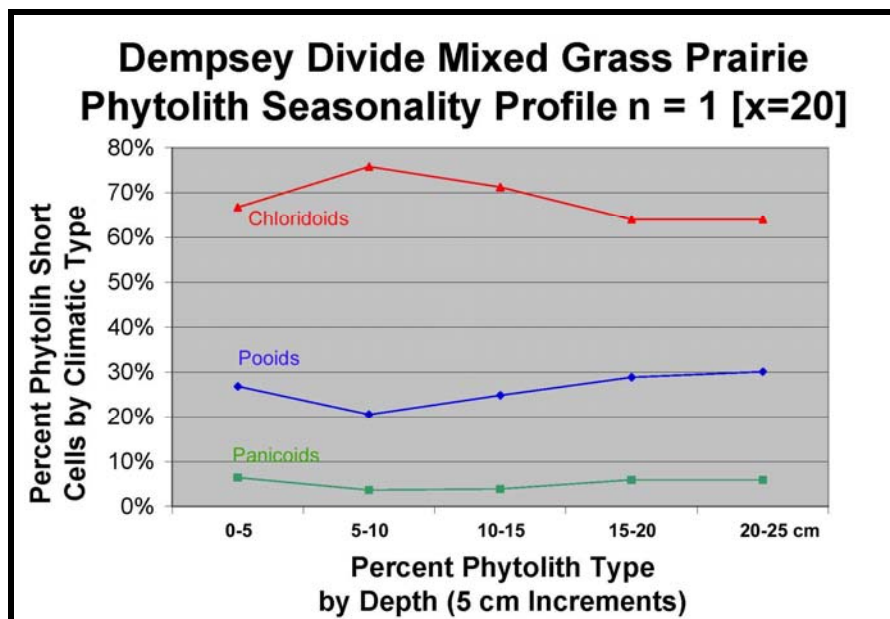
Figure 73. Dempsey Divide Mixedgrass Prairie soil phytolith seasonality profile from 0-
25 cm in depth.

from the lower part of the soil profile studied resulted in a truncated Dempsey Divide Mixedgrass Prairie data set. There was concurrent cooling trend with the increase in charcoal concentration at Manning Tallgrass Prairie, whereas in the limited data available from Dempsey Mixedgrass Prairie the increase in charcoal content occurs with only a moderate temperature decrease. The plot of phytolith/soil concentrations (wt/wt %) from Dempsey is nearly linear (Figure 75); it is probable that this reflects a rate of phytolith dissolution in the basic soil as well as the rate of soil formation, so the phytolith concentration relative to soil depth is presumably skewed via increased dissolution with depth. The very low phytolith recoveries at the site in the lower samples (Table 38) support this theory. The exponential Manning Tallgrass Prairie phytolith profile (Figure 75) suggests long-term soil stability with gradual aggradation occurring while the Dempsey Divide Mixedgrass phytolith data suggest dissolution issues, or possibly a very young soil.

Bull Creek site (Shortgrass Prairie) – Detailed soil sampling (n=1 [x=20]) was initiated at the Dempsey Divide Shortgrass Prairie (Figure 10, location 2). However while sampling the top 5 cm soil interval both available soil probes were twisted into "S" shapes rendering them unusable; the extremely hard soil being a side effect of the 2006 drought. Further Shortgrass Prairie soil sampling at Dempsey Divide was abandoned.

For this reason, the previously collected surface 10 cm soil sample from the Bull Creek site was used as the Shortgrass Prairie control soil sample in this study (n=1). The

Bull Creek site is located in the Oklahoma Panhandle (Figure 61). The eroded high wall

profile that yielded the surface Shortgrass Prairie sample is shown in Figure 74. The

predominant species currently present on the site is Buffalograss. The surface soil

sample, designated sample BC-52, contained 1.65% phytoliths by weight. The raw count

data and normalized short cell values are in Table 45. The climatic summary data is

presented in Table 46; the phytolith signature is a strong hot dry one as would be

expected for a Shortgrass Prairie on the High Plains. The complete soil phytolith profile

was not prepared at Bull Creek although a total of eleven soil samples were analyzed (see

Figure 81). The additional phytolith results from this site are discussed in the Bull Creek

buried soil data section.

Discussion of Bull Creek Shortgrass Prairie Phytolith Data – The last reference

prairie phytolith data present in this series is from the Shortgrass Prairie sample from the

Bull Creek site. However, with the series of eight dated buried soils present at this site

(see next data section; Bement et al. 2007), it is known that the 50 cm interval above the

first buried soil represents less than 6,200 years. Extensive erosion and soil burial events

occurred at the Bull Creek Site over 12,000+ years. The presence of nanodiamonds in a

buried soil at Bull Creek correlating with the hypothesized Younger-Dryas precipitating

event at ~12,900 BP (Firestone et al. 2007, Kennett et al. 2009) may well indicate the

cause for regional climatic disruption and fire. However, this early time interval at the

Bull Creek site is clearly not represented in the Surface A horizon profile soil, so this is

not addressed for the Shortgrass Prairie control sample.

Figure 74. Profile showing soil sampling points at Bull Creek 1 (photograph courtesy of Lee Bement).

Table 45
Bull Creek Surface Soil Sample (BC-52) Phytolith Counts (10 cm, n=1)

Phytolith Form	Phytolith Count	Normalized Short Cells
Keeled	**13**	**5.2%**
Conical	**5**	**2.0%**
Pyramidal	**2**	**0.8%**
Crenate	**3**	**1.2%**
Saddle, Squat	**184**	**73.6%**
Saddle, Tall	**27**	**10.8%**
Stipa	**13**	**5.2%**
Lobate, Simple	**2**	**0.8%**
Lobate, Panicoid	**1.5**	**0.6%**
Lobate, Panicoid (cmpd)	**0**	**0.0%**
Cross, Panicoid (<10 μ)	**1**	**0.4%**
Cross, Panicoid (>10 μ)	**13**	**5.2%**
Spiny Spheroid	9	
Sponge Spicule	1	
Trichome, Hair Cells	1	
Bulliform, square	6	
Bulliform, rectangular	49	
Bulliform, keystone	0	
Bulliform, Y-shaped	2	
Bulliform, other	5	
Elongate, smooth	19	
Elongate, sinuous	11	
Elongate, castillate	21	
Elongate, spiny	2	
Diatoms and fragments	0	

Table 46
Bull Creek Surface Soil Sample (BC-52)
Short Cell Phytoliths Summed by Climatic Grouping (10 cm, n=1)

Climatic Short Cell Phytolith Types	Normalized Percent
Pooids (Cool Wet Phytoliths)	**10.1%**
Chloridoids (Hot Dry Phytoliths)	**82.2%**
Panicoids (Hot Moist Phytoliths)	**7.7%**
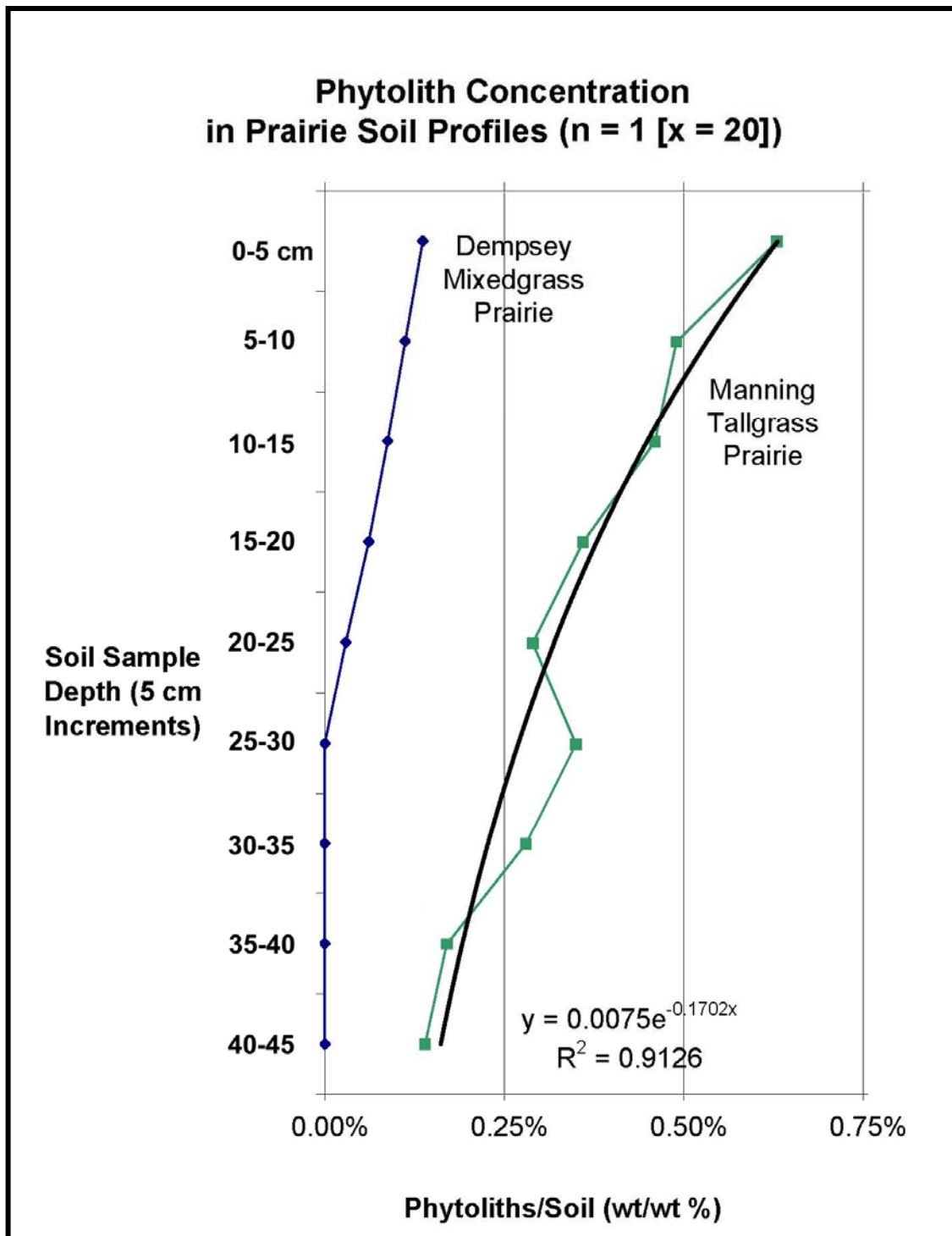
Figure 75. Dempsey Mixedgrass Prairie and Manning Tallgrass Prairie phytolith soil concentrations (wt/wt %). The R^2 value for the six 0-25 cm Manning data points is 0.9966.

Reference Control Prairie Comparison Discussion – The relative surface soil phytolith concentrations at three control prairie sites are shown in Table 47. The low Dempsey Mixedgrass Prairie phytolith concentration may be a reflection of phytolith stability/dissolution issues or rate of soil development. The difference in phytolith concentration may also be related to biomass load and to the actual phytolith concentration present in the dominant plant species at the various prairie locations. Due the amount of annual biomass at the Tallgrass versus the Shortgrass Prairies, it was anticipated that the Tallgrass Prairie would have the highest soil phytolith concentration. However, this clearly was not the case; this difference may be an indicator of the relative rate of soil formation at these two sites (and at the Mixedgrass Prairie as well).

This unexpected observation may be due to a number of possible factors impacting these two sites including:

- different relative rates of soil formation and aggradation at the sites,
- average greater precipitation at the Manning Tallgrass Prairie site may have led to increased erosional losses of shed phytoliths in the runoff,
- possible skewing of the Shortgrass Prairie by only having the upper few cm of soil present in the actual portion of the soil sample that was analyzed, and
- Different land use practices (harvesting prairie hay at Manning Prairie which would remove most of the leaf biomass for the past 100 years), and possible differences in frequency of natural fire events.

The variation the phytolith recoveries for the two different Manning Tallgrass

Prairie sampling templates tested (n=1 [x=20] vs. n=21 replicates values, Table 44)

indicates that significant phytolith concentration differences occur at one given site; these

two sampling locations were centered less than 100 meters apart. The average of the

value from location 2 (n=21) is 48% higher than the average of the values obtained from

location 1 (n=1 [x=20]) (Table 47). Even within sampling location 2, the range of

phytolith concentrations in the 21 discrete sampling locations varied from 0.77 to 1.20

weight % of soil (Table 19) indicating a very non-homogenous phytolith distribution for

21 discrete individual samples collected in a 20 meter diameter circle (314.16 square

meter sample template). Thus, actual horizontal soil phytolith concentration and

distribution is highly variable in a small area, reflecting the variability in plant

distribution, organic material deposition, and possibly other factors (Table 47).

Likewise, as previously noted, the concentration of the individual short cell forms

can be highly variable within a given site based on the evidence from Manning Tallgrass

Prairie (Table 26). The data for the normalized short cell concentrations for the surface

Table 47
Three Control Prairie Surface Soil Sample Phytolith Concentrations

Prairie Type	Phytoliths/Soil (wt/wt %)
Manning Tallgrass Prairie (0-5 cm, n=1 [x=1])	0.69 %
Manning Tallgrass Prairie (0-5 cm, n=1 [x=3])	0.55 %
Manning Tallgrass Prairie (0-5 cm, n=1 [x=20])	0.63 %
Manning Tallgrass Prairie (0-5 cm, 10 replicates)	0.93 %
Manning Tallgrass Prairie (0-5 cm, 21 replicates)	0.93 %
Dempsey Mixedgrass Prairie (0-5 cm, n=1 [x=20])	0.14 %
Shortgrass Prairie at Bull Creek (0-10 cm, n=1)	1.65 %

Table 48
Three Control Prairie Surface Soil Sample Short Cell Phytolith Signatures

Phytolith Form	Normalized Short Cells		
	Manning Tallgrass Prairie (0-5 cm, n=1 [x=20])	Dempsey Mixedgrass Prairie (0-5 cm, n=1 [x=20])	Bull Creek Shortgrass Prairie (0-10 cm, n=1)
Keeled	**9.6%**	**10.2%**	**5.2%**
Conical	**18.0%**	**14.5%**	**2.0%**
Pyramidal	**3.3%**	**1.0%**	**0.8%**
Crenate	**4.4%**	**1.2%**	**1.2%**
Saddle, Squat	**13.2%**	**21.0%**	**73.6%**
Saddle, Tall	**17.3%**	**45.7%**	**10.8%**
Stipa	**1.1%**	**0.7%**	**5.2%**
Lobate, Simple	**2.8%**	**1.8%**	**0.8%**
Lobate, Panicoid	**26.1%**	**3.4%**	**0.6%**
Lobate, Panicoid(cmpd)	**0%**	**0.0%**	**0.0%**
Cross, Panicoid (<10 μ)	**3.5%**	**0.2%**	**0.4%**
Cross, Panicoid (>10 μ)	**0.7%**	**0.2%**	**5.2%**
Tall:Squat saddle ratio	1.31	2.18	0.15

soil of the three control prairies evaluated in this study are summarized in Table 48, and plotted in Figure 76.

The relative normalized concentration of the various short cell forms at these study sites is shown in Figure 76. The concentration of keeled (1), pyramidal (3), crenate (4), stipa (7), simple lobate (8), compound Panicoid lobate (10), large and small Panicoid crosses (11 and 12) are very similar across these three study sites even though they are different prairie types and have very different climatic regimes. As would be expected, the Panicoid lobate (#9) form is much higher at the Tallgrass Prairie site than at the other two sites. The conical form (2) is similar for the Mixedgrass and Tallgrass Prairies which

are both appreciably higher than the conical concentration in the Shortgrass Prairie. The major distinctive difference in these three prairie types is most pronounced in the relative ratios of the two saddle phytolith morphologic forms (#5 and 6) (Figure 76). The two different saddle forms are similar in the Tallgrass Prairie environment, but the relative concentrations are strongly inverted in the Mixedgrass Prairie compared to the Shortgrass Prairie environments. This striking differences suggests that saddle morphology (i.e., short versus tall form, with the difference being which axis of the phytolith is relatively longer) is the most sensitive indicator present in the identified short cell phytolith forms in the modern soils of the three prairie types evaluated in this study. Saddle phytoliths merit future attention in grassland and prairie-related studies.
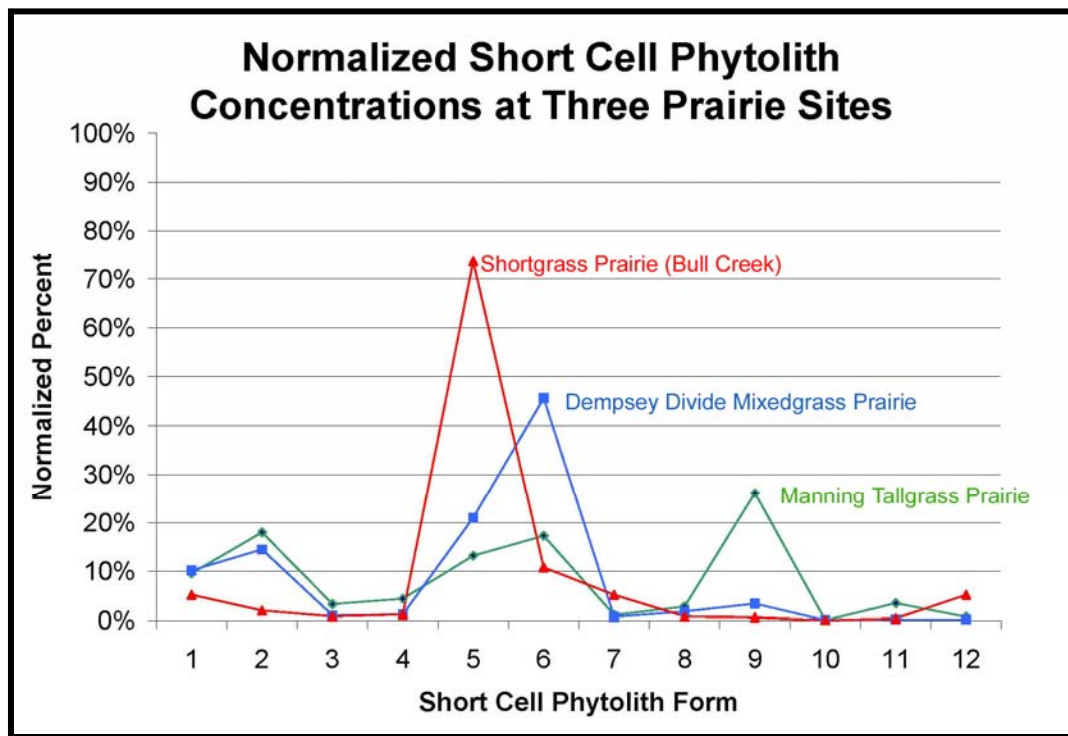
Figure 76. Normalized individual short cell phytolith forms for three prairie sites. Phytolith Form key: 1: Keeled; 2: Conical; 3: Pyramidal; 4: Crenate; 5: Saddle (Squat); 6: Saddle (Tall); 7: Stipa; 8: Lobate (Simple); 9: Lobate (Panicoid); 10: Lobate (Panicoid, Compound), 11: Panicoid Cross (<10 um); and 12: Panicoid Cross (>10 um).

204

A plot of sample saddle ratio verses the total normalized percent of saddles to the short cell count provides another way to look at this data (Figure 77). As expected from the previous values, there are three data clusters by prairie type. The ratio within each sample varied, but linear trends were observed in the data. For instance, the line through the Dempsey Divide Mixedgrass Prairie data has a R^2 value of 0.8695. The grey best fit line through all of the Manning Tallgrass Prairie had a R^2 value of 0.5004. However, in looking at the Manning data, there appear to be two linear subsets in the data (black lines) with the 5-10 cm data point being an outlier (Figure 77).

The meaning of the linear regions in these two data subset is unknown. One potential explanation is that each subset reflects the dominance (or absence) of a particular species or part of the prairie plant association during the time interval reflected in that particular soil sample. This series of comments regarding saddle phytoliths in the samples only considers the relative shape (tall versus squat). Other factions which have not been addressed in this study, such as an understanding of the variation in saddle size, may also have significant importance in the understanding saddle variations among specific plant species and prairie types.

Summing the short cell data (Table 48) by climatic type results in the values given in Table 49 and plotted in Figure 78.

Figure 78 very clearly shows the correlation between prairie types and the summed short cell climatic indicators. The Manning Tallgrass Prairie has roughly equal
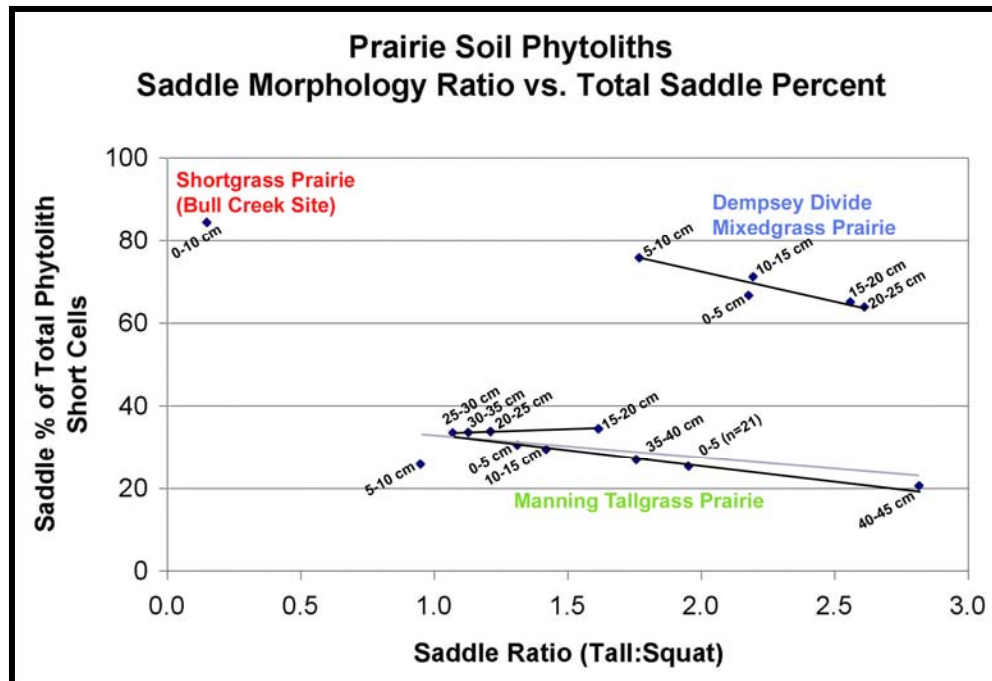
Figure 77. Plot of saddle ratio verses normalized % of saddles in the short cell count. from either subset. The correlation coefficients of these two Manning Prairie subset lines are both better than 0.99 (upper line $R^2 = 0.9976$; lower black line $R^2 = 0.9902$). The two data subsets to share one common point (25-30 cm). The upper portion (0-5 and 10-15, and lower portion (34-45 are on one line, and the intermediate zones (top half of the BA horizon) are on the other line. The deeper samples of the Dempsey Divide Mixedgrass prairie (15-25 cm) also have a higher saddle ratio than the corresponding shallower samples (0-15 cm). For both Dempsey and Manning, the 5-10 cm interval has the lowest ratio of their respective series.

Table 49
Reference Prairie Surface Soil Sample
Short Cell Phytoliths Summed by Climatic Grouping

Climatic Short Cell Phytolith Types	Manning Tallgrass Prairie Normalized Percent	Dempsey Mixedgrass Prairie Normalized Percent	Bull Creek site Shortgrass Prairie Normalized Percent
Cool Wet Phytoliths	33.3%	26.8%	10.1%
Hot Dry Phytoliths	30.5%	66.7%	82.2%
Hot Moist Phytoliths	34.2%	6.4%	7.7%

206
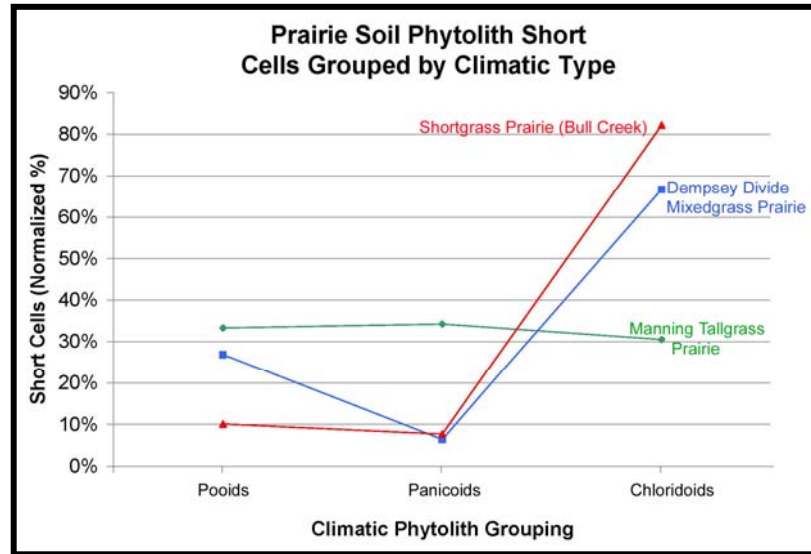
Figure 78. Concentration of phytolith climatic short cell grouping for each prairie type studied.

Pooid, Chloridoid, and Panicoid short cell phytolith composition. As one moves west across the Great Plains to other prairie types, the climate becomes warmer and much drier. The Mixedgrass and Shortgrass Prairies both have a roughly equal low normalized Panicoid component. The Mixedgrass Prairie has an intermediate cool wet season (Pooid) component being somewhat more similar to the Tallgrass Prairie. The Shortgrass Prairie has the lowest Pooid component of all as a result of the extremely xeric conditions.

The largest change between these three plots is the increased Chloridoid component in the Mixedgrass and Shortgrass Prairies. This difference is a direct result of the plant communities adapted to those hotter drier prairie settings. This adaptation occurs by overall increase in frequency in the plant community of hot season adapted plants—those that that use C4 metabolism—which benefits the plants by helping to

conserve plant water. This change is clearly reflected in the phytolith data from these control prairie samples. However, even though both Chloridoid counts are high, the actual Chloridoid forms (i.e., squat vs. tall) making up the count are drastically different between the Mixedgrass and Tallgrass Prairie (Figures 76-78) which may be attributable to actual species differences in the plant communities.

Research Objective 3: Phytolith Samples from Buried Soil Study Sites

Phytolith signatures were determined for buried A horizons at three Oklahoma research sites (Figure 79). Each site contains one or more buried soils whose age has been determined by radiocarbon dating (Bement et al. 2007; Carter et al. 2009). The data from these sites will be presented in order from west to east.

Bull Creek Site (34BV176) – The Bull Creek Site is located along Bull Creek, a small ephemeral tributary of the North Canadian River (Bement et al. 2007). The exposed profile that provided the soil samples for this phytolith study is shown in Figure 74. The soil profile description has been published (Bement et al. 2007). The surface soil sample (BC-52) is the reference Shortgrass Prairie sample described in the previous section. The Bull Creek Site actually has a stacked series of nine distinct A horizons. The lower seven buried soils in this sequence are the subject of this current investigation. Soil phytoliths were quantitatively isolated from the surface A-Horizon (BC-52), the seven lower buried A horizons, and the ABkb3 (BC-42), 2Bkb4 (BC-34) and 2ACb8 (BC-19) horizons. The raw phytolith counts for these eleven soil sample extracts are in Tables 50 and 51. The normalized data by short cell type is in Table 52 and the normalized phytolith seasonality groupings are in Table 53[33]. Figure 80 is a plot of the climatic data. The Chloridoid component of the seasonality profile is shown in more detail in Figure 81.

---

[33] Tables 51 and 52 included recount data for samples BC-34 and BC-47).
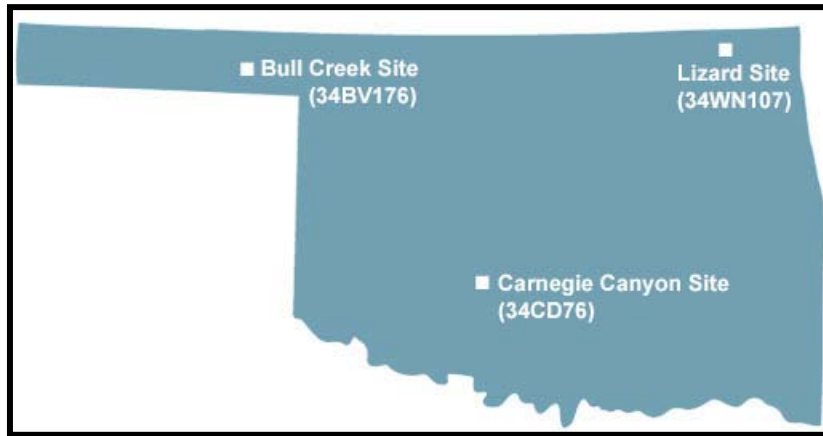
Figure 79. Oklahoma map indicating the location of the three buried soil study sites discussed in this research report. (Base map from http://www.okhistory.org/outreach/map.jpg.)

The stipa morphologic form count is included in the Panicoid fraction in Figure 80[34]. Initially, it was anticipated that the rather ubiquitous rondel forms (Mulholland 1989) would be included with the Pooid fraction. The Bull Creek phytolith data for the saddle and rondel phytolith forms is plotted in Figure 81 (particle count totals taken from Tables 50 and 51). Although there is a low baseline level of rondels present in all of the samples (roughly 0-10 specimens/200 recognizable short cells), it appears that spikes in rondel frequency in these soil samples generally correlate with the higher saddle phytolith form counts. This is most obvious in the modern day soil—where the soil represents the Oklahoma panhandle climate which is exceptionally hot and dry. Thus, as Fredlund and Tieszen (1994, 1997a) did not include rondels in the phytolith counting scheme used to calibrate grasslands of the Great Plains, and because the peak rondel concentrations at

---

[34] In the original publication of this data the stipa fraction is included on the Panicoid side of the graph but remains distinct (Bement et al. 2007). Including both C3 and C4 species, the Stipa count could potentially be included in the Pooid or in the Panicoid fraction. If these fairly low values were switched to the Pooid region, the Chloridoid portion would be shifted slightly to the right in Figure 88, but otherwise relatively unchanged. The stipa morphologic form ranged from 0.9-10.6 normalized percent of the short cell count in these eleven Bull Creek samples (Table 51).

Table 50

Counts of Bull Creek Short Cell and Other Phytolith Forms (BC-34 through BC-52)

Sample No.	BC-52	BC-47	BC-45	BC-42	BC-37	BC-34
Form						
Keeled	**13**	**11**	**18**	**18**	**12**	**21**
Conical	**5**	**49**	**45**	**35**	**36**	**72**
Pyramidal	**2**	**18**	**6**	**17**	**13**	**22**
Crenate	**3**	**56**	**27**	**20**	**16**	**15**
Saddle, Squat	**184**	**41**	**22**	**103**	**42**	**35**
Saddle, Tall	**27**	**11**	**72**	**23**	**74**	**29**
Stipa	**13**	**2**	**13**	**4**	**24**	**26**
Lobate, Simple	**2**	**15.5**	**5.5**	**7.5**	**8.5**	**9.5**
Lobate, Panicoid	**1.5**	**13**	**5**	**7.5**	**5**	**5**
Lobate, Panicoid (cmp'd)	**0**	**1**	**0**	**0**	**0**	**1**
Cross, Panicoid	**1**	**1**	**3**	**2.5**	**5.5**	**3**
Total Short Cell Count	251.5	218.5	216.5	237.5	236	238.5
Ratio saddles (Squat:Tall)	6.815	3.727	0.3056	4.4783	0.568	1.2069
Non-short cell forms:						
Rondel (bipoint)	52	3	0	0	16	0
Rondel, other	8	5	0	7	13	0
Dicot, knobby	2	12	8	4	9	9
Spiny spheroid	9	27	7	12	5	7
WWW	8	2	10	12	7	15
Schlerid	0	0	0	0	0	0
Diatom	0	0	0	2	4	0
Sponge spicule	1	2	1	2	0	1
Trichome	1	15	6	8	8	7
Hair cells	0	1	0	1	2	0
Bulliform, square	6	22	6	3	3	1
Bulliform, rectangular	49	45	12	6	18	8
Bulliform, keystone	0	17	4	5	2	1
Bulliform, Y-shaped	2	0	0	0	1	1
Bulliform, other	5	37	3	8	23	15
Elongate, smooth	19	36	23	15	24	19
Elongate, sinuous	11	15	25	17	14	15
Elongate, castillate	21	21	10	8	13	15
Elongate, spiny	2	23	10	15	17	18
Other Phytolith Count:	202	283	125	125	179	132
Ratio "Short Cell:Other"	1.24	0.772	1.732	1.90	1.318	1.8068

Table 51
Counts of Bull Creek Short Cell and Other Phytolith Forms (BC-19 through BC-31)

Sample No.	BC-31	BC-28	BC-25	BC-22	BC-19[35]
Form					
Keeled	**13**	**13**	**37**	**21**	**46**
Conical	**34**	**70**	**86**	**67**	**45**
Pyramidal	**5**	**20**	**7**	**29**	**7**
Crenate	**29**	**34**	**7**	**27**	**13**
Saddle, Squat	**39**	**50**	**54**	**16**	**49**
Saddle, Tall	**83**	**10**	**3**	**18**	**32**
Stipa	**19**	**2**	**14**	**24**	**3**
Lobate, Simple	**11**	**13.5**	**7**	**12**	**3**
Lobate, Panicoid	**4**	**6.5**	**2**	**9.5**	**3.5**
Lobate, Panicoid (cmp'd)	**1**	**0**	**1**	**0**	**0**
Cross, Panicoid	**2**	**3.5**	**3.5**	**3**	**0**
Total Short Cell Count	240	222.5	221.5	226.5	201.5
Ratio saddles (Squat:Tall)	0.47	5.00	18.00	0.8889	1.5283
Non-short cell forms:					
Rondel (bipoint)	4	0	1	0	1
Rondel, other	18	1	0	0	0
Dicot, knobby	10	8	8	9	14.5
Spiny spheroid	10	20	12	13	7
WWW	8	1	6	2	3
Schlerid	0	0	0	0	0
Diatom	0	0	1	0	3
Sponge spicule	0	0	0	1	1
Trichome	17	10	6	6	17
Hair cells	0	2	0	3	1
Bulliform, square	9	7	8	11	7
Bulliform, rectangular	22	13	8	10	23
Bulliform, keystone	7	7	6	3	1
Bulliform, Y-shaped	0	0	0	1	2
Bulliform, other	44	14	13	35	98
Elongate, smooth	42	17	15	14	39
Elongate, sinuous	15	4	18	6	6
Elongate, castillate	24	12	18	5	11
Elongate, spiny	17	8	20	10	8
Other Phytolith Count:	247	124	140	129	242.5
Ratio "Short Cell:Other"	0.972	1.794	1.582	1.7558	0.8309

---

[35] In addition to the individual phytolith forms counted and reported in this table for sample BC-19, an additional 6300 fragments and unidentifiable fragments were tallied in the same count fields yielding 242.5 short cells.

Table 52. Bull Creek A Horizon Normalized Short Cell Types

Sample:	BC-52	BC-47	BC-45	BC-42	BC-37	BC-34	BC-31	BC-28	BC-25	BC-22	BC-19
Morphology											
Keeled	5.2	5.0	8.3	7.6	5.1	8.8	5.4	5.8	16.7	9.3	22.8
Conical	2.0	22.4	20.8	14.7	15.3	30.2	14.2	31.5	38.8	29.6	22.3
Pyramidial	0.8	8.2	2.8	7.2	5.5	9.2	2.1	9.0	3.2	12.8	3.5
Crenate	1.2	25.6	12.5	8.4	6.8	6.3	12.1	15.3	3.2	11.9	6.5
Saddle (Squat)	73.6	18.8	10.2	43.4	17.8	14.7	16.3	22.5	24.4	7.1	24.3
Saddle (Tall)	10.8	5.0	33.3	9.7	31.4	12.2	34.6	4.5	1.4	7.9	15.9
Stipa	5.2	0.9	6.0	1.7	10.2	10.9	7.9	0.9	6.3	10.6	1.5
Lobate, Simple	0.8	7.1	2.5	3.2	3.6	4.0	4.6	6.1	3.2	5.3	1.5
Lobate, Panicoid	0.6	5.9	2.3	3.2	2.1	2.1	1.7	2.9	0.9	4.2	1.7
Lobate, Panicoid (cmpd)	0.0	0.5	0.0	0.0	0.0	0.4	0.4	0.0	0.5	0.0	0
Cross, Panicoid	0.4	0.5	1.4	1.1	2.3	1.3	0.8	1.6	1.6	1.3	0

Table 53. Bull Creek Short Cell Phytoliths Summed by Climatic Category and Normalized Short Cell Climatic Category

	BC-52	BC-47	BC-45	BC-42	BC-37	BC-34	BC-31	BC-28	BC-25	BC-22	BC-19
Short Cell Counts											
Cool Moist Climate	23	258	96	90	77	187	81	137	137	144	111
Hot Dry Climate	211	120	94	126	116	106	122	60	57	34	81
Warm Moist Climate	17.5	65	26.5	21.5	43	58	37	25.5	27.5	48.5	9.5
total short cell count	251.5	443	216.5	237.5	236	350.5	240	222.5	221.5	226.5	201.5
	BC-52	BC-47	BC-45	BC-42	BC-37	BC-34	BC-31	BC-28	BC-25	BC-22	BC-19
Normalized Short Cell %											
Cool Moist Climate	9.1%	58.2%	44.3%	37.9%	32.6%	53.4%	33.8%	61.6%	61.9%	63.6%	55.1%
Hot Dry Climate	83.9%	27.1%	43.4%	53.1%	49.2%	30.2%	50.8%	27.0%	25.7%	15.0%	40.2%
Warm Moist Climate	7.0%	14.7%	12.2%	9.1%	18.2%	16.4%	15.4%	11.5%	12.4%	21.4%	4.7%
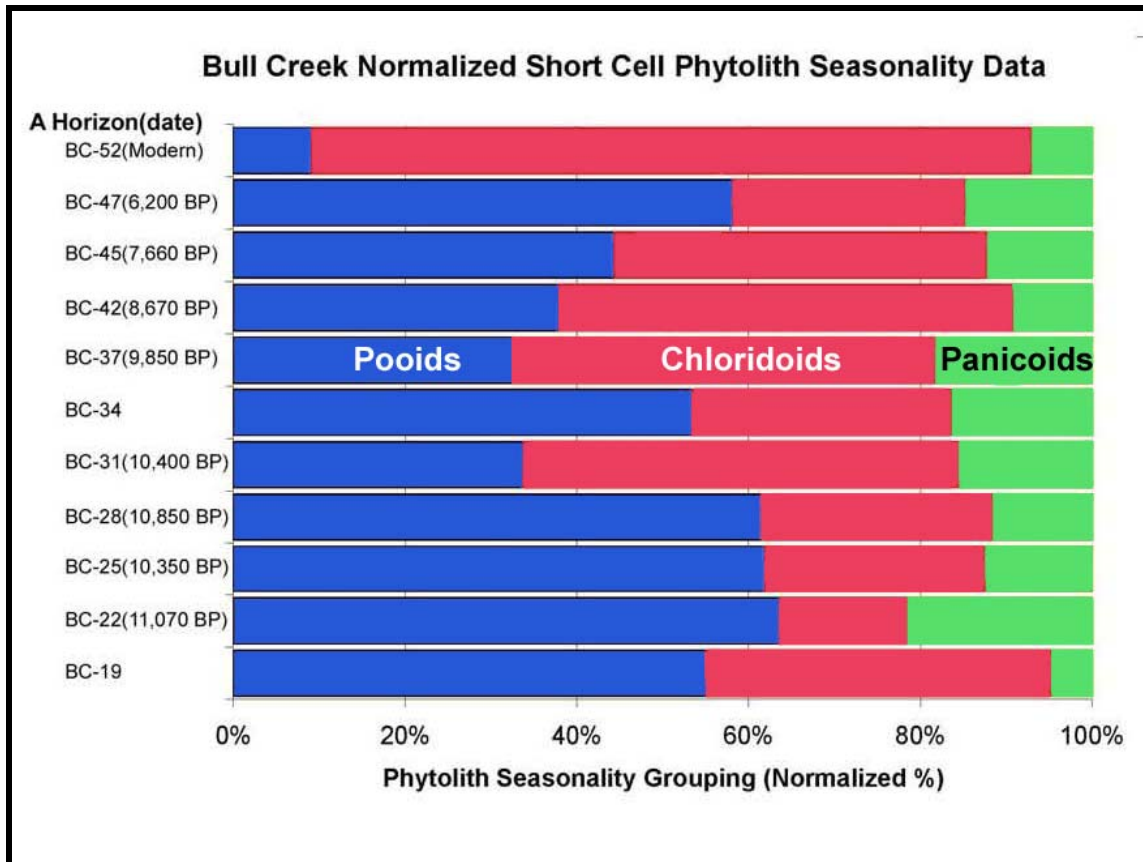
Figure 80. Bull Creek soil sample phytoliths in normalized seasonality groupings (data from Table 53). The dates given are in radiocarbon years before present (RCYBP). (Two non-A horizons were not dated. The non-A horizons analyzed at the Bull Creek Site are BC-42 [ABKb3], BC-34 [2BKb4], and BC-19 [2ACb8]).

Bull Creek correlated with an increase in saddle incidence (Figure 81), it was decided to exclude the rondel form from the short cell count totals and normalization. This is supported by the previous discussion regarding confuser/imposter forms. The so-called saddle form is the only major recognized Chloridoid short cell type used in past prairie studies on the Great Plains Fredlund and Tieszen (1994, 1997a). The actual botanical source of the rondels in soil at the Bull Creek Site has not been determined.

In today's hot dry climate, the Bull Creek Site area's modern Shortgrass Prairie phytolith sample is dominated by the saddle form (BC-52 Chloridoid component in Figure 80); however, none of the Bull Creek Site buried A horizon samples show phytolith evidence of a climate anywhere near as hot and dry as B-52. An increase in the Pooid fraction, as seen in BC-47 and BC-28 through BC-22, represents relatively cooler intervals at this site. Conversely, the increase relative to an adjacent A horizon of the Chloridoid fraction represents a warmer climatic interval (cf. BC-45, BC-37 and BC-31). The Panicoid (including Stipa) fraction is generally the smallest category at this site ranging from 7 to 21.4 %. The modern Manning Tallgrass Prairie control sample Panicoid fraction varied from 34-40% (Tables 17 and 35). The Dempsey Mixedgrass Prairie soil samples never got up to 7% Panicoids (Table 43). Perhaps the most impressive feature about the climate swings evidenced in the Bull Creek buried soil
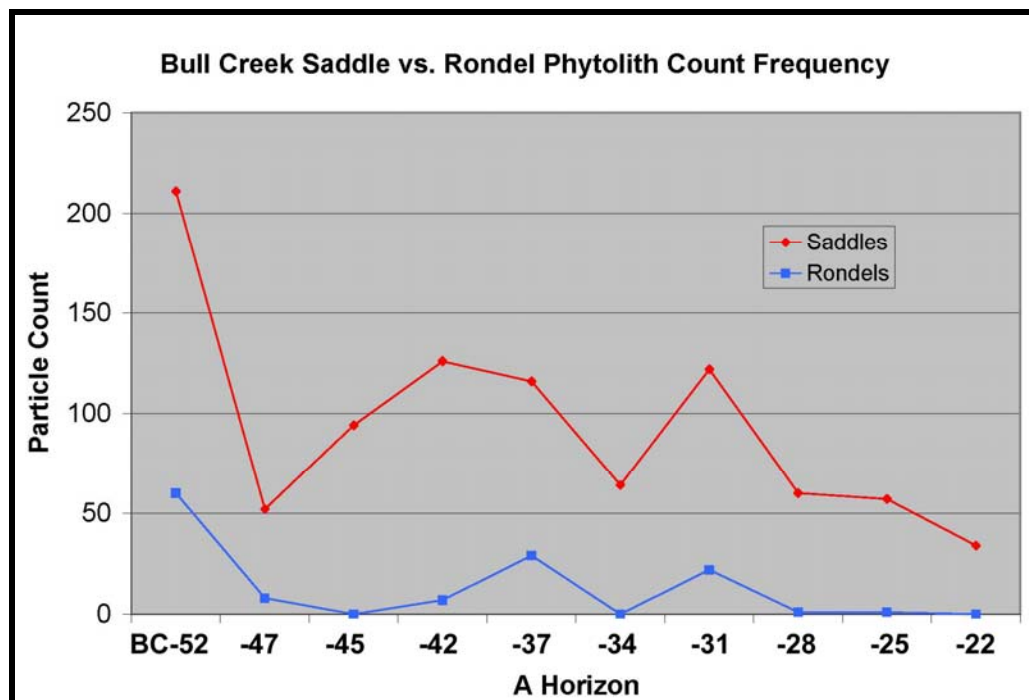
Figure 81. Comparison of actual particle counts of saddle and rondel forms in these eleven Bull Creek Soil Samples.

phytolith data is how large the climate swings are between some of the closely dated

buried soils—particularly during the interval represented by BC-22 through BC-37.

One way to interpret the data in the saddle plot (Figure 82, data from Tables 50

and 51) is that the scatter along the x-axis reflects the speed or extent of climate change

as evidenced by the length of time apparently available for invasive botanical species to

encroach on the site. In this case, the difference between the modern surface sample

(BC-52, in red) and the cluster containing BC-25, BC-28, and BC-47 is that the Pooid

fraction grows relative to the Chloridoid fraction, and the plant community (as reflected
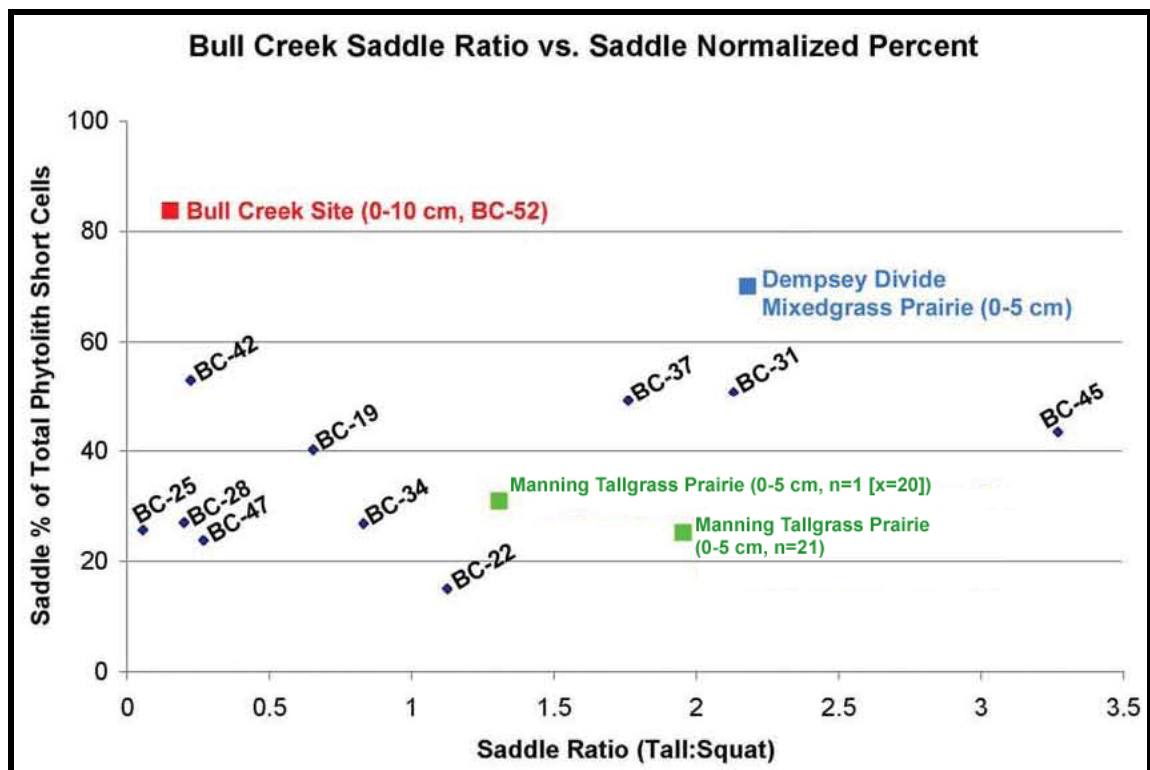
Figure 82. Plot of ratio of Tall:Squat Saddles vs. Normalized Percent Saddles for the
Bull Creek Site. Control Tallgrass and Mixedgrass Prairie surface data points also
included for reference. All black Bull Creek data points (except BC-19 and BC-34) are
buried A Horizons.

in the climatic data summary) was very similar at the times these three earlier A horizons formed. Thus, these three qualitative phytolith signatures (i.e., representing extant plants at the time of soil formation) do not give evidence of vegetation change although the quantitative portion of the data shows that the climate was much cooler than modern day in that Pooid fraction was markedly increased while and the Chloridoid fraction was smaller. The relative saddle composition (i.e., tall verses squat ratio) remained remarkably constant (i.e., the same C4 plants were presumably present, but with much less annual foliage on average resulting in a decrease in total Chloridoid content in the phytolith signature; Figure 82) while the cooler weather enabled the Pooids in the area to flourish and their phytolith composition (i.e., annual biomass) to increase. By the same logic, the BC-42 data point (ABkb3) suggests similar vegetation was present at the site at that time, but indicates an intermediate cooling trend from the previous cluster of three cases relative to modern-day. By this proposed reasoning, one would expect the previously known very cool climate sample (immediately post-glacial interval, 11,070 BP sample BC-22) in this series to have the lowest saddle concentration—and that is the case. During the BC-22 formation interval, the actual plant community composition appears to have been different than that present during BC-52, BC-42, BC-25, BC-28, and BC-47) due to the presumed presence of additional plant species causing a shift in Tall:Squat saddle ratio along the x-axis.

What Figure 82 appears to add to the information about the other samples with a greater tall saddle component is an apparent indication that the extreme cooling (climatic variation) that occurred was either

- extreme enough that the formerly minor plant species with a different saddle ratio became dominant enough to significantly shift the overall saddle ratio, or that

- the phytolith signature change was gradual enough that the actual plant community composition changed via additional plant species with a different saddle signature (tall vs. squat) encroaching on (gradually migrating to) the site in response to the climate change.

In contrast, sample BC-45 shows an extreme change in the soil phytolith saddle morphology ratio (x-axis movement) as well as an intermediate temperature range (y-axis movement). This shift suggests a major change occurred in the plant community at the site. This may mean that enough time lapsed prior to or when developing the BC-45 A horizon (versus BC-42 development) to enable incursion of new plant species into the area which significantly changed the saddle signature. By this reasoning, the samples BC-31 and BC-37 developed somewhat more rapidly than BC-45, but still slowly enough to enable some change in extant plant species in the plant association. The variation in the saddle ratio of two Manning data points (Figure 82) is felt to be the result of different moisture conditions (and thus different dominant botanical species, with no temperature variation) at the two adjacent Manning sampling locations. This potential intra-site moisture variation does not apply to the Bull Creek Site as all of the Bull Creek samples are from one single vertical soil profile.

It should be noted that three of the four A horizon samples that had a relative increase in total Chloridoid fraction (BC-31, BC-37, and BC-45) are the three samples

with the largest change in saddle morphology ratio. This could be explained by invasive

species gradually migrating into the area during an interval of or as a result of climate

change. The relative position on the plot in Figure 82 may indicate how quickly the

migration occurred and/or how long of an interval of new A horizon was stable. If this is

the correct interpretation, the longest period of changed climatic stability (i.e., the speed

of botanical species migration was most rapid) for BC-45, and slower for BC-31 and for

BC-37. The fourth warm interval noted previously (BC-42) shows essentially no change

in saddle morphologic signature which by the above reasoning would suggest the climate

change was relatively fast and/or the period of stability was very short [BC-42 was not an

A horizon]. The saddle signature would change by relative intensity of growth of the

plant community components (i.e., less seasonal time for Chloridoid growth (y-axis)

relative to modern-day, but maintaining the same saddle ratio) and/or with more non-

Chloridoid growth (biomass) in the prolonged cooler seasons (resulting in the ratio

change, seen as movement along the x-axis).

The Bull Creek Site soil profile contained the most buried soils ranging over the

longest dated time interval of any site studied. For this site, primarily A horizon

phytoliths were evaluated so pedogenesis is not addressed in this present discussion. The

soil profile has been published elsewhere, and details of soil formation addressed

(Bement et al. 2007). The Bull Creek Site saddle data (Figure 82) shows considerably

more diversity than was noted in the two previously discussed buried soil sites. The Bull

Creek Site climatic phytolith data is presented as a graph in Figure 83. This Bull Creek

plot differs from previous linear plots in that additional soil samples that occurred

between the analyzed A Horizon samples were omitted resulting in discontinuities in the

data presented from this stratigraphic column.
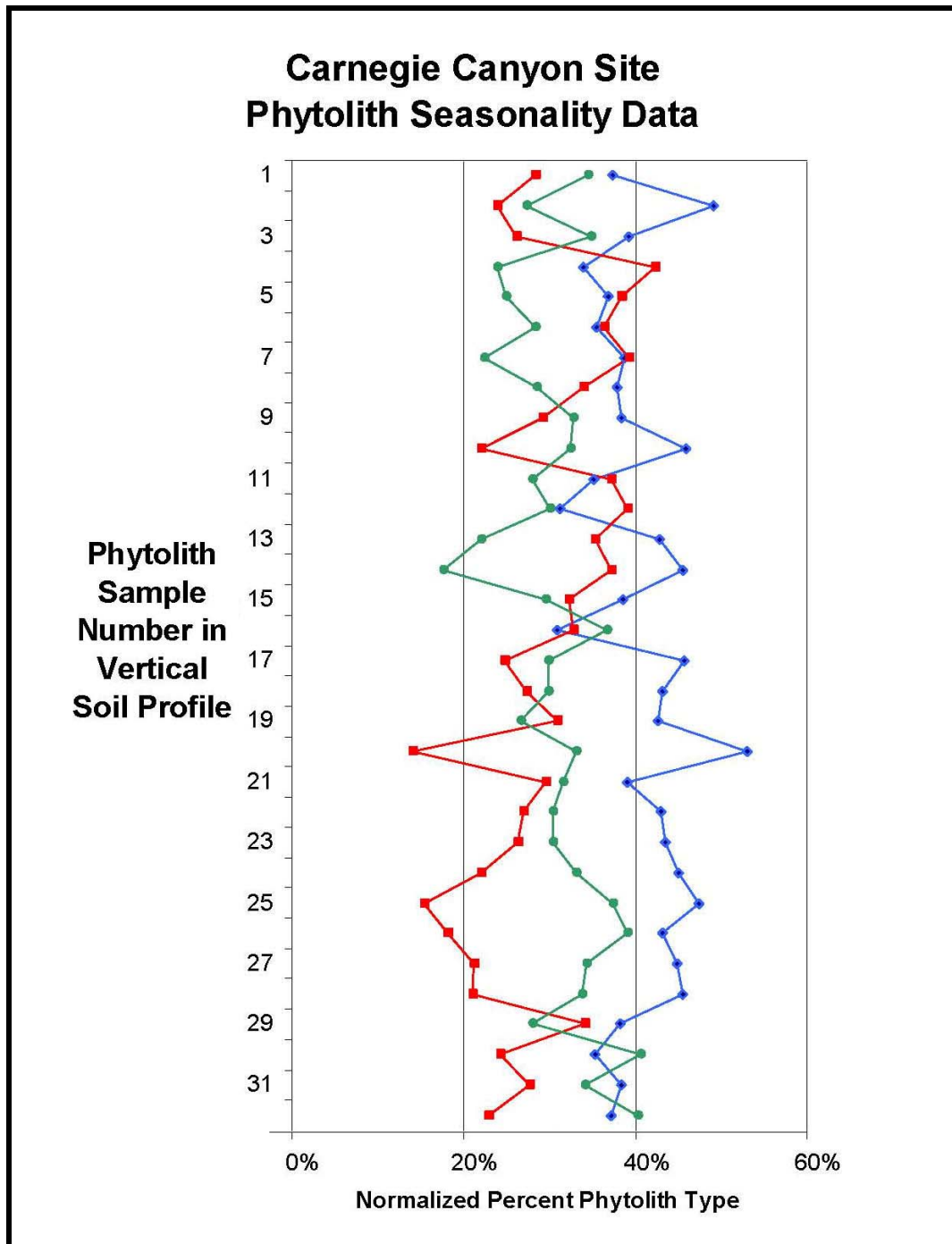
Figure 83. Seasonal plot of Carnegie Canyon Site phytolith data.

The Bull Creek site buried soil sequence begins in the early portion of the

Holocene at the end of the Wisconsin Glacial and Pleistocene Epoch. Although the

topography of the landscape at that time is uncertain, the higher Chloridoid fraction in

BC-19 (2ACb8) verses BC-22 may be indigenous in contrast to what was previously

observed at the Lizard Site when alluvial inputs added to the local phytolith signatures.

The parent material in BC-19 [through BC-37] was colluvium while the BC-42 through

BC-52 soils were loess-derived (Bement et al. 2007).

The phytolith signature of BC-22, dating to 11,070 BP has the lowest Chloridoid

and highest Panicoid content of the samples, and represents the first A horizon sample

analyzed after the beginning of glacial retreat; the climate was still very cool, with the

phytolith signature most similar to the cool moist riparian data observed from the Lizard

Site (Figure 109) of the sites examined in this study. Slight warming occurred in BC-25

and was apparently sustained during BC-28, with an additional warmer spike in BC-31—

with the temperature then being relatively stable through BC-37 and BC-42 (Figure 84).

BC-34 (2Bkb4) was cooler during this interval, but was not an A horizon (Bement et al.

2007). The loess era saw a cooling trend in BC-45 and BC-47, with the modern soil

phytolith sample (BC-52) being extremely hot and dry (Figure 84).

The lower portion of the colluvial sequence has discrepancies in the carbon dates

(Figure 84) within the BC-22 through BC-31 interval. This time interval includes the

BC-22 A horizon from which nanodiamonds were recovered (Kennett et al. 2009); the

nanodiamonds which are thought to be a direct result of the cosmic event proposed by

Firestone et al. (2007) in southeastern Canada during this time interval. If their theory is correct and contributed to the end of the large Pleistocene fauna and demise of the Clovis culture, a major environmental impact occurred. However, a drastic change is not seen in the phytolith signature during this and immediately following this interval; there is slight summer warming with less summer moisture from BC-22 to BC-25, but the Pooid signature remains constant from the BC-22 through BC-28 interval. If the cosmic event did severely alter the landscape at the time of occurrence (and nanodiamonds do occur at Bull Creek Site thousands of kilometers from the event source suggesting a major event), the next buried A horizon that formed at the site had a similar climatic signature to the previous soil sample. There is a distinct warming trend apparent in BC-31 with a higher Chloridoid component offsetting a Pooid decrease, but this is post-event and the climate was significantly warmer during the period of stability reflected in BC-31 (Figure 84).

The problem with the inversion of specific radiocarbon dates at the Bull Creek Site (i.e., BD- 25 and BC-28 in the sampling sequence) may have been caused by the cosmic event which occurred and may be responsible for precipitating the cold Younger-Dryas period in a manner previously described (Firestone and Topping 2001; Firestone et al. 2007). It is interesting to note that a similar date inversion (9,160 and 9,330 BP)—somewhat later and not as extreme—was previously reported from the Dry Creek alluvial fan (profile B) (Fredlund and Tieszen 1997b:212, 214).
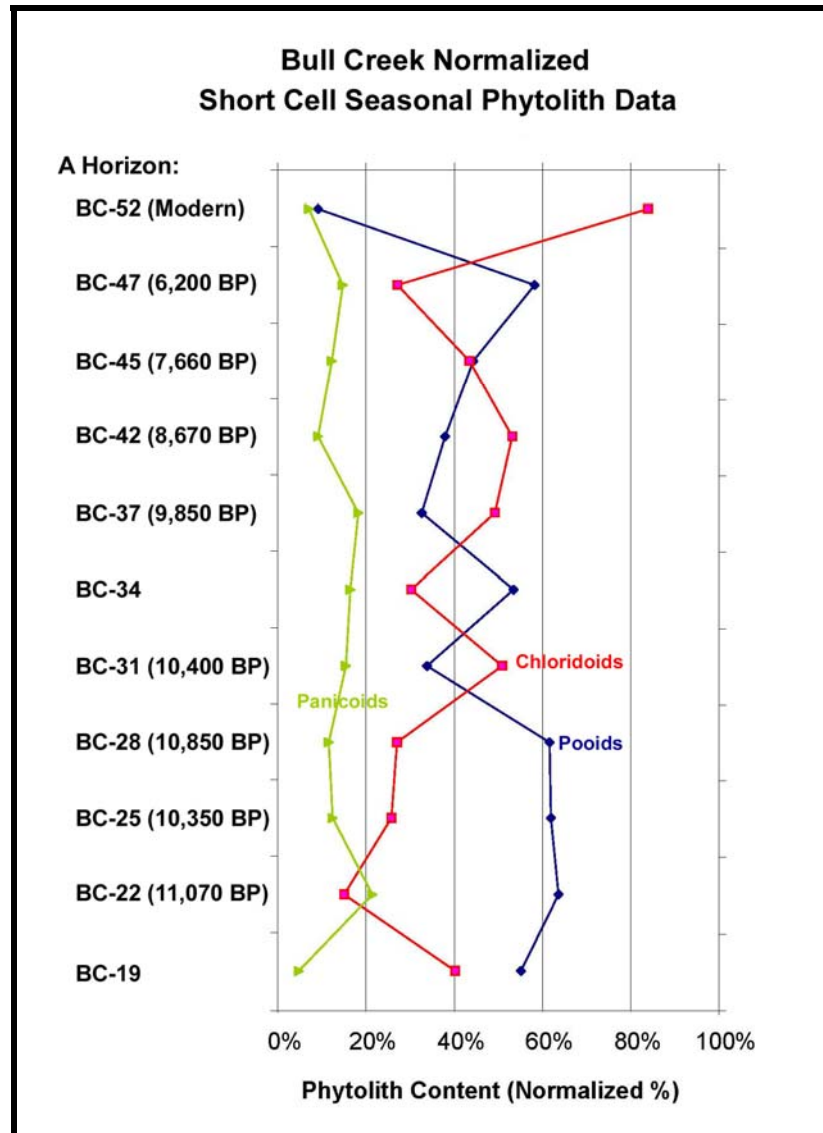
Figure 84. Bull Creek Site climatic phytolith data.

For phytolith research, the most significant finding coming out of the nanodiamond discovery at Bull Creek is that the nanodiamonds did not migrate from their point of deposition (i.e., no vertical scatter or redistribution observed) (Kennett 2009, Bement Personal Communication). Possible phytolith movement and migration in the soil profile has long been theorized and discussed (Rovner 1986b; Piperno 2006:111-

115; Hart and Humphreys 1997; 2003; Fishkis. Ingwersen, and Streck 2009); the Bull Creek nanodiamond evidence suggests that such particle movement does not routinely occur (Kennett et al. 2009)—at least in certain soil types.

The Bull Creek Site saddle data (Figure 82), BC-25, BC-28, and BC-47 are tightly clustered suggesting a similar cool climate and plant community at those three times of A horizon formation. Their total saddle content tends to mirror what was observed in the Carnegie Canyon cluster and in the Tallgrass Prairie controls, but with less morphologic saddle variation (Figure 109). The samples BC-19 and BC-34 [non-A horizons] are actually within the Carnegie Canyon Site cluster (Figure 109). The BC-42 sample, at the beginning of the loess deposition phase, has the same morphologic ratio as BC-25, BC-28, and BC-47, but a significantly lower Pooid component indicating it was much warmer (Figures 84 and 109). The end of the colluvial sequence (BC-37) and the middle of the loess sequence (BC-45) have significantly altered saddle morphology ratios, but retain a similar total saddle concentration to BC-42. This would suggest, as proposed by Bement et al. (2007), that the incursion of invasive species contributed to the change in the phytolith signature. Based on pollen data, cheno-ams were suggested as a possible contributing species (Bement et al. 2007).

Carnegie Canyon Site (34CD76) – Carnegie Canyon is a short southern tributary of the Washita River located in Caddo County, Oklahoma (Lintz and Hall 1983). Four plant associations were identified in the study area (Lintz and Hall 1983) of which "the

Woodland or Creek and River Associations" best describes the Carnegie Canyon Site evaluated in this current phytolith project. The site location is shown in Figures 7, 79, and 85, and the cleaned soil profile is illustrated in Figure 86. The Noble fine sandy loam is a coarse-loamy, siliceous, active, thermic udic haplustept. The soil profile description for this locale has been published (Carter et al. 2009). The raw phytolith counts for the 32 soil samples collected from this profile are given in Tables 54-57, and the normalized short cell values and the seasonality groupings are presented in Tables 58-60. The phytolith concentrations[36] reported as weight percent of dry soil are in Table 61 and plotted in Figure 87. The seasonality profile bar graph is presented in Figure 88.

The Caddo County paleosol (Ab3), beginning at 234 cm below current ground surface, has been carbon dated to 1010 ± 50 rybp (Carter et al. 2009). Thus, the soil above this A horizon filled in at an average accumulation rate of 2.32 mm of sediment per year starting from when the soil was initially buried. It was also suggested that Ab2 probably correlates with the 500 rybp Delaware Creek soil (Carter et al. 2009). Some periods of relative stability occurred in this total sequence—enough so that A horizons had sufficient time to develop. However, the Cb2 horizon between Ab2 and Ab3— apparently representing about 500 years--is nearly 1.6 meters thick and shows no sign of definitive melanization. This indicates a period of rapid alluvial deposition in Carnegie Canyon in the first half of the past millennium.

---

[36] As the separation is based on particle density, the phytolith fraction weight is actually the total biogenic silica weight (including phytoliths, diatoms, and spicules).

The high phytolith concentration in the Ab3 horizon (Figure 87, samples 20-28) indicates that there was a well-developed plant community at the time that the Caddo County paleosol was formed, suggesting a period of stability. The paleosol thickness (1.18 m (Carter et al. 2009)) suggests a prolonged period of stability. The higher total phytolith concentration at the Carnegie Canyon Site than observed at the prairie control sites is possibly an indication of the greater availability of moisture and nutrients in the soil that help nourish and sustain vegetative growth. The flood events that occurred at this site have been detailed based on the soil particle size data (Carter et al. 2009).
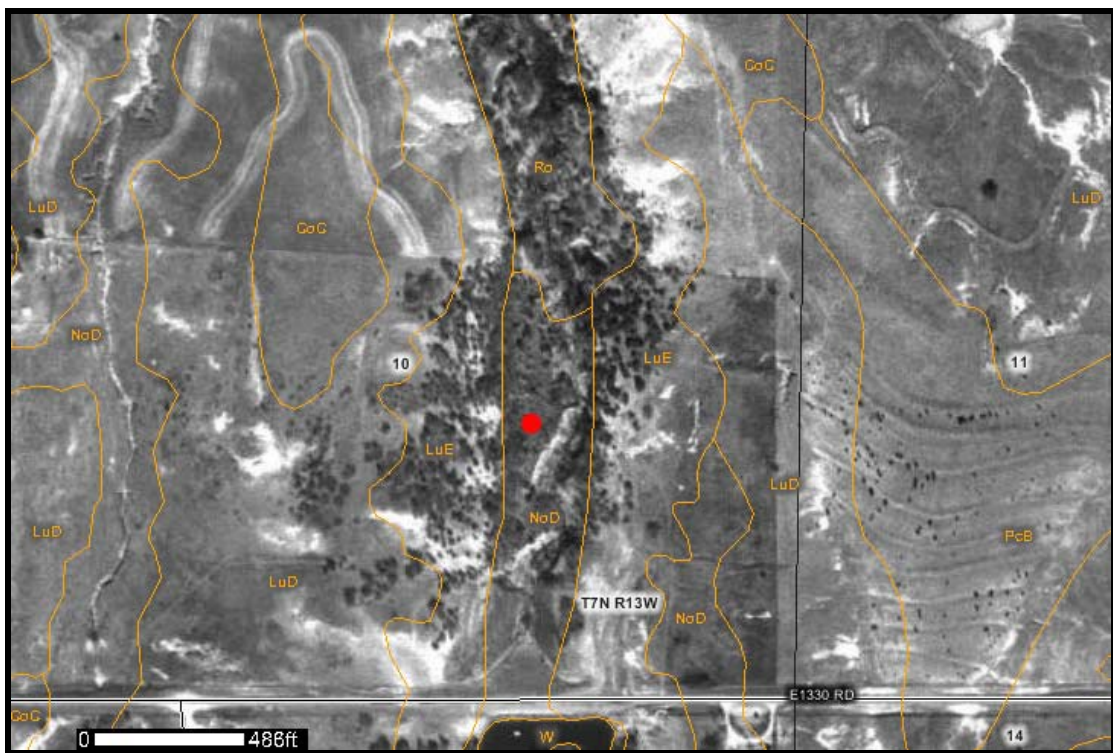
Figure 85. Carnegie Canyon Site (34CD76), Caddo County, Oklahoma. USDA soil series reported as present in this marked aerial photograph are: CoC (Binger fine sandy loam, 3-5 % slopes), LuD (Ironmound-Dill complex, 3-12 % slopes), LuE (Ironmound-Dill complex, 12-30% slopes), NoD (Noble fine sandy loam, 3-8 % slopes), PcB (Pond Creek fine sandy loam, 1-3 % slopes), and Ro (Darnell-Rock outcrop complex, 20-70% slopes). (Aerial photograph with soil designations obtained from NRCS/USDA web site http://websoilsurvey.nrcs.usda.gov/app/HomePage.htm).

Figure 86. Carnegie Canyon Site soil profile showing prominent buried soil Ab3 below 2 meters.

Table 54
Carnegie Canyon Site (34CD76) Phytolith Counts (Samples 1-8)

Sample	S-1	S-2	S-3	S-4	S-5	S-6	S-7	S-8
Morphology								
Keeled	**38**	**44**	**29**	**18**	**21**	**23**	**14**	**35**
Conical	**39**	**42**	**38**	**51**	**48**	**48**	**46**	**43**
Pyramidal	**0**	**2**	**6**	**1**	**4**	**3**	**0**	**4**
Crenate	**2**	**13**	**8**	**4**	**4**	**8**	**19**	**15**
Saddle, Squat	**44**	**30**	**37**	**51**	**55**	**58**	**43**	**46**
Saddle, Tall	**16**	**19**	**17**	**41**	**25**	**26**	**37**	**41**
Stipa	**19**	**8**	**15**	**5**	**13**	**8**	**5**	**6**
Lobate, Simple	**8.5**	**12.5**	**16.5**	**10.5**	**6**	**13**	**5**	**15**
Lobate, Panicoid	**34.5**	**22.5**	**25.5**	**30**	**30**	**41.5**	**34.5**	**44**
Lobate, compound	**0**	**1**	**0**	**0**	**0**	**1**	**0**	**0**
Cross (<10 µ)	**5**	**9**	**8**	**5.5**	**2**	**2**	**1**	**4**
Cross (>10 µ)	**6**	**3**	**7**	**1**	**1**	**0**	**0**	**4**
Maize Rondel	3	0	0	0	1	1	1	5
Rondel, bipoint	0	0	0	0	0	0	0	0
Rondel, other	0	1	0	0	0	1	0	5
Dicot, knobby	0	5	0	0	4	1	1	3
Spiny spheroid	4	1	0	0	0	1	3	1
WWW	0	0	0	0	0	0	0	0
Schlerid	0	0	0	0	0	0	0	0
Diatom	45.5	8	1	1	1	3	2	0
Sponge spicule	5	6	8	0	1	0	1	0
Trichrome	6	6	3	8	15	4	5	7
Hair Cells	0	0	0	0	0	1	0	0
Bulliform, square	5	8	9	7	12	15	12	8
Bulliform, rectangular	4	6	13	17	8	29	12	13
Bulliform, keystone	0	2	1	4	0	2	2	3
Bulliform, Y-shaped	1	0	0	0	0	0	1	0
Bulliform, other	6	24	25	19	35	43	37	23
Elongate, smooth	5	10	5	2	5	15	13	8
Elongate, sinuous	3	3	3	0	3	4	3	4
Elongate, castillate	2	6	3	1	5	17	9	2
Elongate, spiny	9	1	0	2	0	1	1	2
Sedge	3.5	0	1	0	1	0	2	1
Total Phytoliths	314	293	279	279	300	369.5	309.5	342
Total Short Cells	212	206	207	218	209	231.5	204.5	257

Table 55
Carnegie Canyon Site (34CD76) Phytolith Counts (Samples 9-16)

Sample	S-9	S-10	S-11	S-12	S-13	S-14	S-15	S-16
Morphology								
Keeled	**27**	**25**	**30**	**20**	**15**	**25**	**24**	**9**
Conical	**46**	**46**	**36**	**36**	**64**	**54**	**36**	**40**
Pyramidal	**6**	**6**	**3**	**3**	**3**	**2**	**3**	**5**
Crenate	**8**	**19**	**15**	**8**	**10**	**12**	**10**	**9**
Saddle, Tquat	**29**	**28**	**47**	**40**	**38**	**37**	**33**	**39**
Saddle, Tall	**37**	**18**	**42**	**44**	**38**	**39**	**28**	**28**
Stipa	**12**	**11**	**5**	**10**	**6**	**7**	**6**	**5**
Lobate, Simple	**3**	**5**	**6**	**6**	**5**	**3**	**7**	**12.5**
Lobate, Panicoid	**59**	**44**	**49**	**47.5**	**30.5**	**24**	**38**	**55.5**
Lobate (cmpd)	**0**	**0**	**0**	**1**	**0**	**0**	**0**	**0**
Cross (<10 μ)	**0**	**7**	**6**	**0**	**5**	**2**	**5**	**2**
Cross (>10 μ)	**0**	**1**	**1**	**0**	**1**	**0**	**0**	**0**
Maize Rondel	0	1	1	0	1	0	0	0
Rondel, bipoint	0	0	0	0	0	0	0	0
Rondel, other	2	4	4	6	6	4	7	2
Dicot, knobby	0	0	0	0	0	2	0	1
Spiny spheroid	4	1	3	0	3	0	0	0
WWW	0	0	0	0	0	0	0	0
Schlerid	0	0	0	0	0	0	0	0
Diatom	2	1	0	0	0	1	1	0
Sponge spicule	3	2	7	4	4	3	3	2
Trichrome	14	11	6	11	10	10	8	15
Hair Cells	1	0	0	0	0	0	0	0
Bulliform, square	13	4	10	11	11	8	13	20
Bulliform (rect)	15	22	6	17	13	16	8	22
Bulliform, keystone	5	4	11	7	6	4	5	10
Bulliform, Y-shaped	0	2	0	0	0	0	0	0
Bulliform, other	86	94	41	33	36	21	27	27
Elongate, smooth	11	10	9	8	3	4	1	5
Elongate, sinuous	4	11	2	0	3	0	3	4
Elongate, castillate	7	10	5	3	4	4	4	6
Elongate, spiny	0	1	1	4	2	3	1	2
Sedge	3.5	6	3.5	5	0.5	3	1	2
Total Phytoliths	397.5	394	349.5	324.5	318	288	272	323
Total Short Cells	227	210	240	215.5	215.5	205	190	205

Table 56
Carnegie Canyon Site (34CD76) Phytolith Counts (Samples 17-24)

Sample	S-17	S-18	S-19	S-20	S-21	S-22	S-23
Morphology							
Keeled	**31**	**25**	**32**	**36**	**35**	**50**	**30**
Conical	**56**	**43**	**50**	**49**	**37**	**48**	**42**
Pyramidal	**3**	**8**	**7**	**4**	**3**	**7**	**3**
Crenate	**8**	**8**	**8**	**13**	**12**	**13**	**16**
Saddle, Squat	**27**	**35**	**53**	**17**	**39**	**50**	**41**
Saddle, Tall	**26**	**18**	**17**	**10**	**27**	**24**	**14**
Stipa	**8**	**5**	**12**	**17**	**10**	**19**	**7**
Lobate, Simple	**7**	**5**	**8**	**6**	**7**	**5**	**3**
Lobate, Panicoid	**46**	**42**	**31.5**	**36.5**	**47.5**	**48.5**	**49.5**
Lobate, compound	**0**	**1**	**0**	**0**	**0**	**1**	**2**
Cross (<10 μ)	**3**	**4**	**5**	**4**	**4**	**9**	**2**
Cross (>10 μ)	**0**	**1**	**4**	**0**	**2**	**1**	**0**
Maize Rondel	0	1	1	3	1	3	0
Rondel, bipoint	0	0	0	0	0	0	0
Rondel, other	5	3	1	6	7	0	2
Dicot, knobby	0	1	0	1	0	2	1
Spiny spheroid	1	0	2	0	0	0	0
WWW	0	0	0	0	0	0	0
Schlerid	0	0	0	0	0	0	0
Diatom	1	6	69	28	34	45	21
Sponge spicule	3	1	7	5	3	3	0
Trichrome	7	15	6	3	4	6	3
Hair Cells	0	0	0	0	1	0	0
Bulliform, square	18	18	9	1	4	6	6
Bulliform, rectangular	10	19	7	2	9	11	10
Bulliform, keystone	10	18	1	1	4	2	4
Bulliform, Y-shaped	0	0	0	0	0	0	0
Bulliform, other	55	53	13	12	20	24	12
Elongate, smooth	14	10	23	11	9	12	3
Elongate, sinuous	3	4	4	1	4	4	1
Elongate, castillate	8	10	3		7	2	2
Elongate, spiny	2	3	1	3	0	2	0
Sedge	3.5	3	2	1	4	4	4
Total Phytoliths	355.5	360	376.5	270.5	334.5	401.5	278.5
Total Short Cells	215	195	227.5	192.5	223.5	275.5	209.5

Table 57
Carnegie Canyon Site (34CD76) Phytolith Counts (Samples 25-32)

Sample	S-24	S-25	S-26	S-27	S-28	S-29	S-30	S-31	S-32
Morphology									
Keeled	**25**	**29**	**28**	**37**	**21**	**18**	**11**	**7**	**7**
Conical	**49**	**38**	**38**	**39**	**52**	**29**	**21**	**21**	**25**
Pyramidal	**8**	**8**	**10**	**10**	**7**	**13**	**9**	**7**	**1**
Crenate	**8**	**24**	**19**	**16**	**9**	**7**	**10**	**1**	**16**
Saddle, Squat	**30**	**21**	**22**	**25**	**29**	**29**	**20**	**16**	**16**
Saddle, Tall	**14**	**11**	**18**	**23**	**12**	**31**	**15**	**10**	**14**
Stipa	**21**	**11**	**16**	**5**	**3**	**1**	**0**	**1**	**11**
Lobate, Simple	**19**	**11**	**9**	**4**	**1**	**3**	**1.5**	**0**	**3**
Lobate, Panicoid	**19**	**54**	**60**	**63**	**59**	**42**	**54**	**31**	**39**
Lobate, compound	**1**	**0**	**0**	**3**	**1**	**0**	**0**	**0**	**0**
Cross (<10 μ)	**5**	**2**	**1**	**1**	**2**	**1**	**3**	**0**	**0**
Cross (>10 μ)	**1**	**0**	**0**	**2**	**0**	**2**	**0**	**0**	**0**
Maize Rondel	0	0	0	0	0	0	0	0	0
Rondel, bipoint	0	0	0	0	0	0	0	0	0
Rondel, other	2	1	1	3	4	1	1	0	0
Dicot, knobby	1	1	1	1	2	1	1	0	0
Spiny spheroid	0	0	0	3	3	1	2	1	0
WWW	0	0	0	0	0	0	0	0	0
Schlerid	0	0	0	0	0	0	0	0	0
Diatom	28	5	4	3	0	1	0	0	3
Sponge spicule	4	1	3	4	2	0	0	2	3
Trichrome	6	4	6	2	9	8	0	8	19
Hair Cells	0	1	1	0	0	0	0	0	0
Bulliform, square	6	7	6	12	17	22	15	25	39
Bulliform, rectangular	22	14	11	28	22	34	21	25	42
Bulliform, keystone	8	5	2	6	8	25	12	10	22
Bulliform, Y-shaped	0	2	0	1	0	0	0	2	1
Bulliform, other	26	23	38	44	51	31	17	30	11
Elongate, smooth	12	5	7	7	16	1	2	3	2
Elongate, sinuous	4	3	5	8	18	3	0	5	2
Elongate, castillate	8	4	2	4	11	2	4	2	6
Elongate, spiny	0	1	2	1	2	0	0	0	1
Sedge	4	3	4	3	2	4	2	3	3
Total Phytoliths	331	289	314	358	363	310	221.5	210	286
Total Short Cells	200	209	221	228	196	176	144.5	94	132

Table 58. Carnegie Canyon Site (34CD76) Normalized Short Cell Types and Seasonality Groupings (Samples 1-11)

Soil Sample	S-1	S-2	S-3	S-4	S-5	S-6	S-7	S-8	S-9	S-10	S-11
Normalized Short Cells											
Keeled	17.9%	21.4%	14.0%	8.3%	10.0%	9.9%	6.8%	13.6%	11.9%	11.9%	12.5%
Conical	18.4%	20.4%	18.4%	23.4%	23.0%	20.7%	22.5%	16.7%	20.3%	21.9%	15.0%
Pyramidal	0.0%	1.0%	2.9%	0.5%	1.9%	1.3%	0.0%	1.6%	2.6%	2.9%	1.3%
Crenate	0.9%	6.3%	3.9%	1.8%	1.9%	3.5%	9.3%	5.8%	3.5%	9.0%	6.3%
Saddle, squat	20.8%	14.6%	17.9%	23.4%	26.3%	25.1%	21.0%	17.9%	12.8%	13.3%	19.6%
Saddle, Tall	7.5%	9.2%	8.2%	18.8%	12.0%	11.2%	18.1%	16.0%	16.3%	8.6%	17.5%
Stipa	9.0%	3.9%	7.2%	2.3%	6.2%	3.5%	2.4%	2.3%	5.3%	5.2%	2.1%
Lobate, Simple	4.0%	6.1%	8.0%	4.8%	2.9%	5.6%	2.4%	5.8%	1.3%	2.4%	2.5%
Lobate, Panicoid	16.3%	10.9%	12.3%	13.8%	14.4%	17.9%	16.9%	17.1%	26.0%	21.0%	20.4%
Lobate, compound	0.0%	0.5%	0.0%	0.0%	0.0%	0.4%	0.0%	0.0%	0.0%	0.0%	0.0%
Cross (<10)	2.4%	4.4%	3.9%	2.5%	1.0%	0.9%	0.5%	1.6%	0.0%	3.3%	2.5%
Cross (>10)	2.8%	1.5%	3.4%	0.5%	0.5%	0.0%	0.0%	1.6%	0.0%	0.5%	0.4%
total short cell	212	206	207	218	209	231.5	204.5	257	227	210	240
Normalized Seasonality Grouping											
Pooids	37.3%	49.0%	39.1%	33.9%	36.8%	35.4%	38.6%	37.7%	38.3%	45.7%	35.0%
Chloridoids	28.3%	23.8%	26.1%	42.2%	38.3%	36.3%	39.1%	33.9%	29.1%	21.9%	37.1%
Panicoids	34.4%	27.2%	34.8%	23.9%	24.9%	28.3%	22.2%	28.4%	32.6%	32.4%	27.9%

233

Table 59. Carnegie Canyon Site (34CD76) Normalized Short Cell Types and Seasonality Groupings (Samples 12-22)

Soil Sample	S-12	S-13	S-14	S-15	S-16	S-17	S-18	S-19	S-20	S-21	S-22
Normalized Short Cells											
Keeled	9.3%	7.0%	12.2%	12.6%	4.4%	14.4%	12.8%	14.1%	18.7%	15.7%	18.1%
Conical	16.7%	29.7%	26.3%	18.9%	19.5%	26.0%	22.1%	22.0%	25.5%	16.6%	17.4%
Pyramidal	1.4%	1.4%	1.0%	1.6%	2.4%	1.4%	4.1%	3.1%	2.1%	1.3%	2.5%
Crenate	3.7%	4.6%	5.9%	5.3%	4.4%	3.7%	4.1%	3.5%	6.8%	5.4%	4.7%
Saddle, squat	18.6%	17.6%	18.0%	17.4%	19.0%	12.6%	17.9%	23.3%	8.8%	17.4%	18.1%
Saddle, Tall	20.4%	17.6%	19.0%	14.7%	13.7%	12.1%	9.2%	7.5%	5.2%	12.1%	8.7%
Stipa	4.6%	2.8%	3.4%	3.2%	2.4%	3.7%	2.6%	5.3%	8.8%	4.5%	6.9%
Lobate, Simple	2.8%	2.3%	1.5%	3.7%	6.1%	3.3%	2.6%	3.5%	3.1%	3.1%	1.8%
Lobate, Panicoid	22.0%	14.2%	11.7%	20.0%	27.1%	21.4%	21.5%	13.8%	19.0%	21.3%	17.6%
Lobate, compound	0.5%	0.0%	0.0%	0.0%	0.0%	0.0%	0.5%	0.0%	0.0%	0.0%	0.4%
Cross (<10)	0.0%	2.3%	1.0%	2.6%	1.0%	1.4%	2.1%	2.2%	2.1%	1.8%	3.3%
Cross (>10)	0.0%	0.5%	0.0%	0.0%	0.0%	0.0%	0.5%	1.8%	0.0%	0.9%	0.4%
total short cell	215.5	215.5	205	190	205	215	195	227.5	192.5	223.5	275.5
Normalized Seasonality Grouping											
Pooids	31.1%	42.7%	45.4%	38.4%	30.7%	45.6%	43.1%	42.6%	53.0%	38.9%	42.8%
Chloridoids	39.0%	35.3%	37.1%	32.1%	32.7%	24.7%	27.2%	30.8%	14.0%	29.5%	26.9%
Panicoids	29.9%	22.0%	17.6%	29.5%	36.6%	29.8%	29.7%	26.6%	33.0%	31.5%	30.3%

Table 60. Carnegie Canyon Site (34CD76) Normalized Short Cell Types and Seasonality Groupings (Samples 23-32)

Soil Sample	S-23	S-24	S-25	S-26	S-27	S-28	S-29	S-30	S-31	S-32
Normalized Short Cells										
Keeled	14.3%	12.5%	13.9%	12.7%	16.2%	10.7%	10.2%	7.6%	7.4%	5.3%
Conical	20.0%	24.5%	18.2%	17.2%	17.1%	26.5%	16.5%	14.5%	22.3%	18.9%
Pyramidal	1.4%	4.0%	3.8%	4.5%	4.4%	3.6%	7.4%	6.2%	7.4%	0.8%
Crenate	7.6%	4.0%	11.5%	8.6%	7.0%	4.6%	4.0%	6.9%	1.1%	12.1%
Saddle, squat	19.6%	15.0%	10.0%	10.0%	11.0%	14.8%	16.5%	13.8%	17.0%	12.1%
Saddle, Tall	6.7%	7.0%	5.3%	8.1%	10.1%	6.1%	17.6%	10.4%	10.6%	10.6%
Stipa	3.3%	10.5%	5.3%	7.2%	2.2%	1.5%	0.6%	0.0%	1.1%	8.3%
Lobate, Simple	1.4%	9.5%	5.3%	4.1%	1.8%	0.5%	1.7%	1.0%	0.0%	2.3%
Lobate, Panicoid	23.6%	9.5%	25.8%	27.1%	27.6%	30.1%	23.9%	37.4%	33.0%	29.5%
Lobate, compound	1.0%	0.5%	0.0%	0.0%	1.3%	0.5%	0.0%	0.0%	0.0%	0.0%
Cross (<10)	1.0%	2.5%	1.0%	0.5%	0.4%	1.0%	0.6%	2.1%	0.0%	0.0%
Cross (>10)	0.0%	0.5%	0.0%	0.0%	0.9%	0.0%	1.1%	0.0%	0.0%	0.0%
total short cell	209.5	200	209	221	228	196	176	144.5	94	132
Normalized Seasonality Grouping										
Pooids	43.4%	45.0%	47.4%	43.0%	44.7%	45.4%	38.1%	35.3%	38.3%	37.1%
Chloridoids	26.3%	22.0%	15.3%	18.1%	21.1%	20.9%	34.1%	24.2%	27.7%	22.7%
Panicoids	30.3%	33.0%	37.3%	38.9%	34.2%	33.7%	27.8%	40.5%	34.0%	40.2%

Table 61

Carnegie Canyon Site Soil Sample and Recovered Phytolith Weights

34CD76 Profile Sample Number	Soil Sample Wt (g)	Phytoliths Recovered (g)	Phytoliths, Wt% per unit dry soil
1	98.88	0.16807	0.17%
2	101.47	0.10850	0.11%
3	101.28	0.11888	0.12%
4	101.49	0.09206	0.09%
5	107.13	0.11101	0.10%
6	106.20	0.17801	0.17%
7	98.45	0.03970	0.04%
8	107.63	0.02083	0.02%
9	104.15	0.02569	0.02%
10	98.43	0.03056	0.03%
11	104.86	0.02735	0.03%
12	102.80	0.01678	0.02%
13	101.35	0.02462	0.02%
14	100.86	0.05681	0.06%
15	101.48	0.07515	0.07%
16	99.72	0.07561	0.08%
17	102.75	0.04956	0.05%
18	101.95	0.07713	0.08%
19	109.92	0.44615	0.41%
20	107.43	1.23103	1.15%
21	103.78	0.95909	0.92%
22	104.20	0.79590	0.76%
23	103.73	0.70488	0.68%
24	114.99	0.74474	0.65%
25	115.62	0.63827	0.55%
26	101.06	0.53388	0.53%
27	97.40	0.39545	0.41%
28	98.73	0.14569	0.15%
29	103.86	0.04891	0.05%
30	108.16	0.05308	0.05%
31	101.91	0.03349	0.03%
32	99.95	0.00907	0.01%
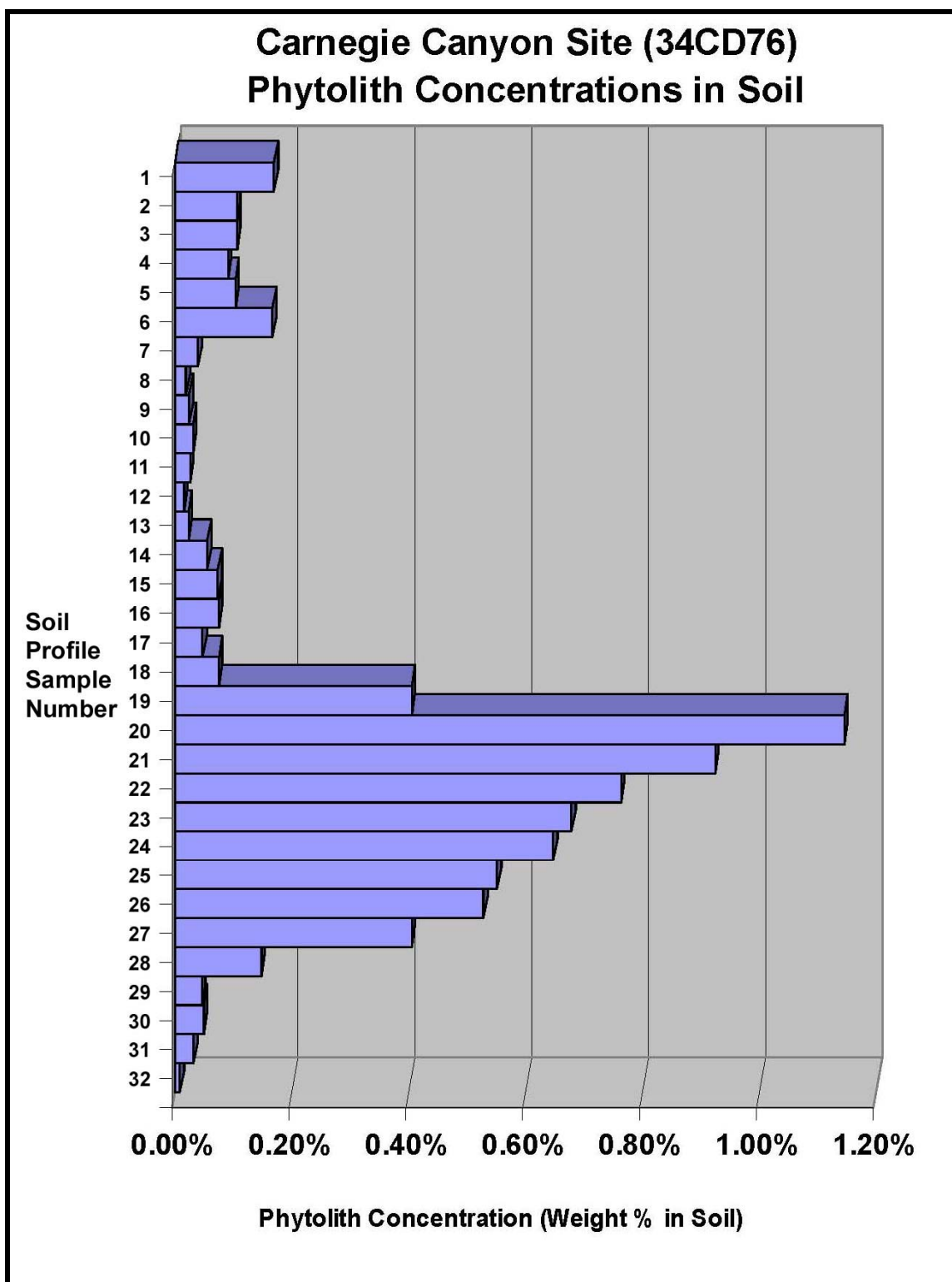
Figure 87. Phytolith (biogenic silica) concentration in the soil profile samples from the Carnegie Canyon Site.
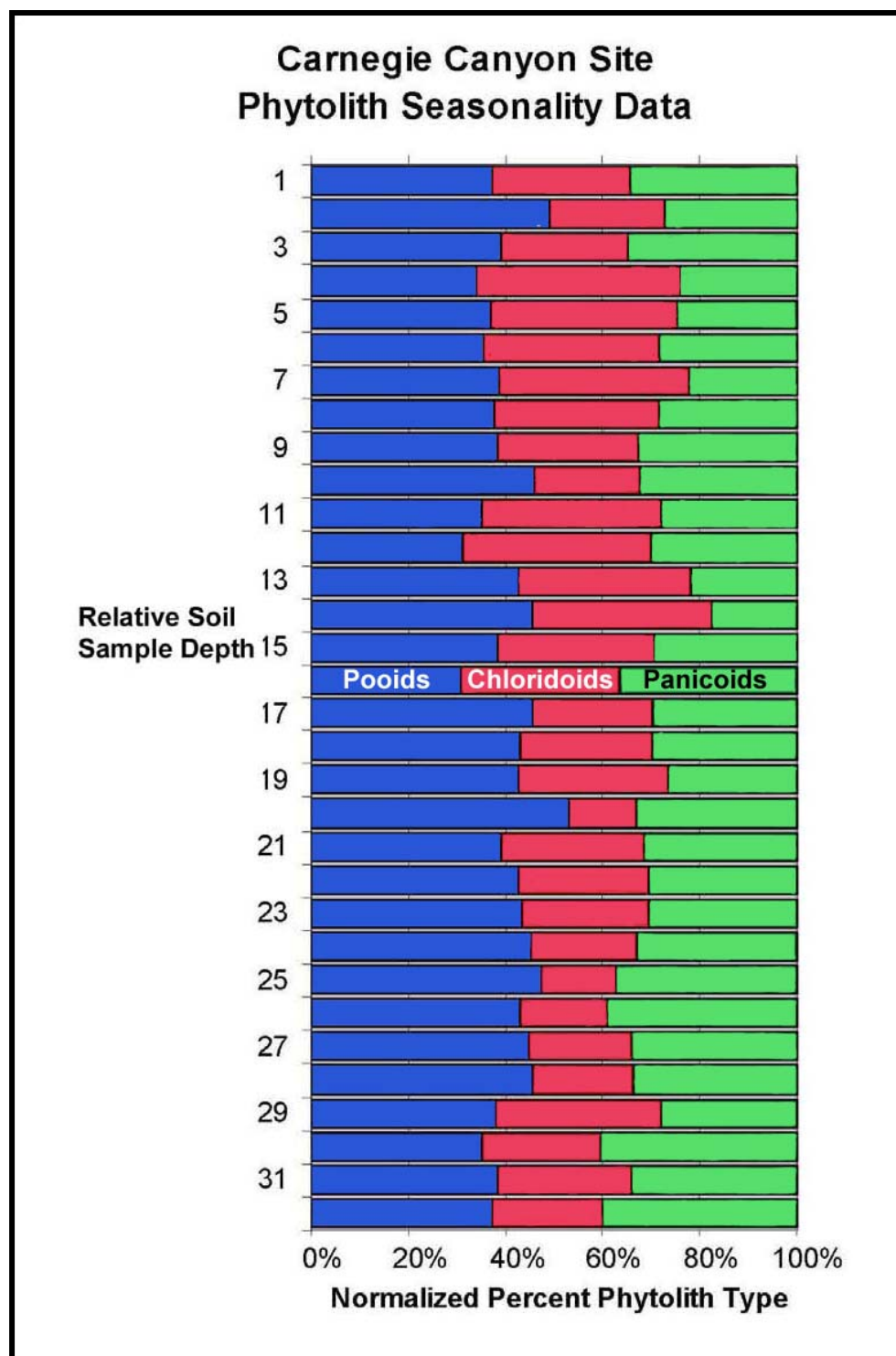
Figure 88. Bar graph of seasonality profile data for the Carnegie Canyon Site. Sample 1 is the modern A Horizon, Sample 3 is Ab, Sample 6 is Ab2, Sample 19 contains "finely dispersed A horizon material", and sample 20 (A1b3) represents the top of Ab3 (Carter et al. 2009).

Another potential contributor is the time interval involved in soil formation. The upper

55% and the lower 10% of the Caddo County paleosol were determined to be formed by

the process of melanization, with the lower portion having much lower phytolith content,

whereas the intervening soil zone was cumulic in nature (Carter et al. 2009).

The morphologic data for the saddle short cell phytoliths for this entire soil profile

sequence is plotted in Figure 89. This sub-fraction of the phytolith samples tends to be

clustered, but does not mirror any of the three control prairie saddle samples. This is

presumably due at least in part to the fact that several of the control sites (Manning

Tallgrass Prairie and Dempsey Divide Mixedgrass Prairie) are in upland prairie settings

whereas the Carnegie Canyon Site study area is located on a short drainage system

dominated by riparian vegetation. This riparian setting would include numerous non-

Poaceae species which would contribute their phytolith signature to the total assemblage

in the soil which would also presumably include phytoliths that may have been

transported into the drainage during rain events.

This same data is further dissected in Figure 91 with the upper A horizons

sampled being highlighted with green diamonds, and the other melanized soil samples

being marked with white diamonds. With this additional winnowing, the data becomes

clearer. Samples 1, 3, 6 and 19 cluster tightly; these are all A horizons (#1 is actually an

AC horizon). Sample 19 showed signs of finely dispersed A material; in this plot it

appears that—although weakly melanized, soil sample 19 rather than soil sample 20 was

actually the upper portion of the Caddo County paleosol and very similar to modern
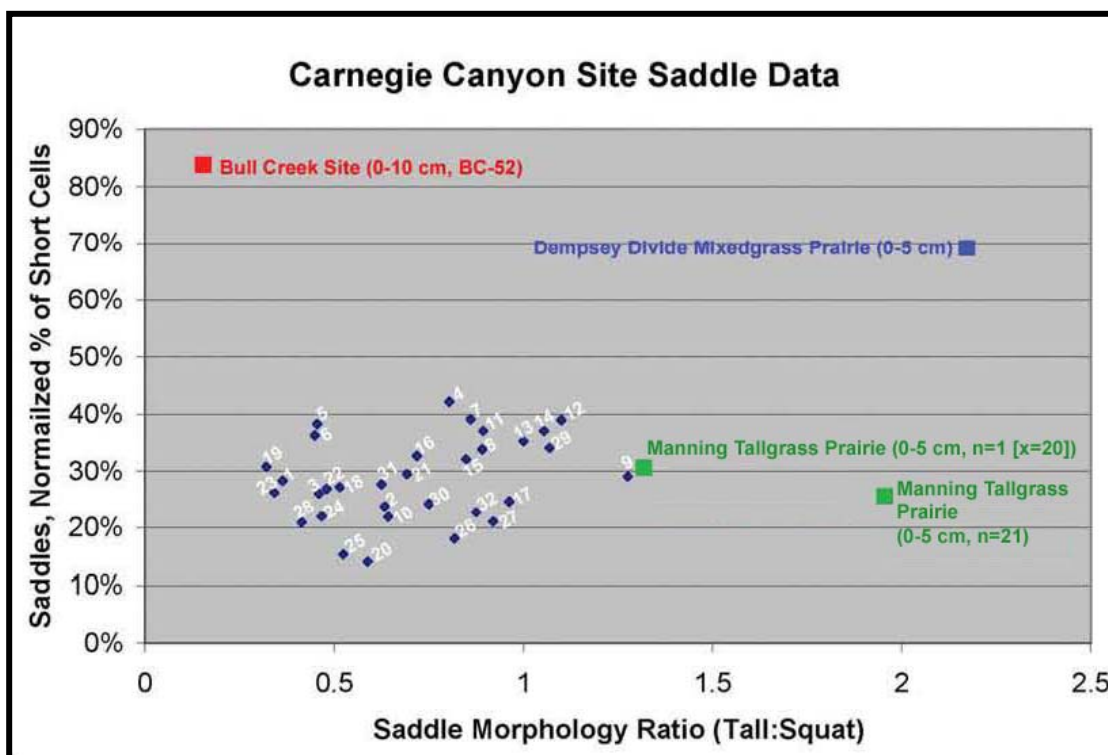
Figure 89. Carnegie Canyon Site data (numbered black diamonds) showing the distribution of relative saddle morphology vs. normalized saddle concentration.

climatic and vegetative conditions. Although there is slight variability in the vertical distribution of 1, 3, 6, and 19 possibly suggesting some temperature variation during this one thousand year interval, overall the climatic conditions at the times that these four A horizons developed (including the modern day AC horizon) appear to have been similar in their vegetative signature. What happened during the intervening cumulic periods between A horizon formations is not addressed in these four samples, but based on Figure 90, the relatively stable periods of A horizon formation all show a somewhat similar soil botanical signature with some temperature variation suggested.
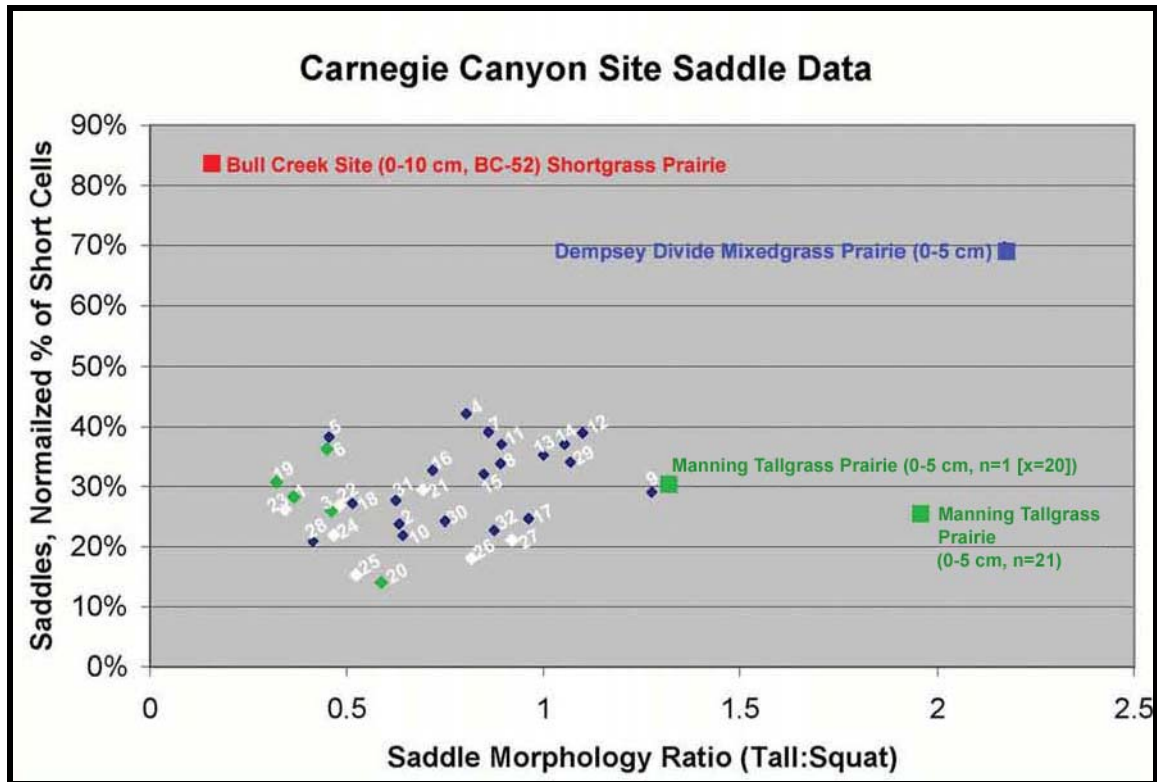
Figure 90. Carnegie Canyon saddle data with top of A horizons denoted by green diamonds (1=AC, 3=Ab, 6=Ab2, 20=Ab3 (top), and 19 contains "finely dispersed A horizon material" (Carter et al. 2009)). The additional lower melanized samples collected from the very thick Ab3 Caddo County paleosol are marked by white diamonds.

The data points for the melanized zone below the top of the Caddo County paleosol does not cluster as closely (Figure 90, white diamonds--numbers 21-27.) However, the two samples judged to be cumulic (26 and 27) do cluster tightly and to the right of the other melanized samples (#21-25). This shift may be a reflection of phytoliths from upstream or upland settings being deposited with the alluvial material during this cumulic period and thus being non-indigenous phytoliths added to the alluvial material that altered the soil saddle signature at the site. Interestingly, based on Figure 90 the absolute coolest interval in the series based on low total Chloridoid count (#20) immediately preceded the burial of the Caddo County paleosol.

Generally, the other soil samples from the profile which primarily represent Bk

and C horizons (denoted by black diamonds) do not overlap with the upper soil from the

four A horizons (green diamonds, Figure 90). The soil samples adjacent to the upper

boundary of the A horizons (2, 5, and 18) do tend to be clustered more closely in saddle

characteristics to the upper A horizon samples than the other non-A horizon samples

(Figure 90).

The two warmest periods as indicated by decline in Pooid frequency (#12 and #16

in Figure 88) both occur in the five hundred year interval between the Ab2 and Ab3

(Delaware and Caddo County paleosols). Conversely, the two intervals with the lowest

Panicoid content (#13, 14) also occurred in this interval, although the Pooid fraction grew

in these two intervals—the summers in these intervals apparently tended to be hotter and

drier than previously. Together, these four out of five sequential intervals—two with a

shorter spring season and two with a hotter drier summer—could have potentially

affected the vegetation to increase regional erosional runoff upstream resulting in more

alluvial deposition at the site. Unfortunately, charcoal particle counts were not collected

for the soil samples from this site so the potential influence of fire affecting area

vegetation and alluvial deposition events at the Carnegie Canyon Site remains unknown.

However there is additional data; counts of sedge phytoliths, diatoms, and sponge

spicules were collected (Figure 91). In order to standardize the data, the values plotted

are the number of indicated particles calculated as percent relative to the total short cell

count for the same sample. Thus by this data, the sedge population spiked in soil samples

10, 12, and 31—the one of which (#12) is in the hotter interval during which time the rate of alluvial deposition increased.

The sponge spicules, which also had a low fluctuating count throughout the soil profile sequence, have their highest concentration at the time that Ab was forming. As sponges require clear water, this suggests the interval was wet if sponge spicule origin and deposition was indigenous to the site. On the other hand, the spicules could also eolian, alluvial, or even originating from animal droppings, so their ultimate source and significance is not absolutely clear.

However, the striking particle data in Figure 91 is the diatom fraction—which made up over 20% of the recognizable biogenic silica particle count in soil sample 19[37]. Indeed, the entire melanized portion of the Caddo County paleosol was a period with a significant elevation in the diatom population at the site. There were actually four diatom concentration peaks within the Caddo County paleosol at samples 19, 22, 24, and a slight shoulder at 26. These peak diatom concentrations appear to mirror the surfaces of the four buried soils reported that later welded to form the thick Caddo County paleosol (Carter et al. 2009). There is also another diatom spike in the modern-day sample (#1). In contrast, the diatom counts in cumulic intervals of sand deposition between A horizon formation are very low. Although diatoms are frequently thought of as water-based organisms, soil diatoms also occur. Diatoms have been reported to colonize sand grains in fresh water (Round 1965, Meadows and Anderson 1966). Identification of diatom

---

[37] All recognizable diatoms and diatom fragments were counted in these samples. The phytolith short cells counted were recognizable and reasonably complete—except for broken Panicoids which were each counted as one-half.

243
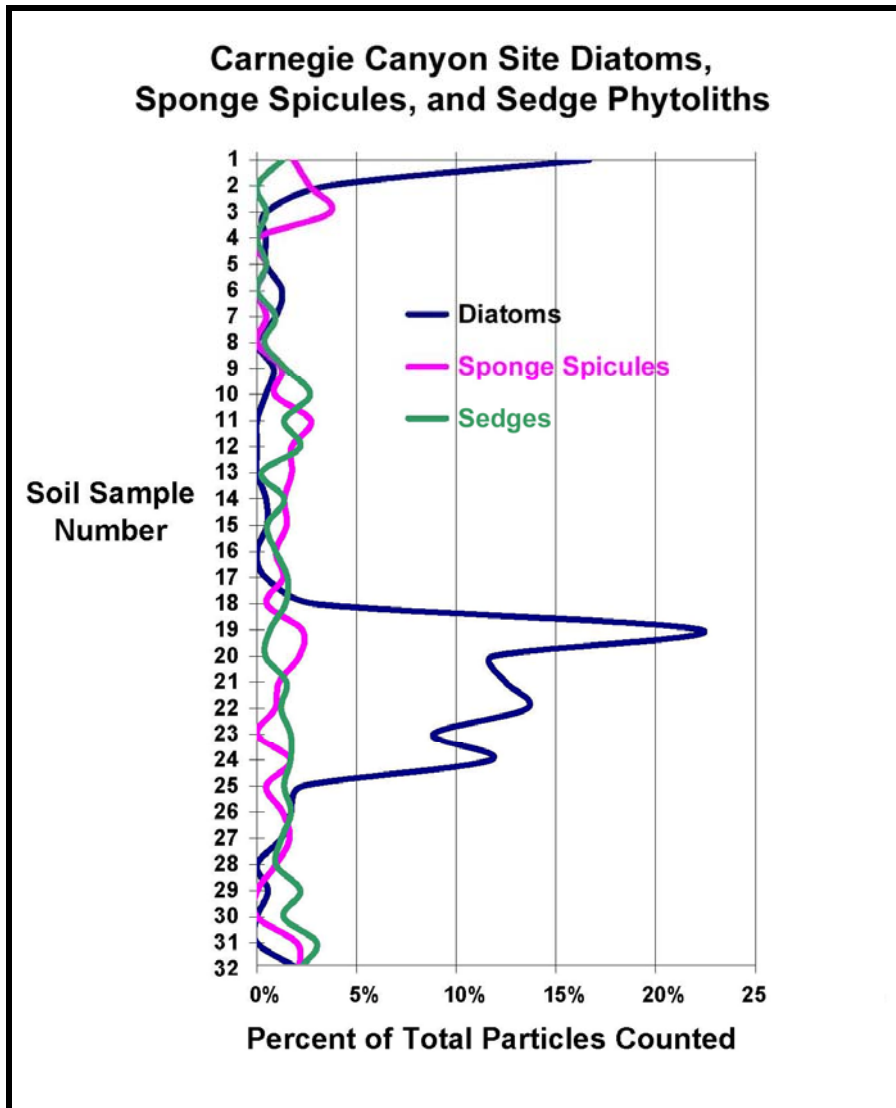
Figure 91. Other biogenic silica and phytolith particles in the Carnegie Canyon Site soil profile (percent determined is the ratio of the specific particle type to the (total number of morphologically distinct phytoliths ["total Phytoliths" in Tables 54-57] counted in each sample less the count for the specific other analyte being evaluated)).

species in the soil samples from this site will be the topic of a future study. The high

diatom content of these A horizons does imply moist conditions conducive to growth.

The thriving diatom community could help explain the low TOC values (i.e., by

consuming organic debris in the soil) that were previously interpreted to indicate cumulic

A horizon development within part of this paleosol (Carter et al. 2009).

One additional noteworthy observation was made during laboratory processing the Carnegie Canyon Site soil samples. A significant variation in sand fraction color was observed in the profile samples; a portion of the clean sand fraction from each soil sample was laid out and the sand samples were photographed at one time while illuminated via overhead lighting (Figure 92). Although #1, #3, and #6 (A, Ab, and Ab2) are slightly darker than the neighboring samples (#11, a sample which had a slightly elevated TOC value, is also darker than #10), all of the samples on the top row are darker than the samples on the two lower rows. Perhaps most interesting is that beginning with sample #19, the sands appear to be nearly white. Although there is some slight darkening beginning with Sample #22, the entire series #19-#27 is lighter than any of the other sand samples obtained from upper portion of the soil profile sequence. This lightest portion of the series correlates with the Caddo County paleosol, and also with the higher observed incidence of diatoms and phytoliths in the soil profile. This same series of samples is shown during the clay removal step where the darker colored Caddo County Paleosol is clearly visible (Figure 16). Below the Caddo County paleosol (beginning with sample 28) the sands again begin to display a reddish brown color (Figure 92).
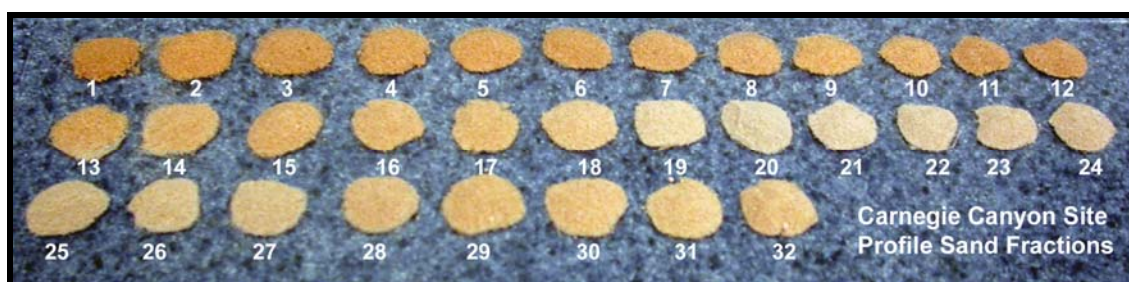
Figure 92. Sand fraction samples from the Carnegie Canyon Site soil profile showing variation in color with sample depth. The number indicates the soil sample of origin (number 1 is the surface AC sample).

All of the sand in this profile is coming from the same short drainage system, so the base sand color would be expected to remain relatively unchanged as the parent material is presumably unchanged. The most plausible explanation for the observed sand color change is related to the presence of water standing at the site. If the site was wet enough frequently enough or for a long enough period of time, the soil bacteria would experience anaerobic conditions. At that point, the anaerobic soil bacteria will use red ferric iron (Fe^{3+}) as an electron acceptor in their metabolism, producing colorless ferrous iron (Fe^{2+}). The result of this metabolic change is that the sand (with surficial and/or included iron deposits such as iron oxide) would lose its red hue, as was observed in the Carnegie Canyon Site soil sands in the Ab3 horizon (samples #19-27, Figure 92). The increased carbon present as organic matter in the buried soil may have also contributed a rich food source for microbes (and also diatoms). Microscopic images of several Carnegie Canyon Site sand fraction samples are shown in Figure 93.
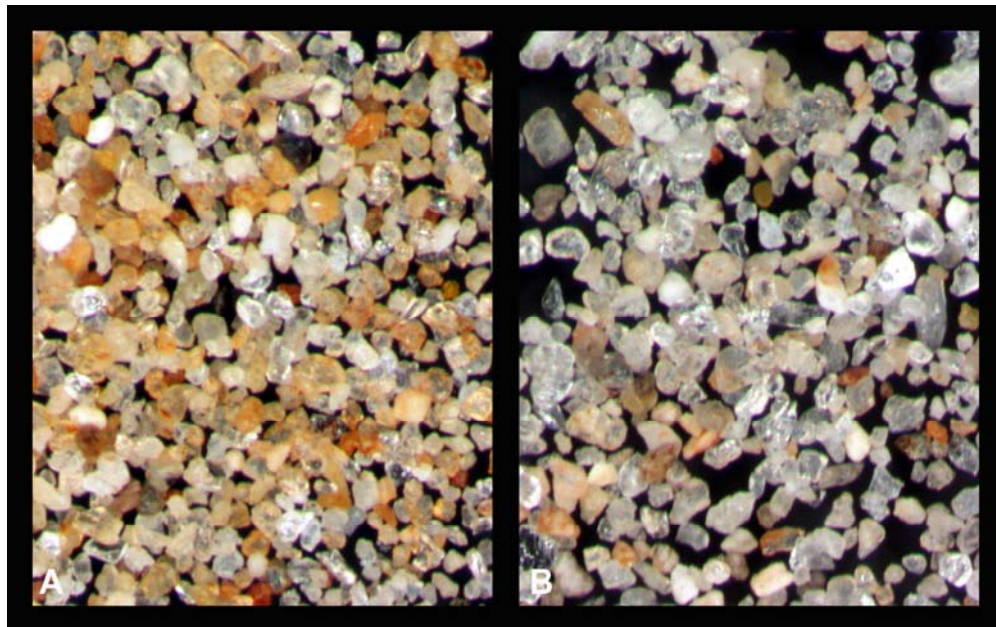
Figure 93. Microscopic images of Carnegie Canyon Site sample sand fraction 18 (A) and 19 (B) showing the relative paucity of sand grains red iron coloration in sample 19 (B).

The interval of the Caddo County paleosol development and melanization also represents the longest prolonged period of low Chloridoid values in the entire sequence, which also implies a cooler and somewhat wetter environment. The sand color observations (Figures 92-93) also tentatively support the previous contention based on the saddle morphology plot (Figure 90) and the diatom concentration (Figure 91) that the top of the Caddo County paleosol actually begins with sample #19 rather than #20. However, the peak in phytolith concentration and the lowest temperature at the site during the time interval studied actually correlates with sample #20. Sample #20 also has the greyest (least red) sand sample suggesting the maximum moisture and/or highest active anaerobic bacterial load during this interval. The high diatom concentration in sample 19 (and perhaps all of the diatom concentration spikes in the buried Ab3 horizons) could actually be a reflection of the diatoms feeding on the recently buried highly concentrated organic plant debris and/or an increase in moisture and/or organic matter at the end of A horizon development during an ongoing wetter interval.

A number of well-preserved tree stumps were reported in the strata below the Caddo County paleosol at this site; these stumps, buried under six to 11 meters of fill, were carbon dated to 2600-3200 years BP (Lintz and Hall 1983; Hall and Lintz 1984) suggesting very rapid sediment deposition and tree burial. The authors postulated a higher water table at the time of the Caddo County paleosol formation, citing "four independent lines of evidence (mollusks, paleosol carbonate, carbonate encrustations, spring conduit)" (Lintz and Hall 1983:40) which would have assisted in preservation of the tree stumps. Now, based on this new data, the support of a high diatom concentration

247

in the soil samples and the loss of reddish hue attributed to bacterial action on the sand attributed to anaerobic (i.e., submerged) conditions can be added to the evidence supporting a higher water table which resulted in tree stump preservation. The image of the soil profile (Figure 86) also shows redoximorphic features visible immediately below the Ab3 buried soil; although there are likely redoximorphice features within the buried soil itself, the dark color of the Ab3 horizon obscures the features.

Overall the saddle phytolith profile of the Carnegie Canyon site clusters more tightly than that of the Lizard site, and with relatively minimal overall x- or y- movement (Figures 90, 104, and 109). The sand and TOC data for the Carnegie Canyon site has been reported (Carter et al. 2009:Figure 2).   On average, the sand content of non-A horizons is significantly higher at the Carnegie Canyon Site than at the Lizard Site, but the saddle data shows less spread. Buried soil Ab3 (#20) "was buried at 1010±50 rybp (Beta 1923130)" (Carter et al. 2009) and Ab2 (#6) is presumed to be the previously reported Delaware Creek Soil dating to about 500 BP (Carter et al. 2009, Ferring 1986).

The Carnegie Canyon Site seasonality profile (Figure 83) shows a very striking cool snap at the time that Ab3 (#20) was buried, followed by a drastic warming in sample #19 (which had the highest diatom concentration (Figure 91) and may or may not actually be the top of Ab3). This dramatic climatic shift may have led to the events that buried this A horizon in Carnegie Canyon. A smaller cool spike occurred farther down the profile in Ab3 (#25). There was a somewhat milder summer compared to adjacent data points at the time Ab2 (#6) ended which was followed by a warming trend (#5 and 4).

The sand concentration (Carter et al. 2009) is very high at this site except during the interval of Ab3 stability and melanization which suggests an interval of a relatively stable environment ending in about 1010 BP; during the process of Ab3 formation, the sand concentration was still high but relatively constant (and lower than at any other point in the soil profile sequence).

Whereas the Lizard site Chloridoid component was relatively stable in the upper half of the profile, the Carnegie Canyon Site Chloridoid values vary constantly with essentially no period of stability. More detail is visible in the in the upper portion of the Carnegie Canyon Site profile because it is less time compressed than the Lizard Site profile. Sample 1 (actually an AC horizon), Ab (#3), and #19 cluster very tightly having a very similar climatic signature based on the saddle data (Figure 109). The reported top of Ab3 (#20) diverges from the cluster as does #6 (Ab2) (#20 is somewhat cooler, and #6 is warmer; Figure 109). With the exception of #26 and #27 (which cluster with each other) the lower portions of each A horizon remain clustered with the upper zones.

Overall, the Carnegie Canyon Site saddle phytolith data clusters more tightly than the Lizard site profile samples (Figure 109). Although the Lizard Site shows more x-axis movement in its spread, the narrower spread at Carnegie Canyon mirrors that seen in the 3000 year era represented at the Lizard Site. However, the Carnegie Canyon site saddle signature is never as cool as the comparable 1000 year segment of the Lizard Site data.

This tight overall clustering suggests that on average, only relatively moderate climate variation occurred at the Carnegie Canyon Site compared to the other two buried soil sites studied in this project. The climate at the time the upper portion of AC (#1) and Ab (#3) were formed was practically identical, while Ab2 (#6) was warmer with a moderate shift in saddle ratio in the direction of the Mixedgrass Prairie control. Sample #20 (Ab3) is the only A horizon that was significantly cooler than the pack—representing the coolest saddle signature sample recovered from the entire Carnegie Canyon Site profile (Figures 83 and 109).

The striking warm snap in sample #19 immediately after the coolest period (#20) may indicate that the climatic change at about 1000 BP led to ending and burying Ab3. The higher sand content in 8-19 suggests higher water flows and/or more erosive runoff occurred. Sample #19 may actually be the top of Ab3, potentially having been partially removed at the time of burial of Ab3 (#20). The highest diatom interval at the site (Figure 91) is in #19 suggesting it may actually be the remnant top of Ab3. An alternative explanation could be that the diatom population was attracted to and concentrated in the organic-rich content of the buried organic material covered by the sand at the top of Ab3. Meadows and Anderson actually report that diatoms colonize the surface of wet or periodically wet sand grains (1966).

Either way, the high diatom concentration throughout Ab3 indicates that conditions were favorable to support a substantial diatom population. The spikes in diatom population accurately mirror the tops of the four buried soils that were later

welded to form Ab3. Thus, in buried soil sites that formed under moist conditions where diatoms thrived, diatom concentration fluctuations may be indicative of different soil surfaces and may help to identify instances when soil welding has later occurred. Similar evidence of multiple A horizons was also faintly visible in the soil phytolith concentrations (Figure 87) although not nearly as strikingly evident as in the diatom data. Presley (et al. 2010) also notes that differences in clay composition may be very useful evidence in confirming the presence of soil welding in complicated profiles (2009).

The final piece of evidence observed relating to soil moisture conditions at the site is related to sand color (Figures 93-94). The loss of iron from sand as observed by whiter sand throughout the Ab3 sequence relative to the redder sand observed elsewhere throughout the profile is interpreted to mean that anaerobic conditions occurred at the site during Ab3 pedogenesis due to very wet conditions at the site. Although this could have occurred at the end of Ab3 when it was truncated and A horizon formation ended, it is also possible that the site was very wet intermittently during Ab3 formation (i.e., as multiple A horizons were forming, and later welded). The diatom concentrations mirroring the various A components within Ab3 would seem to suggest this later explanation. Other evidence for wet conditions at the site includes the presence of sponge spicules and sedge phytoliths throughout much of the profile.

Interestingly, one of the lowest spicule and sedge counts for the site occurred in Ab2 (#6) at ~500 BP—which also correlates with rising temperature saddle signature at the top of the A horizon. Other than the cool snap evidence in #10, samples #4-8 and 11-

251

16 are all warmer saddle signatures than any other samples (except #29). Samples #19 and 21 are also high, with #20 being very low: #17 and 18 are intermediate in saddle temperature signature between #19 and 20 (Figure 109). The Medieval Warm Period, centered around 1,000 years BP, correlates reasonably well with the date of this soil (Ab3, #19) and may be clearly reflected in this saddle phytolith data. If so, this historically documented warm interval may have directly contributed to the termination of Ab3 at the Carnegie Canyon Site and subsequent increasing sand deposition at the site.

Lizard Site (34WN107) – The Lizard site is located in Washington County in northeastern Oklahoma (Figures 7 and 79) on South Cotton Creek (Figure 94). Verdigris silt loam is a fine-silty, mixed, superactive, thermic cumulic hapludoll. Images are shown of the soil profile before (Figure 95) and after cleaning (Figure 96). The soil description of the Lizard Site profile has been previously published (Carter et al. 2009).

As soils from the Lizard Site were the first samples processed in this phytolith research project, the phytolith data were handled somewhat differently than at the previously discussed sites. The deflocculated soil samples were sieved to remove the sand using a 270 mesh sieve, and organic matter removal was by digestion of individual samples in 27 percent sodium hypochlorite while the bottles were in a hot water bath (5-10 days). After flotation, the isolated phytoliths were separated into medium (5-20 micron) and large (20-50 micron) fractions by sedimentation. The lower profile samples (8-27) were initially processed for phytolith recovery; upon review of the data, it was

decided to also quantitatively isolate the phytoliths from the remainder of the soil profile

samples. Several fresh portions of several samples from the initial series were also re-

extracted to replace fractions previously lost during initial processing.
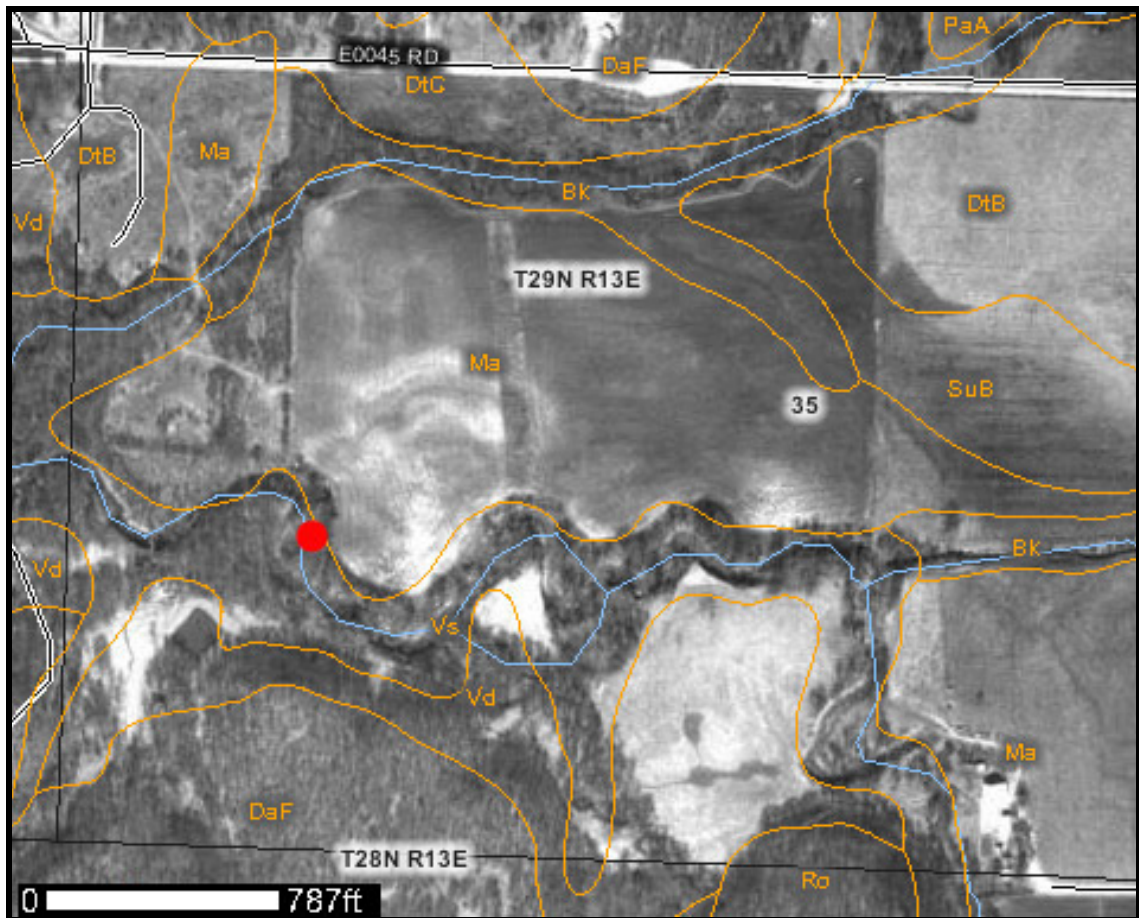
Figure 94. Lizard Site (34WN107), Washington County, Oklahoma. USDA soil series reported as present in this marked aerial photograph are: Bk (Eram-Verdigris complex, 0-12% slopes), DaF (Darnell extremely stony sandy loam, 5-30 % slopes), DtB (Dennis silt loam, 1-3 % slopes), DtC (Dennis silt loam, 3-5% slopes), Ma (Mason silt loam, 0-1 % slopes), PaA (Parsons silt loam, 0-1 % slopes), Ro (Niotaze-Darnell complex, 30-60% slopes), SuB (Summit silty clay loam, 1-3% slopes), Vd (Verdigris silt loam, 0-1 % slopes), and Vs (Verdigris silt loam, 0-2 % slopes). (Aerial photograph with soil designations obtained from NRCS/USDA web site http://websoilsurvey.nrcs.usda.gov/app/HomePage.htm).

Figure 95. South Cotton Creek cutbank exposure at the Lizard Site before the soil profile was cleaned.

Figure 96. Exposed soil profile at the Lizard Site.

Table 62
Lizard Site Phytolith Concentrations

Sample Number	Medium Phytoliths (wt. % in soil)	Coarse Phytoliths (wt. % in soil)	Total Phytoliths (Medium+Coarse) (wt. % in soil)	Ratio Medium:Coarse Phytoliths
1	1.07%	0.39%	1.46%	3.63
2	1.05%	0.26%	1.31%	5.28
3	1.33%	0.33%	1.66%	4.97
4	2.25%	0.62%	2.87%	2.96
5	2.04%	0.50%	2.53%	2.91
6	1.61%	0.68%	2.29%	2.69
7	1.12%	0.50%	1.62%	2.97
8	0.68%	0.37%	0.68%	1.80
9	0.80%	0.51%	0.81%	1.56
10	1.05%	0.72%	1.77%	1.46
11	1.01%	0.65%	1.66%	1.55
12	0.98%	0.59%	1.57%	1.68
13	0.97%	0.54%	1.50%	1.80
14	0.85%	0.41%	1.26%	2.07
15	0.79%	0.35%	1.14%	2.26
16	0.70%	0.33%	1.03%	2.10
17	0.72%	0.20%	0.92%	3.70
18	0.50%	0.25%	0.75%	1.97
19	0.46%	0.22%	0.68%	2.04
20	0.42%	0.18%	0.60%	2.36
21	0.46%	0.14%	0.60%	3.28
22	0.42%	0.092%	0.51%	4.60
23	0.23%	0.10%	0.33%	2.31
24	0.14%	0.03%	0.17%	5.54
25	0.16%	0.08%	0.24%	2.10
26	0.19%	0.02%	0.21%	11.35
27	0.30%	0.093%	0.39%	3.23

The total, medium, and coarse phytolith fraction weights for the entire profile are also given in Table 62, and the phytolith concentration in the soil profile (weight percent total phytoliths in dry soil) is plotted in Figure 97.

As the majority of the short cell phytoliths occur in the 5-20 micron fraction, the medium-size isolate was the portion of the phytolith sample that was counted for short cell morphologic forms. The counts for the medium phytolith fractions are presented in Tables 63-66, the normalized short cell forms and summed climatic values of this data are in Tables 67-69, and the seasonality phytolith plot is in Figure 98. The ratio of total medium phytoliths:total coarse phytoliths (weight % of soil:weight % of soil, Table 62) is also plotted (Figures 99 and 100). Interestingly, a number of the elevated data points in Figure 100 (numbers 2, 7, 22, 24, 26) that indicate a higher relative weight percent medium phytolith concentration correlate with a higher soil sand concentration (Figure 100) reported previously (Carter et al. 2009). The sample sand data are given in Table 70. The original sample 17 sand weight percent value is barely above a line between samples 16 and 18—not nearly as significant as the corresponding phytolith ratio spike (Figure 100). Figure 100 is potentially confusing in that the overlain plots have different scales in order to overlap the different data on the same scale to enable ease of comparison; the phytoliths are presented as a weight to weight direct ratio, whereas the sand values are (weight % /10).

Although there appears to be some correlation between relative elevation of the medium phytolith fraction and increased sand deposition in this alluvial system, it is hard to interpret due to several factors: the samples were not all analyzed at the same time, several intermittent samples were reanalyzed, and the individual parent samples were not well-mixed and homogenized before sampling multiple (soil sample portions were
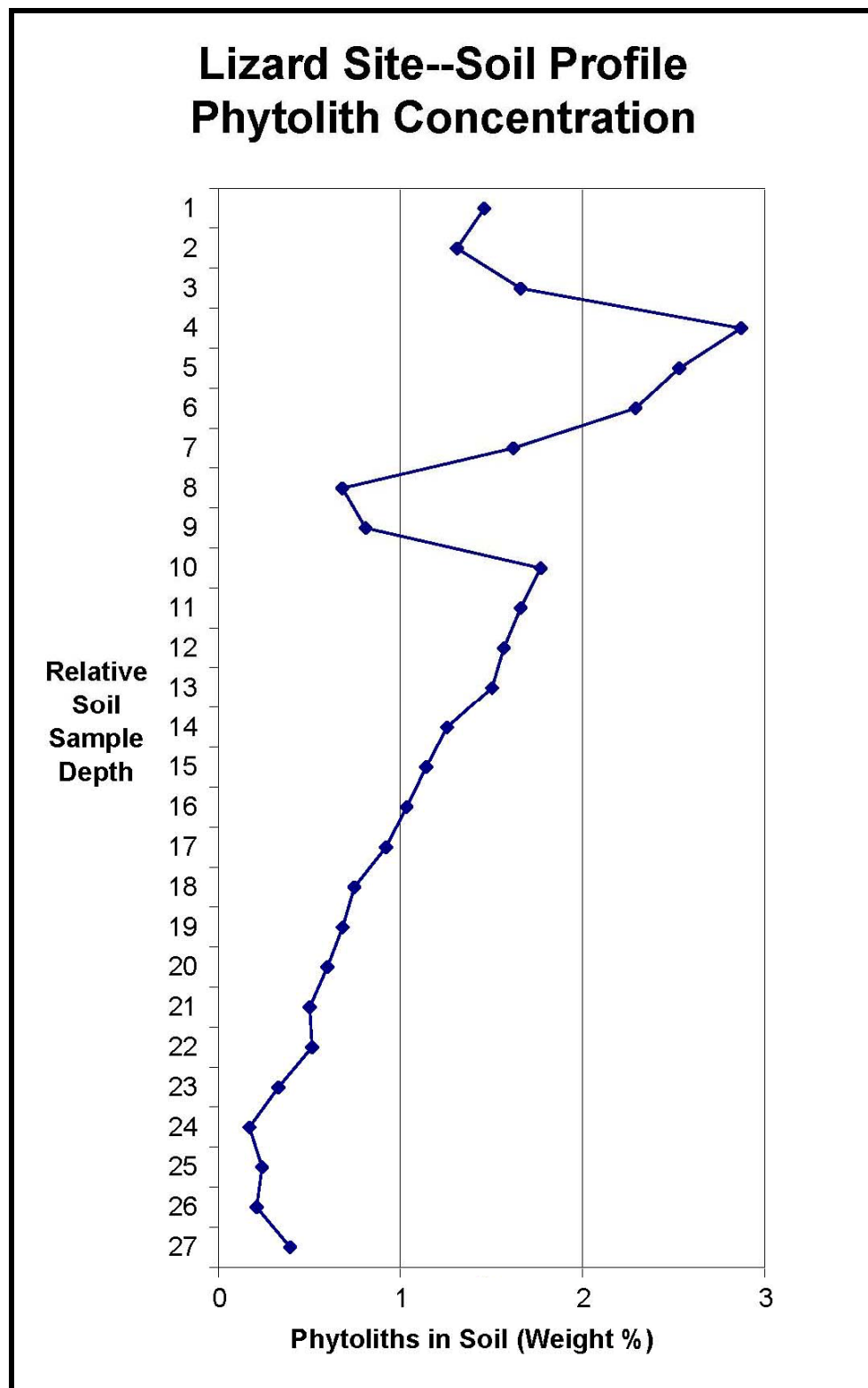
Figure 97. Phytolith concentration in the Lizard Site soil profile (weight % in soil).

Table 63
Lizard Site Medium-sized Raw Phytolith Counts (Samples 1-7)

Morphology/Sample	1	2	3	4	5	6	7
Keeled	**98**	**24**	**34**	**14**	**28**	**39**	**13**
Conical	**23**	**27**	**56**	**33**	**43**	**40**	**25**
Pyramidal	**10**	**11**	**13**	**6**	**7**	**7**	**20**
Crenate	**34**	**24**	**22**	**8**	**4**	**12**	**8**
Saddle, Squat	**12**	**18**	**10**	**10**	**10**	**7**	**4**
Saddle, Tall	**19**	**13**	**11**	**9**	**7**	**7**	**5**
Stipa	**8**	**16**	**9**	**11**	**7**	**8**	**13**
Lobate, Simple	**10**	**15**	**13**	**6**	**9**	**11**	**9**
Lobate, Panicoid	**41**	**68**	**64**	**100.5**	**82.5**	**81.5**	**92**
Lobate, Pan'd (cmpd)	**0**	**1**	**1**	**2**	**2**		**3**
Cross, Panicoid (<10 μ)	**2.5**	**3**	**0**	**5**	**1**	**3**	**7**
Cross, Panicoid (>10 μ)	**12**	**7**	**5**	**8**	**3**	**5**	**10**
Maize Rondel	0	0	0	0	0	5	0
Rondel (bipoint)	2	0	0	0	0	0	0
Rondel, other (Large)	32	5	1	8	0	0	0
Rondel, Ruffled (?)	0	0	2	0	0	0	0
Dicot, knobby	2	0	3	1	1	1	1
Spiny spheroid	0	0	0	1	0	0	1
WWW	0	0	0	0	0	0	0
Schlerid	4	3	0	1	0	1	1
Diatom (fragments)	28	37	30	9	10	14	5
Sponge spicule	6	11	8	4	3	1	5
Trichome	4	3	5	3	3	0	1
Hair cells	0	0	0	0	0	0	0
Bulliform, square	2	2	0	0	1	0	1
Bulliform, rectangular	2	1	2	0	2	2	0
Bulliform, keystone	1	0	0	0	0	0	0
Bulliform, Y-shaped	0	0	0	0	0	0	0
Bulliform, other	0	0	0	0	0	0	0
Elongate, smooth	6	1	6	2	0	0	0
Elongate, sinuous	2	1	3	0	0	0	0
Elongate, castillate	2	3	1	0	0	0	0
Elongate, spiny	0	0	0	0	0	0	0
Sedge	0	0	0	0	0	1	0
Asteraceae	0	0	1	0	0	+	+
Charcoal	0	0	0	0	0	0	0
non-spiny spheres	0	0	0	0	0	0	0
Total Short Cells	269.5	227	238	212.5	203.5	220.5	209
Total Cool	204	133	155	91	106	120	88
Total Hot/Dry	31	31	21	19	17	14	9
Total Warm/Moist	99.5	99	86	129.5	97.5	105.5	121

Table 64
Lizard Site Medium-sized Raw Phytolith Counts (Samples 8-13)

Morphology / Sample	8	9	10	11	12	13	14
Keeled	**20**	**33**	**10**	**19**	**2**	**7**	**12**
Conical	**40**	**45**	**58**	**52**	**38**	**36**	**31**
Pyramidal	**10**	**7**	**8**	**8**	**9**	**4**	**6**
Crenate	**15**	**14**	**11**	**15**	**15**	**10**	**7**
Saddle, Squat	**7**	**13**	**17**	**11**	**12**	**10**	**22**
Saddle, Tall	**5**	**5**	**24**	**7**	**8**	**10**	**6**
Stipa	**6**	**4**	**2**	**7**	**1**	**5**	**3**
Lobate, Simple	**30**	**20.5**	**27.5**	**15**	**21**	**31**	**24**
Lobate, Panicoid	**76**	**88**	**74.5**	**69.5**	**97**	**100.5**	**69**
Lobate, Pan'd (cmpd)	**0**	**2**	**2**	**5**	**2**	**2**	**4**
Cross, Panic'd (<10 µ)	**18**	**10**	**13**	**7**	**5**	**11**	**9**
Cross, Panic'd (>10 µ)	**2**	**3**	**0**	**1**	**0**	**1**	**0**
Maize Rondel	1	2	0	2	0	0	1
Rondel (bipoint)	0	0	0	0	0	0	0
Rondel, other (Large)	19	13	9	7	15	12	6
Rondel, Ruffled (?)	1	0	0	0	0	0	0
Dicot, knobby	0	0	0	0	0	1	0
Spiny spheroid	1	1	0	2	1	1	1
WWW	0	0	0	0	0	0	0
Schlerid	2	1	4	6	2	0	3
Diatom (fragments)	0	0	1	0	0	0	0
Sponge spicule	1	3	2	1	1	1	2
Trichome	3	2	1	3	8	4	10
Hair cells	1	0	0	1	0	0	0
Bulliform, square	2	0	0	0	5	0	0
Bulliform, rectangular	0	1	0	1	1	1	8
Bulliform, keystone	0	0	0	0	1	0	1
Bulliform, Y-shaped	0	0	0	0	0	0	0
Bulliform, other	0	0	0	2	3	0	3
Elongate, smooth	25	33	0	29	27	3	16
Elongate, sinuous	25	27	0	29	31	4	16
Elongate, castillate	16	5	0	3	6	1	4
Elongate, spiny	0	0	0	1	1	2	1
Sedge	0	1	0	0	0	0	0
Asteraceae	0	0	0	0	0	0	0
Charcoal	4	4	3	15	21	13	34
non-spiny spheres	1	0	6	0	6	6	1
Total Short Cells	228.5	244.5	247	216.5	209.5	227.5	193
Total Cool	103	121	130	119	85	82	87
Total Hot/Dry	12	18	41	18	20	20	28
Total Warm/Moist	146.5	138.5	126	106.5	139.5	157.5	113

Table 65
Lizard Site Medium-sized Raw Phytolith Counts (Samples 15-21)

Phytolith Form / Sample	15	16	17	18	19	20	21
Keeled	**5**	**4**	**8**	**8**	**11**	**8**	**7**
Conical	**17**	**39**	**39**	**26**	**37**	**36**	**24**
Pyramidal	**4**	**6**	**12**	**9**	**3**	**8**	**11**
Crenate	**19**	**21**	**8**	**22**	**15**	**17**	**18**
Saddle, Squat	**24**	**32**	**35**	**34**	**19**	**24**	**32**
Saddle, Tall	**33**	**51**	**38**	**43**	**37**	**68**	**35**
Stipa	**5**	**0**	**1**	**1**	**0**	**1**	**0**
Lobate, Simple	**23.0**	**31.5**	**39**	**12.5**	**33.5**	**22.0**	**17.0**
Lobate, Panicoid	**55**	**66**	**42**	**46.5**	**52.5**	**41.0**	**35.5**
Lobate, Panicoid (cmpd)	**3**	**0**	**1**	**3**	**1**	**0**	**0**
Cross, Panicoid (<10 μ)	**6**	**6**	**3**	**3**	**6**	**4**	**5**
Cross, Panicoid (>10 μ)	**0**	**0**	**0**	**0**	**0**	**0**	**0**
Maize Rondel	1	0	1	0	0	0	0
Rondel (bipoint)	0	0	0	0	0	0	0
Rondel, other (Large)	11	10	19	17	20	12	13
Rondel, Ruffled (?)	0	0	0	0	1	0	0
Dicot, knobby	0	0	0	0	1	0	0
Spiny spheroid	4	1	14	7	11	7	15
WWW	0	0	0	0	0	0	0
Schlerid	1	2	1	1	5	1	3
Diatom (fragments)	0	0	0	0	0	0	1
Sponge spicule	1	0	1	0	0	4	2
Trichome	4	0	8	5	7	10	5
Hair cells	0	0	0	0	0	0	0
Bulliform, square	1	3	2	2	7	3	2
Bulliform, rectangular	4	3	4	1	1	6	3
Bulliform, keystone	0	0	0	0	0	0	1
Bulliform, Y-shaped	0	0	2	0	0	0	0
Bulliform, other	2	0	2	0	0	0	0
Elongate, smooth	9	4	8	1	0	0	0
Elongate, sinuous	4	1	12	3	0	0	0
Elongate, castillate	1	1	4	0	0	0	1
Elongate, spiny	1	1	0	1	0	0	1
Sedge	1	2?	0	0	0	1	1
Asteraceae	0	0	0	0	0	0	0
Charcoal	27	42	54	58	124	147	141
non-spiny spheres	4	16	5	47	26	22	33
Total Short Cells	193.5	256.5	226	208	215	229	184.5
Total Cool	107	153	141	143	122	162	127
Total Hot/Dry	57	83	73	77	56	92	67
Total Warm/Moist	98.5	113.5	105	82	114	79	70.5

Table 66
Lizard Site Medium-sized Raw Phytolith Counts (Samples 22-27)

Phytolith Form / Sample	22	23	24	25	26	27
Keeled	**0**	**5**	**2**	**2**	**0**	**2**
Conical	**21**	**17**	**31**	**19**	**7**	**10**
Pyramidal	**6**	**2**	**11**	**2**	**0**	**0**
Crenate	**12**	**9**	**30**	**18**	**1**	**5**
Saddle, Squat	**38**	**3**	**15**	**5**	**2**	**5**
Saddle, Tall	**64**	**6**	**24**	**6**	**3**	**8**
Stipa	**0**	**0**	**0**	**0**	**0**	**0**
Lobate, Simple	**25.0**	**3.5**	**38.5**	**8**	**4**	**3**
Lobate, Panicoid	**38.5**	**7.0**	**39.5**	**16**	**1**	**12**
Lobate, Panicoid (cmpd)	**1**	**0**	**0**	**1**	**0**	**0**
Cross, Panicoid (<10 μ)	**3**	**2**	**4**	**2**	**0**	**0**
Cross, Panicoid (>10 μ)	**0**	**0**	**0**	**0**	**1**	**2**
Maize Rondel	0	0	0	0	0	0
Rondel (bipoint)	0	0	0	0	0	0
Rondel, other (Large)	4	2	14	6	4	10
Rondel, Ruffled (?)	0	0	0	0	0	0
Dicot, knobby	0	0	0	0	0	0
Spiny spheroid	8	4	14	16	5	12
WWW	0	0	0	0	0	0
Schlerid	1	1	1	1	0	0
Diatom (fragments)	0	0	0	0	0	0
Sponge spicule	1	0	10	2	1	4
Trichome	3	0	1	1	0	4
Hair cells	0	0	0	0	0	0
Bulliform, square	0	2	3	0	1	1
Bulliform, rectangular	1	0	0	0	0	0
Bulliform, keystone	0	0	1	0	0	1
Bulliform, Y-shaped	0	0	0	0	1	0
Bulliform, other	0	0	0	0	0	0
Elongate, smooth	0	1	0	0	0	0
Elongate, sinuous	0	0	0	0	0	0
Elongate, castillate	0	0	0	2	0	0
Elongate, spiny	0	0	1	0	0	0
Sedge	3	0	2	14	6	5
Asteraceae	1	1	0	0	0	0
Charcoal	89	4	156	7	9	28
non-spiny spheres	15	10	41	24	6	33
Total Short Cells	208.5	54.5	195	78.5	18.5	47
Total Cool	141	42	113	52	13	30
Total Hot/Dry	102	9	39	11	5	13
Total Warm/Moist	71.5	14.5	96	32.5	9.5	27

Table 67. Lizard Site Normalized Climatic Data for Medium-sized Phytoliths (Samples 1-9)

Sample Number	1	2	3	4	5	6	7	8	9
Morphology									
Keeled	36.4%	10.6%	14.3%	6.6%	13.8%	17.7%	6.2%	8.8%	13.5%
Conical	8.5%	11.9%	23.5%	15.5%	21.1%	18.1%	12.0%	17.5%	18.4%
Pyramidal	3.7%	4.8%	5.5%	2.8%	3.4%	3.2%	9.6%	4.4%	2.9%
Crenate	12.6%	10.6%	9.2%	3.8%	2.0%	5.4%	3.8%	6.6%	5.7%
Saddle, squat	4.5%	7.9%	4.2%	4.7%	4.9%	3.2%	1.9%	3.1%	5.3%
Saddle, tall	7.1%	5.7%	4.6%	4.2%	3.4%	3.2%	2.4%	2.2%	2.0%
Stipa	3.0%	7.0%	3.8%	5.2%	3.4%	3.6%	6.2%	2.6%	1.6%
Lobate, Simple	3.7%	6.6%	5.5%	2.8%	4.4%	5.0%	4.3%	13.1%	8.4%
Lobate, Panicoid	15.2%	30.0%	26.9%	47.3%	40.5%	37.0%	44.0%	33.0%	36.0%
Lobate, Panicoid (cmpd)	0.0%	0.4%	0.4%	0.9%	1.0%	0.0%	1.4%	0.0%	0.8%
Cross, Panicoid (<10 µ)	0.9%	1.3%	0.0%	2.4%	0.5%	1.4%	3.3%	7.9%	4.1%
Cross, Panicoid (>10 µ)	4.5%	3.1%	2.1%	3.8%	1.5%	2.3%	4.8%	0.9%	1.2%
Total Short Cells	269.5	227	238	212.5	203.5	220.5	209	228.5	244.5
Climatic Data									
Cool/Moist	61.2%	37.9%	52.5%	28.7%	40.3%	44.4%	31.6%	37.2%	40.5%
Hot/Dry	11.5%	13.7%	8.8%	8.9%	8.4%	6.3%	4.3%	5.3%	7.4%
Warm/Moist	27.3%	48.5%	38.7%	62.4%	51.4%	49.2%	64.1%	57.5%	52.1%

262

Table 68. Lizard Site Normalized Climatic Data for Medium-sized Phytoliths (Samples 10-18)

Sample Number	10	11	12	13	14	15	16	17	18
Morphology									
Keeled	4.0%	8.8%	1.0%	3.1%	6.2%	2.6%	1.6%	3.5%	3.8%
Conical	23.5%	24.0%	18.1%	15.8%	16.1%	8.8%	15.2%	17.3%	12.5%
Pyramidal	3.2%	3.7%	4.3%	1.8%	3.1%	2.1%	2.3%	5.3%	4.3%
Crenate	4.5%	6.9%	7.2%	4.4%	3.6%	9.8%	8.2%	3.5%	10.6%
Saddle, squat	6.9%	5.1%	5.7%	4.4%	11.4%	12.4%	12.5%	15.5%	16.3%
Saddle, tall	9.7%	3.2%	3.8%	4.4%	3.1%	17.1%	19.9%	16.8%	20.7%
Stipa	0.8%	3.2%	0.5%	2.2%	1.6%	2.6%	0.0%	0.4%	0.5%
Lobate, Simple	11.1%	6.9%	10.0%	13.6%	12.4%	11.9%	12.3%	17.3%	6.0%
Lobate, Panicoid	30.2%	32.1%	46.1%	44.2%	35.8%	28.2%	25.7%	18.6%	22.4%
Lobate, Panicoid (cmpd)	0.8%	2.3%	1.0%	0.9%	2.1%	1.6%	0.0%	0.4%	1.4%
Cross, Panicoid (<10 μ)	5.3%	3.2%	2.4%	4.8%	4.7%	3.1%	2.3%	1.3%	1.4%
Cross, Panicoid (>10 μ)	0.0%	0.5%	0.0%	0.4%	0.0%	0.0%	0.0%	0.0%	0.0%
Total Short Cells	247	216.5	209.5	227.5	193	193.5	256.5	226	208
Climatic Data									
Cool/Moist	35.2%	43.4%	30.5%	25.1%	29.0%	23.3%	27.3%	29.6%	31.3%
Hot/Dry	16.6%	8.3%	9.5%	8.8%	14.5%	29.5%	32.4%	32.3%	37.0%
Warm/Moist	48.2%	48.3%	59.9%	66.2%	56.5%	47.3%	40.4%	38.1%	31.7%

Table 69. Lizard Site Normalized Climatic Data for Medium-sized Phytoliths (Samples 19-27)

Sample Number	19	20	21	22	23	24	25	26	27
Morphology									
Keeled	5.1%	3.5%	3.8%	0.0%	9.2%	1.0%	2.5%	0.0%	4.3%
Conical	17.2%	15.7%	13.0%	10.1%	31.2%	15.9%	24.2%	37.8%	21.3%
Pyramidal	1.4%	3.5%	6.0%	2.9%	3.7%	5.6%	2.5%	0.0%	0.0%
Crenate	7.0%	7.4%	9.8%	5.8%	16.5%	15.4%	22.9%	5.4%	10.6%
Saddle, squat	8.8%	10.5%	17.3%	18.2%	5.5%	7.7%	6.4%	10.8%	10.6%
Saddle, tall	17.2%	29.7%	19.0%	30.7%	11.0%	12.3%	7.6%	16.2%	17.0%
Stipa	0.0%	0.4%	0.0%	0.0%	0.0%	0.0%	0.0%	0.0%	0.0%
Lobate, Simple	15.6%	9.6%	9.2%	12.0%	6.4%	19.7%	10.2%	21.6%	6.4%
Lobate, Panicoid	24.4%	17.9%	19.2%	18.5%	12.8%	20.3%	19.7%	2.7%	25.5%
Lobate, Panicoid (cmpd)	0.5%	0.0%	0.0%	0.5%	0.0%	0.0%	1.3%	0.0%	0.0%
Cross, Panicoid (<10 µ)	2.8%	1.7%	2.7%	1.4%	3.7%	2.1%	2.5%	0.0%	0.0%
Cross, Panicoid (>10 µ)	0.0%	0.0%	0.0%	0.0%	0.0%	0.0%	0.0%	5.4%	4.3%
Total Short Cells	215	229	184.5	208.5	54.5	195	78.5	18.5	47
Climatic Data									
Cool/Moist	30.7%	30.1%	32.5%	18.7%	60.6%	37.9%	52.2%	43.2%	36.2%
Hot/Dry	26.0%	40.2%	36.3%	48.9%	16.5%	20.0%	14.0%	27.0%	27.7%
Warm/Moist	43.3%	29.7%	31.2%	32.4%	22.9%	42.1%	33.8%	29.7%	36.2%

264
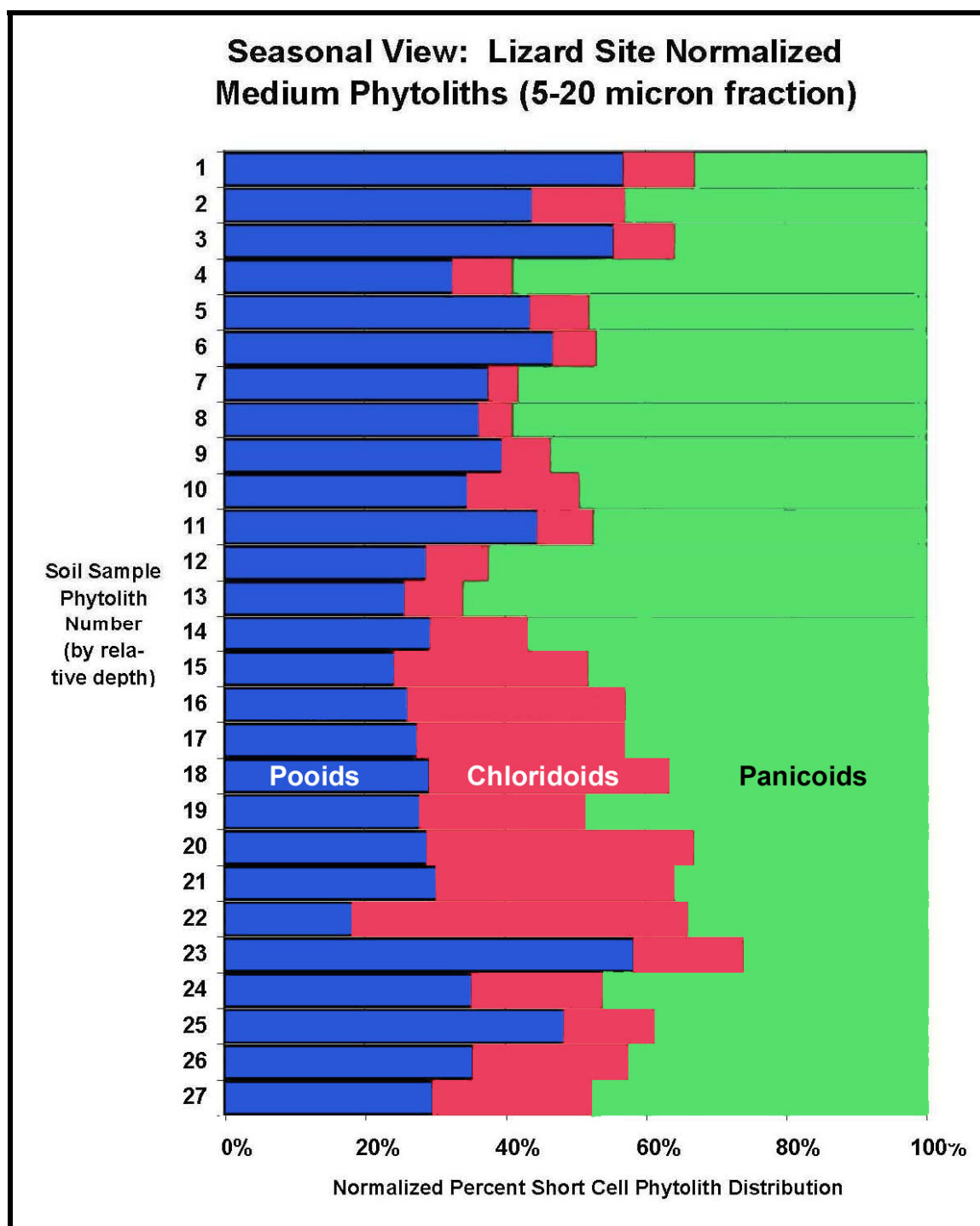
Figure 98. Seasonality profile of Lizard Site short cell phytoliths.
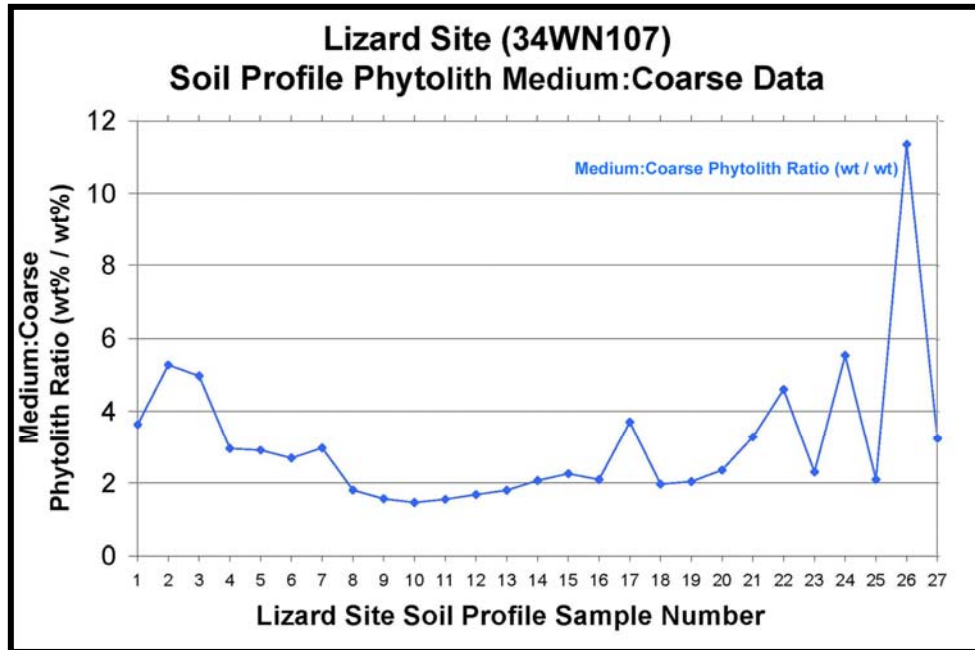
Figure 99. Ratio of medium to coarse phytoliths (weight/weight) in the Lizard Site soil profile.
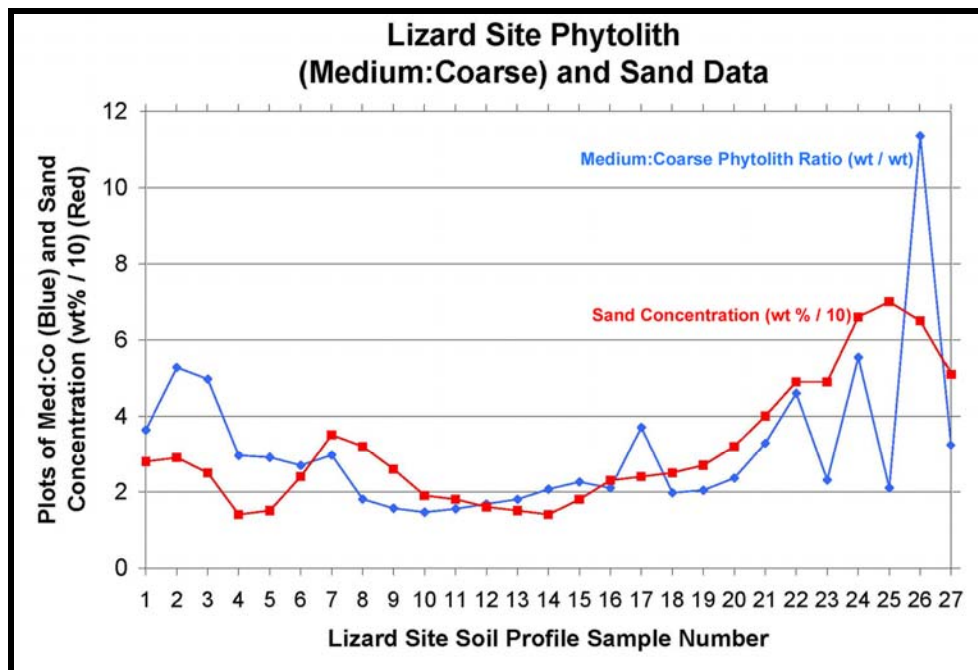
Figure 100. Plots of medium:coarse phytolith ratio and the sand concentration (times 0.10) in the Lizard Site soil profile.

Table 70
Lizard Site Phytolith and Sand Data

Lizard Site Soil Sample	Ratio Medium:Coarse Phytoliths (wt/wt)	Sand (% / 10)	Sand (%)
1	3.632	2.8	28
2	5.276	2.9	29
3	4.972	2.5	25
4	2.960	1.4	14
5	2.912	1.5	15
6	2.694	2.4	24
7	2.973	3.5	35
8	1.804	3.2	32
9	1.562	2.6	26
10	1.460	1.9	19
11	1.550	1.8	18
12	1.680	1.6	16
13	1.800	1.5	15
14	2.070	1.4	14
15	2.260	1.8	18
16	2.097	2.3	23
17	3.700	2.4	24
18	1.970	2.5	25
19	2.040	2.7	27
20	2.360	3.2	32
21	3.282	4.0	40
22	4.600	4.9	49
23	2.309	4.9	49
24	5.538	6.6	66
25	2.101	7.0	70
26	11.353	6.5	65
27	3.230	5.1	51

removed from the bulk sample for various analyses). The poorest data, at the lower end

of the soil profile, correlates with very low phytolith content (<0.2 weight percent) and

very low total short cell counts. The elevated medium phytolith concentration, if

confirmed in future studies, could be explained by enhanced Poaceae biomass associated

with additional moisture as indicated by increased sand deposition and/or erosional runoff from rains preferentially transporting the lighter phytoliths from upland settings.

After later encountering the high diatom counts at the Carnegie Canyon site buried soil (Figure 91), I recounted 250 fields of the phytolith prep slides from Lizard Site sample numbers 10-15 buried soil to make certain that diatoms had not been overlooked during the early stages of this project. This recount data is reported in Table 71. Evidence of maize as represented by observing the distinctive ruffle-top rondel was noted (Figure 101; also previously reported from other soil samples—see Tables 63-66). There was certainly not an abundance of diatoms at the Lizard site, with the number of spicules and sedges both being higher than the diatoms. As sedges indicate a wet environment whereas sponges require clear flowing water, the ratio of these two particle types was plotted for the buried A horizon (Figure 102). Although there appears to be a general trend in the data, a best fit line through the data resulted in a poor correlation coefficient (0.6863). However, if one divides the six data points into two sets of 3 data points, the sample 10-12 value results in a correlation coefficient of 0.9968 and the sample 13-15 data results in a 0.9922 correlation coefficient. Although these trends are visible when looking at Figure 102, both of these zones were judged based on soil properties to be due to cumulic soil formation (Carter et al. 2009). However, the phytolith curve shows a clear inflection point between these two data subsets in the middle of a melanized zone (Figure 97). This sedge/spicule data suggests that the inflection in the biogenic silica data, which correlated with an inflection within the melanized zone (15-13 and 12-10) which was not visible in the TOC data (Carter et al.

2009) was not simply due to moist conditions but rather to a change in flowing water as

tentatively suggested by the relative increase in relative sponge spicule count.

Table 71
Additional Counts of Particles in Medium Size Phytolith Fraction

Lizard Site Sample No.	Spicule	Diatom	Sedges	Asteraceae	Curcubit	Maize Rondel	Sedge/Spicule Ratio
2-10	11	1	1	0	0	0	0.0909
2-11	13	1	4	0	0	0	0.3077
2-12	14	1	8	2	1	1	0.5714
2-13	5	1	1	0	0	0	0.2000
2-14	12	0	9	0	0	0	0.7500
2-15	2	0	3	0	0	0	1.5000

Figure 101. Ruffled top rondel diagnostic for maize from Lizard site phytolith fraction from soil sample 12 (immediately above 20 micron scale bar).
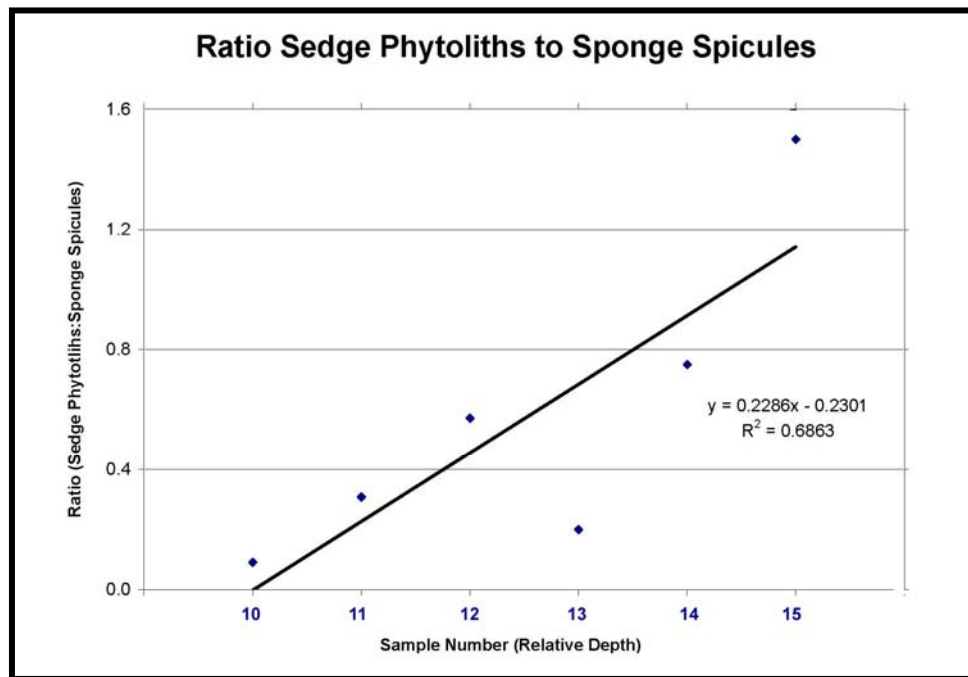
Figure 102. Plot of ratio of sedge phytoliths to sponge spicules.

Specifically, based on this limited data for Ab2 (Table 71), sample 13—with lower total and spicule count [non-normalized] appears to have possibly formed during an interval of very low water flow, before and after which water flows at the site were higher. In the seasonality graph (Figure 98), sample 13 correlates with a shortened cool season and the largest panicoid sample recovered from the entire site profile indicating an interval of relatively cooler summers.

Whether the sponge spicules in this profile are actually indigenous to the site, or transported in during frequent small overbank depositional episodes is not clear. However, although the spicules in the medium phytolith fraction tended to be fragmentary, they were relatively unworn suggesting minimal movement (Figure 103 B,

C, E, and F)[38]; the coarse phytolith fraction actually contained pristine complete spicules (Figure 103 A and D). No gemmules were observed during particle counting from any of the sites studied (for an example of gemmules, see Sudbury 2007:156 (Figure 17C-E)); the adult spicules recovered from the research sites in this current project are not identifiable to species. The adult spicules illustrated do suggest that several species are represented in this sample. The one recounted sample below the Ab2 horizon (2-15) also had a very low spicule and sedge count. The increase in incidence of both biogenic silica forms observed in 2-14 (i.e., wetter conditions and running water) correlates with the lowest portion of Ab2 (more stability, plant growth, and A horizon development).

The counts of the same biogenic silica particles in the original short cell data (Tables 63-66) were too small to see any definitive trend although sample 24 had a notably high spicule count and sample 25 had a very high sedge count. Although admittedly a small data set (Figure 102), the R^2 values of these two previously noted Lizard Site buried soil subsets (10-12, 13-15) are striking enough that this type of data merits a more in depth evaluation on other buried soil sites in alluvial settings.

The Lizard site Tall:Squat Saddle ratio was also processed (Table 72) and plotted (Figure 104). The three A horizons (green diamonds) are not clustered quite as tightly as the Carnegie Canyon Site A horizons (Figure 90) suggesting somewhat more climatic fluctuation and difference between periods of stability resulting in A horizon formation. However, at the Lizard Site, the top of Ab2 (sample 10) plots very close to

---

[38] Some spicules may have been broken in processing; this is the only sample set reported in this dissertation that was sieved to remove the sand fraction.

the modern A horizon (sample 1) suggesting a climate very similar to our modern climate

at the time that the buried A horizon terminating in sample 10 was forming. On the other

hand, sample 4 (top of Ab, the presumed Copan geosol (Carter et al. 2009) is shifted to

the left in Figure 104 putting it about half the distance between climate represented by the

modern A horizon at the Lizard Site (Figure 104) and the cluster at the Carnegie Canyon

Site (Figure 90), likely indicating a climatic shift—but much cooler and/or wetter at the
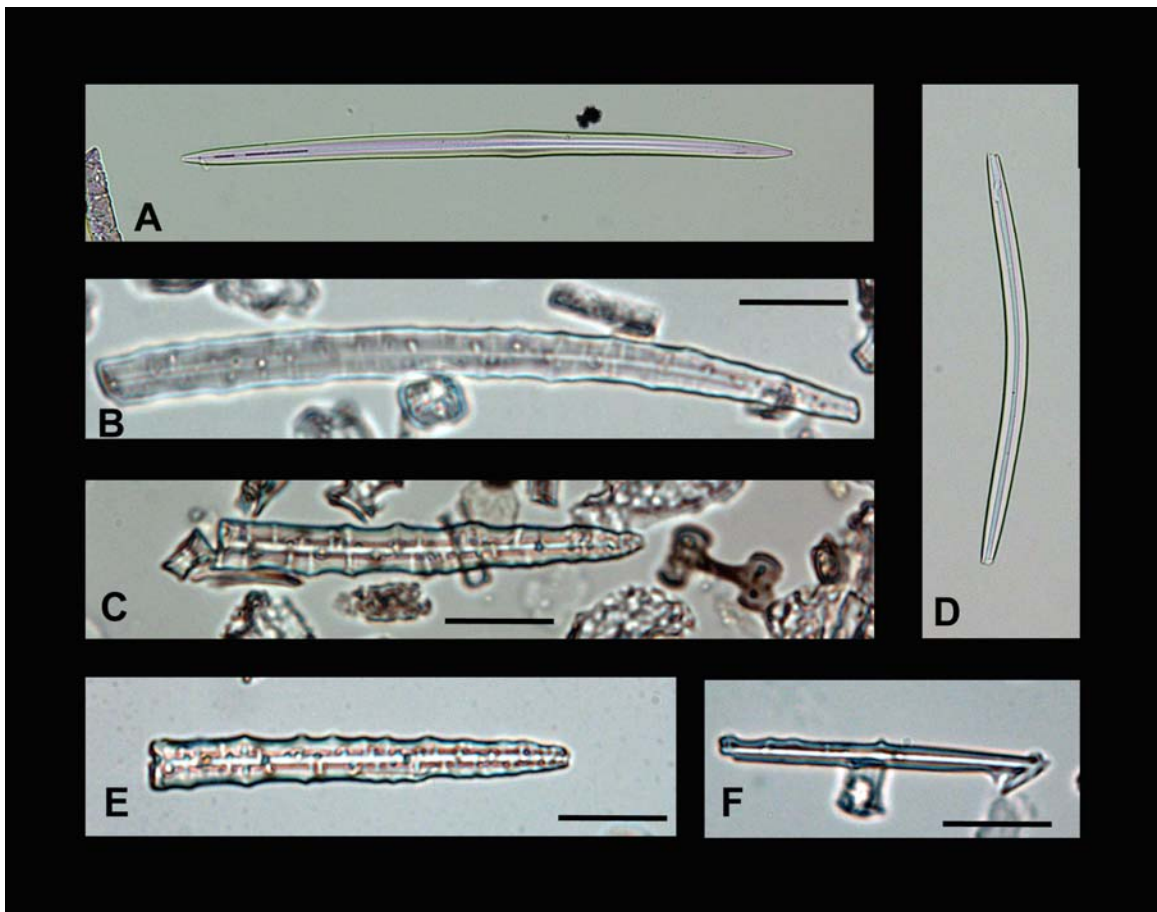
Figure 103. Sponge Spicules recovered from the phytolith fractions of soil sample 12 from the Lizard Site. The bar scales are 20 microns (500x); unscaled images (A and D) are specimens recovered from the coarse phytolith fraction (200x). Note the burned panicoid phytolith in C.

Table 72
Lizard Site Saddle Phytolith Ratio
and Normalized Percent of Short Cells[39]

Soil Sample	Ratio (Tall:Squat)	Normalized Percent
1	1.583	11.50%
2	0.722	13.66%
3	1.100	8.82%
4	0.900	8.94%
5	0.700	8.35%
6	1.000	6.35%
7	1.250	4.31%
8	0.714	5.25%
9	0.385	7.36%
10	1.412	16.60%
11	0.636	8.31%
12	0.667	9.55%
13	1.000	8.79%
14	0.273	14.51%
15	1.375	29.46%
16	1.594	32.36%
17	1.086	32.30%
18	1.265	37.02%
19	1.947	26.05%
20	2.833	40.17%
21	1.094	36.31%
22	1.684	48.92%
23	2.000	16.51%
24	1.600	20.00%
25	1.200	14.01%
26	1.500	27.03%
27	1.600	27.66%

Lizard Site (i.e., a lower chloridoid content) than at Carnegie Canyon. Even more

interesting, sample 13 (a lower Ab2 horizon sample)—marking the proposed transition

to temporary lower water flow at the Lizard site during Ab2 (via sedge/spicule data,

Figure 102) almost directly overlies that of sample 4 (Ab). This can be interpreted to

---

[39] Samples 22-27 were too low in total short cells for the counts to be reliable.

indicate that the Lizard Site climate during sample 4 (i.e., the plant community that

deposited phytoliths at the time that A horizon was forming) was very similar to that

present at the time of the formation of the soil zone represented by sample 13. This

evidence may indicate that soil welding of two A horizons, as reported at the Carnegie

Canyon site (Carter et al. 2009), may have also occurred within what has been identified

as the Ab2 Horizon at the Lizard Site. Alternatively the process of melanization

continued at the stable developing A horizon during intermittent water flow fluctuations.
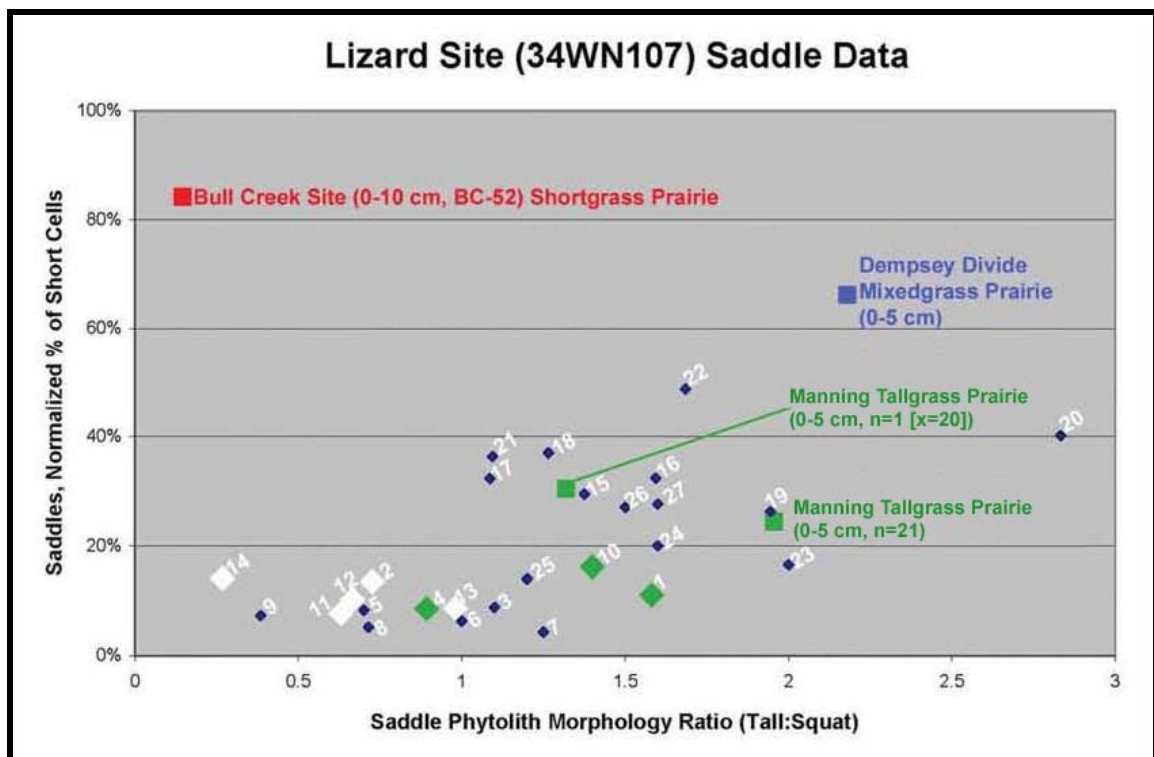
Figure 104. Saddle data from the Lizard Site (34WN107). Green diamonds are the top of A horizons, white diamonds are lower portions of A horizons, and small blue diamonds are non-A horizon samples. (In the Carnegie Canyon sample, the white diamonds remained in the A horizon cluster or shifted right in the saddle plot (Figure 90). In the Lizard Site plot (Figure 104), the white diamonds shifted to the left—possibly suggesting different processes or inputs occurring at the two sites.)

The charcoal data (charcoal particle count / total short cell phytolith count in the same fields (Tables 63-66)) is shown in Figure 105 along with the sand and phytolith weight percent concentrations for the same samples. Overall, charcoal concentrations were very low until the top of Ab2 (sample 10), with charcoal concentration higher from sample 10 through most of the rest of lower profile. Again, sample 13 is an anomalous point—perhaps with lower water flow correlating with less run off and thus less charcoal deposition from the upper portion of the drainage system. The charcoal concentration increases in 14, briefly drops off and then increases much more with the higher sand concentration in the lower samples in the profile. The highest sand concentration correlates with at time of high charcoal incidence, suggesting that fires and vegetation loss may have resulted in more severe erosion following upland fires that deposited charcoal in the drainage system. Even though the entire specimen slides were counted, the short cell counts were too low for samples 23 and 25-27 to feel comfortable with the actual numerical value. However, Figure 105 suggests a very high charcoal concentration in the predominantly sandy sediment load that occurred when the alluvium now at the bottom of the profile was being deposited. This possibly suggests a high rate of erosion, or a high velocity runoff, and also suggests that fires were more prevalent on the landscape. The spicule and sedge data from the portion of the profile also suggested a very wet period during this interval of high sand deposition. Based on the low phytolith short cell counts for some of these lower profile samples, larger samples of high sand content alluvial soils should be processed for phytolith recovery.
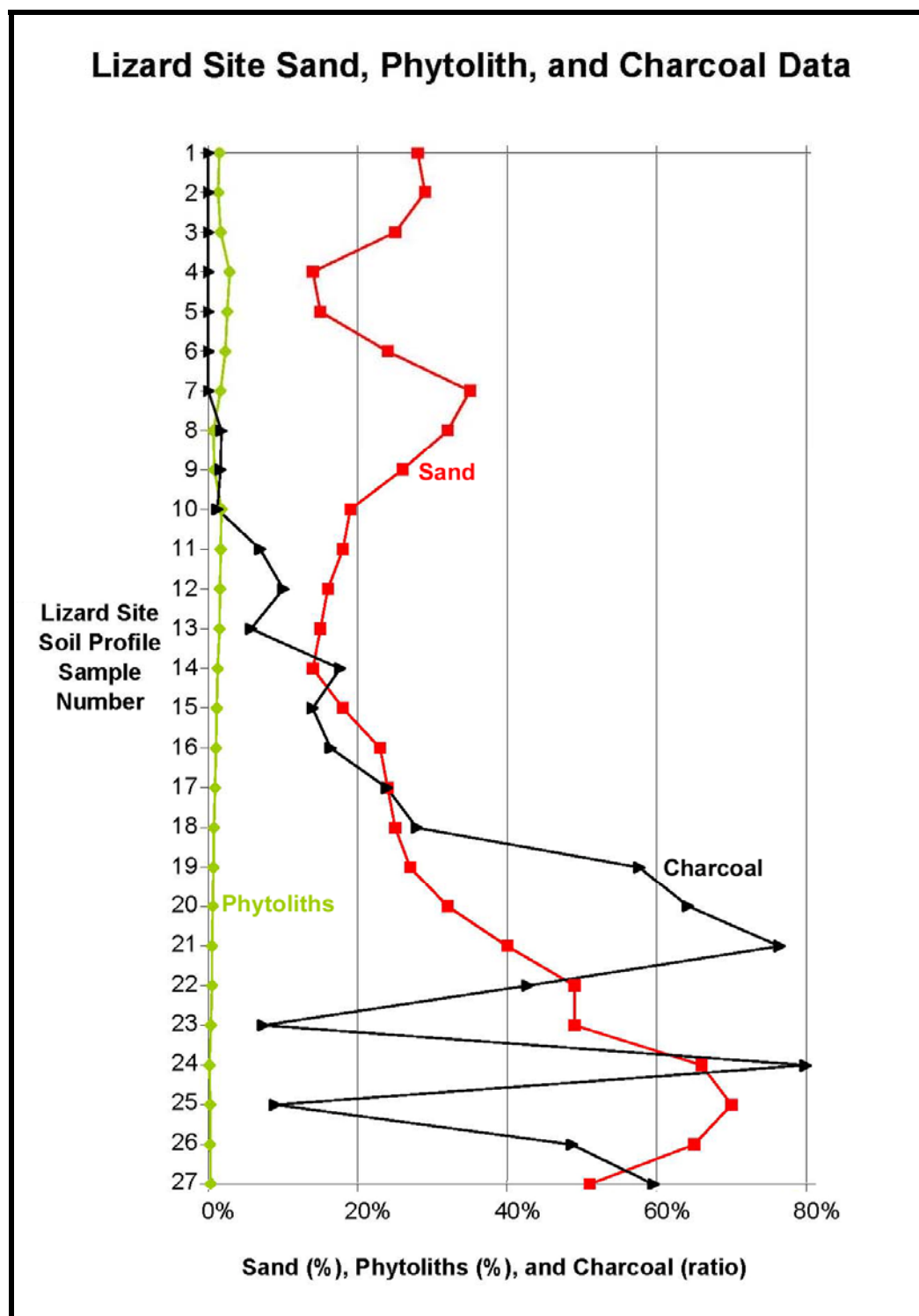
Figure 105. Phytolith, sand, and charcoal data from the Lizard Site soil profile (34WN107). Phytolith and sand data are weight %; the charcoal data is a numerical ratio of charcoal fragments to short cell phytoliths overlain on the same graph. (The charcoal data [and all particle data] in #22-25 is suspect due to low particle counts.)

The Lizard Site shows considerable variation in placement of the three A horizons on the saddle plot (Figure 109) while still indicating that each sample represents a cool moist climate in a known riparian setting. The placement variation of the asterisks suggests that the climate/vegetation regime of A horizon samples 1 and 10 were relatively similar, and while that of 4 was somewhat different; Figure 98 indicated that sample 4 had a much stronger Panicoid content and a smaller total Chloridoid content than the other two A horizons (Figure 98). The sample 4 A-horizon was concluded to be the Copan Soil geosol dated to about 1200 BP (Carter et al. 2009, Hall 1990). The sample 10 A horizon "was buried at 3120±60 rybp (Beta 192314)." (Carter et al. 2009).

The TOC data for the A (1) and Ab (4) samples supported melanization whereas the TOC data for Ab2 (10) and below (down to sample 14) indicated a cumulization process of soil formation (Carter et al. 2009). However, as previously discussed in this current chapter (Figure 97), the phytolith data showed an exponential drop-off in phytolith concentration with depth in each of these three A horizons suggesting that all three A horizons were formed by the process of melanization. On potential explanation for this dichotomy between the two data sets (TOC vs. phytolith soil concentration in Ab2) is that the moist riverbank environment at the Lizard site immediately after inundation of the Ab2 horizon may have supported extensive microbial growth that over time would have lowered the TOC values but not had an effect on the inorganic phytolith concentration. It is not known if there were any erosional losses from the Lizard Site between 3120 and 1200 BP; however, based on the [remaining] deposits recovered (#5-9) conditions were not suitable for formation of another A horizon during that time interval.

If the site remained wet enough during this time interval, microbial activity in the organic rich layer would have tended to decrease the buried soil TOC, perhaps resulting in the apparent cumulic TOC values that were observed. The evidence at the Lubbock Lake Site suggested deterioration of the strong TOC signature of a soil by one thousand years after burial (Holliday 1988:601). The Lizard Site soil profile has been previously published (Carter et al. 2009).

The saddle plot data for the Lizard site (Figure 109) is very interesting with considerable spread along each axis. However, as noted previously the three A horizons are all situated within a zone that is consistent with what would be expected from a riparian setting; of these three A horizons, Ab2 (#10) and A (#1) are somewhat more similar in relative placement to the Tallgrass Prairie controls than Ab(#4). All of the sample data points number 1-14 are essentially lower than any of the points from Carnegie Canyon Site (Figure 109) while #15-27 are more in line with the y-axis value (warming) noted at Carnegie Canyon (except for the temporary decrease seen in #23-25).

The seasonality data from Figure 98 is plotted in Figure 106 in a way to make it easier to judge individual relative plant metabolic type contributions. The top of Ab2 (sample #10) correlates with a significantly warmer period with a lesser contribution from the cooler Pooid fraction; this 3,200 BP buried soil formation ended after this warm interval spike. In the lower Ab2 horizon, sample #11 had cooler summers and more prolonged C3 growing seasons, whereas #12-13 had much stronger Panicoid component (longer cooler moister summers) and less C3 growing interval.

278

At this point, the two dimensional plot in Figure 109 is very useful when compared with the sand data (Carter et al. 2009). FE 2 resulted in relatively low sand content in the soil compared to the overall sand load in FE 3 (Carter et al. 2009). In looking at Figure 109, it appears that the saddle signature during FE 2 interval samples (#4-9) mirrors that of the relatively cool riparian phytolith signature of Ab (#4) whereas the signature of the samples below Ab2 (#15-27) generally move closer to that to the Tallgrass Prairie. This observation may indicate that the apparent relatively lower flow FE 2 interval tended to move and redeposit sands that were already present in the stream drainage system (and thus have a strong cool Pooid signature), while the erosion that occurred during FE-3 from higher flows (i.e. much more sand deposition) actually moved in much more material (including phytoliths) from a surrounding upland Tallgrass Prairie. Thus, in the Cotton Creek alluvial system, non-A horizons, such as the Bw, BC, BTss, Bt, and Bc at the Lizard site, the entombed phytolith signature in these samples appears to mirror the stream bottom riparian vegetation in low flow (relatively low quantity of sand depositional events), and the surrounding uplands in high flow erosional events. The apparent anomaly in this data set is samples 23-25 which occurred at the very peak flow (sand deposition) would show an intermediate stage between Tallgrass and riparian phytolith signature (Figures 106 and 109); however, in actuality there was so much sand and so few phytoliths recovered that these specific counts are not reliable. Samples 20 and 22 are more far afield in their scatter.

The sedge and sponge spicule data (Figure 102) shows intriguing indicators of changes in water flow at the site which are suggestive of climatic changes, with periods
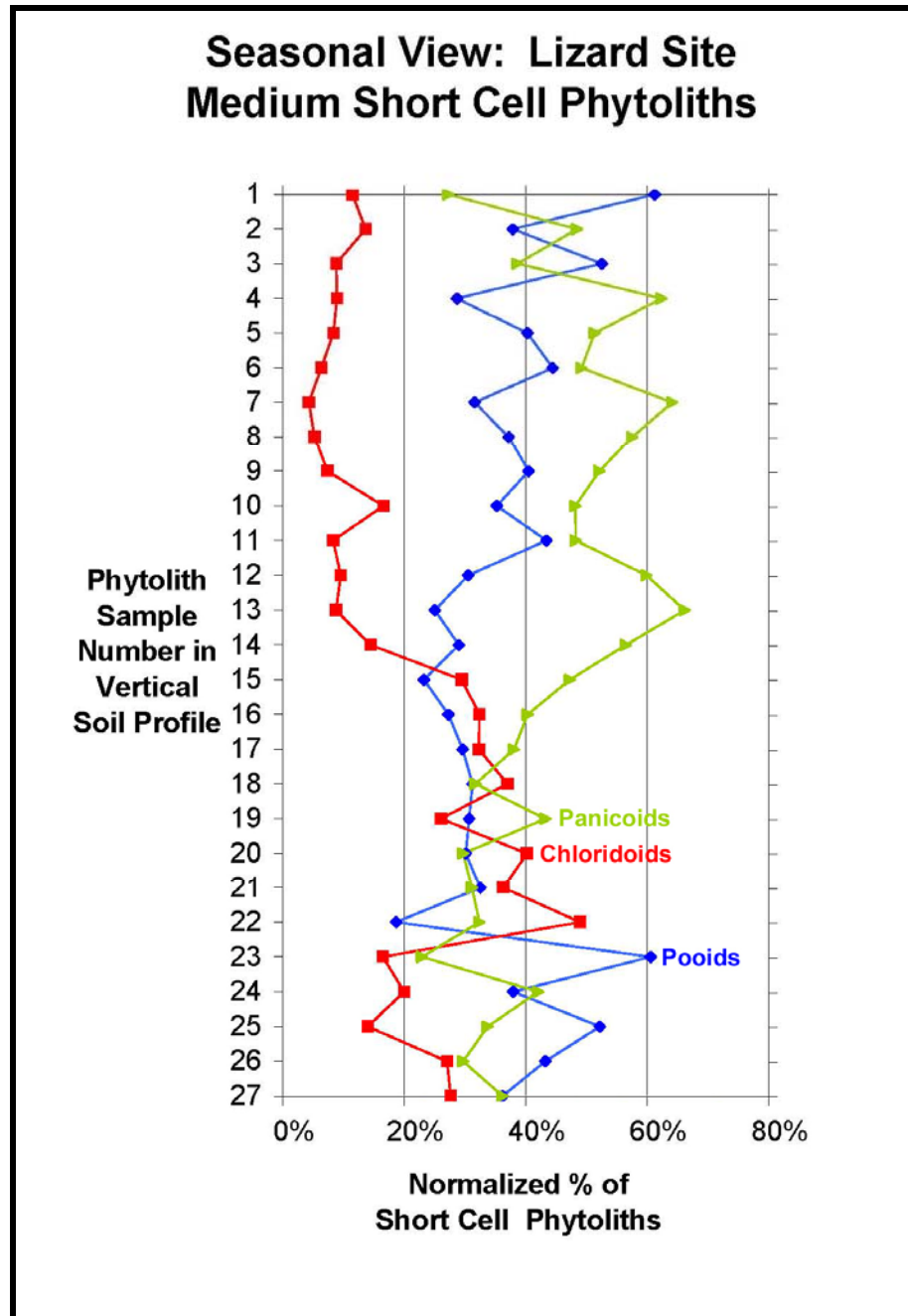
Figure 106. Seasonal plot of Lizard Site phytolith data. (Short cell phytolith total counts below sample 22 are significantly lower than desirable).

of lower and higher flow during development of Ab2. Phytoliths representing maize, curcubits, and asteraceae were also noted in the profile (#12). Diatom incidence remained very low farther down the profile than sample #7. The occurrence of charcoal

flecks (Figure 106) in the phytolith fraction isolates increased in Ab2, dropping off in temporarily in sample 13 which the sedge/spicule ratio (Figure 103) indicated was a period of relatively higher spicule ratio with somewhat lower particle counts. This presumably indicates that the charcoal was entering the drainage system from the uplands, and the lower flows cut back charcoal entry into the system. It also suggests a much higher incidence of fire in the area in the interval prior to 3,100 BP. The Panicoid fraction peaked in #13 for the whole profile, and was elevated somewhat throughout the development interval of Ab2. The lower Panicoid fraction in #10 and 11, and the Chloridoid spike in #10 offsetting the drop in the Pooid fraction may have combined to create the environmental change that led to burial of Ab3. The Chloridoid fraction from #7 gradually increased until present day, although the Pooid and Panicoid components of the phytolith signature were in a constant state of flux—continually offsetting each other suggesting a variation in the relative amount of cool season growth throughout the past 3,000 years. The zone from #15-21 (Figure 106) confirms what was seen in the saddle morphology data (Figure 109)—that the vegetation represented in the profile appears similar to that originating from a Tallgrass Prairie. The sand data (Carter et al. 2009) indicating high sand content in the profile suggests that the phytoliths (and charcoal) in the lower part of the profile are likely of upland setting and contributed to the profile by erosive runoff. Charcoal incidence above Ab2 in the profile is very low presumably reflecting a lower fire incidence post-3,100 BP. The higher charcoal incidence earlier clearly correlates with a significantly warmer period than encountered on average during the past three millennia.

Discussion of Buried Soils and Saddle Phytolith Signature Data – The three

Oklahoma research sites contained buried A horizons with dates ranging from about 500

to 11,000 BP. The soil phytolith concentrations of these buried soils is summarized in

Table 73 [control site data ppresented in Table 47]. The large range in observed soil

phytolith concentration is felt to be due to a variety of interacting factors including the

length of time that the soil horizon was the stable ground surface, the rate of aggradation

(i.e., the rate at which added material dilutes the phytolith concentration of the soil), the

biomass load at the site, the relative phytolith concentration

Table 73
Buried Soil Site A Horizon Soil Phytolith Concentrations

Site	Sample	Horizon Designation	Phytolth/Soil (wt/wt %)
Carnegie Canyon	1	AC	0.17%
Carnegie Canyon	3	Ab	0.12%
Carnegie Canyon	6	AB2	0.17%
Carnegie Canyon	19	CAb2	0.41%
Carnegie Canyon	20	A1b3	1.15%
Carnegie Canyon	21	A1b3	0.92%
Carnegie Canyon	22	A2b3	0.76%
Carnegie Canyon	23	A2b3	0.68%
Carnegie Canyon	24	A3b3	0.65%
Carnegie Canyon	25	A3b3	0.55%
Carnegie Canyon	26	A4b3	0.53%
Carnegie Canyon	27	A4b3	0.41%
Lizard Site	1	A	1.46%
Lizard Site	2	A	1.31%
Lizard Site	4	Ab	2.87%
Lizard Site	10	Ab2	1.77%
Lizard Site	11	Ab2	1.66%
Lizard Site	12	Ab2	1.57%
Lizard Site	13	Ab2	1.50%
Lizard Site	14	Ab2	1.26%
Bull Creek Site	52	A	1.65%
Bull Creek Site	47	Akb2	0.90%
Bull Creek Site	45	Akb3	1.85%
Bull Creek Site	42	ABkb3	2.12%
Bull Creek Site	37	2Akb4	2.77%
Bull Creek Site	31	2Ab5	0.76%
Bull Creek Site	28	2Ab6	0.24%
Bull Creek Site	25	2Akb7	1.07%
Bull Creek Site	22	2Akb8	0.49%

of the particular botanical species present, the stability of the phytoliths in the soil environment, and relative soil fertility. The soil types at the six study sites (Table 74) show that both Inceptisols (newly forming soils) and Mollisols (well-developed fertile prairie soils) were both represented. Before discussing the individual site saddle data, a brief additional discussion about saddle morphology is warranted.

Table 74
Modern A Horizon Soil Types Present at Study Sites

Site/Location	Soil Series	Soil Description
Bull Creek	Mansic	fine-loamy, mixed, superactive, thermic aridic calciustoll
Carnegie	Noble	coarse-loamy, siliceous, active, thermic udic haplustept
Dempsey	Quinlan	loamy, mixed, superactive, thermic, shallow typic haplustept
Divide	Woodward	coarse-silty, mixed, superactive, thermic typic haplustept
Lizard	Verdigris	fine-silty, mixed, superactive, thermic cumulic hapludoll
Manning	Coyle Loam	fine-loamy, siliceous, active, thermic udic argiustoll

The Bull Creek Site Shortgrass Prairie has a very high saddle phytolith concentration and a very minor tall saddle phytolith component. Several saddle phytolith images from sample BC-52 relevant to morphology are shown in Figures 107 and 108. These images include numerous tall and squat saddle phytoliths. There are also several that are nearly square in dimension, and two that actually measure to be a different ratio than what they visually appear to be. Several saddle imposter forms (*Aristida* sp.?) are also present in these images (labeled "I" in Figure 108 H, I, and K).

Moving south-southeast about 145 kilometers to the Dempsey Divide Mixedgrass Prairie sampling area (Figure 7), which is adjacent to a Shortgrass Prairie also dominated
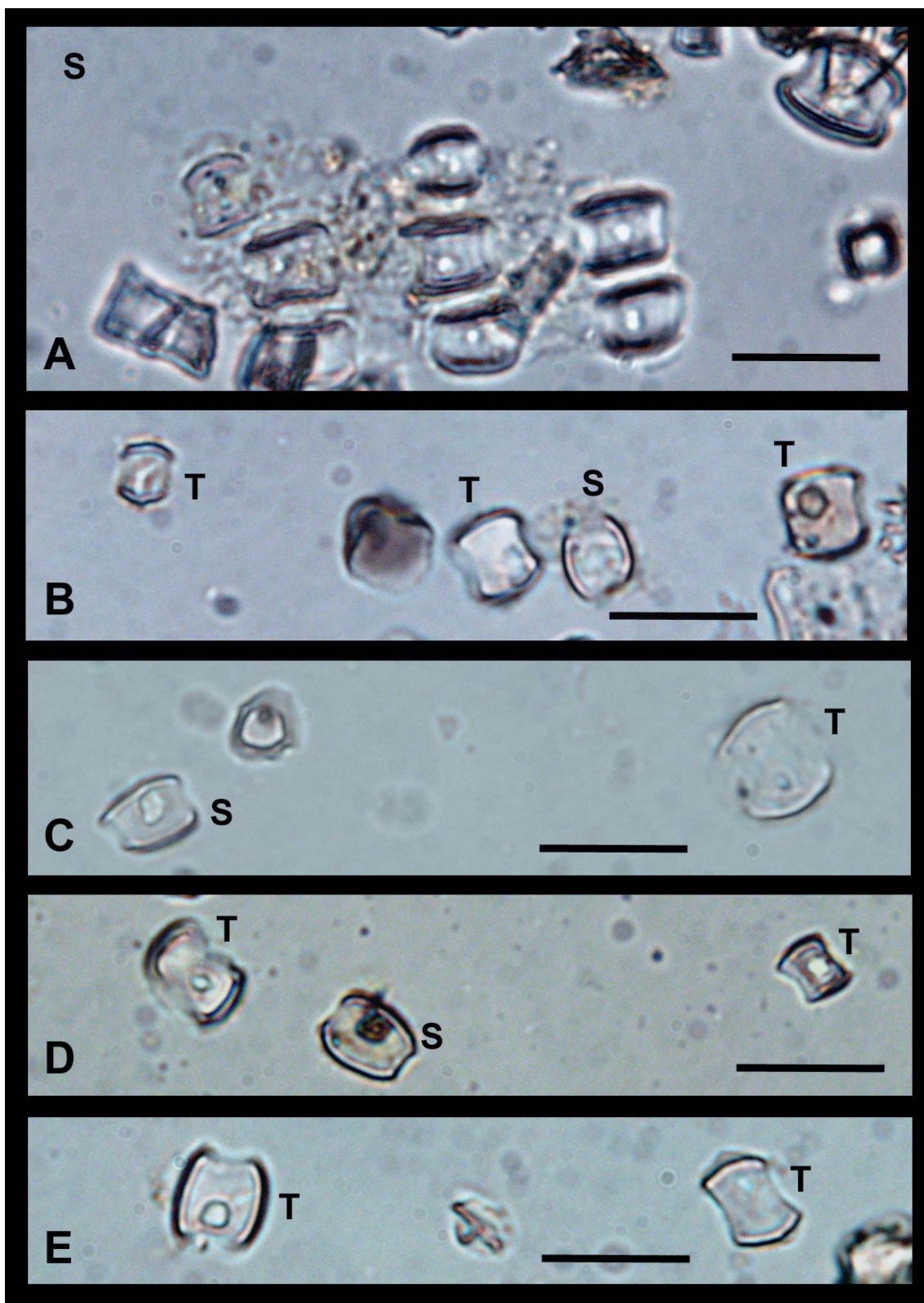
Figure 107. BC-52 Tall ("T") and Squat ("S") phytoliths. Bar scale is 20 microns.

Figure 108. BC-52 Tall ("T"), Squat ("S"), and imposter ("I") phytoliths. Bar scale is 20 microns.

by Buffalo Grass (Figures 10-13), the saddle signature changes very abruptly. Although the total saddle content is still very high, the relative saddle morphology (tall verses squat) changed drastically with the addition of new plant species to the landscape in the Mixedgrass Prairie. Although perhaps slightly more moist, the Dempsey Divide climate is still very hot and dry (agreeing with high overall saddle content); however the saddle signature ratio shifts distinctly along the x-axis indicating a strong vegetative change compared to the Shortgrass Prairie.

Moving 250 kilometers east from the Dempsey Divide Mixedgrass Prairie to the virgin Manning Tallgrass Prairie, the total Chloridoid fraction in the surface soil samples is essentially halved, and the saddle ratio moderates to an intermediate position. The Tallgrass Prairie is a more balanced mixture of C4 hot, C4 warm and moist, and C3 cool season species (see Figure 64 soil sample 1). The new species present in the Tallgrass Prairie are a reflection of more moisture which helps decrease the relative incidence of C4 hot dry species, and increases the cool moist season C3 species. Phytolith assemblages, such as those from cooler climates or shady moist riparian settings, are predicated to plot on this chart lower than the Tallgrass Prairie data points due to their higher incidence of cool/most vegetation decreasing the relative Chloridoid content.

For the southern Great Plains, based on this limited data set, the big mover on the x-axis (i.e., saddle morphology) appear to significantly be affiliated with species in the sampled Mixedgrass Prairie assemblage. The increase in Panicoid fraction in the

Tallgrass Prairie seems to dilute the saddle morphologic change on the x-axis as the total

Mixedgrass Prairie species contribution to the Tallgrass Prairie declines, with a

concomitant significant downward shift on the y-axis (i.e., total Chloridoid content)

reflecting an increase in average available annual moisture.

Summarizing the saddle data from the buried soil sites and the control prairie sites

resulted in Figure 109. Here, the asterisks denote the upper sample taken from each A

horizon, the closed circles indicate the non-upper A horizon samples (when present), and

the diamonds represent the non-A horizon samples. The three prairie control samples are

plotted. The buried soil site samples are red (Bull Creek Site), purple (Carnegie Canyon

Site), and blue (Lizard Site). Figure 110, showing the saddle data plot for the A Horizons

(and the upper sample from A horizons when thick A horizons were subsampled), is less

cluttered and shows a relatively tight data cluster at Carnegie Canyon (squares),

somewhat more species variation at the Lizard Site (circles), and broad ranges along both

axes (i.e., temperature and species variations) at the Bull Creek Site (asterisks).

In the Bull Creek saddle plot (Figure 83) and the earlier phytolith short cell type

plot (Figure 79), both the Shortgrass and Mixedgrass prairie controls [Table 48] have

high saddle concentrations (84.4% and 66.7%), but a considerable spread in the saddle

morphology ratio (0.147% vs. 2.176%). The data and the current site conditions suggest

that the y-axis (concentration) is related to thermal conditions. The main difference in

the Short- and Mixedgrass Prairies (both have hot climate with limited moisture) is the

addition of new plant species that make up the Mixedgrass Prairie which effectively
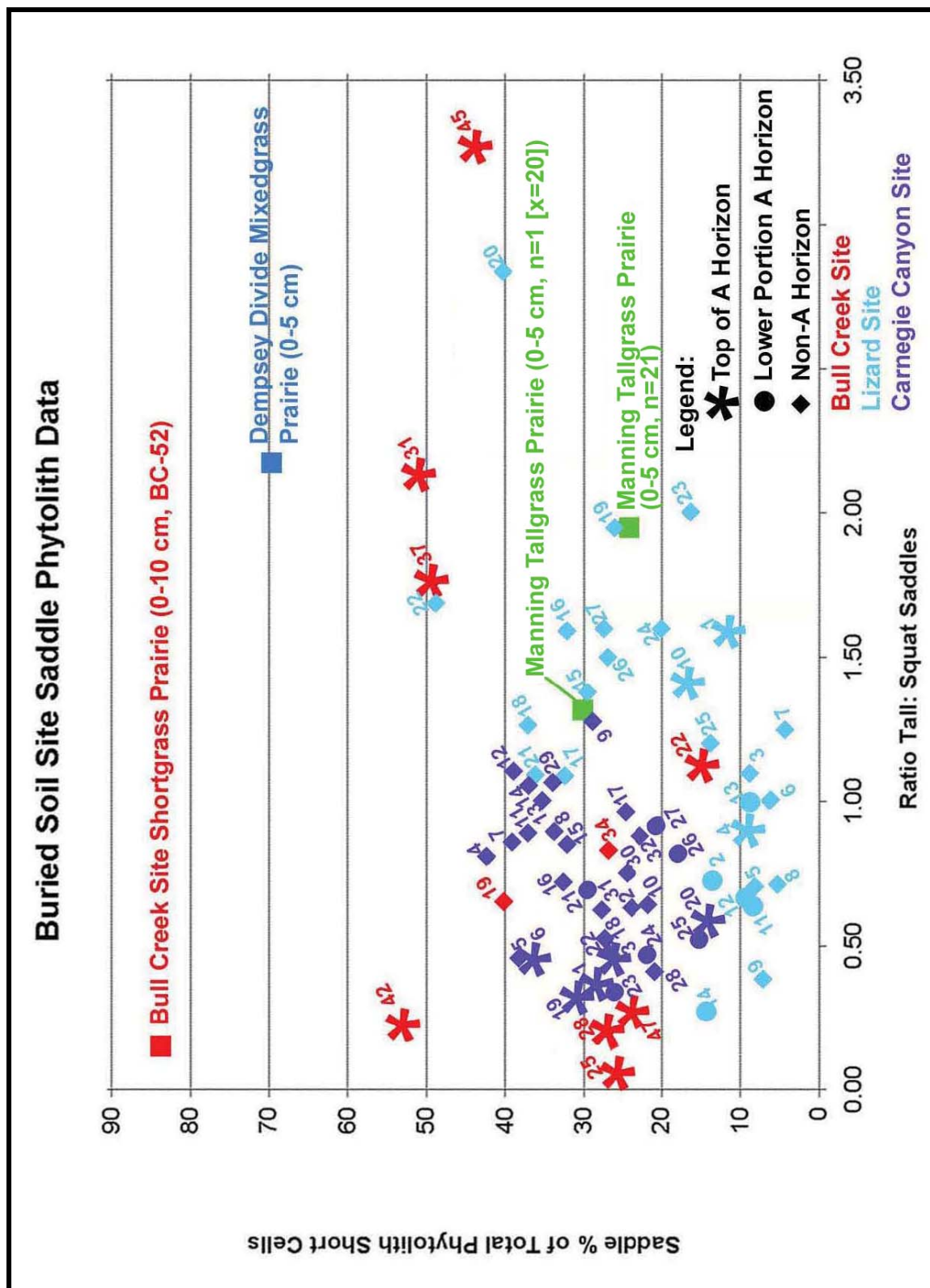
Figure 109. Composite plot of saddle morphology verses total saddle concentration for the three prairie control sites, and for all buried soil site samples evaluated.

dilutes the Shortgrass species input. This particular compositional change results in a strong shift along the x-axis, suggesting this movement is due to species change (such as the "invasive species" noted previously (Bement et al. 2007)).

An examination of the individual saddle data from the 21 surface A horizon replicate samples from Manning Tallgrass Prairie (Experiment 3) shows a fairly tight y-axis clustering and a very large x-horizon deviation of the data (Figure 111)—larger than the range observed in the various Bull Creek buried A horizon samples (Figures 82, 109, and 110). This supports the interpretation that climate indicated by the Bull Creek saddle signatures for samples 31, 37, 42, and 45 was relatively constant although there was
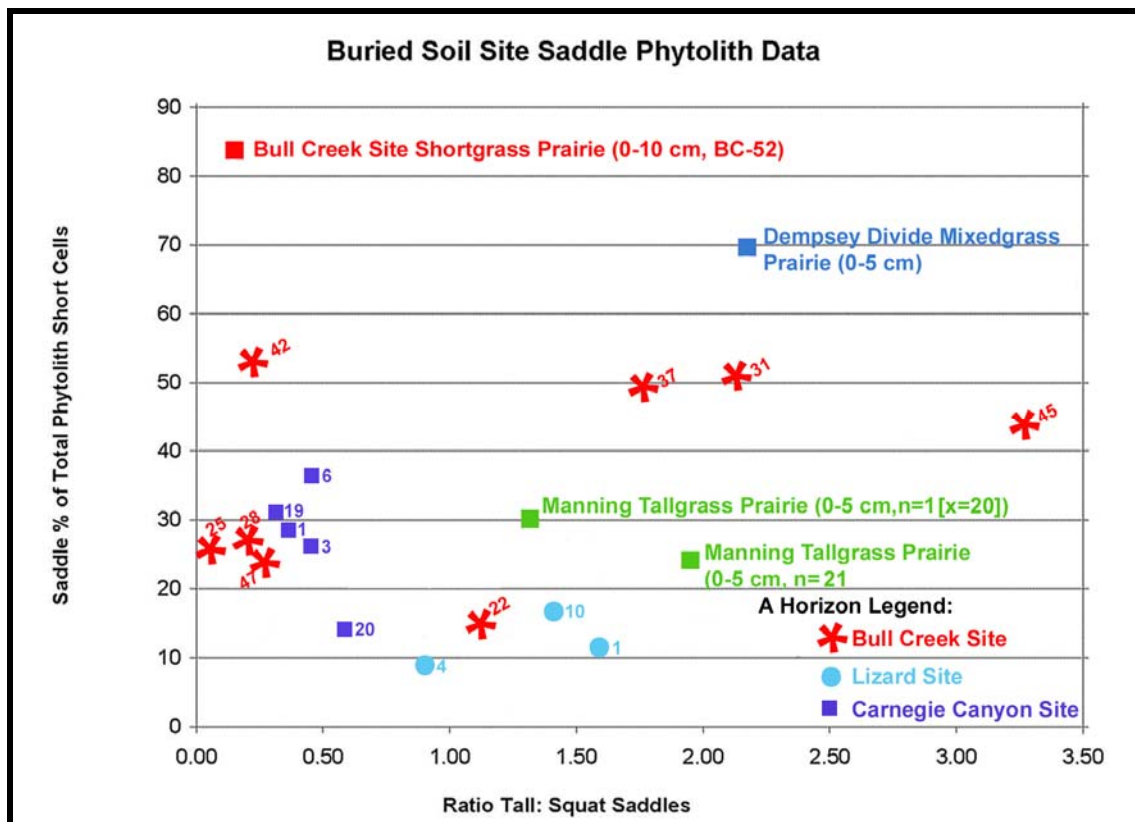
Figure 110. Plot of buried soil site A horizons (and upper A horizon sample when the horizon was subdivided into fractions) saddle signatures.

considerable variation in the actually botanical species represented in the soil phytolith

signature at the sampling point over time. The individual Manning replicate surface

samples (that produced the average Manning value for Experiment 3, n=21) are plotted in

Figure 111.

There are two noticeable outliers to the n=21 data cluster (samples #8 and #14 in

Figure 111); even so, the average of the remaining 19 data points is still to the right and

below that of the n=1 sample average data value. As the temperature was consistent at

these two locations, some other factor(s) must lead to the species variation that is

represented in the soil saddle phytolith signature. These differences could be a

combination of a variety of factors including soil moisture, mineral composition, organic

matter, and overall fertility. Regardless of the specific cause, the x-axis variation appears
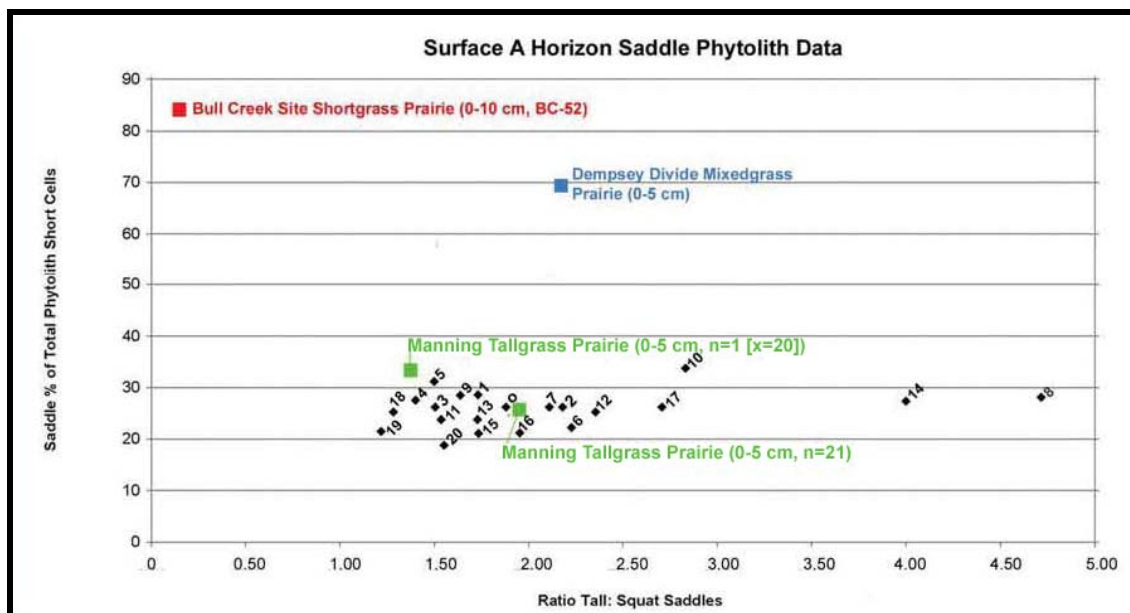
Figure 111. Plot of saddle data from individual replicates from Manning Tallgrass Prairie
experiment 3 (saddle and short cell count data from Tables 22 and 23).

to be due to local site factors, whereas the y-axis variation is primarily due to temperature variations (with a possible smaller moisture component)

Supporting this same reasoning, the two Manning Tallgrass Prairie sampling areas show significant variability in plant species (i.e., the saddle ratio varied from 1.31 (n=1 [x=20] composite sample) [Table 15] to 1.95 (n=21) [Table 26]), while the actual total chloridoid concentration (i.e., the proposed relative thermal indicator based on normalized saddle phytolith concentration (y-axis)) only varied from 30.50% (n=1 [x=20]) to 26.38% (n=21), or 32.8% variation in the saddle ratio due to species variation versus 15.6% variation for the total saddle concentration (i.e., climatic factors— predominantly temperature (x-axis)). Thus, even with the variation caused by the extremely irregular horizontal phytolith morphologic distribution of various species across the Manning Tallgrass Prairie site (as noted previously in Tables 26-30), the overall climatic signature—meaning moisture and especially temperature—were the same (Tables 33-35).

With these thoughts in mind regarding the variation in the Manning Prairie replicates data, additional comments can be made about the A horizon saddle data in Figure 110. The Bull Creek data shows a very large x-axis variation (species variation) and a large y-axis deviation (primarily thermal changes, with some possible local moisture input). In contrast, the Carnegie Canyon data (a very small drainage area) shows minimal species variation (x-axis) and a larger variation in thermal conditions (y-axis); the thermal deviation is larger than that observed in the two samples (n=1 [x=20]

and n=21) at Manning Tallgrass Prairie. On the other hand, the Lizard site data (on a

larger drainage basin) shows minimial environmental thermal change over the time

interval studied (y-axis) although it does show more species variation (x-axis). The range

of species variation recorded in the Lizard site saddle data is less than the modern range

noted at Manning Tallgrass Prairie (Figure 111).

Environmentally, the Bull Creek Shortgrass Prairie and the Dempsey Divide

Mixedgrass Prairie are similar (Tables 8 and 75). The difference in these two average

modern soil saddle phytolith ratios values thus reflect a difference in the predominant

plant species rather than in the actual temperature and moisture conditions prevalent at

both sites.   At Manning Tallgrass Prairie, the overall normalized saddle concentration

moderates from the Shortgrass and Mixedgrass extremes (on the y-axis), but the

predominant species present tend to have an intermediate tall:short saddle ratio. Thus,

Manning Tallgrass Prairie–with a different moisture and temperature regime—shows a

significant thermal change (y-axis difference in normalized saddle concentration) from

the other two prairie types, and an intermediate species saddle signature (x-axis).

Paleoclimate Temperature Calculations – One product of prior Great Plains'

phytolith research investigations was development of a formula that correlated current

prairie soil phytolith morphologies with local mean July temperature (Fredlund and

Tieszen 1997a):

July Mean Temp (ºC) =

$$(-0.263)[\text{Stipa}] + (0.135)[\text{Saddle}] + (0.324)[\text{C4 Lobates}] + (0.246)[\text{Crenate}].$$

where the percent of each morphologic type named in the bracket is taken from the previous data tables with normalized percent of each short cell for a given site. Developed during the study of 34 modern prairie locations across the plains, Fredlund and Tieszen (1997a) also applied this formula to soil phytolith samples from earlier Holocene deposits in order to calculate the environmental temperatures at the time that the deposits formed.

In this current study, this formula was used to estimate the temperature at time of formation/deposition of modern A Horizons, dated buried soil deposits, and other previously discussed samples. Based on the phytolith sample concentrations determined in this study (presented earlier in this chapter), the calculated temperatures of the various isolated soil phytoliths are presented in Tables 75, 77-78, and 80-81, and discussed in this section.

The calculated dates for the five surface A horizons in this study are in Table 75. The modern mean July temperature for each site was needed in order to make the temperature calculations. This temperature data was obtained from the National Weather Service mean values for the period 1971-2000 (NWS nd). No NWS temperature collection sites were close to Bull Creek, so the sites used to calculate the modern mean July Temperature were to the east (Buffalo and Fort Supply, Oklahoma) and north and

northeast (Liberal and Ashland, Kansas) of the site. The Dempsey Divide Mixedgrass

Prairie temperature average was based on NWS values from Reydon, Hammon, Elk City,

Sayre, and Arnette, Oklahoma (n=5). No NWS data collection sites were available from

immediately east of Manning Prairie, so the average temperature value was based on data

from Cushing, Perkins, and Stillwater. Although the local Carnegie NWS site reading

was 27.7ºC, there was considerable variation in the immediately surrounding area.

For this reason the composite Carnegie value (ºC) was used based on the average of eight

locations (Anadarko, Apache, Carnegie, Chickisha, Cordell, Hobart, Weatherford, and

Wichita Mountain Wildlife Refuge). There were no local NWS reporting sites near the

Lizard Site locality; the default value of the closest sites would be in Kay County (over

Table 75
Temperature Calculation of Modern Soil Samples from Study Sites

Field Site	Horizon (cm)	Calculated Deviation from T (ºC)	Mean Modern July Temperature (ºC)[40]	Number of Locations used to Determine Modern Mean July T
Bull Creek Site (Shortgrass Prairie)	A (0-10)	**-0.163**	27.02	n=4
Dempsey Mixedgrass Prairie	A (0-5)	**-0.029**	26.91	n=5
Manning Tallgrass Prairie	A (0-5)	**+3.962**	27.82	n=3
Carnegie Canyon	AC (0-11)	**-2.301**	28.19	n=8
Lizard Site	A (0-6)	**-1.242**	26.46	n=1

---

[40] The modern temperature value is based on adjacent modern geographically local collection sites. The temperature deviation is blue (negative value) when the calculated temperature is less than the modern temperature, and red (positive value) when above modern temperature.

140 kilometers away, but at approximately the same latitude as the Lizard Site, with a temperature of 27.7ºC). Due to this large distance, the available local Oklahoma Mesonet July temperature average mean from 1994-2009 (Table 76) was used for the relative temperature calculation for Copan. As an example of the normal annual variation in local temperatures over a sixteen year interval the annual mean July temperature data is shown in Table 76, which includes a range of 4.9ºC at the Copan data collection location.

Although slightly lower, the calculated modern temperature values based on phytolith soil data for Bull Creek and Dempsey Divide Mixedgrass Prairie Sites were very close to the known modern temperature (Table 75). The cause of the significantly higher aberration in the temperature calculated from the Manning Prairie data is not known and should be addressed in future research. As the Manning location was the most heavily sampled surface A horizon in this study, this variation presumably may be due to the specific botanical signature at the site and/or an error in the local modern temperature value.

Based on the reported phytolith assemblage for all soil samples analyzed at each site, the environmental temperature correlating with each sample collected from the profile that was analyzed for phytolith content was calculated. The Fredlund and Tieszen temperature formula was developed based on the surface of A horizons, so it is anticipated that the B and C horizon samples analyzed for phytolith composition may not be suitably addressed by this formula. Thus, calculations will only be performed on A (and one AC) horizons.

Eight of the eleven Bull Creek samples were A horizons. The calculated

environmental temperature correlating with each deposit based on the phytolith record is

presented in Table 77. The bottom of the tested sequence at the Bull Creek site, starting

with BC-22, represents the period of retreat from the glacial maximum on the North

American continent following the end of the Wisconsin Glacial. Interpretation of pollen

records on the Great Plains has helped track the glacial retreat (Wendland 1978). Thus,

the colder calculated temperatures at this the early Holocene Bull Creek Site time agree

with the regional climate picture developed for this interval.

The radiocarbon dates obtained for BC-25, BC-28, and BC-31 are not in the

expected chronological order (Table 77).   The calculated temperatures for BC-31 and

BC-28 indicate a relatively warm climate, much more similar to modern day than to the

then immediately preceding glacial episode.   In contrast, calculated temperature based on

BC-25 is actually somewhat colder than the adjacent temperatures (BC-22 and BC-28).

If one were to look at the bracketing dates that appear to be in correct time sequence (i.e.,

BC-22 and BC-31), this time interval corresponds with what is referred to as the

Younger-Dryas period; one or both samples yielding questionable radiocarbon date/s

(10,840 and/or 10,350 BP) are potentially included in the Younger Dryas period.

The relative temperature data calculated via Fredlund and Tieszen's formula

(Table 75) does not correlate well with the previous normalized short cell seasonal

phytolith data (Figure 84; Bement 2007 et al. Figure 7) even though the same base

phytolith data set was used. The difference is that, when developed to obtain the best

correlation based on modern prairie soil A horizons, the final Fredlund formula excluded

several major C3 short cell phytolith morphologic types (C3 short cells excluded from

Fredlund's final formula include keeled, conical, and pyramidal forms) whereas the Bull

Creek data in this report (Figure 84) includes all of the short cell forms.   Whether

Fredlund's formula is applicable to immediately post-glacial conditions which had a high

Table 76
Mean July Temperature, Copan and Beaver Mesonet Sites (1994-2009)

Year	Mean July Temp (ºF)	
	Copan	Beaver[41]
2009	77.7	80.1
2008	79.7	80.1
2007	78.1	78.7
2006	82.6	83.8
2005	79.1	79.0
2004	75.8	76.5
2003	81.9	84.2
2002	80.2	81.1
2001	84.6	87.1
2000	79.0	81.7
1999	81.7	82.2
1998	81.8	81.0
1997	71.9	80.3
1996	80.2	80.2
1995	80.3	79.8
1994	79.5	81.6
Mean	79.63	81.09
Mean	26.5 ºC	27.7 ºC
SDev	1.6 ºC	1.4 ºC

---

[41] The NWS values from the surrounding reporting sites were used to obtain the Bull Creek average July temperature in Beaver County that used were for the Bull Creek temperature calculations. This decision was made because NWS temperature records were the data source Fredlund and Tieszen used to derive the original correlation formula. However, as the Oklahoma Mesonet Beaver data collection point is very near the Bull Creek site (Mesonet nd), the Mesonet data is recorded here for comparative purposes. The average temperature for the interval at Beaver from 1994-2009 Mesonet data was 81.09ºF (27.72ºC), close to the composite NWS data from 1971-2000 (27.02ºC, or 80.63ºF) used in the actual preceding Bull Creek Site temperature calculations.

Table 77
Bull Creek Site A-Horizon Paleotemperature Calculations

Sample	Date	Calculated Relative T (°C)	Stipa (%)	Saddle (%)	C4 Lobates (%)	Crenate (%)
BC-52	Modern	-0.2	5.2	84.4	1.8	1.2
BC-47	6,200 BP	+2.7	0.9	23.8	14.0	25.6
BC-45	7,660 BP	-1.7	6.0	43.5	6.2	12.5
BC-42	8,760 BP	+0.2	1.7	53.1	7.5	8.4
BC-37	9,850 BP	-2.8	10.2	49.2	8.0	6.8
BC-31	10,400 BP	-0.9	7.9	50.9	7.5	12.1
BC-28	10,850 BP	-0.5	0.9	27.0	10.6	15.3
BC-25	10,350 BP	-6.4	6.3	25.8	6.2	3.2
BC-22	11,070 BP	-5.4	10.6	15.0	10.8	11.9

incidence of C3 species phytoliths present in the botanical signature remains to be clearly

demonstrated. Further information from the delta 13 values obtained from buried soils

across Great Plains is also available and shows temperature variations (cooler and

warmer) over time during the Holcene (Nordt et al. 2007). A 6°C temperature drop

during in the Younger-Dryas was reported based on oxygen isotope data obtained from

biogenic silica (i.e., diatoms) in a lake core (Shemesh and Peteet 1998), which is similar

to the temperature change noted at Bull Creek based on phytolith signature (Table 77).

Rather than being in an upland prairie setting as were the three control prairies,

the other two study site profiles providing buried soil data were exposed by erosion from

adjacent active modern streams. The paleotemperature data derived from these two sites

is considerably more problematic and less informative than those from the earlier Bull

Creek Site although it was also originally in an alluvial setting. The data from the Lizard

Site (Table 78) shows what an erroneously high modern temperature, and even higher

temperatures in the buried soils. This is presumably due to the riparian site setting and

the possibility of contamination from adjacent upland settings. Thus, a brief

consideration of the Lizard Site setting is in order.

Table 78
Lizard Site Paleotemperature Calculations

Sample	Date (BP)	Calculated Relative T (ºC)	Stipa (%)	Saddle (%)	C4 Lobates (%)	Crenate (%)
1	Modern	**+1.2**	3.0	11.6	24.3	12.6
4	~1,200BP	**+8.8**	5.2	8.9	57.2	3.8
10	3,120 BP	**+7.9**	0.8	16.6	47.4	4.5

The Lizard site is on South Cotton Creek, a second order meandering steam with

additional input feeding in from intermittent drainages (Reid and Artz 1984, DeLorme

2003).   The drainage area above the Lizard Site location on South Cotton Creek is about

73 square kilometers. The soil profile sampled in this study was initially observed in the

cutbank exposed by South Cotton Creek. The phytolith climatic/temperature signature of

the modern A horizon is not in good agreement with the mean modern July temperature

readings (Table 75). The sand content in the soil samples from this alluvial Lizard Site

setting ranged from approximately12-70%, and particle size analysis documented that

numerous flood events had occurred impacting the site (Kelley 2006:51). Whereas

Fredlund used several collection sites near the Bull Creek Site to develop the temperature

calibration formula, all of the control sites used in development of the temperature

formula were more than 300 kilometers away from the Lizard Site locality (Fredlund and

Tieszen 1997a:201 (Figure 1)). Thus, the Lizard site may simply lie outside of the

effective geographical boundaries where the temperature formula is effective.

The majority of the soil samples from this profile are not from established A

horizons, and thus the Fredlund/Tieszen temperature correlation formula developed based

on modern prairie A horizons would not be expected to apply for these samples.

However, even in cases of the Lizard Site buried A horizon samples, the temperatures

obtained via the prairie temperature calibration formula seem high. This result is

presumably attributable to a combination of the fluvial action occurring at the site and the

dissimilarity of a riparian site setting to the upland prairie reference samples used to

develop Fredlund's formula. Grade and flooding frequency in the riparian setting do

affect vegetation species diversity (Hupp 1982; Harris 1987). Indeed, bot flooding and

soil characteristics at a given site affect the plant community (Burke, King, Gartner, and

Eisenbies 2003). Erosional losses would be expected to occur from the site, and

deposition also could occur from upstream erosional runoff. As spring rains are

generally the highest volume water input in this region (Table 79, Figure 112), this low

biomass/high moisture interval spring prairie setting might tend to deposit dead vegetal

debris from the previous summer's growing season along with the alluvium. Also, higher

spring runoff could increase the erosional loss of riparian species plant debris along the

stream. Any input, removal, or dissimilarity of the study site to the controls would tend

to skew the phytolith data. The botanical composition in this riparian setting is not the

same as the up-drainage established prairie; the tree and woody species at the site would

also be represented the phytolith sample potentially further altering the sample

composition. Irregardless of the specific cause, in this case the alluvial-based A horizons

in a riparian setting representing moderate-sized drainage basins of upland grasslands do

Table 79. Lizard Site Average Monthly Rainfall (Based on Oklahoma Mesonet Data, Copan Location)

Year/Month	Jan	Feb	Mar	Apr	May	Jun	Jul	Aug	Sep	Oct	Nov	Dec	Total
2009	0.12	2.42	4.29	5.20	6.08	2.22	4.66	4.93	3.20	6.36	-	-	
2008	0.68	2.40	3.54	4.58	7.12	11.78	5.44	4.39	4.51	3.91	2.13	1.70	52.18
2007	1.89	0.96	7.90	3.03	8.05	18.45	1.18	1.60	2.63	4.45	0.43	2.25	52.82
2006	1.22	0.00	2.08	6.82	3.11	2.15	2.76	2.81	0.79	0.89	1.37	3.31	27.31
2005	3.84	1.89	1.78	2.19	5.00	7.55	2.81	3.29	1.74	2.75	0.32	0.55	33.71
2004	2.49	1.60	6.93	3.68	1.72	5.59	4.59	1.86	0.44	6.45	3.38	1.37	40.10
2003	0.12	1.58	3.83	2.81	7.60	5.09	0.93	7.43	2.48	3.43	2.36	2.96	40.62
2002	2.74	0.57	0.64	3.27	7.82	4.92	4.07	3.05	5.19	1.94	0.24	1.75	36.20
2001	2.34	3.41	1.60	1.60	3.00	2.19	0.91	0.99	1.70	3.02	0.41	1.41	22.58
2000	0.57	1.39	5.17	3.95	5.75	7.22	2.25	0.11	0.47	4.81	1.48	0.44	33.61
1999	2.14	1.58	3.61	5.73	10.05	6.82	2.12	1.45	3.46	0.00	0.47	3.91	41.34
1998	2.57	0.29	5.75	0.36	3.58	2.27	4.70	1.08	3.76	4.95	3.86	1.86	35.03
1997	0.45	4.73	1.48	3.01	7.00	5.39	2.22	4.31	4.01	3.87	1.11	4.02	41.60
1996	0.90	0.10	1.45	3.95	1.67	3.64	1.05	3.34	NA	NA	2.99	0.17	
1995	0.65	0.53	1.34	6.11	7.16	7.85	4.05	2.39	1.41	0.30	0.10	1.97	33.86
1994	NA	NA	1.89	9.73	3.68	0.92	5.07	2.42	1.99	3.46	5.27	1.20	
Avg. Monthly (inches)	1.51	1.56	3.33	4.13	5.52	5.88	3.05	2.84	2.52	3.37	1.73	1.92	37.77
Avg. Monthly (cm)	3.90	4.02	8.59	10.66	14.24	15.17	7.87	7.33	6.50	8.69	4.46	4.95	97.45
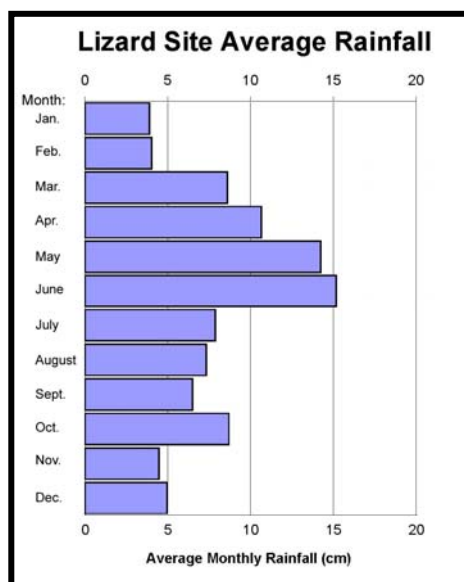
Figure 112. Average Monthly Rainfall at the Lizard Site (Oklahoma Mesonet Data 1994-2009).

not appear to provide an accurate site phytolith signature to use for temperature

correlation calculation based on upland prairie phytolith samples.

The Carnegie Canyon Site is another alluvial site in a modern riparian setting.

However, at this site, the skewing of the calculated temperature is not as severe as at the

Lizard Site. At the Carnegie Canyon Site, the channel is only eight meters wide

immediately above the site profile location which is only about one-third of the way

down the short 2.7 kilometer long stream (Lintz and Hall 1983:4). An even more

significant measurement is that the land area above the Carnegie Canyon Site draining

into the stream is slightly less than one square kilometer. Thus, although this site is in

another riparian/non-upland prairie setting, the Carnegie Canyon Site is dissimilar from

the Lizard Site in that there is less total land area in the drainage and less total runoff

occurs in the stream. However, the narrower channel may indicate that higher flow

velocities do occur at Carnegie Canyon during and following rainfall events. Thus, again interpretation of the phytolith results in an alluvial/riparian setting for temperature correlation purposes remains to be elucidated.   The Carnegie Canyon Site is actually more similar to the Bull Creek Site than the Lizard Site.

In examining the Fredlund temperature calculations based on phytolith content at Carnegie Canyon (Table 80), there is some variation in the temperatures obtained around zero difference (in contrast to the uniformly high temperature values obtained at the Lizard Site relative to the modern temperature (Table 78)). The modern day Carnegie Canyon temperature calculation is several degrees low which is potentially explained by the observation that the sampled site phytolith assemblage is not from an established A horizon in a prairie setting (i.e., not equivalent to the upland prairie controls).   Given the observations made on the previous Lizard Site temperatures, temperature calculations in a riparian setting encompassing alluvial conditions should certainly be viewed as suspect.

The buried Ab3 horizon soil actually extends from sample S-19 to S-27 (the 1,010 BP date was obtained from sample S-20). This particular A horizon has a complex formation history, including periods of cumulization and melanization, and the welding of multiple buried A horizons into a single thick buried soil (Carter et al. 2009).

In addition to the reported elevated TOC (Total Organic Carbon) values and relatively low sand values associated with Ab3 (Carter et al. 2009), this current research also showed an elevated phytolith concentration and an elevation in the diatom content in

Table 80
Carnegie Canyon Site Paleotemperature Calculations

Sample	Date (BP)	Calculated Relative T (°C)	Stipa (%)	Saddle (%)	C4 Lobates (%)	Crenate (%)
S-1	Modern	**-2.3**	9.0	28.3	25.5	0.9
S-3	NA	**-0.7**	7.2	26.1	27.6	3.9
S-20	1,010BP	**-3.1**	8.8	14.0	24.2	6.8

Table 81
Microfossils and Calculated Temperatures for the Carnegie Canyon Ab3 Horizons

Horizon (Carter et al. 2009)	Sample No.	Phytolith Conc. (wt %)	Diatom Conc. (% of Other Particles Counted)	Calculated Temperature (°C)
C8b2	18	0.08%	1.69%	**+0.56**
CAb2	19	0.41%	22.44%	**-1.71**
A1b3	20	1.15%	11.55%	**-3.15**
	21	0.92%	11.31%	**+0.67**
A2b3	22	0.76%	12.62%	**-1.73**
	23	0.68%	8.16%	**+4.30**
A3b3	24	0.65%	9.24%	**-6.83**
	25	0.55%	1.76%	**-5.79**
A4b3	26	0.53%	1.29%	**+0.70**
	27	0.41%	0.85%	**+2.12**
ABb3	28	0.15%	0.00%	**+1.72**

the Ab3 horizon (Figures 87 and 91). Interestingly, the diatom concentration plot shows

three spikes one small shoulder that generally correlate within the welded A horizons; the

A4b3 diatom concentration is lowest in the series (and this horizon also provided the

warmest temperature value indicated in A4b). The phytolith concentration spiked in S-20

suggesting this upper zone of Ab3 experienced the longest period of stability in this series

of welded soils. The A4b3 region from S-26 to S-27 was determined to have formed by

cumulization, whereas the other portions of Ab3 were formed by melanization (Carter et

al. 2009). The Ab3 data is summarized in Table 81 (for the sand concentration in these

Ab3 sub samples, see Carter et al. 2009). The one other significant environmental indicator associated with this buried A Horizon was the change observed in the sand color in this interval relative to other deposits in the same profile (Figures 92-93); this color change is felt to be an indicator of anaerobic (i.e., wet) conditions in the A horizon resulting in bacterial conversion of Fe^{3+} to Fe^{2+}. The seasonality plot discussed earlier (Figure 88) suggests that S-20 was the coolest, wettest interval in the Carnegie Canyon soil sample series.

The use of the Fredlund/Tieszen correlation formula for determining paleo temperatures in riparian/alluvial settings appears to not always be appropriate. It does not appear to be relevant for modern A horizons formed in a moderate sized drainage basin such as the Lizard Site location, although it performed somewhat better in a much a smaller drainage system (i.e., at the Carnegie Canyon Site). These results indicate that a different correlation formula needs to be developed and tailored for non-upland/riparian settings due to alluvial inputs, possible losses to erosion, contamination and dilution of the phytolith signature by numerous non-Poaceae species that do not occur on upland prairies, and the lack of dominant prairie grass species in a lowland setting.   With the exception of Manning Tallgrass Prairie, the Fredlund formula held up well for the three modern A horizons at the other upland prairie sites (Dempsey Divide Mixedgrass Prairie and at the Bull Creek Site (Shortgrass Prairie)). Although the buried Bull Creek Site consists of alluvial deposits and is on the modern Bull Creek drainage, it is being incised and eroded by the drainage system in modern day and thus the modern surface is actually an upland prairie setting.

Discussion of Soil Phytolith Distribution, Pedogenesis, and Paleoclimate

Soil Phytolith Distribution and Pedogenesis – The soil samples from modern prairies and buried A horizons provide important information about phytolith distribution in soil and about soil pedogenesis. The most detailed modern control prairie sample data was obtained from Manning Tallgrass Prairie. The three Manning experiments involved collection and analysis of replicate samples (pages 143-183). Using the fixed 5 cm deep soil probe increment, the surface soil samples had a fairly consistent texture and phytolith concentration (Tables 12, 19-21). The vertical phytolith distribution showed an exponential decrease in concentration with depth (Figure 66, Table 12) suggesting a long-term stable environment and period of melanization at this virgin Tallgrass Prairie site developed on a Mollisol.

In addition to soil samples and phytolith concentrations, the Manning samples provide an excellent example of the wide variability in individual phytolith morphologic form content (Tables 22-25). As expected, and as predicted by others (c.f., Strömberg 2009), the phytolith forms present at a relatively low concentration have very high standard deviations whereas the higher concentration phytolith forms have lower deviations (Tables 26-30). This is the type of individual data—for twelve distinctive phytolith morphotypes—on which the temperature calibration formula developed by Fredlund and Tieszen (1997a) was based; the original formula was arrived at by picking the individual morphotype combinations from their dataset that provided the best statistical result. Although this current researcher is historically a splitter rather than a

lumper[42], the morphologic phytolith data from Manning Tallgrass Prairie is improved

when it is grouped into three climatic categories (Tables 33-35) as the overall percent

standard deviations for these three grouped categories (Table 35) are significantly better

than those of the twelve individual phytolith morphotypes (Tables 29-30). Thus—except

for performing the actual temperature calculations based on the published Fredlund/-

Tieszen formula (pages 292-305)—these three combined climatic or seasonality

groupings are used in the discussions in the remainder of this dissertation.

The original eureka event that led to evaluating lumping the various phytolith

forms together for climatic interpretation was prompted by the fortuitous selection a

single non-native reference botanical species (Kentucky Bluegrass) in order to obtain

representative images of pyramidal phytoliths which had not been observed in the other

Poaceae reference specimens selected at that time.   The visible morphologic gradation

observed from keeled to pyramidal phytolith in close proximity suggested that the

recognized individual morphotypes may actually be gradations or variations of a general

form rather than discrete morphotypes (see Figures 47 A and D; also note the conical

forms present in Figure 47B); this observation led to investigation and subsequent

adoption of the three broader climatic groupings of phytoliths for seasonality evaluations.

The tremendous phytolith form variability between adjacent samples (Tables 22-

25) helps to explain why the adjacent sampling sites of Fredlund and Tieszen (1994,

1997a) had such extensive variation in phytolith signatures. The fact that the Manning

---

[42] For examples of this researcher's tendency toward splitting, see the glass trade bead descriptions
(Sudbury 1976) and white clay trade pipe descriptions (Sudbury 2009b).

Prairie has at least 105 plant species present based botanical surveys conducted during this project (Table 9)[43] is indicative of the extensive species diversity present at this 13.4 hectare (33 acre) site, and demonstrates why there can be such tremendous variability in individual seasonality markers (i.e., keeled, conical, etc.) in adjacent samples—even on a level consistent virgin prairie surface. Based on this Manning Tallgrass Prairie phytolith control data, the three proposed seasonality groupings[44] are considered to be more reproducible than the individual phytolith morphologic types. Likewise, the benefits of composite samples to average out the variations in phytolith morphotype content are also shown to be beneficial for the climate groupings, although not as much so as for the specific individual forms (particularly those present in relatively low concentrations).

The phytolith profile at Dempsey Divide was linear rather than exponential (Figure 75).   The current soil pH values (Table 39), the deteriorated bulliform phytoliths through the upper portion of the profile (Figure 70), and the dearth of phytoliths in the soil below 25 cm (Table 38) all suggest that phytolith preservation is poor in the young soil at this particular Dempsey Divide Mixedgrass Prairie locale. Thus, the linear phytolith concentration plot obtained may actually be more akin to a dissolution plot rather than an actual unaltered soil phytolith concentration curve. Overall similar biogenic silica preservation issues were noted previously during the analysis of the Sewright Site samples (Sudbury 2007:12-18, Figure 23). Phytolith preservation issues

---

[43] The other botanical survey during this project, conducted at Dempsey Divide Mixedgrass Prairie, yielded 15 different species collected from within the 20 m sampling circle during a single visit (Table 37). The Manning Tallgrass Prairie sample was collected during different seasons over several years from the entire 13.4 hectare (33 acre) property. Species identifications from both prairies were performed by Mary Gard.

[44] These three groupings, are as originally proposed by others early in Poaceae phytolith studies (see page 39), are Pooids (cool moist climate), Panicoids (warm moist climate) and Chloridoids (hot dry climate).

have been previously been reported to occur in basic pH soils and also to be affected by the presence of iron and aluminum in the soil, as well as other factors (Piperno 2006:108)[45].

At the Bull Creek Site, primarily A horizons were analyzed from the profile; thus, the phytolith concentration profile for the entire stratigraphic column under this modern Shortgrass Prairie was not obtained[46]. One interesting feature at the Bull Creek Site is how rapidly some A horizons developed in the early Holocene (see the radiocarbon dates in Figure 80) indicating repeated intermittent periods of climatic stability during what has been identified as periods of colluvial deposition (Bement et al. 2007).

The other two buried soil sites studied are both in alluvial settings situated in different size drainage systems. Of the two sites, the Carnegie Canyon Site (pages 225-251) provided the most pedogenic information. The phytolith concentration in all three Carnegie Canyon Site buried A horizons showed an exponential phytolith concentration curve indicating that melanization had occurred (Table 61; Figure 87; Carter et al. 2009); this finding is in direct opposition to Hall's previous assertion that the all of the buried soils in Carnegie Canyon were "cumulic A-Horizons" (Hall 1983:36-38).

---

[45] The charcoal concentration was also noted to increase in the lowest Mixedgrass Prairie sample analyzed, 20-25 cm (Table 44). Processing the lower four Dempsey Divide Mixedgrass samples (25-45 cm) was suspended when no phytoliths were recovered from the silt fraction, so the charcoal content in the 25-45 cm interval is unknown. The possible affinity of charcoal to alter metal ion concentration in the soil water solution has been previously mentioned as a possible mechanism to potentially affect phytolith preservation issues (Sudbury 2007:18). However, the hypothesis that charcoal may affect phytolith preservation under some soil conditions remains untested.

[46] Of the 52 Bull Creek soil samples, eleven were analyzed including nine A horizons (Figure 80).

The thick Carnegie Canyon Ab3 soil is particularly noteworthy for several reasons. First, the phytolith concentration curve is much stronger than the corresponding TOC (Total Organic Carbon) curve (Carter et al. 2009)[47]. Second, the soil profile properties indicate that the Ab3 soil is actually four A horizons that have been welded together (Carter et al. 2009). The diatom concentration in these same soil samples (i.e., the Ab3 soils, Figure 91) mirrors the soil phytolith concentration (Figure 87); both the diatom and the phytolith concentration spikes correlate with the position of the upper surfaces of the four recognized welded buried A horizons (Carter et al. 2009). Thus, the wet conditions in this particular drainage at the time of the development of this series of welded soils (ending at about 1010 B.P.) were suitable to support a high diatom concentration and stable landscapes—confirmation of which is preserved in the soil biogenic silica record—both diatoms and phytoliths. Third, soil wetness, previously documented by the presence of preserved buried tree stumps and mollusks (Lintz and Hall 1983; Hall and Lintz 1984), is also supported by the properties observed in the welded buried A horizon record. In this case, the soil was wet enough beginning with soil sample 19 that the reddish sand lost its coloration and became near-white (Figures 92-93); this visual difference is interpreted as being due to wet soil conditions which caused anaerobic bacteria to chemically reduce the iron deposited on the sand grains resulting in a lower chroma. The close-up image of the sand grains does document their overall change from red-tinted to near white supporting the theory that the iron oxidation state was changed rather than the actual sand composition. Thus, sand grain coloration,

---

[47] Holliday reports that the organic material in a buried A horizon can disappear in less than one-thousand years (1988); thus, this profile intensity difference has a logical explanation (i.e., stable inorganic phytoliths vs. gradually degrading TOC).

phytolith concentration, and the concentration of other biogenic silica (i.e., in this case diatoms), all contribute to a better understanding of past environmental conditions and pedogenesis at the Carnegie Canyon Site. This same biogenic silica data for sample 19 suggests that 19 may actually be the top portion of the buried A horizon rather than sample 20 as determined by standard soil particle analysis.

For the buried soils present at the Lizard site, phytoliths again served as a good proxy for the TOC in the younger buried soil; where the deeper buried soil Ab2 TOC values suggested cumulic formation, the phytolith data again suggested that the soil formed by melanization (Table 62, Figure 97; Carter et al. 2009).

Paleoclimate Information from Phytolith and Soil Data – The previous section discussed the pedogenic information revealed by biogenic silica during this research project. Several major limitations of phytolith analysis are the dual issues of redundancy and multiplicity. Redundancy refers to the fact that the same phytolith shape is present in numerous different plant species, whereas multiplicity refers to the fact that each plant often contains a large variety of different phytolith forms (Rovner 1971). Thus, selecting morphologically significant phytolith forms for analysis is at times less that straightforward. Over the decades, Poaceae short cell phytoliths have consistently been recognized as very useful forms upon which to base paleoclimatic interpretations. These phytolith morphotypes tend to be most frequently affiliated with certain grasses based primarily on their metabolic differences and thus the optimal environmental conditions

under which they thrive. These metabolic/climatic differences are recorded as the

phytolith signature left behind in any given soil.

The assortment of the twelve short cell forms of interest for the three control

prairie soils are summarized in Table 48 and in Figure 76. As evident in Figure 76, the

distinctive short cell phytolith form for the Manning Tallgrass Prairie is the Lobate

Panicoid, and the major differentiator between the Dempsey Divide Mixedgrass Prairie

and the Bull Creek Shortgrass Prairie are the tall and squat saddles, respectively.

Although other differences are present within the soil phytolith data, those are clearly the

three most significant differences, and include one stand-out form from each of the three

prairie types studied.[48]

The biogenic silica morphologic form counts for the various buried soil samples

were performed, and their climatic signatures plotted as both bar and linear graphs for the

Manning Tallgrass (Figures 64 and 67) and Dempsey Divide Shortgrass Prairies (Figures

71 and 73). The same seasonality groupings plots were prepared for the Bull Creek Site

(Figures 80 and 84 [the Bull Creek soil phytolith samples represent only part of the

stratigraphic column]), Carnegie Canyon Site (Figures 83 and 88), and the Lizard Site

(Figures 98 and 106). Discussion regarding the climatic information contained in these

various figures is in the pertinent sections of Chapter 4.

---

[48] It is interesting to note that the saddle phytolith plots of total normalized saddle phytolith concentration
versus tall:short saddle phytolith ratio for the Mixedgrass and Tallgrass Prairie samples tend to be linear
with only moderate slopes (Figure 77 [complete profile of the Shortgrass Prairie not available]). The
significance of this observation remains unknown.

The climatic summaries of the three modern prairie soils are plotted in Figure 78 (data in Table 49). The Manning Tallgrass Prairie has a fairly constant concentration of the three different phytolith seasonality groupings, whereas the Bull Creek Shortgrass and Dempsey Divide Mixedgrass Prairies have higher chloridoid components, very similar panicoid concentrations, and the Shortgrass Prairie has low pooid and panicoid components whereas the Mixedgrass Prairie has an intermediate Pooid content between the Tallgrass and Shortgrass Prairie pooid concentrations (Figure 78). Although the Shortgrass and Mixedgrass Prairies are discernable in both the pooid and chloridoid components, the chloridoid values are further isolated from the panicoid fraction and thus potentially easier to study and interpret. Thus, the chloridoid fraction (i.e., saddle phytoliths) were scrutinized more closely in this study.

The saddle phytolith data for the three sites, reported as saddle ratio (tall:squat) vs. normalized chloridoid (saddle) concentration (as percent of total short cells counted in the same microscopic fields of view), was plotted for the three surface control prairie A horizon soil samples (Figure 78 and 82). This modern prairie information was included as the base plot reference/control for the same type of saddle data for all of the samples from each buried soil site (Carnegie Canyon Site (Figures 89-90); Lizard Site (Figure 104); and Bull Creek Site (Figure 82)). Representative examples of the tall and short saddles are shown in Figures 107-108. All surface control prairie samples and buried soil samples analyzed were also included in one single plot (Figure 109). The large squares are the three prairie control surface sample values (color coded red, blue, and green, which correlates with the data colors in the tables in Chapter 4). The figure legend

identifies which geometric shape represents an A horizon, the lower portion of an A

horizon, and a non A-horizon. This plot was discussed in some detail previously (pages

282-292). As a brief summary, several data highlights are:

- The two different Manning Tallgrass Prairie surface composite sample values

  from the two different sample template areas gave a larger x-axis variation than y-

  axis variation in this particular data scatter (large green squares). This is

  interpreted to mean that the species composition varied quite a bit between the

  two adjacent sampling locations although the actual total saddle concentration at

  the site was fairly stable [49].

- Three Bull Creek buried A horizons (25, 28, and 47) cluster very tightly,

  suggesting similar vegetation and climate at those three times. The two earlier

  samples in this cluster (25 and 28) are the two samples with inverted radiocarbon

  dates that occurred during the Younger Dryas[50].

- Bull Creek sample 22 shows appreciable x-axis (i.e., species) deviation from the

  two immediately following A horizons, but was actually somewhat colder and/or

  moister. Three later Bull Creek samples 37, 31 and 45 showed much larger x-axis

  deviations, with 45 being the largest deviation noted of all buried A horizon

  samples analyzed during this study (i.e., species variation); all three of these later

---

[49] While performing the spring botanical inventories, it was observed that different species tended to be clustered in various portions of the prairie setting, giving living visual evidence of the non-uniform distribution of species across the site.

[50] These two sample dates were potentially impacted by the proposed early Holocene asteroid event (Firestone et al. 2007; Kennett et al. 2009).

stable soil environments appear to have been warmer/drier than the earlier Bull Creek Samples (i.e., more y-axis excursion).

- No buried soil site sample has a chloridoid content close the very hot dry modern Bull Creek surface Shortgrass Prairie soil sample (BC-52, top red square). The modern Dempsey Divide Mixedgrass Prairie profile samples also demonstrated a high chloridoid concentration (top blue square) but showed considerable species variation from the Shortgrass Prairie (i.e., x-axis deviation).

- Both riparian setting sample series (Carnegie Canyon and Lizard Sites) were dissimilar from the control prairie samples, and somewhat similar to each other, with the Carnegie Canyon samples clustering fairly tightly and the Lizard Site tending to be slightly cooler/drier and showing more species variation. The Lizard Site A horizon saddle samples showed more intra-x-axis range, whereas the Carnegie Canyon Site A horizons showed more saddle sample deviation along the y-axis. This may be a reflection of drainage parameters and/or other local environmental conditions within these riparian settings.

Although this saddle data is difficult to interpret with such a small series of control samples, the juxtaposition of A horizons from several sites (notably Bull Creek 25, 28, and 47; and Carnegie Canyon 1 [AC horizon], 3, and 19) suggest that the surface horizons within each of these two individual clusters had similar botanical signatures. Conversely, the signature of the Lizard Site A horizons were not as similar suggesting more species variation over time at the Lizard Site, while the other Bull Creek A horizons exhibit an even greater species variation.

The potential occurrence of broken panicoids being imposters that superficially appear to be saddles (Figures 57-59) was given additional attention due to the significance placed on saddle-shaped phytoliths in interpreting this buried soil data. Likewise, the concern over retaining smaller saddles, if present, supported the laboratory concerns regarding silt definitions, settling times, and potential particle and solution density issues[51]; all of these method improvements were developed with the intent of resolving specific potential problems encountered in the procedures employed during the course of this research. Based on the three prairie control samples investigated, saddle phytolith morphology appears to be a sensitive indicator and a potentially significant tool for evaluating landscape stability and plant species changes—thus, additional study appears to be merited[52]. Considerable deviation and variety was also observed in the crenate forms (see reference images in Figures 42-47) and in bulliform phytolith morphology, but time constraints did not permit pursuit of these observations.

At the Manning Tallgrass Prairie, a significant spike in spheroid phytoliths, spicules, and charcoal occurred in the 35-40 cm sample (Table 14; Figure 65) which correlates with a cooler wetter interval via the Poaceae phytolith signature (Figures 64 and 67) that extended to the 40-45 cm level [both samples from non-A horizons]. The only other significant climatic deviation noted at Manning was that the time interval

---

[51] I.e., to make certain to retain any lower density and/or smaller phytoliths and also to keep the effective flotation solvent density of 2.35 g/cm^3 which prompted the decision to float phytoliths from dry silt samples rather than risk having a potential negative effect on the flotation recovery.

[52] Previously, Brown provided measurements for saddles from 24 species, and looked at saddle size from 43 *Bouteloua gracilis* specimens over two years to correlate size with June/July rainfall (1984:364-365). Lu and Liu (2003b) reported relative saddle type morphologies for a number of reference specimens from the southeastern USA, and developed associations between other phytolith morphotypes and coastal plant communities.

316

represented by the 5-10 cm interval appears to have been warmer (Figures 64 and 67).

Concurrently, the per cent of burned panicoid phytoliths was also higher during these

same intervals (5-10, and 35-45 cm) (Table 18). The noted increase in spiny spheroids

(35-40 cm) is often associated with trees and woody species (Lejju 2009). As Manning

Prairie is in an upland setting, this spheroid spike may indicate a major vegetation change

at the time of the cooler weather (35-40 cm). Whether this climate change and particle

increase (i.e., charcoal) is associated with a past glacial episodes and/or known fire events

remains uncertain. A spike in the charcoal concentration was also observed in the lowest

Dempsey Divide soil sample processed (Table 44, Figure 72) again suggesting a

significant fire history—possibly indicating regional fires. The radiocarbon dates of

these particular control prairie soil samples have not been determined, so further

interpretation is not currently possible. Due to the riparian conditions which support non-

Poaceae growth, the spiny spheroid content fluctuations at the Carnegie Canyon and

Lizard Sites cannot confidently be climatically interpreted[53]. Additional known

vegetative control samples containing spiny spheroids from these various settings are

needed.

When applying the temperature correlation formula to this site phytolith data, the

modern prairie temperature calculation based on the modern Bull Creek Site surface A

horizon phytolith signature is very accurate (Table 75) and the temperature calculations

for the Bull Creek Site buried soils (Table 77) seems to correlate reasonably well with the

values from other sites reported by Fredlund and Tieszen (1997b).   The calculated

---

[53] The absolute charcoal concentration at the Lizard site clearly peaked during the development of the Ab2
horizon which had a terminal radiocarbon date of 3120 BP (Tables 62-65). This soil evidence indicates
extensive fire activity.

modern temperature value for the Dempsey Divide Mixedgrass Prairie was also dead on

(Table 75), although the value for Manning Tallgrass Prairie was significantly off and

will be investigated further in the future.   Of the temperature values for the two riparian

buried soils, the calculated values for the Lizard Site were way off (Table 78) and the

Carnegie Canyon values are suspicious (Table 80). These later two calculated

temperatures are felt to be erroneous primarily due to the fact that the prairie controls

used to develop the original formula (Fredlund and Tieszen 1997a) are apparently not

applicable in riparian settings because the phytolith signature of those soils reflect

considerable contamination from the watershed and/or species growing in the moister

setting, and thus are not totally representative of an upland prairie setting reference

materials used to establish the temperature formula.

The proposed Bond Cycles that have been correlated with climatic change are

based on multiple evidence lines of Holocene ice rafting episodes in the North Atlantic

(Bond et al. 1997; Bond et al. 1999; Bond et al. 2001). One composite Bond plot is

reproduced in Figure 113 with this current study's buried soil data superimposed on the

chart. The correlation is inexact, at least in part because the radiocarbon dates obtained

for the buried soils[54] are not directly translatable to the corresponding Bond data which

was presented in calendar years. The three data points from the most recent 2000 years

correlate with Bond peaks; however, presumably the farther back the dates are in time,

the greater the degree of divergence in the two dating systems. A good correlation

---

[54] The buried soils plotted over the Bond Cycle graph were previously noted in this dissertation: the
Lizard Site buried dates are in Table 78, the Carnegie Canyon Site dates are in Table 80, and the Bull Creek
dates are listed in Table 77. These radiocarbon dates were published by Bement et al. (2007) and Carter et
al. (2009).

between these two series of dates remains to be established. Prior comments suggest that a cosmic event may have distorted the radiocarbon dates around the time of the Younger Dryas (Firestone and Topping 2001).
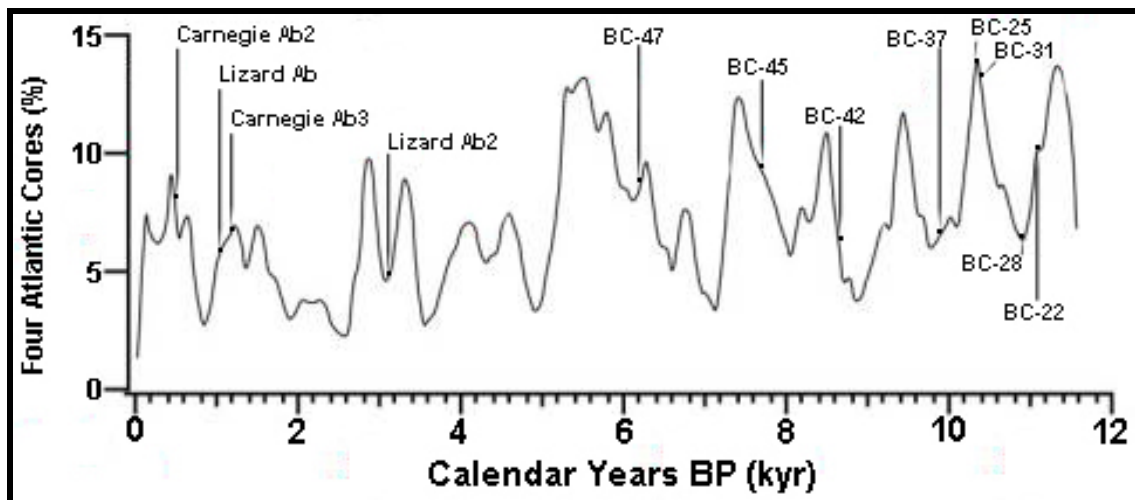
Figure 113. Buried Soil A horizon radiocarbon dates superimposed on Bond Cycle calendar year date ice rafting composite data regarding 1500 year Bond Cycles (Bond Cycle chart from Bond 2001:2130).

In addition to these various lines of investigation, the relative weight/weight concentration of coarse (20-50 μ) to medium (5-20 μ) size phytoliths was determined for the Lizard Site soil sequence (Table 70, Figure 99)[55]. Although variation in the ratio was noted, this data subset—which likely indicates the relative change in the bulliform phytolith concentration in the samples (and thus changes in moisture conditions and in species present)—was not pursued further on soil samples from the other research sites; this is because the improved laboratory protocol used on samples processed later resulted

---

[55] The Lizard Site samples were the first samples processed in this project using the initial laboratory methods presented in Appendix C. As later work progressed toward complete saddle recovery, the phytolith fraction was left intact when processing samples from subsequent sites.

in keeping the phytolith assemblage intact rather than subdividing the phytoliths into medium and coarse silt fractions.

The Lizard and Carnegie Canyon Sites are both in alluvial settings, with buried soils that formed on a stable landscape being buried by water-borne sand deposits. The three most recent radiocarbon dates (500, 1010, and 1200 BP) which are the terminal dates for three buried soils tend to correlate with the data reported by Ely (1997; dates in radiocarbon years). Ely, studying sites in Arizona and Utah, reported peak flooding intervals during 900-1100 BP and subsequent to 500 BP (Ely 1997). Ferring reports stable buried soils in Oklahoma [including the Caddo and Copan soils included in this current study] near the time of each of these intense flooding intervals, as well as noting similar sites from Texas (1990). Interestingly, Ely reports a relatively calm interval between 5000 and 3600 BP (1997), which in the Figure 113 data is closely followed by the 3200 Lizard Ab2 soil (and preceded by Bull Creek-47 (6,200 BP)).

Investigation of buried soils in the Kansas sand prairie yielded dates of stability of 500 and 1000 years, in addition to others (Arbogast 1996). Also noted was that "valley filling between 5000 and 1000 yr B.P. was interrupted by soil formation about 1800, 1500, and 1200 yr BP" (Arbogast and Johnson 1993). In reviewing other reported instances of area floodplain stability, significant dates of stability noted are 10,500, 8900, 5700, 5000, 4200, 2600, 2000, and 1200 years BP (Arbogast and Johnson 1993). Several of these dates are near the dates reported in this current report (Figure 113) suggesting similar environmental trends over much of the Great Plains during the Holocene.

The Bull Creek data from the Oklahoma panhandle shows gradual warming in the early Holocene with numerous periods of landscape stability. The first buried soil (BC-22) contains nanodiamond evidence that is thought to mark the start of the much colder Younger Dryas (Kennett et al. 2009); the second and third buried soils (BC-25 and BC-28) share a common vegetative and climatic signature although they have inverted radiocarbon dates which are possibly due to the after effects of the earlier North American cosmic event that correlated with BC-22 (which in turn was responsible for the nanodiamond deposit). While the climatic signature of BC-31 indicates a warming trend at the end of the Younger Dryas (Figure 80), the saddle data shows a major change in plant composition (Figure 82). Although there was slight moderation in BC-37 species composition, the climate appears to have been stable and samples 31 and 37 have a very similar phytolith signature. The next three buried soils (BC-42, 45, and 47) show a significant gradual cooling trend and increase in moisture (Figure 80) which was accompanied by major swings in vegetation (Figure 82) which ended with BC-47 which has a signature remarkably similar to that observed during the Younger Dryas interval (Figures 80, 82). The modern climate at the Bull Creek site, represented by the BC-52 phytolith signature of the Bull Creek Shortgrass Prairie, is hotter and drier than anything observed previously (Figures 80, 82)[56].

---

[56] The modern Bull Creek Shortgrass Prairie saddle concentration is also higher than in any of the prairie phytolith signatures reported by Fredlund and Tieszen (1994, 1997a) or any other samples processed during this current project. One possible reason may be that the laboratory methodology changes in this current research may have improved recovery of smaller saddle phytoliths. The analyst was careful to exclude broken *Aristida* lobate phytoliths (see Figures 57-59) from the count so that potential error is not felt to have affected the current saddle counts reported in this dissertation.

The other two buried soil sites help to fill in the gaps in the last half of the

Holocene that are not represented in the soil record preserved at the Bull Creek Site

(which is located in the Oklahoma Panhandle (Figure 79)). Both the Carnegie Canyon

Site (south central Oklahoma) and the Lizard Site (northeastern Oklahoma) show

intervals of extensive alluvial fill interspersed with periods of climatic stability marked

by development of A horizons that later became buried soils.

As noted previously, the buried soil dates from 3,200 through 500 BP at the

Carnegie Canyon and Lizard Sites, and those at the Bull Creek Site (11,010-6,200 BP),

frequently correlate with the dates of other buried soils reported from the Plains and

indicate that the climatic events and periods of stability were happening on a regional

scale. The common environmental factors causing these broad changes include the end

of the Wisconsin glacial, the melting and withdrawl of the Laurentide ice sheet, the

apparent cosmic event at the start of the Younger Dryas, the gradual climatic change to a

hotter drier climate by the mid-Holocene which was accompanied by major vegetative

shifts, a cooling trend, and then extensive flooding episodes in the last third of the

Holocene—again brought on by changing climate.

Summary – It is evident that phytolith analysis and research is a relevant,

multidisciplinary, viable, rapidly growing discipline which can address a variety of

research issues including paleoclimate, environmental change, and pedogenesis.

Although ubiquitous across the landscape, buried soils are most frequently observed when exposed by environmental conditions such as water erosion. The three sites with buried soils selected to study in this project were exposed in stream cut banks. Additionally, radiocarbon dates have been determined for the buried soils at these sites. In order to utilize established prairie short cell phytolith research protocols to evaluate these sites for their climatic phytolith signature, pristine prairie locations were sought as grassland controls. The areas selected for sampling and analysis are representative Tallgrass, Mixedgrass, and Shortgrass Prairies. Intentionally, the locations selected were not included in previous published studies (Fredlund and Tieszen 1994, 1997a) in order to add additional study site data to the prairie control points for the Great Plains. Both the control prairie and buried soil sites cover a wide swatch of Oklahoma from the hot dry panhandle, to south central Oklahoma, and to the moister northeast portion of the state.

Approaching phytolith analysis from the viewpoint of soil science and chemistry, significant climatic and soil pedogenic observations were made. Obtaining a good uniform representative sample is critical to success of the investigation. Making significant improvements in established laboratory methodology, a quantitative phytolith recovery protocol was developed, and several common protocol errors embedded in the literature were noted and alternate procedures developed and recommended.

Quantitative phytolith recovery from stratigraphic soil columns enabled determination that soil phytolith concentration mirrored total organic carbon (TOC) and

323

thus can serve as a TOC proxy. In instances where the soil carbon signature had faded, the phytolith content continued to indicate the occurrence of soil melanization in place of what in the past has frequently been assumed to be cumulic formation. Due to their plant origin, phytolith concentration mirrors soil A-horizon development (i.e., cumulic vs. melanization), so phytolith concentration confirms the existence of and the mechanism of A horizon formation. Diatoms and phytoliths also help confirm moisture conditions, and the presence of soil welding; in one case, changes in sand color also helped address the issue of past moisture conditions present at the site. In the future, in order to study buried soils in riparian site settings, control samples from similar settings are needed rather than using upland control prairie soil phytolith samples.

A tremendous variability in phytolith morphologic distribution was documented across a virgin Tallgrass Prairie site location (21 individual soil probe samples collected in a 314 m^2 area). Grouping various phytolith morphologic forms into their broad environmental/climatic categories based on three groupings rather than twelve individual phytolith morphotypes improved the reproducibility of the results as far as paleoclimatic interpretation. Saddle-shaped phytoliths have been long reported, occasionally studied, and are recognized as being indicative of hotter drier climate. During the course of this study, evidence indicated that dimensionally different saddles (i.e., the ratio of tall:squat forms) may turn out to be a useful interpretive tool for variations in the composition of vegetative cover while the total saddle concentration continues to mirror temperature and moisture conditions (i.e., hot and dry vs. cool and moist).

When looking at the saddle signatures of various soil samples, tight data clusters are tentatively interpreted to indicate similar vegetation in the buried soils represented in the cluster whereas differences in either the total normalized saddle concentration (i.e., different relative hot/dryness) or in the tall:squat saddle ratio (which is postulated to represent a change in vegetative composition) indicate different climatic and/or vegetative conditions. Thus, saddle phytolith characterization potentially represents a significant undeveloped opportunity to help improve the understanding of paleoenvironmental conditions and to offer an additional level of discernment. Saddles are sometimes one of the smaller diagnostic phytoliths, making the issue of optimal phytolith recovery in the laboratory an important objective. Likewise, other particle types (including diatoms, sponge spicules, and charcoal) also contribute to our understanding of past environmental conditions and climate change.

During the Holocene the Great Plains were in a period of climatic fluctuation. The Phytolith data from the Bull Creek site, with buried A horizons spanning the range from 6,200-11,070 BP shows the general warming trend that occurred on the Great Plains following the retreat from the Wisconsin Glacial period. The Younger Dryas cooling interval, the start of which appears to be clearly visible at the Bull Creek Site profile as marked by the nanodiamond deposit (Kennett et al. 2009), is not recorded in the recovered soil phytolith signature from the buried A horizons. The colluvial interval at Bull Creek shows good general agreement regarding stability of the land surface when compared with intervals of stability reported in Kansas, although the correlation breaks down in the eolian period (Johnson and Martin 1997). At the end of the altithermal, the

final buried A horizon that was dated shows a distinct cooling interval (based on seasonality groupings)—which is the opposite result of what is indicated by Fredlund's calibration formula. The compressed or missing millennia above BC-47 are known to have been a time of heavy erosional activity on the plains. Sand dune studies in Nebraska indicate that dune formation there occurred during the 3,000-1,500 B.P interval, suggesting considerable environmental activity during part of this period (Ahlbrandt, Swinehart, Maroney 1983).

The 3,120 BP buried A horizon at the Lizard Site correlates with a time of stability flanked by extensive erosion on the plains. The estimated 1,200 BP buried A horizon at the Lizard Site (Figures 98 and 106) seems to represent a period with a wetter summer interval similar to that seen in the middle of the Ab2 (peaking in S-13.) There is warming trend seen in the slightly later ~500 BP soil (S-5) at Carnegie Canyon after which time pedogenesis ceased. The final Ab horizon—a very cool interval—at Carnegie Canyon was not dated, but it may correlate with what is often referred to as the Little Ice Age. Subsequent to formation of the Ab horizon, another true A horizon has not formed at the Carnegie Canyon Site.

CHAPTER V

CONCLUSIONS

The phytolith samples evaluated in this research were collected from three control prairie sites and from three buried soil sites. The modern reference prairies are good representative examples of Shortgrass, Mixedgrass, and Tallgrass Prairies. Botanical specimens were collected and identified from two of the prairie locations. The three buried soil sites included fifteen buried A horizons (including four A horizons that had welded into one unit); many of the A horizons formed while exposed to alluvial environments.

In order to quantitatively recover phytoliths from these soil samples, a number of modifications and significant improvements were made to the laboratory methods published in the literature. Issues regarding definitions (silt particle size) and techniques (relevant density values, settling times, and dilution of heavy density flotation liquid with soil water) were clearly addressed and cost saving equipment ideas effectively demonstrated. The final laboratory method utilized a reversed order of particle separation by decanting rather than sieving, zinc bromide solution as the heavy density liquid for flotation, and longer particle settling times based on the lowest possible phytolith density. Vacuum filtration using ashless filter paper was determined to be the

most efficient silt recovery method for this project. The result of this procedure was to include all biogenic silica in one fraction and to recover a more complete fraction including the larger, smaller, and/or less dense particles that might ordinarily be lost using other isolation schemes.

After phytoliths were quantitatively recovered from the soil samples, the phytolith signature was ascertained of each of the A horizons and a number of the other soil horizons. Extensive study of the Manning Tallgrass Prairie phytolith samples demonstrated the variability the horizontal phytolith concentration (wt/wt % in soil), and permitted determination of the phytolith morphological composition or signature (normalized percent of twelve established short cell phytolith forms). The fortuitous observation of a Western Wheatgrass spodogram (Figure 43A) showed how variable some of the short cells were in a small area, with the distinctive forms rapidly grading into related distinctive forms. This gradation implied there are families of similar short cell types rather than distinct unrelated morphotypes, which led to summing the twelve forms into the three broad recognized climatic categories. The climatic interpretation was based on these three groupings rather than twelve individual groupings as had been proposed by others in the recent past. The problem of imposter phytolith forms was also recognized and addressed.

The reference botanical specimens showed considerable species variability in a number of phytolith forms which all hold considerable promise for future research (crenates, bulliforms, and saddles to name a few). Of these, the soil saddle phytolith

composition at the three reference prairie sites (Figures 76-78) demonstrated the most

promise for helping to discern differences in plant association composition as indicators

of variations in environmental conditions. In particular, a simple ratio based on the

predominant saddle morphology in a soil phytolith sample (i.e., the tall:short saddle ratio,

based on which particle axis was longest) vs. the total saddle concentration normalized

relative to the total short cell count, provided a great deal of information about changes in

plant composition at the sites over time (Figure 109).

The vertical soil phytolith concentration profile proved to be a good proxy for

total organic carbon (TOC). Variations in the phytolith concentration profile in a massive

buried A horizon mimicked the other soil evidence and helped to mark the location of the

welded buried A subunits. The normalized concentration of diatoms in the same profile

also mirrored the phytolith concentration changes and soil welding evidence. The color

change of the recovered sand fractions collected from the stratagraphic column also

corroborated the observation of redoximorphic features observed in the soil and

confirmed that at the time of the buried A horizon formation, the site had experienced

very wet conditions. Numerous other components observed in the recovered phytolith

fractions (burned phytoliths, sedge phytoliths, sponge spicules, and charcoal) provided

additional information about past environments and site conditions. A number of proxies

for soil wetness were observed in this study.

The phytolith signature data for two of the three modern control prairies gave

accurate temperature values (Table 75) based on the temperature correlation developed to

study paleoenvironments on the Great Plains corroborating the effectiveness of that earlier work for upland prairie settings. The older Bull Creek buried A horizon samples also yielded calculated temperature values that agree with similar age sites reported from across the plains. The data from the two later buried soil sites was not as clear cut, and is felt to reflect the difficulties and limitations of using an upland prairie-based temperature correlation in active riparian settings. The non-Poaceae dominated plant communities present in drainages and riparian settings are not necessarily appropriate for evaluation by the prairie derived temperature formula. The instances of erosional losses and valley filling episodes at these Oklahoma sites fit well with the regional picture of climatic conditions and changes across the Great Plains during the Holocene.

LITERATURE CITED

AAPG. 2005. North American Stratigraphic Code. *AAPG Bulletin* 89(11):1547-1591.

Ahlbrandt, T.S., J.B. Swinehart, and D.G. Maroney. 1983. The Dynamic Holocene Dune Fields of the Great Plains and Rocky Mountain Basins, U.S.A. *In Eolian Sediment and Processes*. Brookfield, M.E., and T.S. Ahlbrandt (Eds.). Elsevier, Amsterdam.

Akai, S. 1939. On the ash figures of leaves of the rice plants transplanted from the different kinds of nursery beds and their susceptibilities to the blast disease. *Annals of the Phytopathological Society of Japan* 9:223-235.

Albert, R.M., and M. Madella (Eds.). 2009. Perspectives on Phytolith Research: 6th International Meeting on Phytolith Research. *Quaternary International* 193. 191 p.

Aleinikoff, J.N., D.R. Muhs, E.A. Bettis, III, W.C. Johnson, C.M., Fanning, and R. Benton. 2008. Isotopic evidence for the diversity of late Quaternary loess in Nebraska: Glacial and non-glacial sources. *Geological Society of America Bulletin* 120:1362-1377.

Alexandre, A., and L. Brémond. 2009. Forum Comment Methodological concerns for analysis of phytolith assemblages: Does count size matter? (C.A.E. Strömberg). *Perspectives on Phytolith Research: 6th International Meeting on Phytolith Research. Quaternary International* 193:141-142.

Alexandre, A., J.-D. Meunier, F. Colin, and J.-M. Koud. 1997. Plant impact on the biogeochemical cycle of silicon and related weathering processes. *Geochimica et Cosmochimica Acta* 61:677-682.

Alexandre, A., J.-D. Meunier, A.-M. Lézine, A. Vincens, and D. Schwartz. 1997. Phytoliths: indicators of grassland dynamics during the late Holocene in intertropical Africa. *Palaeogeography, Palaeoclimatology, Palaeoecology* 136:213-229.

Alexandrovskiy, A.L., M.P. Glasko, N.A. Krenke, and A. Chichagova. 2004. Buried soils of floodplains and paleoenvironmental changes in the Holocene. *Revista Mexicana de Ciencias Geológicas* 21(1):9-17.

Anderson, P.C. 1980. A testimony of prehistoric tasks: diagnostic residues on stone tool working edges. *World Archaeology* 12(2):181-198.

Anderson, R.C. 1982. An Evolutional Model Summarizing the Roles of Fire, Climate, and Grazing Animals in the Origin and Maintenance of Grasslands: An End Paper, pp. 297-308. In Estes, J.R., R.J. Tyrl, and J.N. Brunken (Eds.) *Grasses and Grasslands Systematics and Ecology.* University of Oklahoma Press, Norman, Oklahoma.

Andrejko, M.J. 1982. Notes on procedures for extraction and analysis of plant phytoliths. *Phytolitharien Newsletter* 1:5.

Arbogast, A.F. 1996. Stratigraphic evidence for late-Holocene aeolian sand mobilization and soil formation in south-central Kansas, U.S.A. *Journal of Arid Environments* 34:403–414.

Arbogast, A.F., and W.C. Johnson. 1994. Climatic Implications of the Late Quaternary Alluvial Record of a Small Drainage Basin in the Central Great Plains. *Quaternary Research* 41:298-305.

Arbogast, A.F., and W.C. Johnson. 1998. Late-Quaternary Landscape Response to Environmental Changes in South-Central Kansas. *Annals of Association of American Geographers* 88(1):126-145.

Armitage, P.L. 1975. The Extraction and Identification of Opal Phytoliths from the Teeth of Ungulates. *Journal of Archaeological Science* 2:187-97.

Baker, G. 1961. Opal Phytoliths and Adventitious Mineral Particles in Wheat Dust. *Mineragraphic Investigations Technical Paper* 4:3-12.

Baker, R.G., G.G. Fredlund, R.D. Mandel, and E.A. Bettis III. 2000. Holocene environments of the central Great Plains: multi-proxy evidence from alluvial sequences, southeastern Nebraska. *Quaternary International* 67:75-88.

Ball, T.B., J.D. Brotherson, and J.S. Gardner. 1993. A typologic and morphometric study of variation in phytoliths from einkorn wheat (*Triticum monococcum*). *Can. J. Bot.* 71:1182-1192.

Ball, T.B., J.S. Gardner, and N. Anderson. 1999. Identifying inflorescence phytoliths from selected species of wheat *(Triticum monococcum, T. dicoccon. T. dicoccoides,* and *T. aestivum)* and barley *(Hordeum vulgare* and *H. spontaneum)* (Gramineae). *American Journal of Botany* 86:1615-1623.

Bartoli, E, and L.P. Wilding. 1980. Dissolution and surface properties of biogenic opal of forest origin. *Soil Sci. Soc. of Am. Jour.* 44:873-878.

Bazzaz, F.A., and J.A.D. Parrish. 1982. Organization of Grassland Communities, pp. 233-254. In Estes, J.R., R.J. Tyrl, and J.N. Brunken (Eds.) *Grasses and Grasslands Systematics and Ecology.* University of Oklahoma Press, Norman, Oklahoma.

Beavers, A.H., and I. Stephen. 1958. Some Features of the Distribution of Plant Opal in Illinois Soils. *Soil Science* 86:1-5.

Bement, L.C., and B.J. Carter. 2008. A Younger Dryas Signature on the Southern Plains. *Current Research in the Pleistocene* 25:193-194.

Bement, L.C., B.J. Carter, R.A. Varney, L.S. Cummings and J.B. Sudbury. 2007. Paleo-environmental reconstruction and bio-stratigraphy, Oklahoma Panhandle, USA. *Quaternary International* 169-170:39-50

Betts-Piper, A.M., B.A. Zeeb, and J.P. Smol. 2004. Distribution and autecology of chrysophyte cysts from high Arctic Svalbard lakes: preliminary evidence of recent environmental change. *Journal of Paleolimnology* 31(4):467-481.

Blackman, E. 1971. Opaline silica bodies in the range grasses of southern Alberta. *Canadian Journal of Botany* 49:769-781.

Blecker, S.W., C.M. Yonker, C.G. Olson, and E. F. Kelly. 1997. Paleopedologic and geomorphic evidence for Holocene climate variation, Shortgrass Steppe, Colorado, USA. *Geoderma* 76:113-130.

Blinnikov, M.S. 2005. Phytoliths in plants and soils of the interior Pacific Northwest, USA. *Review of Palaeobotany and Palynology* 135:71-98.

Blinnikov, M., A. Busacca, and C. Whitlock. 2001. A New 100,000-Year Phytolith Record from the Columbia Basin, Washington, USA*, pp. 27-55. In Meunier, J.-D., and E. Colin (Eds.) *Phytoliths: Applications in Earth Sciences and Human History.* AA Balkema Publishers, Lisse, Netherlands.

Blinnikov, M., A. Busacca, and C. Whitlock. 2002. Reconstruction of the Late Pleistocene Grassland of the Columbia Basin, Washington, USA, Based on Phytolith Records in Loess. *Palaeogeography, Palaeoclimatology, Palaeoecology* 177:77-101.

Boardman, R.S., A.H. Cheetham, and A.J. Rowell (Eds.) 1987. *Fossil Invertbrates*. Blackwell Scientific Publications, London. 713 p.

Bodén, P. 1991. Reproducibility in the random settling method for quantitative diatom analysis. *Micropaleontology* 37(3):313-319.

Bond, G., B. Kromer, J. Beer, R. Muscheler, M.N. Evans. W. Showers, S. Hoffmann, R. Lotti-Bond, I. Hajdas, and G. Bonani. 2001. Persistent Solar Influence on North Atlantic Climate during the Holocene. *Science* 294:2130-2136.

Bond, G., W. Showers, M. Cheseby, R. Lotti, P. Almasi, P. deMenocal, P. Priore, H. Cullen, I. Hajdas, and G. Bonani. 1997. A Pervasive Millennial-Scale Cycle in North Atlantic Holocene and Glacial Climates. *Science* 278(5341):1257-1266

Bond, G.C., W. Showers, M. Elliot, M. Evans, R. Lotti, I. Hajdas, G. Bonani, and S. Johnson. 1999. The North Atlantic's 1-2 kyr Climate Rhythm: Relation to Heinrich Events, Dansgaard/Oeschger Cycles and the Little Ice Age, pp. 35-58. Clark, P., R. Webb, and L.D. Keigwin (Eds.). *Mechanisms of Global Climate Change at Millennial Time Scales.* Geophysical Monograph 112. American Geophysical Union, Washington, D.C.

Bonnett, O.T. 1972. Silicified Cells of Grasses: A Major Source of Plant Opal in Illinois Soils. *Illinois Agricultural Experiment Station, Bulletin* No 742. 32 p.

Bouyoucos. 2009. "An Urgent Appeal for Soil Stewardship." Statement issued from the *2009 Bouyoucos Conference on Soil Stewardship in an Era of Global Climate Change.* http://pss.okstate.edu/home/rightsidebar/anurgentappealforsoilstewardship.pdf. [Reproduced in Appendix H].

Bowdrey, D. 1998. *Phytolith Analysis Applied to Pleistocene-Holocene Archaeological Sites in the Australian Arid Zone.* BAR Int. Ser. 695. 216 p.

Bowdery, D., D.M. Hart, C. Lentfer, and L.A. Wallis. 2001. A Universal Phytolith Key*, pp. 267-278. In Meunier, J.-D., and E. Colin (Eds.) *Phytoliths: Applications in Earth Sciences and Human History.* AA Balkema Publishers, Lisse, Netherlands.

Boyd, M. 2002. Identification of Anthropogenic Burning in the Paleoecological Record of the Northern Prairies: A New Approach. *Annals of the Association of American Geographers* 92:471-487.

Boyd, M. 2005. Phytoliths as paleoenvironmental indicators in a dune field on the northern Great Plains. *Journal of Arid Environments* 61:357-375.

Bozarth, S. 1993. Biosilicate Assemblages of Boreal Forests and Aspen Parklands*, pp. 95-105. In Pearsall, D.M., and D.R. Piperno (Eds.) *Current Research in Phytolith Analysis: Applications in Archaeology and Paleoecology* MASCA Research Papers in Science and Archaeology, Vol. 10. The University Museum of Archaeology and Anthropology, University of Pennsylvania, Philadelphia.

Bozarth, S. 1995. Fossil biosilicates. *Stratigraphy and Paleoenvironments of Late Quaternary Valley Fills on the Southern High Plains*, pp. 47-50. Holliday, V. (Ed.) Geological Society of American Memoir 186.

Brady, N.C., and R.R. Weil. 2002. *The Nature and Properties of Soils Thirteenth Edition.* Prentince Hall, Upper Saddle River, New Jersey. 960 p.

Brazle, F.K., L.H. Harbers, and C.E. Owensby. 1979. Structural Inhibitors of Big and Little Bluestem Digestion Observed by Scanning Electron Microscopy. *Journal of Animal Science* 48:1457-1463.

Brémond, L., A. Alexandre, O. Peyron, and J. Guiot. 2005a. Grass water stress estimated from phytoliths in West Africa. *Journal of Biogeography* 32:311-327.

Bremond, L., A. Alexandre, C. Hély, and J. Guiot. 2005b. A phytolith index as a proxy of tree cover density in tropical areas: Calibration with Leaf Area Index along a forest-savanna transect in southeastern Cameroon. *Global and Planetary Change* 45:277-293.

Bremond, L., A. Alexandre, O. Peyron, and J. Guiot. 2008. Definition of grassland biomes from phytoliths in West Africa. *Journal of Biogeography* 35:2039–2048.

Bremond, L., A. Alexandre, M.J. Wooller, C. Hély, D. Williamson, P. A. Schäfer, A. Majule, and J. Guiot. 2008. Phytolith indices as proxies of grass subfamilies on East African tropical mountains. *Global and Planetary Change* 61:209-224.

Brizuela, M.A., J.K. Detling, and M.S. Cid. 1986. Silicon Concentration of Grasses Growing in Sites with Different Grazing Histories. *Ecology* 67(4):1098-1101.

Broecker, W. S. 2006. Was the Younger Dryas Triggered by a Flood? *Science* 312:1146–1148.

Brown, D.A. 1984. Prospects and Limits of a Phytolith Key for Grasses in the Central United States. *Journal of Archaeological Science* 11:345-368.

Brown, D. 1986a. Taxonomy of a Midcontinent Grasslands Phytolith Key, pp. 67-86. In Rovner, I. (Ed.) *Plant Opal Phytolith Analysis in Archaeology and Paleoecology* Occasional Papers No. 1 of the Phytolitharien. North Carolina State University, Raleigh.

Brown, D. 1986b. Geographic and Taxonomic Aspects of Research Design for Opal Phytolth Analysis in the Midcontinent Plains, pp. 89-101. In Rovner, I. (Ed.) *Plant Opal Phytolith Analysis in Archaeology and Paleoecology* Occasional Papers No. 1 of the Phytolitharien. North Carolina State University, Raleigh.

Brown, L. 1979. *Grasses An Identification Guide*. Houghton Mifflin Company, Boston. 240 p.

Brown, D.A. 1993. Early Nineteenth-Century Grasslands of the Midcontinent Plains. *Annals of the Association of American Geographers* 83(4):589-612.

Brush, G.S., and L.M. Brush. 1994. Transport and deposition of pollen in an estuary: signature of the landscape, pp. 33-46. In Traverse, A. (Ed.). *Sedimentation of Organic Particles*. Cambridge University Press, Cambridge.

Buol, S.W., R.J. Southard, R.C. Graham, and P.A. McDaniel. 2003. *Soil Genesis and Classification Fifth Edition*. Iowa State Press, Ames, Iowa. 494 p.

Burke, M.K., S.L. King, D. Gartner, and M.H. Eisenbies. 2003. Vegetation, Soil, and Flooding Relationships in a Blackwater Floodplain Forest. *Wetlands* 23(4):988-1002.

de Campos, A.C., and L.G. Labouriau. 1969. Corpos silicosos de gramíneas dos Cerrados II. (Silica bodies of grasses of the Cerrados II.) *Pesquisa Agropecuraria Brasileira* 4:143-151.

Carter, B.J., J.P. Kelley, J.B. Sudbury, and D.K. Splinter. 2009. Key Aspects of A Horizon Formation for Selected Buried Soils in Late Holocene Alluvium; Southern Prairies, USA. *Soil Science* 174(7):408-416.

Carter, J.A. 1999. Late Devonian, Permian and Triassic Phytoliths from Antarctica. *Micropaleontology* 45(1):56-61.

Cavalcante, P.B. 1968. Contribuição ao estudo dos corpos silicosos das gramineas Amazônicas. I. Panicoideae (Melinideae, Andropogoneae, e Tripsaceae). [Contribution to the study of silica bodies from Amazonian grasses. I. Panicoideae (Melinideae, Andropogoneae and Tripsaceae)]. *Boletim do Museu Paraense Emilio Goeldi, Botanica,* No 30. 30 pages, 26 figures.

Chaffey, N.J. 1983. Epidermal Structure in the Ligule of Rice *(Oryza sativa* L.). *Annals of Botany* 52:13-21.

Chevalier, L., C. Desbuquois, J. Le Lannic, and M. Charrier. 2001. Poaceae in the natural diet of the snail *Helix aspersa* Müller (Gastropoda, Pulmonata). *C.R. Acad. Sci. Paris, Sciences de la vie / Life Sciences* 324:979-987.

Ciochon, R.L., D.R. Piperno, and R.G. Thompson. 1990. Opal phytoliths found on the teeth of the extinct ape *Gigantopithecus blackii:* Implications for paleodietary studies. *Proceedings of the National Academy of Sciences USA* 87:8120-8124.

Clarke, J. 2003. The occurrence and significance of biogenic opal in the regolith. *Earth-Science Reviews* 60:175-194.

Cohen, A.S. 2003. *Paleolimnology: the History and Evolution of Lake Systems*. Oxford University Press, New York. 500 p.

Coleman, W.C. 1969. Cysts of Chrysomonadacea, Chrysostomatacea and Archaeomonadacea: Their Status in Paleontology [Abstract]. *Journal of Paleontology* 43(3):885.

Constable, G., et al. (Eds.). 1985. *Planet Earth Grasslands and Tundra*. Time-Life Books, Alexandria, Virginia. 175 p.

Constantini, E., A. Makeev, and D. Sauer (Eds.). 2009. Recent Developments and New Frontiers in Palaeopedology. *Quaternary International* 209. 186 p.

Cordova, C.E**.**, and L. Agenbroad. 2009. Opal phytoliths from Teeth Calculus in the Mammoths of the Hot Springs Site, South Dakota. *Current Research in the Pleistocene* 26:145-147.

Cordova, C.E., and W.C. Johnson. 2007. Paleobiomes and Paleopastures: A reconstruction of interactions of vegetation, climate, grazing, and fire in south-central North America since the Last Glacial Maximum. *Current Research in the Pleistocene* 24:196-198.

Cordova, C.E., J.C. Porter, K. Lepper, R. Kalchgruber, and G. Scott. 2005. Preliminary Assessment of Sand Dune Stability along a Bioclimatic Gradient, North-Central and Northwestern Oklahoma. *Great Plains Research* 15:227-249.

Cornell, W.C. 1969. Cysts of Chrysomonadacea, Chrysostomatacea and Archaeomonadecea: Their status in paleontology. *Journal of Paleontology* 43(3):885.

Coyle, H.M. (Ed.). 2005. *Forensic Botany Principle and Applications to Criminal Casework*. CRC Press, Boca Raton, Florida. 318 p.

Cummings, L.S. 1996. Paleoenvironmental Interpretations for the Mill Iron Site: Stratigraphic Pollen and Phytolith analysis, pp. 177-193. G. C. Frison (Ed.) *The Mill Iron Site.* University of New Mexico Press, Albuquerque.

Cummings, L.S., and A. Magennis. 1997. A phytolith and starch record of food and grit in Mayan human tooth tartar*, pp.* 211-218. In Pinilla, A., J. Juan-Tresserras, and M.J. Machado (Eds.) *The State-of-the-Art of Phytoliths in Soils and Plants*. Monografías del Centro de Ciencias Medioambientales, Consejo Superior de Investigaciones Científicas, Madrid.

Darke, R., and M. Griffiths (Eds.). 1994. *Manual of Grasses.* Timber Press, Portland, Oregon. 169 p.

Darwin, C. 1846. An account of the fine dust which often falls on vessels in the Atlantic Ocean. *Quarterly Journal of the Geological Society of London,* 22:26-30.

De La Rocha, C.L. 2003. Silicon isotope fractionation by marine sponge and the reconstruction of the silicon isotope composition of ancient deep water. *Geology* 31:423-426.

Dean, W.E., R.M. Forester, and J. Platt Bradbury. 2002. Early Holocene change in atmospheric circulation in the Northern Great Plains: an upstream view of the 8.2 ka cold event. *Quaternary Science Reviews* 21:1763-1775.

DeLorme. 2003. *Oklahoma Atlas and Gazetteer.* DeLorme, Yarmouth, Maine. 68 p.

337

Djamin, A., and M.D. Pathak. 1967. Role of Silica in Resistance to Asiatic Rice Borer, *Chilo suppressalis* (Walker), in Rice Varieties. *Journal of Economic Entomology* 60:347-351.

Drees, L.R., L.P. Wilding, N.E. Smeck, and A.L. Senkayi. 1989. Silica in Soils: Quartz and Disordered Silica Polymorphs, pp. 913-974. Dixon, J.B., and S.B. Weed (Eds.) *Minerals in Soil Environments Second Edition*. Soil Science Society of America, Madison, Wisconsin.

Dröscher, I., and J. Waringer. 2007. Abundance and microhabitats of freshwater sponges (Spongillidae) in a Danubean floodplain in Austria. *Freshwater Biology* 52(6):998-1008.

Duff, K.E., B.A. Zeeb, and J.P.Smol. 1997. Chrysophyte Cyst Biogeographical and Ecological Distributions: A Synthesis. *Journal of Biogeography* 24(6):791-812.

Easterbrook, D.J. 1999. *Surface Processes and Landforms, Second Edition*. Prentice Hall, Upper Saddle River, New Jersey. 546 p.

Elbaum, R., C. Melamed-Bessudo, N. Tuross, A.A. Levy, and S. Weiner. 2009. New methods to isolate organic materials from silicified phytoliths reveal fragmented glycoproteins but no DNA. *Perspectives on Phytolith Research: 6th International Meeting on Phytolith Research. Quaternary International* 193:11-19.

Elger, A., D.G. Lemoine, M. Fenner, and M.E. Hanley. 2009. Plant ontogeny and chemical defence: older seedlings are better defended. *Oikos* 118: 767-773.

Ely, L.L. 1997. Response of extreme floods in the southwestern United States to climatic variations in the late Holocene. Geomorphology 19:175-201.

Epstein, E. 1994. The anomaly of silicon in plant biology. *PNAS* 91:11-17.

Ernst, W.H.O., R.D. Vis*, and F. Piccoli. 1995. Silicon in Developing Nuts of the Sedge *Schoenus nigricans*. *Journal of Plant Physiology* 146:481-488.

d'Errico, F., G. Giacobini, J. Hather, A.H. Powers-Jones, and A.M. Radmilli. 1995. Possible bone threshing tools from the Neolithic levels of the Grotta dei Piccioni (Abruzzo, Italy). *Journal of Archaeological Science* 22:537-549.

Evan, A.T., J. Dunion, J.A. Foley, A.K. Heidinger, and C.S. Velden. 2006. New evidence for a relationship between North Atlantic tropical cyclone activity and African dust outbreaks. *Geophys. Res. Lett., 33*, L19813, doi:10.1029/2006GL026408.

Evett, R.R., R.A. Woodward, W. Harrison, J. Suero, P. Raggio, and J.W. Bartolome. 2006. Phytolith Evidence for the Lack of a Grass Understory in a *Sequoiadendron giganteum* (Taxodiaceae) Stand in the Central Sierra Nevada, California. *Madroño* 53(4):351-363.

Faegri, K., and J. Iversen. 1950. *Text-book of Modern Pollen Analysis.* Copenhagen. 168 p.

FAOSTAT. 2009. http://faostat.fao.org/site/567/default.aspx#ancor. (accessed 8-14-09)

Fearn, M.L. 1995. Louisiana's Cajun Prairie: Holocene History of a Southern Grassland. Ph.D. Dissertation, Louisiana State University. 283 p.

Fearn, M.L. 1998. Phytoliths in sediment as indicators of grass pollen source. *Review of Palaeobotany and Palynology* 103:75-81.

Feng, Z-D., W.C Johnson, D.R. Sprowl, Y. Lu. 1994. Loess Accumulation and Soil Formation in Central Kansas, United States, During the Past 400,000 Years. *Earth Surface Processes and Landforms* 19:55-67.

Fernández, O.A., M.E. Gil, and R.A. Distel. 2009. The Challenge of Rangeland Degradation in a Temperate Semiarid Region of Argentina: The Caldenal. *Land Degrad. Develop.* 20:431–440.

Fernández Honaine, M., V. Bernava Laborde, and A.F. Zucol. 2008. Contenido de Sílice en Gramíneas del Pastizal Nativo del Sudeste Bonaerense, Argentina [Silica Content in Grasses from Native Grassland of Southeastern Buenos Aires Province, Argentina], pp. 57-63. In Korstanje, M.A. and M. Babot (Eds.) *Matices Interdisciplinarios en Estudios Fitolíticos y de Otros Microfósiles* [*Interdisciplinary Nuances in Phytoliths and Other Microfossil Studies*]. *BAR Int. Ser.* 1870.

Fernández Honaine, M., M.L. Osterrieth, and A.F. Zucol. 2009. Plant communities and soil phytolith assemblages relationship in native grasslands from southeastern Buenos Aires province, Argentina. *Catena* 76:89-96.

Ferring, C.R. 1992. Alluvial Pedology and Geoarchaeological Research, pp. 1-39. In Holliday, V.T. (Ed.) *Soils in Archaeology Landscape Evolution and Human Occupation.* Smithsonian Institution Press, Washington.

Figueiredo, R.C.L., and W. Handro. 1971. Corpos silicosos de gramíneas dos Cerrados-- V. (Silica bodies of grasses from Cerrados V.) *III Simpósio sôbre o Cerrado:* 215-230.

Fiorentino, G., and D. Magri (Eds.). 2008. *Charcoals from the Past: Cultural and Palaeoenvironmental Implications.* Proceedings of the Third International Meeting of Anthracology, Cavallino - Lecce (Italy), June 28th - July 1st 2004. *BAR Int. Ser.* 1807. 318 p.

Firestone, R.B., and W. Topping. 2001. Terrestrial Evidence of a Nuclear Catastrophe in Paleoindian Times. *Mammoth Trumpet* 16(1):9-16.

Firestone, R.B., A. West, J.P. Kennett, L. Becker, T.E. Bunch, Z.S. Revay, P.H. Schultz, T. Belgya, D.J. Kennett, J.M. Erlandson, O.J. Dickenson, A.C. Goodyear, R.S. Harris, G.A. Howard, J.B. Kloosterman, P. Lechler, P.A. Mayewski, J. Montgomery, R. Poreda, T. Darrah, S.S. Que Hee, A.R. Smith, A. Stich, W. Topping, J.H. Wittke, and W.S. Wolbach. 2007. Evidence for an extraterrestrial impact 12,900 years ago that contributed to the megafaunal extinctions and the Younger Dryas cooling. *PNAS* 104(41):16016-16021.

Fisher, R.F., M.J. Jenkins, and W.F. Fisher. 1986. Fire and the Prairie-forest Mosaic of Devils Tower National Monument. *The American Midland Naturalist* 117(2):251-257.

Fontana, P., Jr. 1954. Studies on the deposition of silica on the leaves of the grass *Panicum maximum. Revista Brasiliera de Biologica* 14:35-40.

Forman, S.L., M. Spaeth, L. Marín, J. Pierson, J. Gómez, F. Bunch, and A. Valdez. 2006. Episodic Late Holocene dune movements on the sand-sheet area, Great Sand Dunes National Park and Preserve, San Luis Valley, Colorado, USA . *Quaternary Research* 66:97–108.

Fredlund, G.G. 1986. Problems in the Simultaneous Extraction of Pollen and Phytoliths from Clastic Sediments*, pp. 102-111. In Rovner, I. (Ed.) *Plant Opal Phytolith Analysis in Archaeology and Paleoecology* Occasional Papers No. 1 of the Phytolitharien. North Carolina State University, Raleigh.

Fredlund. G.G., C.B. Bousman, and D.K. Boyd. 1998. The Holocene Phytolith Record from Morgan Playa in the Rolling Plains of Texas. *Plains Anthropologist* 43:187-200.

Fredlund, G.G., W.C. Johnson, and W. Dort, Jr. 1985. A Preliminary Analysis of Opal Phytoliths from the Eustis Ash Pit, Frontier County, Nebraska. *Institute for Tertiary-Quaternary Studies – TER-QUA Symposium Series* 1:147-167.

Fredlund, G.G., and L.T. Tieszen. 1994. Modern phytolith assemblages from the North American Great Plains. *Journal of Biogeography* 21:321-335.

Fredlund, G.G., and L.T. Tieszen. 1997a. Calibrating grass phytolith assemblages in climatic terms: Application to late Pleistocene assemblages from Kansas and Nebraska. *Palaeogeography,Palaeoclimatology,Palaeoecology* 136:199-211.

Fredlund, G.G., and L.T. Tieszen. 1997b. Phytolith and Carbon Isotope Evidence for Late Quaternary Vegetation and Climate Change in the Southern Black Hills, South Dakota. *Quaternary Research* 47:206-27.

Frey, D.G. 1955. A Differential Flotation Technique for Recovering Microfossils from Inorganic Sediments. *New Phytologist* 54(2):257-258.

Fried, B., and J. Sherma. 1999. *Thin-Layer Chromatography Fourth Edition, Revised and Expanded*. Chromatographic Science Series Volume 81. Marcel-Dekker, Inc. New York. 1047 p.

Fullagar, R., and J. Field. 1997. Pleistocene seed-grinding implements from the Australian arid zone. *Antiquity* 71:300-307.

Gali-Muhtasib, H.U., C.C. Smith, and J.J. Higgins. 1992. The Effect of Silica in Grasses on the Feeding Behavior of the Prairie Vole, *Microtus ochrogaster*. *Ecology* 73(5):1724-1729.

Gallego, L., and R.A. Distel. 2004. Phytolith Assemblages in Grasses Native to Central Argentina. *Annals of Botany* 94:865-874.

Gallego, L., R.A. Distel, R. Camina, and R.M. Rodríguez Iglesias. 2004. Soil phytoliths as evidence for species replacement in grazed rangelands of central Argentina. *Ecography* 27:725-732.

García-Rodríguez, F. 2006. Inferring paleosalinity trends using the chrysophyte cyst to diatom ratio in coastal shallow temperate/subtropical lagoons influenced by sea level changes. *Journal of Paleolimnology* 36(2):165-173.

Geis, J.W. 1973. Biogenic Silica in Selected Species of Deciduous Angiosperms. *Soil Science* 116:113-130.

Geis, J.W. 1978. Biogenic Opal in Three Species of *Gramineae*. *Annals of Botany* 42:1119-1129.

Geis, J.W., and R.L. Jones. 1973. Ecological significance of biogenic opaline silica, pp. 74-85. In Dindal, D.L. (Ed.) *Proceedings of the first soil Microcommunities Conference*. Oak Ridge, Tennessee. U. S. Atomic Energy Commission.

Goble, R.J., J.A. Mason, D.B. Loope, J.B. Swinehart. 2004. Optical and radiocarbon ages of stacked paleosols and dune sands in the Nebraska Sand Hills, USA. *Quaternary Science Reviews* 23:1173-1182.

Goss, D.W., A.R. Ross, P.B. Allen, and J.W. Naney. 1972. Geomorphology of the Central Washita River Basin. *Proceedings of the Oklahoma Academy of Science* 52:145-149.

Gould, F.W. 1968. *Grass Systematics*. McGraw-Hill Book Company, New York. 382 p.

GPWG (Grass Phylogeny Working Group). 2001. Phylogeny and Subfamilial Classification of the Grasses (Poaceae). *Annals of the Missouri Botanical Garden* 88:373-457.

von Grafenstein, U., H. Erlenkeuser, J. Müller, J. Jouzel, and S. Johnsen. 1998. The cold event 8200 years ago documented in oxygen isotope records of precipitation in Europe and Greenland. *Clim. Dyn.* 14:73-81.

Gregory, W. 1855. On the presence of Diatomaceae, Phytolitharia and Sponge Spicules in soils which support Vegetation. *Proceedings of the Botanical Society*, Edinburgh pp. 69-72.

Grousset, F.E., and P.E. Biscaye. 2005. Tracing dust sources and transport patterns using Sr, Nd and Pb isotopes. *Chemical Geology* 222(3-4):149-167.

Hagemeyer, J., and S-W. Breckle. 1996. Growth Under Trace Element Stress, pp. 415-433. In Waisel, Y, A. Eshel, and U. Kafkafi (Eds.) *Plant Roots The Hidden Half Second Edition, Revised and Expanded*. Marcel Dekker, Inc., New York.

Hall, S.A. 1983. A Paleosol in Central Oklahoma and its Archaeological Significance. *Bulletin of the Oklahoma Anthropological Society* XVI:151-154.

Hall, S.A. and C. Lintz. 1984. Buried trees, water table fluctuations, and 3000 years of changing climate in west-central Oklahoma. *Quaternary Research* 22:129-133.

Harbers, L.H., D.J. Raiten, and G.M. Paulsen. 1981. The role of plant epidermal silica as a structural inhibitor of rumen microbial digestion in steers. *Nutrition Reports International* 24:1057-1066.

Harbers, L.H., and M.L. Thouvenelle. 1980. Digestion of corn and sorghum silage observed by scanning electron microscopy. *Journal of Animal Science* 50:514-526.

Harper, H.J. 1932. Studies of the Origin of the Sandy Land along the Cimarron River in Oklahoma. *Proceedings of the Oklahoma Academy of Science* 13:24-27.

Harper, H.J. 1933. Further Investigations of Buried Soils in Relation to Climatic Changes in Oklahoma. *Proceedings of the Oklahoma Academy of Science* 14:65-67.

Harper, H., and C.A. Hollopeter. 1931. Buried Soils and their Significance. *Proceedings of the Oklahoma Academy of Science* 12:63-66.

Harris, R.R. 1987. Occurrence of Vegetation on Geomorphic Surfaces in the Active Floodplain of a California Alluvial Stream. *American Midland Naturalist* 118(2): 393-405.

Hart, D.M., and G.S. Humphreys. 2003. Phytolith Depth Functions in Surface Regolith Materials, pp. 159-163. In Roach, I.C. (Ed.) *Advances in Regolith*. CRC LEME.

Hart, D.M., and G.S. Humphreys. 1997. The mobility of phytoliths in soils; pedological considerations, pp. 93-100. In Pinilla, A., J. Juan-Tresserras, and M.J. Machado (Eds.) *The State-of-the-Art of Phytoliths in Soils and Plants*. Monografías del Centro de Ciencias Medioambientales, Consejo Superior de Investigaciones Científicas, Madrid.

Hart, D.M., and L.A. Wallis (Eds.). 2003. *Phytolith and Starch Research in the Australian-Pacific-Asian Regions: The State of the Art.* Terra Australis 19. Pandanus Books, Australian National University, Canberra. 200 p.

Hodson, M.J., A.G. Parker, M.J. Leng, and H.J. Sloane. 2008**.** Silicon, oxygen and carbon isotope composition of wheat (*Triticum aestivum* L.) phytoliths: implications for palaeoecology and archaeology. In *Special Issue: Isotopes in Biogenic Silica (IBiS)*. Leng, M.J., F.A. Street-Perrott, and P.A. Barker (Eds.) *Journal of Quaternary Science* 23(4):331-339.

Leng, M.J., F.A. Street-Perrott, and P.A. Barker (Eds.). *Journal of Quaternary Science* 23(4):331-339.

Hodson, M.J., and A.G. Sangster. 1988. Silica deposition in the inflorescence bracts of wheat *(Triticum aestivum).* I. Scanning electron microscopy and light microscopy. *Canadian Journal of Botany* 66:829-838.

Holliday, V.T. 1988. Genesis of a Late-Holocene Soil Chronosequence at the Lubbock Lake Archaeological Site. *Annals of the Association of American Geographers* 78(4):594-610.

Holliday, V.T. 1995. *Stratigraphy and Paleoenvironments of Late Quaternary Valley Fills on the Southern High Plains.* Geological Society of America Memoir 186. The Geological Society of America, Inc., Boulder, Colorado. 135 p.

Holliday, V.T. 2004. *Soils in Archaeological Research.* Oxford University Press, New York. 448 p.

Holliday, V.T., J.H. Mayer, and G.G. Fredlund. 2008. Late Quaternary sedimentology and geochronology of small playas on the Southern High Plains, Texas and New Mexico, U.S.A. *Quaternary Research* 70:11-25.

Houyuan, L., W. Naiqin, and L. Baozhu. 1997. Recognition of rice phytoliths, pp. 159-174. In Pinilla, A., J. Juan-Tresserras, and M.J. Machado (Eds.) *The State-of-the-Art of Phytoliths in Soils and Plants*. Monografías del Centro de Ciencias Medioambientales, Consejo Superior de Investigaciones Científicas, Madrid.

Hupp, C.R. 1982. Stream-Grade Variation and Riparian-Forest Ecology Along Passage Creek, Virginia. *Bulletin of the Torrey Botanical Club* 109(4):488-499.

Iler, R.K. 1979. *The Chemistry of Silica Solubility, Polymerization, Colloid and Surface Properties, and Biochemistry*. John Wiley & Sons, New York. 866 p.

Jackson, M.I. 1956. Soil Chemical Analysis-Advanced Course. Mimeograph published by the Department of Soil Science, University of Wisconsin, Madison.

Jacobs, B.F., J.D. Kingston, and L.L. Jacobs. 1999. The Origin of Grass-Dominated Ecosystems. *Annals of Missouri Botanical Garden* 86:590-643.

Jenkins, E. 2009. Phytolith taphonomy: a comparison of dry ashing and acid extraction on the breakdown of conjoined phytoliths formed in *Triticum durum. Journal of Archaeological Science* 36:2402–2407.

Jiang, Q. 1995. Searching for evidence of early rice agriculture at prehistoric sites in China through phytolith analysis: an example from central China. *Review of Palaeobotany and Palynology* 89:481-485.

Johnson, W.C., and B. Logan. 1990. Geoarchaeology of the Kansas River Basin, Central Great Plains: in *Archaeological Geology of North America,* pp. 267-299. Lasca, N.P, and J.E. Donahue (Eds.) *Decade of North American Geology (DNAG) Centennial Special Volume 4*. Geological Society of America.

Johnson, W.C. and C.W. Martin. 1987. Holocene Alluvial-Stratigraphic Studies from Kansas and Adjoining States of the East-Central Plains, pp. 109-122. In Johnson, W.C. (Ed.) *Quaternary Environments of Kansas*, Kansas Geological Survey *Guidebook Series 5.*

Johnson, W.C., K.L. Willey, and G.L. Macpherson. 2007. Carbon isotope variation in modern soils of the Tallgrass prairie: analogues for the interpretation of isotopic records derived form paleosols. *Quaternary International* 162-163:3-20.

Johnston, A, L.M. Bezeau, and S. Smoliak. 1967. Variation in silica content of range grasses. *Canadian Journal of Plant Science* 47:65-71.

Jones, D.J. 1956. *Introduction to Microfossils*. Harper & Brothers, New York. 406 p.

Jones, J.G., and V.M. Bryant, Jr. 1992. Phytolith Taxonomy in Selected Species of Texas Cactis*, pp. 215-238. In Rapp, G., Jr., and S.C. Mulholland (Eds.) *Phytolith Systematics: Emerging Issues*. Plenum Press, New York.

Jones, L.H.P., and K.A. Handreck. 1963.   Effects of iron and aluminum oxides on silica in soils. *Nature* 198:852-853

Jones, L.H.P., and K.A. Handreck. 1965. Studies of Silica in the Oat Plant III. Uptake of Silica from Soils by the Plant. *Plant and Soil* 23:79-96.

Jones, L.H.P., and K.A. Handreck. 1967. Silica in Soils, Plants and Animals, pp. 107-149. In Nolman, G. (Ed.) *Advances in Agronomy* 19. Academic Press, New York.

Jones, L.H.P., and A.A. Milne. 1963. Studies of Silica in the Oat Plant I. Chemical and Physical Properties of the Silica. *Plant and Soil* 18:207-220.

Jones, R.L., and A.H. Beavers. 1963. Some Mineralogical and Chemical Properties of Plant Opal. *Soil Science* 96:375-379.

Jones, R.L., and A.H. Beavers. 1964a. Aspects of Catenary and Depth Distribution of Opal Phytoliths in Illinois Soils. *Soil Science Society of America Proceedings* 28:413-416.

Jones, R.L, and A.H. Beavers. 1964b. Variation of Opal Phytolith Content Among Some Great Soil Groups in Illinois. *Soil Science Society of America Proceedings* 28:711-712.

Jones, R.L., W.W. Hay, and A.H. Beavers. 1963. Microfossils in Wisconsin Loess and Till from Western Illinois and Eastern Iowa. *Science* 140:1222-1224.

Jones, R.L., L.J. McKenzie, and A.H. Beavers. 1964. Opaline Microfossils in some Michigan Soils. *The Ohio Journal of Science* 64(6):417-423.

Kanno, I., and S. Arimura. 1958. Plant opal in Japanese soils. *Soil Science and Plant Nutrition (Soil and Plant Food)* 4:62-67.

Kaufman, P.B., P. Dayanandan, Y. Takeoka, W.C. Bigelow, J.D. Jones, and R. Iler. 1981. Silica in shoots of higher plants*,* pp. 409-449. In Simpson, T.L., and B.E. Volcani (Eds.) *Silicon and siliceous Structures in Biological Systems.* Springer Verlag, New York.

Kealhofer, L. 1996. The Human Environment During the Terminal Pleistocene and Holocene in Northeastern Thailand: Phytolith Evidence from Lake Kumphawapi. *Asian Perspectives* 35:229-254.

Kealhofer, L. 2002. Changing perceptions of risk. The development of agro-ecosystems in Southeast Asia. *American Anthropologist* 104(1):178-194.

Kealhofer, L. 2003. Looking into the Gap: Land Use and the Tropical Forests of Southern Thailand. *Asian Perspectives* 42:72-95.

Kealhofer, L., and D. Penny. 1998. A combined pollen and phytolith record for fourteen thousand years of vegetation change in northeastern Thailand. *Review of Palaeobotany and Palynology* 103:83-93.

Kealhofer, L., and D.R. Piperno. 1994. Early agriculture in southeast Asia: phytolith evidence from the Bang Pakong Valley, Thailand. *Antiquity* 68:564-572.

Kealhofer, L., and D.R. Piperno. 1998. Opal Phytoliths in Southeast Asian Flora. *Smithsonian Contributions to Botany. No.88.* Smithsonian Institution Press, Washington, D.C. 39 p.

Kealhofer, L., R. Torrence, and R. Fullagar. 1999. Integrating Phytoliths within Use-Wear/Residue Studies of Stone Tools. *Journal of Archaeological Science* 26:527-546.

Kelley, J.P. 2006. Influence of Alluvial Sedimentation Rate on Floodplain Soil Development and Vegetation. Unpublished M.S. Thesis, Oklahoma State University. 126 pp.

Kennett, D.J., J.P. Kennett, A. West, C. Mercer, S.S. Que Hee, L. Bement, T.E. Bunch, M. Sellers, and W.S. Wolbach. 2009. Nanodiamonds in the Younger Dryas Boundary Sediment Layer. *Science* 323:94.

Kerns, B.K. 2001. Diagnostic Phytoliths for a Ponderosa Pine-Bunchgrass Community Near Flagstaff, Arizona. *The Southwestern Naturalist* 46:282-294.

Kerns, B.K., M.M. Moore, and S.C. Hart. 2001. Estimating forest-grassland dynamics using soil phytolith assemblages and δ13C of soil organic matter. *Ecoscience* 8:478-488.

Kido, M., and S. Yanatori. 1964. (Studies on Silicified Tissues of Leaf in Rice Plant by Spodogram – Hydrogen Chloride Treatment Method.) *Nihon Sakumotsu Gakkai Kiji. (Proceedings of the Crop Science Society of Japan) (Japanese Journal of Crop Science)* 33:115-118.

Kirk, G. 2004. *The Biogeochemistry of Submerged Soils.* John Wiley & Sons, Ltd. 304 p.

Knox, A.S. 1942. The use of bromoform in the separation of non-calcareous microfossils. *Science* 95(2464):107-108.

Kondo, R., C. Childs, and L Atkinson. 1994. *Opal Phytoliths of New Zealand.* Manaaki Press, Lincoln, New Zealand. 85 p.

Korstanje, M.A. and M. Babot (Eds.). 2008. *Matices Interdisciplinarios en Estudios Fitoliticos y de Otros Microfosiles. Interdisciplinary Nuances in Phytoliths and Other Microfossil Studies. BAR Int. Ser.* 1870. 218 p.

Kramer, P.J., and J.S. Boyer. 1995. *Water Relations of Plants and Soils.* Academic Press, San Diego. 495 p.

Krull, E.S., J.O. Skjemstad, D. Graetz, K. Grice, W. Dunning, G. Cook, and J.F. Parr. 2003. 13C-depleted charcoal from C4 grasses and the role of occluded carbon in phytoliths. *Organic Geochemistry* 34:1337-1352

Lanning, F.C. 1963. Silicon in Rice. *Journal of Agriculture and Food Chemistry* 11:435-437.

Lanning, F.C., and L.N. Eleuterius. 1987. Silica and Ash in Native Plants of the Central and Southeastern Regions of the United States. *Annals of Botany* 60:361-375.

Lanning, F.C., T.L. Hopkins, and J.C. Loera. 1980. Silica and Ash Content and Depositional Patterns in Tissues of Mature *Zea mays* L. Plants. *Annals of Botany* 45:549-554.

Laruelle, G.G.. V. Roubeix, A. Sferratore, B. Brodherr, D. Ciuffa, D.J. Conley, H.H. Dürr, J. Garnier, C. Lancelot, Q. Le Thi Phuong, J.-D. Meunier, M. Meybeck, P. Michalopoulos, B. Moriceau,S. Nı´ Longphuirt, S. Loucaides, L. Papush, M. Presti, O. Ragueneau, P.A.G. Regnier, L. Saccone, C.P. Slomp, C. Spiteri, and P. Van Cappellen. 2009. Anthropogenic perturbations of the silicon cycle at the global scale: Key role of the land-ocean transition. *Global Biogeochemical Cycles* 23 GB4031, doi:10.1029/2008GB003267.

Laws, F. 2009. 'Land grants' could lead hunger fight. *Southwest Farm Press*, October 14. http://southwestfarmpress.com/grains/land-grants-1014/ (10-15-09). [Reproduced in Appendix G]

Lejju, J.B. 2009. Vegetation dynamics in western Uganda during the last 1000 years: climate change or human induced environmental degradation? *Afr. J. Ecol.* 47 (Suppl. 1):21–29.

Leng, M.J., and H.J. Sloane. 2008. Combined oxygen and silicon isotope analysis of biogenic silica. In *Special Issue: Isotopes in Biogenic Silica (IBiS)*. Leng, M.J., F.A. Street-Perrott, and P.A. Barker (Eds.). *Journal of Quaternary Science* 23(4):313-319.

Leng, M.J., G.E.A Swann, M.J. Hodson, J.J. Tyler, S.V. Patwardhan, and H.J. Sloane. 2009. The Potential use of Silicon Isotope Composition of Biogenic Silica as a Proxy for Environmental Change. *Silicon* 1(2):65-77.

Lentfer, C.J., and W.E. Boyd. 1998. A Comparison of Three Methods for the Extraction of Phytoliths from Sediments. *Journal of Archaeological Science* 25:1159-1183.

Lentfer, C.J., and W.E. Boyd. 1999. An Assessment of Techniques for the Deflocculation and Removal of Clays from Sediments Used in Phytolith Analysis. *Journal of Archaeological Science* 26:31-44.

Lentfer, C.J., W.E. Boyd., and D. Gojak. 1997. Hope Farm Windmill: Phytolith Analysis of Cereals in Early Colonial Australia. *Journal of Archaeological Science* 24:841-856.

Leopold, E.B., and M.F. Denton. 1987. Comparative Age of Grassland and Steppe East and West of the Northern Rocky Mountains. *Ann. Missouri Bot. Gard.* 74:841-867.

Lepper, K., and G.F. Scott. 2002. Late Holocene episodic aeolian activity and landscape development in the Cimarron River Valley, Western Oklahoma, pp. 463-466. In *Proceedings of ICAR5/GCTE-SEN Joint Conference*. Center for Arid and Semiarid Lands Studies, Lubbock, Texas.

Levi, C., J.L. Barton, C. Guillemet, E. Le Bras, and P. Lehuede. 1989. A remarkably strong natural glassy rod: the anchoring spicule of the *Monorhaphis* sponge. *Journal of Materials Science Letters* 8(3):337-339.

Lintz, C. and S. A. Hall. 1983. The Geomorphology and Archaeology of Carnegie Canyon, Ft. Cobb Laterals Watershed, Caddo Co., Oklahoma. Archaeological Research Report No. 10. Oklahoma Conservation Commission, Oklahoma City, Oklahoma. 221 p.

Lopez, P.J., J. Descle´s, A.E. Allen, and C. Bowler. 2005. Prospects in diatom research. *Current Opinion in Biotechnology* 16:180–186.

Lotter, A.F., H.J.B. Birks, W. Hofmann, and A. Marchetto. 1997. Modern diatom, cladocera, chironomid and chrysophyte cyst assemblages as quantitative indicators for the reconstruction of past environmental conditions in the Alps. 1. Climate. *Journal of Paleolimnology* 18(4):395-420.

Lu, H., and K.-B. Liu. 2003a. Morphological variations of lobate phytoliths from grasses in China and the south-eastern United States. *Diversity and Distributions* 9:73-87.

Lu, H., and K.-B. Liu. 2003b. Phytoliths of common grasses in the coastal environments of southeastern USA. *Estuarine, Coastal and Shelf Science* 58:587-600.

MacFadden, B.J. 2000. Cenozoic Mammalian Herbivores from the Americas: Reconstructing Ancient Diets and Terrestrial Communities. *Annu. Rev. Ecol. Syst.* 31:33-59.

Madella, M., A. Alexandre, and T. Ball. 2005. International Code for Phytolith Nomenclature 1.0. *Annals of Botany* 96:253-260.

Madella, M., A.H. Powers-Jones, and M.K. Jones. 1998. A Simple Method of Extraction of Opal Phytoliths from Sediments Using a Non-Toxic Heavy Liquid. *Journal of Archaeological Science* 25:801-803.

Madella, M., and D. Zurro (Eds.). 2007. *Plants, People and Places Recent Studies in Phytolith Analysis*. Oxbow Books, Oxford. 237 p.

Maiorana, V.C. 1978. What Kinds of Plants do Herbivores Really Prefer? *The American Naturalist* 112(985):631-635.

Marshner, H. 1995. *Mineral Nutrition of Higher Plants*. Academic Press, London.

Martin, C.W., and W.C. Johnson. 1987. Historic Channel Narrowing and Riparian Vegetation Expansion in the Medicine Lodge River Basin, Kansas, 1871-1983. Association of American Geographers *Annals* 77:436-449.

Martin, C.W., and W.C. Johnson. 1995. Variation in Radiocarbon Ages of Soil Organic Matter Fractions from Late Quaternary Buried Soils. *Quaternary Research* 43:232-237.

Marumo, Y., and H. Yanai. 1986. Morphological Analysis of Opal Phytoliths for Soil Discrimination in Forensic Science Investigation. *Journal of Forensic Sciences* 31: 1039-1049.

Mason, J.A., Z. Miao, P.R. Hanson, W.C. Johnson, P.M. Jacobs, and R.J. Goble. 2008. Loess record of the Pleistocene-Holocene transition on the northern and central Great Plains, USA. *Quaternary Science Reviews* 27:1772-1783.

Massey, F.P., A.R. Ennos, and S.E. Hartley. 2006. Silica in grasses as a defence against insect herbivores: contrasting effects on folivores and a phloem feeder. *Journal of Animal Ecology* 75:595–603.

Massey, F.P., and S.E. Hartley. 2009. Physical defences wear you down: progressive and irreversible impacts of silica on insect herbivores. *Journal of Animal Ecology* 78**:**281–291.

Matichenkov, V.V., and D.V. Calvert. 2002. Silicon as a Benefical Element for Sugarcane. *Journal American Sociey of Sugarcane Technologies* 22:21-30.

McCarty, R., and L. Schwandes. 2006. Biogenic Silica as an Environmental Indicator, pp. 471-491. In Webb, S.D. (Ed.) *First Floridians and Last Mastodons: The Page-Ladson Site in the Aucilla River.* Springer.

McClenahen, J.R., and D.B. Houston. 1998. Comparative age structure of a relict prairie transition forest and indigenous forest in southeastern Ohio, USA. *Forest Ecology and Management* 112:31-40.

McKee, T.R., and J.L. Brown. 1977. Preparation of Specimens for Electron Microscopic Examination, pp. 809-846. In Dixon, J.B., S.B. Weed, J. A. Kittrick, M.H. Milford, and J.L. White (Eds.) *Minerals in Soil Environments.* Soil Science Society of America, Madison, Wisconsin.

McNaughton, S. A., C. Bolton-Smith, G.D. Mishra, R. Jugdaohsingh, and J.J. Powell. 2005. Dietary Silicon intake in post-menopausal women. *British Journal of Nutrition* 94:813-817.

McNaughton, S.J., M.B. Coughenour, and L.L. Wallace. 1982. Interactive Processes in Grassland Ecosystems, pp. 167-193. In Estes, J.R., R.J. Tyrl, and J.N. Brunken (Eds.) *Grasses and Grasslands Systematics and Ecology.* University of Oklahoma Press: Norman, Oklahoma.

McNaughton, S.J., and J.L. Tarrants. 1983. Grass leaf silicification: Natural selection for an inducible defense against herbivores. *Proceedings of the National Academy of Sciences* 80:790-791.

Meadows, P.S., and J.G. Anderson. 1966. Micro-organisms attached to marine and freshwater sand grains. *Nature* 212:1059-1060.

Metcalfe, C.R. 1960. *Anatomy of the Monocotyledons. I. Gramineae.* Oxford University Press, London. 731 p.

Meunier, J.D., and F. Colin (Eds.). 2001. *Phytoliths: Applications in Earth Sciences and Human History.* A.A. Balkema Publishers, Lisse, Netherlands. 378 p.

Miao, X., J.A. Mason, W. C. Johnson, and H. Want. 2007. High–resolution proxy record of Holocene climate from a loess section in Southwestern Nebraska, USA. *Palaeogeography, Palaeoclimatology, Palaeoecology* 245:368-381.

Middleton, W. 1990. An Improved Method for Extraction of Opal Phytoliths from Tartar Residues on Herbivore Teeth. *The Phytolitharien* 6:2-6.

Middleton, W.D., and I. Rovner. 1994. Extraction of Opal Phytoliths from Herbivore Dental Calculus. *Journal of Archaeological Science* 21:469-473.

Morgan, R.M., and P.A. Bull. 2007. The philosophy, nature and practice of forensic sediment analysis. *Progress in Physical Geography* 31(1):43-58.

Morrow, J.R., and G.D. Webster. 1989. A Cryogenic Density Separation Technique for Conodont and Heavy Mineral Separations. *Journal of Paleontology* 63(6):953-955.

Muhs, D.R., E.A. Bettis, III, J.N. Aleinikoff, J.P. McGeehin, J. Beann, G. Skipp, B.D. Marshall, H.M. Roberts, W.C. Johnson, R. Benton, and T.A. Ager. 2008. Origin and paleoclimatic significance of late Quaternary loess in Nebraska: Evidence from stratigraphy, chronology, sedimentology, and geochemistry. *Geological Society of America Bulletin* 120:1378-1407.

Mulholland, S.C. 1982. Various Wet-Ashing Procedures for Phytolith Extraction from Plants. *Phytolitharien Newsletter* 1:5.

Mulholland, S.C. 1986a. Classification of Grass Silica Phytoliths, pp. 41-52. In Rovner, I. (Ed.) *Plant Opal Phytolith Analysis in Archaeology and Paleoecology* Occasional Papers No. 1 of the Phytolitharien. North Carolina State University, Raleigh.

Mulholland, S.C. 1986b. Identification of Plants in a Sediment*, pp. 123-129. In Rovner, I. (Ed.) *Plant Opal Phytolith Analysis in Archaeology and Paleoecology* Occasional Papers No. 1 of the Phytolitharien. North Carolina State University, Raleigh.

Mulholland, S.C. 1986c. Phytolith studies at Big Hidatsa, North Dakota: Preliminary results*, pp. 21-24. In Clambey, G.K., and R.H. Pemble (Eds.) *The Prairie: Past, Present and Future. Proceedings of the Ninth North American Prairie Conference, July* 29 *to August 1, 1984, Moorhead, Minnesota.* Tri-College University Center for Environmental Studies, Fargo, North Dakota.

Mulholland, S.C. 1989. Phytolith Shape Frequencies in North Dakota Grasses: A Comparison to General Patterns. *Journal of Archaeological Science* 16:489-511.

Mulholland, S.C. 1993. A Test of Phytolith Analysis at Big Hidatsa, North Dakota*, pp. 131-145. In Pearsall, D.M., and D.R. Piperno (Eds.) *Current Research in Phytolith Analysis: Applications in Archaeology and Paleoecology* MASCA Research Papers in Science and Archaeology, Vol. 10. The University Museum of Archaeology and Anthropology, University of Pennsylvania, Philadelphia.

Mulholland, S.C., E.J. Lawlor, and I. Rovner. 1992. Annotated Bibliography of Phytolith Systematics*, pp. 277-322. In Rapp, G., Jr., and S.C. Mulholland (Eds.) *Phytolith Systematics: Emerging Issues*. Plenum Press, New York.

Mulholland, S.C., and C. Prior. 1993. AMS Radiocarbon Dating of Phytoliths*, pp. 21-23. In Pearsall, D.M., and D.R. Piperno (Eds.) *Current Research in Phytolith Analysis: Applications in Archaeology and Paleoecology* MASCA Research Papers in Science and Archaeology, Vol. 10. The University Museum of Archaeology and Anthropology, University of Pennsylvania, Philadelphia.

Mulholland, S.C., and G. Rapp, Jr. 1989. Characterization of Grass Phytoliths for Archaeological Analysis. *Materials Research Society Bulletin 14(3):36-39.* Errata, *MRS Bulletin* 14(5):50.

Mulholland, S.C., and G. Rapp, Jr. 1992b. A Morphological Classification of Grass Silica-Bodies*, pp. 65-89. In Rapp, G., Jr., and S.C. Mulholland (Eds.) *Phytolith Systematics: Emerging Issues*. Plenum Press, New York.

Mulholland, S.C., G.R. Rapp, Jr., and J.A. Gifford. 1982. Phytoliths, pp. 117-137. In Rapp, G.R., Jr., and J.A. Gifford (Eds.) *Troy: The Archaeological Geology*. Princeton University Press, Cincinnati.

Mulholland, S.C., G. Rapp, Jr., and A.L. Ollendorf. 1988. Variation in phytoliths from corn leaves. *Canadian Journal of Botany* 66:2001-2008.

Muller, W.E.G., K.P. Jochum, B. Stoll, and X. Wang. 2008. Formation of Giant Spicule from Quartz Glass by the Deep Sea Sponge *Monorhaphis*. *Chem. Mater.*, 20 **(**14**):**4703–4711.

Murray, R.C. 2004. *Evidence from the Earth.* Mountain Press, Missoula, Montana. 226 p.

Murray, R.C., and J. Tedrow. 1992. *Forensic Geology*. Prentice Hall, Englewood Cliffs, New Jersey.

Murray. R.C., and L.P. Solebello. 2002. Forensic Examination of Soil, pp. 615-633. In Saferstein, R. (Ed.) *Forensic Science Handbook* Volume 1. Prentice Hall, Upper Saddle River, New Jersey.

Myers, J.H., and D. Bazely. 1991. Thorns, Spines, Prickles, and Hairs: Are They Stimulated by Herbivory and do They Deter Herbivores?, pp. 325-344. In Tallamy, D.W., and M.J. Raupp (Eds.) *Phytochemical Induction by Herbivores.* John Wiley & Sons, Inc., New York.

Neethirajan, S., R. Gordon, and L. Wang. 2009. Potential of silica bodies (phytoliths) for nanotechnology. *Trends in Biotechnology* 27(8):461-467.

Newman, R.H. 1986. Fine biogenic silica fibres in sugar cane: a possible hazard. *Ann. Occup. Hyg.* 30(3):365-370.

Newman, R.H. 1986b. Association of Biogenic Silica with Disease. *Nutrition and Cancer* 8(3):217-221.

Newman, R.H., and A.L. MacKay. 1983. Silica Spicules in Canary grass. *Annals of Botany* 52:927-929.

Neymark. L.A., Y.V. Amelin, and J.B. Paces. 2000. ^{206}Pb—^{230}Th—^{234}U—^{238}U and ^{207}PB—^{235}U geochronology of Quaternary opal, Yucca Mountain, Nevada. *Geochimica et Cosmochimica Acta* 64(17):2913-2928.

Nordt, L., J. von Fisher, and L. Tieszen. 2007. Late Quaternary temperature record from buried soils on theNorth American Great Plains. *Geology* 35(2):159-162.

O'Neill, C.H., G.M. Hodges, P.N. Riddle, P.W. Jordan, R.H. Newman, R.J. Flood, and E.C. Toulson. 1980. A Fine Fibrous Silica Contaminant of Flour in the High Oesophageal Cancer Area of North-east Iran. *International Journal of Cancer* 26:617-628.

O'Neill, C., P. Jordan, T. Bhatt, and R. Newman. 1986. Silica and oesophageal cancer, pp. 214-243. In *Silicon Biochemistry* Ciba Foundation Symposium No 121, Chichester, UK, John Wiley and Sons.

O'Neill, C., Q.-Q. Pan, G. Clarke, F.-S. Liu, G. Hodges, M. Ge, P. Jordan, Y.-M. Chang, R. Newman, and E. Toulson. 1982. Silica Fragments from Millet Bran in Mucosa Surrounding Oesophageal Tumors in Patients in Northern China. *The Lancet* 319:1202-1206.

Osterrieth, M., M. Madella, D. Zurro and M. F. Alvarez. 2009. Taphonomical aspects of silica phytoliths in the loess sediments of the Argentinean Pampas. *Perspectives on Phytolith Research: 6th International Meeting on Phytolith Research. Quaternary International* 193:70-79.

Paces, J.B., L.A. Newark, J.L. Wooden, and H.M. Persing. 2004. Improved spatial resolution for U-series dating of opal at Yucca Mountain, Nevada, USA, using ion-microprobe and microdigestion methods. *Geochimica et Cosmochimica Acta* 68(7):1591-1606.

Palmer, P.G. 1976. Grass cuticles: A new paleoecological tool for East African lake sediments. *Canadian Journal of Botany* 54:1725-1734.

Palmer, P.G., and S. Gerbeth-Jones. 1986. A scanning electron microscope survey of the epidermis of East African grasses: IV. *Smithsonian Contributions to Botany,* No. 62. Smithsonian Institution Press, Washington, D.C. 120 p.

Palmer, P.G., and S. Gerbeth-Jones. 1988. A scanning electron microscope survey of the epidermis of East African grasses, V, and West African supplement. *Smithsonian Contributions to Botany,* No. 67. Smithsonian Institution Press, Washington, D.C. 157 p.

Palmer, P.G., S. Gerbeth-Jones, and S. Hutchinson. 1985. A scanning electron microscope survey of the epidermis of East African grasses: III. *Smithsonian Contributions to Botany,* No. 55. Smithsonian Institution Press, Washington, D.C. 136 p.

Palmer, P.G., and A.E. Tucker. 1981. A scanning electron microscope survey of the epidermis of East African grasses: I. *Smithsonian Contributions to Botany,* No. 49. Smithsonian Institution Press. Washington, D.C. 84 p.

Palmer, P.G., and A.E. Tucker. 1983. A scanning electron microscope survey of the epidermis of East African grasses: II. *Smithsonian Contributions to Botany,* No. 53. Smithsonian Institution Press, Washington, D.C. 72 p.

Parr, J.F. 2002. A comparison of heavy liquid floatation and microwave digestion techniques for the extraction of fossil phytoliths from sediments. *Review of Palaeobotany and Palynology* 120:315-336.

Parr, J.F. 2006. Effect of Fire on Phytolith Coloration. *Geoarchaeology: An International Journal* 21(2):171-185.

Parr, J.F., V. Dolic, G. Lancaster, and W.E. Boyd. 2001. A microwave digestion method for the extraction of phytoliths from herbarium specimens. *Review of Palaeobotany and Palynology* 116:203-212.

Parr, J.F., and L.A. Sullivan. 2005. Soil carbon sequestration in phytoliths. *Soil Biology and Biochemistry* 37:117-124.

Parry, D.W. and M.J. Hodson. 1982. Silica Distribution in the Caryopsis and Inflorescence Bracts of Foxtail Millet *(Setaria italica* (L.) Beauv.) and its Possible Significance in Carcinogenesis. *Annals of Botany* 49:531-540.

Parry, D.W., M.J. Hodson, and A.G. Sangster. 1984. Some recent advances in studies of silicon in higher plants. *Philosophical Transactions of the Royal Society of London, Series B* 304:537-549.

Parry, D.W., C.H. O'Neill, and M.J. Hodson. 1986. Opaline Silica Deposits in the Leaves of *Bidens pilosa* L. and their Possible Significance in Cancer. *Annals of Botany* 58:641-647.

Pearsall, D.M. 1978. Phytolith Analysis of Archaeological Soils: Evidence for Maize Cultivation in Formative Ecuador. *Science* 199:177-178.

Pearsall, D.M. 1979. The application of ethnobotanical techniques to the problem of subsistence in the Ecuadorian Formative. Ph.D. dissertation, University of Illinois. 270 p.

Pearsall, D.M. 1987. Evidence for Prehistoric Maize Cultivation on Raised Fields at Peñon del Rio, Guayas, Ecuador, pp. 279-295. In Denevan, W. M., K. Mathewson, and G. Knapp (Eds.) *Prehispanic Agricultural Fields in the Andean Region. BAR Int. Ser.* 359i, Oxford.

Pearsall, D.M. 1989. *Paleoethnobotany: A Handbook of Procedures.* Academic Press, New York. 470 p.

Pearsall, D.M. 2000. *Paleoethnobotany: A Handbook of Procedures.* 2nd Ed. Academic Press, San Diego. 700 p.

Pearsall, D.M., and R.H. Dinan. 1992. Developing a Phytolith Classification System, pp. 37-64. In Rapp, G., Jr., and S.C. Mulholland (Eds.) *Phytolith Systematics: Emerging Issues*. Plenum Press, New York.

Pearsall, D.M., and D.R Piperno. 1990. Antiquity of Maize Cultivation in Ecuador: Summary and Reevaluation of the Evidence. *American Antiquity* 55:324-337.

Pearsall, D.M., and D.R. Piperno (Eds.). 1993. *Current Research in Phytolith Analysis: Applications in Archaeology and Paleoecology.* MASCA Research Papers in Science and Archaeology, Vol. 10. The University Museum of Archaeology and Anthropology, University of Pennsylvania, Philadelphia. 211 p.

Pearsall, D.M., D.R. Piperno, E.H. Dinan, M. Umlauf, Z. Zhao, and R.A. Benfer, Jr. 1995. Distinguishing Rice *(Oryza sativa* Poaceae) from Wild *Oryza* Species through Phytolith Analysis: Results of Preliminary Research. *Economic Botany* 49:183-196.

Pinilla, A., J. Juan- Tresserras, and M. J. Machado (Eds.). 1997. *The State-of the-Art of Phytoliths in Soils and Plants.* Monografias del Centro de Ciencias Medioambientales, Consejo Superior de Investigaciones Cientificas, Madrid. 292 p.

Piperno, D.R. 1984. A Comparison and Differentiation of Phytoliths from Maize and Wild Grasses: Use of Morphological Criteria. *American Antiquity* 49:361-383.

Piperno, D.R. 1985a. Phytolithic analysis of geological sediments from Panama. *Antiquity* 59:13-19.

Piperno, D.R. 1985b. Phytolith Taphonomy and Distributions in Archeological Sediments from Panama. *Journal of Archaeological Science* 12:247-267.

Piperno, D.R. 1985c. Phytolith Analysis and Tropical Paleo-Ecology: Production and Taxonomic Significance of Siliceous Forms in New World Plant Domesticates and Wild Species. *Review of Paleobotany and Palynology* 45:185-228.

Piperno, D.R. 1988. *Phytolith Analysis: An Archaeological and* Geo*logical Perspective.* Academic Press, San Diego. 280 p.

Piperno, D.R. 2001. On Maize and the Sunflower. *Science* 292:2260-2261.

Piperno, D.R. 2006. *Phytoliths A Comprehensive Guide for Archaeologists and Paleoecologists.* AltaMira Press, New York. 237 p.

Piperno, D.R., and I. Holst. 1998. The Presence of Starch Grains on Prehistoric Stone Tools from the Humid Neotropics: Indications of Early Tuber Use and Agriculture in Panama. *Journal of Archaeological Science* 25:765-776.

Piperno, D.R., and D.M. Pearsall. 1998a. The Silica Bodies of Tropical American Grasses: Morphology, Taxonomy, and Implications for Grass Systematics and Fossil Phytolith Identification. *Smithsonian Contributions to Botany* No. 85. Smithsonian Institution Press, Washington, D.C. 40 p.

Piperno, D.R., and D.M. Pearsall. 1998b. *The Origins of Agriculture in the Lowland Neotropics.* Academic Press, San Diego. 400 p.

Piperno, D.R., and H.–D. Sues. 2005. Dinosaurs Dined on Grass. *Science* 310:1126-1128.

Pla, S., and N.J. Anderson. 2005. Environmental Factors Correlated with Chrysophyte Cyst Assemblages in Low Arctic Lakes of Southwest Greenland. *Journal of Phycology* 41(5):957-974.

Powell, J.J., S.A. McNaughton, R. Jugdaohsignh, S.H.C. Anderson. J. Dear, K. Khot, L. Mowatt, K.L. Gleason. M. Sykes, R.P.H. Thompson, C. Bolton-Smith, and M.J. Hodson. 2005. A provisional database for the silicon content of foods in the United Kingdom. *British Journal of Nutrition* 94:804-812.

Powers, A.H., and D.D. Gilbertson. 1987. A Simple Preparation Technique for the Study of Opal Phytoliths from Archaeological and Quaternary Sediments. *Journal of Archaeological Science* 14:529-535.

Prasad, V., C.A.E. Strömberg, H. Alimohammadian, and A. Sahni. 2005. Dinosaur Coprolites and the Early Evolution of Grasses and Grazers. *Science* 310:1177-1180.

Prat, H. 1936. La systématique des Graminées. (Systematics of the Gramineae.) *Annales des Sciences Naturelles, Botanique, Series 10,* 18:165-258.

Presley, D.R., P.E. Hartley, and M.D. Ransom. 2010. Mineralogy and morphological properties of buried polygenetic paleosols formed in late quaternary sediments on upland landscapes of the central plains, USA. *Geoderma* 154(3-4):508-517.

Pye, K. 2007. *Geological and Soil Evidence Forensic Applications*. CRC Press, Boca Raton, Florida. 335 p.

Rapp, G., and C.L. Hill. 2006. *Geoarchaeology The Earth–Science Approach to Archaeological Interpretation, 2nd Edition*. Yale University Press, London. 339 p.

Rapp, G., Jr., and S.C. Mulholland (Eds.). 1992. *Phytolith Systematics: Emerging Issues*. Plenum Press, New York. 350 p.

Raven, P.H., and G.B. Johnson. 1995. *Understanding Biology Third Edition*. Wm. C. Brown Publishing Company, Dubuque, Iowa.

Reider, R.G., G.A. Huckleberry, and G.C. Frison. 1988. Soil Evidence for Postglacial Forest-Grassland Fluctuation in the Absaroka Mountains of Northwestern Wyoming, U.S.A. *Arctic and Alpine Research* 20(2):188-198.

Retallack, G.J. 2001. *Soils of the Past An Introduction to Paleopedology. Second Edition*. Blackwell Science, Oxford. 404 p.

Retallack, G.J., D.P. Dugas, and E.A. Bestland. 1990. Fossil Soils and Grasses of a Middle Miocene East African Grassland. *Science* 247:1325-1328.

Rigby, J.K. (Coordinating Author). 2003. *Treatise on Invertebrate Paleontology Part E Porifera revised Volume 2 Introduction to the Porifera*. The Geological Society of America, Boulder, CO. 384 p.

Rigby, J.K. (Coordinating Author). 2004. *Treatise on Invertebrate Paleontology Part 3 Porifera revised Volume 3 Porifera (Demospongea, Hexactinellida, Heteractinida), Calcarea)*. The Geological Society of America, Boulder, CO.

Rondeau, V., H. Jacqmin-Gadda, D. Commenges, C. Helmer, and J.F. Dartigues. 2009. Aluminum and silica in drinking water and the risk of Alzheimer's disease or cognitive decline: findings from 15-year follow-up of the PAQUID cohort. *American Journal of Epidemiology* 169 (4): 489–96.

Rosen, A.M., and S. Weiner. 1994. Identifying Ancient Irrigation: A New Method Using Opaline Phytoliths from Emmer Wheat. *Journal of Archaeological Science* 21:125-132.

Round, F.E. 1965. The Epipsammon; A Relatively Unknown Freshwater Algal Association. *Br. Phycol. Bull.* 2(6):456-462.

Rovner, I. 1971. Potential of Opal Phytoliths for Use in Paleoecological Reconstruction. *Quaternary Research* 1:343-359.

Rovner, I. (Ed.). 1986a. Plant Opal Phytolith Analysis in Archaeology and Paleoecology. Proceedings of the 1984 Phytolith Research Workshop. North Carolina State University, Raleigh, North Carolina. Occasional Papers No. 1 of the Phytolitharien. Raleigh, N.C. 147 p.

Rovner, I. 1986b. Downward Percolation of Phytoliths in Stable Soils: A Non-Issue, pp. 23-30. In Rovner, I. (Ed.) Plant Opal Phytolith Analysis in Archaeology and Paleoecology Occasional Papers No. 1 of the Phytolitharien. North Carolina State University, Raleigh.

Rovner, I. 2004. Appendix F Phytolith Analysis of Selected Soil Samples from the Puncheon Run Site. *Archaeology of the Puncheon Run Site (7K-C-51) Volume II: Technical Appendices.* The Louis Berger Group, Inc.

Ruhe, R.V. 1965. Quaternary Paleopedology, pp. 755-764. In Wright, H.E., and D.E. Frey *The Quaternary of the United States*. Princeton University Press, Princeton, N.J.

Ruhe, R.V., and G.G. Olson. 1980. Soil Welding. *Soil Science* 130:132-139.

Runge, F. 2000. *Opal-Phytolithe in den Tropen Afrikas.* BoD GmbH, Norderstedt, Germany. 285.

Runge, J., and F. Runge. 1995. Late Quaternary Palaeoenvironmental Conditions in Eastern Zaire (Kivu) Deduced from Remote Sensing, Morpho-Pedological and Sedimentological Studies (Phytoliths, Pollen, C-14 data), pp. 109-122. In *2nd Symposium on African Palynology, Tervuren (Belgium). Publ. Occas. CIFEG 1995/31, CIFEG.*

Runge, F., and J. Runge. 1997. Opal Phytoliths in East African Plants and Soils, pp. 71-81. In Pinilla, A., J. Juan-Tresserras, and M.J. Machado (Eds.) *The State-of-the-Art of Phytoliths in Soils and Plants*. Monografías del Centro de Ciencias Medioambientales, Consejo Superior de Investigaciones Científicas, Madrid.

Russell, E.W. 1973. *Soil Conditions and Plant Growth*. Tenth Edition. Longman, London. 849 p.

Sakr, K. 2006. Effects of Silica Fume and Rice Husk Ash on the Properties of Heavy Weight Concrete. *Journal of Materials in Civil Engineering.* 18(3):367-376.

Sandgren, C.D. (Ed.). 1991a. Application of Chrysophyte Stomatocysts in Paleolimnology. *Journal of Paleolimnology* 5.

Sandgren, C.D. 1991b. Chrysophyte reproduction and resting cysts: a paleolimnologist's primer. *Journal of Paleolimnology* 5:1-9.

Sanson, G.C. 2006. The Biomechanics of Browsing and Grazing. *American Journal of Botany* 93(10)1531-1545.

Schaetlz, R.J., and S. Anderson. 2005. *Soils: Genesis and Geomorphology*. Cambridge University Press, New York. 817 p.

Schenk, W.M. 2004. Cereal Murder in Spokane, pp. 165-190. In Houck, M.M. (Ed.) *TRACE EVIDENCE ANALYSIS More Cases in Mute Witnesses*. Elsevier: New York.

Schoeneberger, P.J., D.A. Wysocki, E.C. Benham, and W.D.Broderson (Eds.). 2002. *Field book for describing and sampling soils. Version 2.0.* Natural Resources Conservation Service, National Soil Survey Center, Lincoln, NE.

Schwandes, L.P. and M. E. Collins. 1994. Distribution and Significance of Freshwater Sponge Spicules in Selected Florida Soils. *Trans. Amer. Microsc. Soc.* 113(3):242-257.

Scott, H.D. 2000. *Soil Physics Agricultural and Environmental Applications*. Iowa State University Press, Ames, Iowa. 421 p.

Sears, P.B, and G.C. Couch. 1934. Humus Stratigraphy as a Clue to Past Vegetation in Oklahoma. *Proceedings of the Oklahoma Academy of Science* 15:33-34.

Ségalen, L., J.A. Lee-Thorp, and T. Cerling. 2007. Timing of C4 grass expansion across sub-Saharan Africa. *Journal of Human Evolution* 53:549-559.

Sendulsky, T., and L.G. Labouriau. 1966. Corpos Silicosos de Gramineas dos Cerrados-I. *Anais da Academia Brasileira de Ciencias* 38:159-85.

Sheldrick, B.H., and C. Wang. 1993. Chapter 47 Particle Size Distribution, pp. 499-511. In Carter, M.R. (Ed.) *Soil Sampling and Methods of Analysis.* Lewis Publishers, New York

Shemesh, A., and D. Peteet. 1998. Oxygen isotopes in fresh water biogenic opal – Northeastern US Allerod-Younger Dryas temperature shift. *Geophysical Research Letters* 25(11):1935-1938.

Shringarpure, R., S. Venugopal, L.T. Clark, D. R. Allee, and E. Bawolek. 2008. Localization of Gate Bias Induced Threshold Voltage Degradation in a-Si:H TFTs. *IEEE Electron Device Letters* 29(1):93-95.

Slatyer, R.L., and S.A. Taylor. 1960. Terminology in plant and soil-water relations. *Nature* (London) 187:922-924.

Smith, F.A., and K.B. Anderson. 2001. Characterization of Organic Compounds in Phytoliths: Improving the Resolving Power of Phytolith δ13C as a Tool for Paleoecological Reconstruction of C3 and C4 Grasses*,* pp. 317-327. In Meunier, J.-D., and E. Colin (Eds.) *Phytoliths: Applications in Earth Sciences and Human History.* A.A. Balkema Publishers, Lisse, Netherlands.

Smith, F.A., and J.W.C. White. 2004. Modern calibration of phytolith carbon isotope signatures for C3/C4 paleograssland reconstruction. *Palaeogeography, Palaeo-climatology, Palaeoecology* 207:277-304.

Smithson, F. 1956. Plant Opal in Soil. *Nature* 178:107.

Smithson, F. 1958. Grass Opal in British Soils. *Journal of Soil Science* 9:148-155.

Smithson, F. 1959. Opal Sponge Spicules in Soil. *Journal of Soil Science* 10(1):105-109.

Soil Survey Staff. 1992. *Keys to Soil Taxonomy*, *Fifth Edition.* SMSS technical monograph No. 19. Blacksburg, Virginia, Pocahontas Press, Inc. 556 p.

Soil Survey Staff. 1999. *Soil Taxonomy A Basic System of Soil Classification for Making an Interpreting Soil Surveys*. United States Department of Agriculture Natural Resources Conservation Services Agriculture Handbook Number 436. U.S. Government Printing Office, Washington, D.C. 869 p.

Sondahl, M.R., and L.G. Labouriau. 1970. Corpos silicosos de gramineas dos Cerrados. IV. (Silica bodies of grasses from the "Cerrados." IV.) *Pesquisa Agropecuraria Brasileira* 5:183-207.

Sosman, R.B. 1965. *The Phases of Silica*. Rutgers University Press, New Brunswick, New Jersey. 388 p.

Staller, J.E., R.H. Tykot, and B.F. Benz. 2006. *Histories of Maize. Multidisciplinary Approaches to the Prehistory, Linguistics, Biogeography, Domestication, and Evolution of Maize.* Elsevier, New York. 678 p.

Stewart, D.R.M. 1965. The epidermal characters of grasses, with special reference to East African plain species. *Botanische Jahrbucher fur Systematik, Pflanzengeschichte, und flanzengeographie* 84:63-116, 117-174.

Stirling, C.H., D.-C. Lee, J.N. Christensen, and A.N. Halliday. 2000. High-precision in situ ^{238}U-^{234}U-^{230}Th isotopic analysis using laser ablation multiple-collector ICPMS. *Geochimica et Cosmochimica Acta* 64(11):3737-3750.

Street-Perrott, F.A., and P.A. Barker. 2008. Biogenic silica: a neglected component of the coupled global continental biogeochemical cycles of carbon and silicon. *Earth Surf. Process. Landforms* 33:1436–1457.

Strömberg, C.A.E. 2002. The origin and spread of grass-dominated ecosystems in the late Tertiary of North America: preliminary results concerning the evolution of hypsodonty. *Palaeogeography, Palaeoclimatology, Palaeoecology* 177:59-75.

Strömberg, C.A.E. 2007. Can slide preparation methods cause size biases in phytolith assemblages? Results from a preliminary study, pp. 1-12. In Madella, M., and D. Zurro (Eds.) *Plants, People and Places Recent Studies in Phytolith Analysis.* Oxbow Books, Oxford.

Strömberg, C.A.E. 2009a. Methodological concerns for analysis of phytolith assemblages: Does count size matter? *Perspectives on Phytolith Research: 6th International Meeting on Phytolith Research. Quaternary International* 193:124-140.

Strömberg, C.A.E. 2009b. Reply to Comment on "Methodological concerns for analysis of phytolith assemblages: Does count size matter?" (A. Alexandre and L. Brémond). *Perspectives on Phytolith Research: 6th International Meeting on Phytolith Research. Quaternary International* 193:143-145.

Sudbury, B. 1976. Ka-3, The Deer Creek Site. An Eighteenth Century French Contact Site in Kay County, Oklahoma. *Bulletin of the Oklahoma Anthropological Society* XXIV:1-135.

Sudbury, J.B. 2000. SEM Evaluation of Plant Remains in Selected Soil and Ash Samples from the Waugh Site, 34HP42: A Folsom Campsite and Buffalo Processing Station in Western Oklahoma. MS in possession of the author. 58 p.

Sudbury, J.B. 2003. Soil/Dust from Unpaved Roadways–An Important Evidentiary Tool in the Fight Against Crime and Terrorism. Manuscript in author's files (3-25-03). 35 p.

Sudbury, J.B. 2006. Appendix C: Phytolith Analysis Indicates Activity Areas at a Late Prehistoric Site (34CN176), pp. 145-156. In Drass, R.R., and M.W. McKay, *A Reconnaissance Survey Defining Prehistoric through Historic Occupation of the Divide Separating the Canadian and North Canadian Rivers between Geary and Calumet, Oklahoma*. Oklahoma Archeological Survey, Archeological Resource Survey Report No. 53. The University of Oklahoma, Norman.

Sudbury, J.B. 2007. Sewright Site (39FA1603) Phytolith Analysis. J. S. Enterprises Project Report 2007-2. MS in possession of the author. 56 p.

Sudbury, J.B. 2009a. Phytoliths from Features at Two Gunnison County Archaeological Sites (5GN2404 and 5GN2262) [Appendix C]. In Moore, S., and J. Firor *Archaeological Data Recovery At Six Sites Along The Blue Mesa-Skito 115-Kv Transmission Line, Gunnison County, Colorado*. Western Area Power Administration Contract Report.

Sudbury, J.B. 2009b. *Politics of the Fur trade: Clay Tobacco Pipes at Fort Union Trading Post NHS (32WI17)*. Clay Pipes Press, Ponca City, Oklahoma. 225 p.

Swann, G.E.A., and M.J. Leng. 2009. A review of diatom $\delta^{18}O$ in palaeoceanography. *Quaternary Science Reviews* 28(5-6):384-398.

Sweeney, M.R., A.J. Busacca, C.A. Richardson, M. Blinnikov, and E.V. McDonald. 2004. Glacial anticyclone recorded in Palouse loess of northwestern United States. *Geology* 32(8):705-708.

Sylvia, D.M., J.J. Fuhrmann, P.G. Hartel, and D.A. Zuberer. 1999. *Principles and Applications of Soil Microbiology*. Prentice Hall, Upper Saddle River, New Jersey. 550 p.

Taiz, L, and E. Zeiger. 2002. *Plant Physiology Third Edition*. Sinauer Associates, Inc., Sunderland, Massachusetts. 690 p.

Tarbuck, E.J., and F.K. Lutgens. 1999. *EARTH An Introduction to Physical Geology* Sixth Edition. Prentice Hall, Upper Saddle River, New Jersey. 638 p.

Tassara, G., and M. Osterrieth. 2008. Silicofitolitos en Artefactos de Molienda de Sitios Arqueológicos del Área Interserrana, Buenos Aires. Un Estudio Preliminar [Silica phytoliths on Ground Stone Artifacts from Archaeological Sites in the Buenos Aires Province's Interserrana Area, Argentina. A Preliminary Study], pp. 163-171. In Korstanje, M.A. and M. Babot (Eds.) *Matices Interdisciplinarios en Estudios Fitolíticos y de Otros Microfósiles* [*Interdisciplinary Nuances in Phytoliths and Other Microfossil Studies*]. *BAR Int. Ser.* 1870.

Teaford, M.F., P.W. Lucas, P.S. Ungar, and K.E. Glander. 2006. Mechanical Defenses in Leaves Eaten by Costa Rican Howling Monkeys (Alouatta palliate). *American Journal of Physical Anthropology* 129:99-104.

Tegen, I. 2003. Modeling the mineral dust aerosol cycle in the climate system. *Quaternary Science Reviews* 22:1821-1834.

Teixeira da Silva, S., and L.G. Labouriau. 1970. Corpos silicosos de gramineas dos Cerrados. III. (Silica bodies of grasses from the "Cerrados." III.) *Pesquisa Agropecuraria Brasileira* 5:167-182.

Teixeira, S.R., J.B. Dixon, G.N. White, and L.A. Newsom. 2002. Charcoal in Soils: A Preliminary View, pp. 819-830. In Dixon J.B., and D.G. Schultze (Eds.) *Soil Mineralogy with Environmental Applications*. Soil Science Society of America, Inc., Madison, Wisconsin.

Thomasson, J.R. 1980. *Paleoriocoma* (Gramineae, Stipeae) from the Miocene of Nebraska: Taxonomic and Phylogenetic Significance. *Systematic Botany* 5:233-240.

Thomasson, J.R., M.E. Nelson, and R.J. Zakrzewski. 1986. A Fossil Grass (Gramineae: Chloridoideae) from the Miocene with Kranz Anatomy. *Science* 233: 876-878.

Thompson, L.G., and E. Mosley-Thompson. 1981. Microparticle Concentration Variations Linked with Climatic Change: Evidence from Polar Ice Cores. *Science* 212:812-815.

Thorn, V.C. 2004. *An Annotated Bibliography of Phytoliths Analysis and Atlas of Selected New Zealand Subantarctic and Subalpine Phytoliths*. Antarctic Data Series No. 29. Victoria University of Wellington. 67 p.

Thurmond, P. 1990. Late Paleoindian Utilization of the Dempsey Divide on the Southern Plains. *Plains Anthropological Society Memoir* 25.

Thurmond, J.P., C.C. Freeman, K. Kindscher, H. Loring, C.A. Morse, and B.W. Hoagland. 2002. Preliminary Report of an Ethnobotanical Survey along the Ogallala Ecotone on the Dempsey Divide Roger Mills County, Oklahoma. *Oklahoma Archeology* 50(2):10-37.

Tibbet, M., and D. O. Carter (Eds.). 2008. *Soil Analysis in Forensic Taphonomy Chemical and Biological Effects of Buried Human Remains*. CRC Press, Boca Raton, Florida. 340 p.

Tubb, H.J., M.J. Hodson, and G.C. Hodson. 1993. The Inflorescence Papillae of the Triticeae: a New Tool for Taxonomic and Archaeological Research. *Annals of Botany* 72:537-545.

Twiss, P.C. 1980. Opal Phytoliths as Indicators of C3 and C4 Grasses. Abstracts with Programs, Geological Society of America 12(1):17.

Twiss, P.C. 1983. Dust Deposition and Opal Phytoliths in the Great Plains. *Transactions of the NebraskaAcademy of Sciences* 11:73-82.

Twiss, P.C. 1986. Morphology of Opal Phytoliths in C3 and C4 Grasses, pp. 4-12. In Rovner, I. (Ed.) *Plant Opal Phytolith Analysis in Archaeology and Paleoecology* Occasional Papers No. 1 of the Phytolitharien. North Carolina State University, Raleigh.

Twiss, P.C. 1987. Grass-opal phytoliths as climatic indicators of the Great Plains Pleistocene. *In Quaternary Environments of Kansas,* pp. 179-188. Johnson, W.C. (Ed.) Kansas *Geological Survey Guidebook Series* 5.

Twiss, P.C. 1992. Predicted World Distribution of C3 and C4 Grass Phytoliths, pp. 113-128. In Rapp, G., Jr., and S.C. Mulholland (Eds.) *Phytolith Systematics: Emerging Issues*. Plenum Press, New York. Twiss, P.C. 2001. A Curmudgeon's View of Grass Phytolithology, pp. 7-25. In Meunier, J.-D., and E. Colin (Eds.) *Phytoliths: Applications in Earth Sciences and Human History.* A.A. Balkema Publishers, Lisse, Netherlands.

Twiss, P.C. 2001. A Curmudgeon's View of Grass Phytolithology, pp. 7-25. In Meunier, J.-D., and E. Colin (Eds.) *Phytoliths: Applications in Earth Sciences and Human History.* A.A. Balkema Publishers, Lisse, Netherlands.

Twiss, P.C., E. Suess, and R.M. Smith. 1969. Morphological Classification of Grass Phytoliths. *Soil Science Society of America Proceedings* 33:109-115.

Tyrl, R.J., T.G. Bidwell, R.E. Masters, and B.P. Jansen. 2002. *Field Guide to Oklahoma Plants Commonly Encountered Prairie, Shrubland, and Forest Species*. Oklahoma State University, Stillwater, OK. 515 p.

Valentine, K.W.G., and J.B. Dalrymple. 1976. Quaternary Buried Paleosols: A Critical Review. *Quaternary Research* 6:209-222.

Vankat, J.L. 1979. The Natural Vegetation of North America An Introduction. John Wiley & Sons, New York. 261 p.

Vanlandingham, Sam L. 2008. Diatoms and Chrysophyte Cysts: Powerful Tools for Determining Paleoenvironment and Age of the Hueyatlaco Early Man Site, Puebla, Mexico. Joint Meeting of The Geological Society of America, Soil Science Society of America, American Society of Agronomy, Crop Science Society of America, Gulf Coast Association of Geological Societies with the Gulf Coast Section of SEPM. Geological Society of America *Abstracts with Programs*, 40(6):241.

Vehik, S.C. 2001. Hunting and Gathering Tradition: Southern Plains, pp. 146-158. In DeMallie, R.J. (Ed.) *Handbook of North American Indians Volume 13:1 Plains*. Smithsonian Institution Press, Washington, D.C.

Virden, S.T. 1886. Discomforts arising from sponge spicules in pond-soils. *Science* VII:218.

Vlamis, J., and D.E. Williams. 1967. Manganese and silicon interaction in the Gramineae. *Plant Soil* 2:131-140.

Waltman, S.W., and E.J. Ciolkosz. 1995. Prairie Soil Development in Northwestern Pennsylvania. *Soil Science* 160(3):199-208.

Watanabe, N. 1968. Spodographic Evidence of Rice from Prehistoric Japan. *Journal of Faculty of Science, University of Tokyo, Section 5,* 3:217-235.

Waters, M.R. 1996. *Principles of Geoarchaeology A North American Perspective*. University of Arizona Press, Tucson. 398 p.

Web Soil Survey. nd. http://websoilsurvey.nrcs.usda.gov/app/HomePage.htm

Wendland, W.M. 1978. Holocene Man in North America: The Ecological Setting and Climatic Background. *Plains Anthropologist* 23(1):273-287.

Wendland, W.M., and R.A. Bryson. 1974. Dating Climatic Episodes of the Holocene. *Quaternary Research* 4:9-24.

Weyl, W.A., and E.C. Marboe. 1967. *The Constitution of Glasses, Volume 2*. Wiley, New York.

Wilding, L.P. 1967. Radiocarbon Dating of Biogenetic Opal. *Science* 156:66-67.

Wilding, L.P., R.E. Brown, and N. Holowaychuk. 1967. Accessibility and Properties of Occluded Carbon in Biogenetic Opal. *Soil Science* 103:56-61.

Wilding, L.P., and L.R. Drees. 1968. Biogenic opal in soils as an index of vegetative history in the Prairie Peninsula*,* pp. 96-103. In Bergstrom, R.E. (Ed.) *The Quaternary of Illinois.* University of Illinois College of Agriculture, Special Publication 14, Urbana.

Wilding, L.P., and L.R. Drees. 1971. Biogenic Opal in Ohio Soils. *Soil Science Society of America Proceedings* 35:1004-1010.

Wilding, L.P., and L.R. Drees. 1974. Contributions of Forest Opal and Associated Crystalline Phases to Fine Silt and Clay Fractions of Soils. *Clays and Clay Minerals* 22:295-306.

Wilkins, G.R., P.A. Delcourt, H.R. Delcourt, F.W. Harrison, and M.R. Turner. 1991. Paleoecology of Central Kentucky since the last Glacial Maximum*. Quaternary Research* 36:224-239.

Williams, M., D. Dunkerley, P. De Deckker, P. Kershaw, and J. Chappell. 2003. *Quaternary EnvironmentsSecond Edition*. Arnold: London. 329 p.

Yeck, R.D. 1969. Selected Characteristics of Opaline Phytoliths Between Some Udolls and Ustolls. Unpublished Ph.D. dissertation, Oklahoma State University. 55p.

Yeck, R.D., and F. Gray. 1969. Preliminary Studies of Opaline Phytoliths from Selected Oklahoma Soils. *Proceedings of the Oklahoma Academy of Science for 1967* 48:112-116.

Yeck, R.D., and F. Gray. 1972. Phytolith Size Characteristics Between Udolls and Ustolls. *Soil Science Society of America Proceedings* 36(4):639-641.

Yool, A., and T. Tyrrell. 2003. *Role of diatoms in regulating the ocean's silicon cycle*. *Global Biogeochemical Cycles* **17:**1103, doi:10.1029/2002GB002018.

Zhao, Z. 1998. The Middle Yangtze region in China Is one place where rice was domesticated: phytolith evidence from the Diaotonghuan Cave, Northern Jiangxi. *Antiquity* 72:885-897.

Zhao, Z., and D.M. Pearsall. 1998. Experiments for Improving Phytolith Extraction from Soils. *Journal of Archaeological Science* 25:587-598.

Zucol, A.F. 1996. Microfitolitos de las Poaceae argentinas: I. Microfitolitos foliares de algunas especies del género *Stipa* (Stipeae: Arundinoideae), de la provincia de Entre Ríos. *Darwiniana* 34:151-172.

Zucol, A.F. 1998. Microfitolitos de las Poaceae Argentinas: II. Microfitolitos Foliares de Algunas Especies del Genero *Panicum* (Poaceae, Paniceae) de la Provincia de Entre Ríos. *Darwiniana* 36:29-50.

Zucol, A. F., and M. Bonomo. 2008. Estudios Arqueobotánicos del Sitio Nutria Mansa I. (Partido de General Alvarado, Provincia de Buenos Aires): II. AnáIisis Fitolíticos Comparativos de Artefactos de Molienda [Archaeobotanical Studies of The Nutria Mansa I Site (General Alvarado, Buenos Aires Province): II. Comparative Phytolith Analysis of Milling Stone Artefacts], pp. 173-185. In Korstanje, M.A. and M. Babot (Eds.) *Matices Interdisciplinarios en Estudios Fitolíticos y de Otros Microfósiles* [*Interdisciplinary Nuances in Phytoliths and Other Microfossil Studies*]. *BAR Int. Ser.* 1870.

APPENDICES

APPENDIX A

Amorphous Silica in Foods

Comments about sources of silicon in the diet are of interest. Despite the health

warnings noted in the literature review regarding silicon inhalation and ingestion[57], fine

amorphous silica is now widely used as a common food additive. Silicon dioxide at

levels of less than 2% has been an approved food additive for over three decades (Iler

1979:757). This product goes by a variety of names, and is widely advertised as an

approved anti-caking ("keep free flowing") food additive. This silicon component is

probably best described by the sales literature phrase of precipitated amorphous silica,

but is apparently marketed commercially under a variety of descriptors—based on

specific manufacturing protocols to produce numerous closely related materials including

fumed silica and colloidal silica.

Sosman (1965:231) referred to fumed and precipitated silica as "micro-

amorphous granular silica". One commercial form of precipitated silica is called "white

carbon black" by a number of manufacturers, a number of whom identify the material

specifically as "hydrated silica dioxide"[58] and indicate that it is used as a filler in rubber

---

[57] The reported ingestion problem is presumably due to phytoliths acting as an abrasive (irritant) problem in food.

[58] Described and for sale by http://sanjichemical.en.made-in-china.com/product/bevQPsMTAHkW/China-White-Carbon-Black.html and http://www.made-in-china.com/showroom/amy-guo/product-detailrbTxjqSGCDWC/China-White-Carbon-Black.html (11-27-09). Another producer indicates that white carbon is used in production of tires, shoe soles, medicine, feedstuff, silicone rubber, and food (http://uboliaxiamen.en.made-in-china.com/product/bqymWYNlCTRe/China-White-Carbon.html (11-27-09)). Yet another producer touts fumed silicas use as a "thickener in milkshakes", as an abrasive in toothpaste, and that its "light-diffusing properties" make it useful in cosmetics (http://may-ally.en.made-in-china.com/product/rovERxAKsDci/China-Fumed-Silica.html (11-27-09)).

tires (thus replacing carbon black)--perhaps implying this material's pervasive presence in our modern world. Silica gel, a well-known separation media used in many laboratory settings, is also amorphous hydrated silicon dioxide (Fried and Sherma 1999:25). Representative MSDSs in Appendix B present useful information about amorphous $SiO_2 \bullet \eta H_2 0$ in commerce including CAS number, numerous synonyms, end-products incorporating the material, and the density of the different product forms.

A brief perusal of in stock kitchen seasoning ingredients[59] show that "silicon dioxide" is present in 5[th®] Season Chili Powder, Cain's[®] Sugar Substitute, Cook Shack Rib Rub, Fruit-Fresh[®], Great Value[TM] Paprika, Head Country All Purpose Championship Seasoning, Mc[®] McCormick Garlic Season-All Seasoned Salt, Tones[®] Lemon Pepper, and Cajun Grill Smokeless No Fry Seasoning.

The ramifications of this widespread use of amorphous silica in food remain to be seen. However, as this is a relatively soluble form of silica, widespread adoption as a common anti-caking agent in foods (and applications in other high volume commercial end uses) may potentially gradually impact the global soluble silicon balance. This new high volume application of fairly soluble silicon (both commercial processing and usage)

---

[59] Other anti-caking food additives encountered during this brief kitchen self-survey include "calcium silicate" (in KP Sugar Substitute [Saccharin], McCormick[®] Garlic Salt, Morton[®] Iodized Salt, S[®] Schilling Meat Tenderizer, Sweet'n Low [Saccharin], and Sweet Plus[®] [Saccharin]), "calcium phosphate" (Sugar Free Crystal Light[®] Diet Soft Drink Mix), "silica gel" (in Original Mesquite Longhorn Grill Seasoning), "sodium silico aluminate" (Best Choice[®] Poultry Seasoning, Pizza Hut[®] Parmesan, Pizza Hut[®] Romano and Hard Grating Cheese Blend), and 'tricalcium phosphate" (Ever-Fresh[TM], Junket[®] Rennet Tablets, L[®] Lawry's Seasoned Salt, McCormick[®] Szechuan Style Pepper blend, and Spice Island[®] Beau Monde[®] Seasoning). Sodium silico aluminate, (alternatively spelled sodium silicoaluminate or sodium silico-aluminate), is also universally present in all individual serving size salt packets that I have observed over the years, presumably suggesting a common sodium chloride supplier (available samples include Arbys[®], Borden[®], Church's Fried Chicken[®], Diamond Crystal Salt Company, Diamond Crystal Specialty Foods, Hardee's[®], Kraft[®], McDonald's[®] Corporation, PPI Portionpac, Red & White International, and Sonic[®]).

could potentially, over time, essentially have the effect of gradually increasing the overall global rate of silica weathering. Although perhaps only a slight possibility, this increased large scale production and marketing of amorphous silica could conceivably result in a small increase in ocean silicon concentration. The global silica cycle and balance is an area of active research (c.f. Yool and Tyrrell 2003; Street-Perrott and Barker 2008; Laurelle et al. 2009). Diatoms are a very important component in this cycle, being recognized as a major silicon cycler (Lopez, Descle´s, Allen, and Bowler 2005) and crucial to CO_2 absorption by the oceans.

The theoretical possibility that increased world-wide synthetic amorphous silica production and use may coincidentally increase overall worldwide silica weathering rates, thereby increasing the ocean Si load, which in turn may result in higher diatom populations which in turn may process more CO_2 and thus potentially impact global warming may be the most important concept to result from this phytolith research project.

APPENDIX B

Representative Material Safety Data Sheets Relevant to Amorphous Silica

1.   Chem Abstracts MSDS Information

2.   WACKER FUMED SILICA HDK H20 Material Safety Data Sheet

3.   Allied High Tech Products, Inc. MATERIAL/CHEMICAL SAFETY

        DATA SHEET

4.   Fisher: Material Safety Data Sheet Silica Gel Desiccant

5.   PPG INDUSTRIES INC -- HI-SIL 233 -- 6850-01-022-7031

The first document, although not as up to date as the following four MSDSs (Material Safety Data Sheets), is included because it provides 28 synonyms for "amorphous fumed silica" and also provides the CAS (Chem Abstract Service) compound numbers.

The Chem Abstracts MSDS information for amorphous fumed silica[60]:

```
MSDS       :  Silica, amorphous fumed
CAS        :  112945-52-5
SYNONYMS   : * Acticel
             * Aerosil
             * Amorphous silica dust
             * Aquafil
             * Cab-O-grip II
             * Cab-O-sil
             * Cab-O-sperse
             * Cataloid
             * Colloidal silica
             * Colloidal silicon dioxide
             * Davison SG-67
             * Dicalite
             * Dri-Die insecticide 67
             * ENT 25,550
             * Fossil flour
             * Fumed silica
             * Fumed silicon dioxide
             * Ludox
             * Nalcoag
             * Nyacol
             * Nyacol 830
             * Nyacol 1430
             * Santocel
             * SG-67
             * Silica, amorphous
             * Silicic anhydride
             * Silikill
             * Vulkasil
```

---

[60] These five pages copied verbatim from http://www.chemcas.com/msds/cas/msds126/112945-52-5.asp (11-29-09).

Catalog of Chemical Suppliers Buyers Distributors And Custom Synthesis & Organic Synthesis & Bio-Synthesis Companies [Silica, amorphous fumed 112945-52-5]

Suppliers:
Not Available
Buyers:
Not Available

```
                        *** CHEMICAL IDENTIFICATION ***

RTECS NUMBER            : VV7310000
CHEMICAL NAME           : Silica, amorphous fumed
CAS REGISTRY NUMBER     : 112945-52-5
OTHER CAS REGISTRY NOS. : 50926-93-7
                          67256-35-3
LAST UPDATED            : 199710
DATA ITEMS CITED        : 18
MOLECULAR FORMULA       : O2-Si
MOLECULAR WEIGHT        : 60.09
WISWESSER LINE NOTATION :  SI  O2
COMPOUND DESCRIPTOR     : Tumorigen
                          Mutagen
SYNONYMS/TRADE NAMES :
   * Acticel
   * Aerosil
   * Amorphous silica dust
   * Aquafil
   * Cab-O-grip II
   * Cab-O-sil
   * Cab-O-sperse
   * Cataloid
   * Colloidal silica
   * Colloidal silicon dioxide
   * Davison SG-67
   * Dicalite
   * Dri-Die insecticide 67
   * ENT 25,550
   * Fossil flour
   * Fumed silica
   * Fumed silicon dioxide
   * Ludox
   * Nalcoag
   * Nyacol
   * Nyacol 830
   * Nyacol 1430
   * Santocel
```

```
      * SG-67
      * Silica, amorphous
      * Silicic anhydride
      * Silikill
      * Vulkasil


                    *** HEALTH HAZARD DATA ***

                   ** ACUTE TOXICITY DATA **

TYPE OF TEST          : LD50 - Lethal dose, 50 percent kill
ROUTE OF EXPOSURE     : Oral
SPECIES OBSERVED      : Rodent - rat
DOSE/DURATION         : 3160 mg/kg
TOXIC EFFECTS :
   Details of toxic effects not reported other than lethal dose value
REFERENCE :
   ARSIM* Agricultural Research Service, USDA Information Memorandum.
   (Beltsville, MD 20705)  Volume(issue)/page/year: 20,9,1966

TYPE OF TEST          : LDLo - Lowest published lethal dose
ROUTE OF EXPOSURE     : Intraperitoneal
SPECIES OBSERVED      : Rodent - rat
DOSE/DURATION         : 50 mg/kg
TOXIC EFFECTS :
   Details of toxic effects not reported other than lethal dose value
REFERENCE :
   AHBAAM Archiv fuer Hygiene und Bakteriologie.  (Munich, Fed. Rep. Ger.)
   V.101-154, 1929-71.  For publisher information, see ZHPMAT.
   Volume(issue)/page/year: 136,1,1952

TYPE OF TEST          : LD50 - Lethal dose, 50 percent kill
ROUTE OF EXPOSURE     : Intravenous
SPECIES OBSERVED      : Rodent - rat
DOSE/DURATION         : 15 mg/kg
TOXIC EFFECTS :
   Lungs, Thorax, or Respiration - acute pulmonary edema
REFERENCE :
   BSIBAC Bolletino della Societe Italiana di Biologia Sperimentale.  (Casa
   Editrice Idelson, Via A. de Gasperi, 55, 80133 Naples, Italy)  V.2- 1927-
   Volume(issue)/page/year: 44,1685,1968

TYPE OF TEST          : LDLo - Lowest published lethal dose
ROUTE OF EXPOSURE     : Intratracheal
SPECIES OBSERVED      : Rodent - rat
DOSE/DURATION         : 10 mg/kg
TOXIC EFFECTS :
   Details of toxic effects not reported other than lethal dose value
REFERENCE :
   AHBAAM Archiv fuer Hygiene und Bakteriologie.  (Munich, Fed. Rep. Ger.)
   V.101-154, 1929-71.  For publisher information, see ZHPMAT.
   Volume(issue)/page/year: 136,1,1952

              ** OTHER MULTIPLE DOSE TOXICITY DATA **

TYPE OF TEST          : TCLo - Lowest published toxic concentration
```

373

```
ROUTE OF EXPOSURE        : Inhalation
SPECIES OBSERVED         : Rodent - rat
DOSE/DURATION            : 154 mg/m3/6H/4W-I
TOXIC EFFECTS :
   Lungs, Thorax, or Respiration - structural or functional change in trachea
   or bronchi
   Biochemical - Enzyme inhibition, induction, or change in blood or tissue
   levels - dehydrogenases
   Biochemical - Metabolism (Intermediary) - other proteins
REFERENCE :
   FAATDF Fundamental and Applied Toxicology.  (Academic Press, Inc., 1 E.
   First St., Duluth, MN 55802) V.1-   1981-  Volume(issue)/page/year:
   16,590,1991
```

                         ** TUMORIGENIC DATA **

```
TYPE OF TEST             : TCLo - Lowest published toxic concentration
ROUTE OF EXPOSURE        : Inhalation
SPECIES OBSERVED         : Rodent - rat
DOSE/DURATION            : 50 mg/m3/6H/2Y-I
TOXIC EFFECTS :
   Tumorigenic - Carcinogenic by RTECS criteria
   Lungs, Thorax, or Respiration - tumors
REFERENCE :
   CREMEX Cancer Research Monographs.  (Praeger Pub., 521 Fifth Ave., New York,
   NY 10175)  V.1-   1983-  Volume(issue)/page/year: 2,255,1986
```

                         ** MUTATION DATA **

```
TYPE OF TEST             : Unscheduled DNA synthesis
ROUTE OF EXPOSURE        : Intratracheal
TEST SYSTEM              : Rodent - rat
DOSE/DURATION            : 120 mg/kg
REFERENCE :
   ENVRAL Environmental Research.  (Academic Press, Inc., 1 E. First St.,
   Duluth, MN 55802) V.1-   1967-  Volume(issue)/page/year: 41,61,1986


TYPE OF TEST             : Body fluid assay
TEST SYSTEM              : Rodent - rat Lung
DOSE/DURATION            : 120 mg/kg
REFERENCE :
   ENVRAL Environmental Research.  (Academic Press, Inc., 1 E. First St.,
   Duluth, MN 55802) V.1-   1967-  Volume(issue)/page/year: 41,61,1986
```

                         *** REVIEWS ***

```
   IARC Cancer Review:Animal Inadequate Evidence
   IMEMDT IARC Monographs on the Evaluation of Carcinogenic Risk of Chemicals
   to Man.  (WHO Publications Centre USA, 49 Sheridan Ave., Albany, NY 12210)
   V.1-   1972-  Volume(issue)/page/year: 42,39,1987


   IARC Cancer Review:Human Inadequate Evidence
   IMEMDT IARC Monographs on the Evaluation of Carcinogenic Risk of Chemicals
   to Man.  (WHO Publications Centre USA, 49 Sheridan Ave., Albany, NY 12210)
   V.1-   1972-  Volume(issue)/page/year: 42,39,1987
```

IARC Cancer Review:Human Inadequate Evidence
IMEMDT IARC Monographs on the Evaluation of Carcinogenic Risk of Chemicals
to Man. (WHO Publications Centre USA, 49 Sheridan Ave., Albany, NY 12210)
V.1-   1972- Volume(issue)/page/year: 68,41,1997

IARC Cancer Review:Group 3
IMEMDT IARC Monographs on the Evaluation of Carcinogenic Risk of Chemicals
to Man. (WHO Publications Centre USA, 49 Sheridan Ave., Albany, NY 12210)
V.1-   1972- Volume(issue)/page/year: 68,41,1997

TOXICOLOGY REVIEW
NTIS** National Technical Information Service. (Springfield, VA 22161)
Formerly U.S. Clearinghouse for Scientific & Technical Information.
Volume(issue)/page/year: CONF-691001

TOXICOLOGY REVIEW
ECRVE8 Environmental Carcinogenesis Reviews. (Marcel Dekker, 270 Madison
Ave., New York, NY 10016) V.3-   1985- Volume(issue)/page/year: 6,197,1988

*** U.S. STANDARDS AND REGULATIONS ***

MSHA STANDARD-dust in air:TWA 20 mppcf
DTLWS* "Documentation of the Threshold Limit Values for Substances in
Workroom Air," Supplements. For publisher information, see 85INA8.
Volume(issue)/page/year: 3,33,1973

*** STATUS IN U.S. ***

EPA TSCA TEST SUBMISSION (TSCATS) DATA BASE, JUNE 1998

NIOSH Analytical Method, 1994: Silica, amorphous, 7501

OSHA ANALYTICAL METHOD #ID-125G

*** END OF RECORD ***

Following is the Fumed silica MSDS copied verbatim from the Wacker web site noting five product end uses[61]:

Material Safety Data Sheet

Material: 60003956   HDK® H20
                      HYDROPHOBIC FUMED SILICA

Version: 1.8 (US)   Date of print: 08/06/2008   Date of last alteration: 08/05/2008

---

1   Product and company identification

1.1   Identification of the substance or preparation:

Commercial product name: HDK® H20
                            HYDROPHOBIC FUMED SILICA

Use of substance / preparation: Industrial.
                            Auxiliary agent for: Plastics , Lacquer , Building
                            materials , elastomer products , cosmetics .

1.2   Company/undertaking identification:

Manufacturer/distributor: Wacker Chemie AG
                            Hanns-Seidel-Platz 4
                            81737 München
                            Germany

Customer information: Wacker Chemical Corporation
                            3301 Sutton Roauc1d
                            Adrian, Michigan 49221-9397
                            USA
                            InfoLine:
                            Tel (517) 264uc1-8240, Fax (517) 264-8740
                            Hours of uc1operation:
                            Monday - Friday, 8 am tuc1o 5 pm (eastern standard
                            time)
                            Corporate websuclite: www.wackersilicones.com

Emergency telephone no. (24h):   (517) 264-8500
Transportation emergency: (800) 424-9300 (CHEMTREC, USA)
                            (703) 527-3887 (CHEMTREC, international)

This MSDS was prepared by the Regulatory Affairs and Product Safety Department (RAPS) of Wacker Chemical Corporation.

---

2   Composition/information on ingredients

2.1   Chemical characterization (substance):

CAS No.	Chemical characteristics
68611-44-9	Hydrophobized highly dispersed silica, synthetic, x-ray amorphous silicon dioxide

2.2   Information on ingredients:

Type	CAS No.	Substance	Content [wt. %] Lower	Upper	Note
INHA	68611-44-9	hydrophobic silicic acid	>=100.0	<=100.0	

Type: HYD - by-product upon hydrolysis, INHA - ingredient, NEBE - by-product, MONO - residual monomer, VERU - impurity, VUL - by-product upon vulcanization. *** **Note:** C1 - IARC carcinogen, C2 - NTP carcinogen, C3 - OSHA carcinogen, NH - non-hazardous, R - reproductive toxin.

Substances listed in the Subsections "HAPS" and "California Proposition 65 Carcinogens / Reproductive Toxins" that are not listed in Section 2 are only present at quantities below 0.1% for California Proposition 65 listed toxins or below 1% for non-carcinogenic HAPS or they are inextricably bound in the product.

---

3   Hazards identification

3.1   Hazards classifications
HMIS® rating (product as packaged):
Health: 1   Fire: 0   Reactivity: 0   PPE: E

Page: 1/8

---

[61] Eight page document copied from http://candmz04.brenntag.ca/MSDS/Fr/00066334.pdf (11-29-09). An MSDS in French is also included in the same pdf file. Searching the MSDS literature reveals the intended end uses of the product; also the final materials where fumed silica is an ingredient are described.

Material Safety Data Sheet

Material: 60003956   HDK® H20
                        HYDROPHOBIC FUMED SILICA

Version: 1.8 (US)   Date of print: 08/06/2008   Date of last alteration: 08/05/2008

Note: Respiratory protection is only recommended in the event that ventilation or engineering controls are unable to maintain exposures below recommended levels; or in the event of a spill or other emergency response situation. Hazardous Materials Identification System and HMIS are registered trademarks of the National Paint and Coatings Association. (HMIS codes are based on contact with the product as packaged and any hydrolysis by-products, if present.)

Canadian WHMIS Classification: None.

3.2   **Emergency overview and potential hazards**
      Physical Hazards:
      Nuisance dust.

      Acute health effects
      Route of entry or possible contact:
      eyes , skin , inhalation
      Eye contact:
      No acute toxic effects are expected. Slight irritation by mechanical effects can not be excluded.
      Skin contact:
      No acute toxic effects are expected. Temporary discomfort like feeling of dryness on the skin.
      Inhalation:
      No acute toxic effects are expected. May cause physical discomfort to the respiratory tract.
      Ingestion:
      Not expected in industrial use.
      Additional information on acute health effects:
      No adverse effects observed at manufacture and during use. Re Sect. 11.2 "Toxicological data", LC50 (inhalative): no mortalities at highest technical achievable concentration (rat) .

3.3   **Further information:**
      Chronic health effects:
      Toxicological test results with a similar hydrophobic amorphous silica: A long term exposure exceeding TLV can lead to damaging effect as a result of mechanical overloading of the respiratory tract. Chronic respiratory exposure: Changes in respiratory organs observed in animal experiments (inflammatory processes) were reversible; no indication of silicosis. Animal tests have shown no indication to carcinogenic or to reproduction effects.
      Medical conditions which may be aggravated by exposure:
      unknown
      Carcinogens/Reproductive toxins:
      This material does not contain any reportable carcinogenic ingredients. This material does not contain any reproductive toxins at or above OSHA or WHMIS reportable levels.

      See Section 11 for Toxicological Information, if any.

4	First-aid measures

4.1   **General information:**
      Get medical attention if irritation occurs or if breathing becomes difficult.
4.2   **After inhalation:**
      If inhaled, remove to fresh air.
4.3   **After contact with the skin:**
      If contact with skin, wash skin with plenty of water or with water and soap.
4.4   **After contact with the eyes:**
      If contact with eyes, immediately flush eyes with plenty of water.
4.5   **After swallowing:**
      Drink plenty of water. Get medical attention if symptoms occur. Show label if possible.

377

Material Safety Data Sheet

5	Fire-fighting measures

5.1   **Flammable properties:**   Method
      Flash point..........................: not applicable
      Boiling point / boiling range........: not applicable
      Lower explosion limit (LEL)..........: not applicable
      Upper explosion limit (UEL)..........: not applicable
      Ignition temperature ....: not applicable
5.2   **Fire and explosion hazards:**
      Material does not burn. Electrostatic charging is possible. Ensure all components are well
      earthed. Use inert gas when working with combustible and explosive liquids.
5.3   **Recommended extinguishing media:**
      Use extinguishing measures appropriate to the source of fire.
5.4   **Unsuitable extinguishing media:**
      not applicable
5.5   **Special exposure hazards arising from the substance or preparation itself, combustion products,**
      resulting gases:
      not applicable
5.6   **Fire fighting procedures:**
      Fire fighters should wear full protective clothing including a self-contained breathing
      apparatus.

6	Accidental release measures

6.1   **Precautions:**
      Avoid dust formation. Do not breathe dust. Wear personal protection equipment (see section 8).
      HAZWOPER PPE Level: D
6.2   **Containment:**
      Cover any spilled material in accordance with regulations to prevent dispersal by wind.
      Spills of material which could reach surface waters must be reported to the United States Coast
      Guard National Response Center's toll free phone number (800) 424-8802.
6.3   **Methods for cleaning up:**
      Take up mechanically and dispose of according to local/state/federal regulations.

7	Handling and storage

7.1   **Handling**
      Precautions for safe handling:
      Avoid dust formation.
      Precautions against fire and explosion:
      Electrostatic discharge possible during transport and processing. Take precautionary measures
      against electrostatic charging. Ensure all parts of equipment are well earthed. Use inert gas
      when working with combustible and explosive liquids. Avoid dust deposit, remove dust regularly.

7.2   **Storage**
      Conditions for storage rooms and vessels:
      none known
      Advice for storage of incompatible materials:
      not applicable
      Further information for storage:
      Keep container tightly closed.

8	Exposure controls and personal protection

8.1   **Engineering controls**
      Ventilation:
      Use only with adequate ventilation.
      Local exhaust:
      In case of dust formation: (To maintain concentration below TLV.) Local exhaust ventilation
      which meets the requirements of ANSI Z9.2 is recommended to control airborne contaminants at
      the point of use.

Material: 60003956   HDK® H20
                             HYDROPHOBIC FUMED SILICA

Version: 1.8 (US)   Date of print: 08/06/2008   Date of last alteration: 08/05/2008

8.2 Associate substances with specific control parameters such as limit values
Maximum airborne concentrations at the workplace:

CAS No.	Material	Type	mg/m³	ppm	Dust fract.
7631-86-9	Silica, amorphous	OSHA PEL	0.8		
	Particulates not otherwise classified	ACGIH TWA	10.0		Inhalable dust/mist
	Particulates not otherwise classified	ACGIH TWA	3.0		Respirable dust/mist

Re Silica, amorphous: The exposure limits given for CAS-No. 7631-86-9 cover all types of synthetic amorphous silica; it appears, that there is an error in the OSHA PEL entry for amorphous silica. There should have been a footnote to the Z-3 Table indicating that the percent SiO2 in formula (80 mg/m3 + % SiO2) refers to crystaline silica content and not to amorphous silica. For evaluation of U.S. exposure measurements WACKER recommends use of the current NIOSH REL (6 mg/m3) instead of the old Z-3 Table entry.
Re Particulates not otherwise classified: The value is for particulate matter containing no asbestos and < 1% crystalline silica (ACGIH).

8.3 Personal protection equipment (PPE)
Respiratory protection:
In case of dust formation: A NIOSH approved particulate respirator with a P95 or higher rating.
Hand protection:
Recommendation: rubber gloves .
Eye protection:
Recommendation: Safety glasses with side shields or chemical safety goggles.
Other protective clothing or equipment:
Barrier cream may be used to prevent dryness of skin. If working with hydrophobic silica powder in areas where flammable or combustible vapors are present, measures to control static electric charging are recommended. This may include wearing personal anti-static clothing and conductive shoes in addition to process and equipment related engineering controls.

8.4 General hygiene and protection measures:
Do not breathe dust/vapor/mist/gas/aerosol. Avoid contact with eyes and skin. Preventive skin protection recommended. Do not eat, drink or smoke when handling.

---

9   Physical and chemical properties

9.1 Appearance
Physical state / form................: solid - powder
Colour..............................: white
Odour...............................: odourless

9.2 Safety parameters   Method
Melting point / melting range........: 1700 °C (3,092 °F)
Boiling point / boiling range........: not applicable
Flash point..........................: not applicable
Ignition temperature ....: not applicable
Lower explosion limit (LEL)..........: not applicable
Upper explosion limit (UEL)..........: not applicable
Vapour pressure......................: not applicable
Density..............................: approx. 2.2 g/cm³ at 20 °C (68 °F)
Bulk density.........................: 30 - 100 kg/m³
Water solubility / miscibility.......: virtually insoluble at 20 °C (68 °F)
pH-Value.............................: 3.6 - 5.6
Viscosity (dynamic)..................: not applicable

9.3 Further information
Thermal decomposition................: > 150 °C (> 302 °F)

10 Stability and reactivity

10.0 General information:
Stable under normal conditions of use.

10.1 Conditions to avoid:
none known

10.2 Materials to avoid:
none known

10.3 Hazardous decomposition products:
If stored and handled in accordance with standard industrial practices and local regulations where applicable: none known .

10.4 Further information:
Hazardous polymerization cannot occur.

11 Toxicological information

11.1 General information:
The following data were taken from literature.

11.2 Toxicological data:
Acute toxicity (LD50/LC50-values relevant to classification):

Exposition	Value/value range	Species	Source
oral	> 5000 mg/kg	rat (Limit Test)	literature
by inhalation	> 0.477 mg/l/4h	rat (Limit Test)	literature

Primary irritation:

Exposition	Effect	Species/Testsystem	Source
to skin	not irritating	rabbit	literature
to eyes	not irritating	rabbit	literature

Experience with man:
Product degreases the skin. By handling the product for many years no damage to health was observed.

12 Ecological information

12.1 Information on elimination (persistence and degradability)

Biodegradation / further information:
Inorganic substance: Not applicable.

Further information:
Separation by sedimentation.

12.2 Behaviour in environmental compartments

Mobility
Insoluble in water.

Further information:
No adverse effects expected.

12.3 Ecotoxicological effects:

Species	Test method	Exp. time	Result	Source
Daphnia magna	acute	24 h	> 10000 mg/l (EC50)	literature
zebra fish (Brachydanio rerio)	acute	96 h	> 10000 mg/l (LC50)	literature

No expected damaging effects to aquatic organisms.

Effects in sewage treatment plants (bacteria toxicity: respiration-/reproduction inhibition):

According to current knowledge adverse effects on water purification plants are not expected. Can be removed mechanically from waste water.

Material Safety Data Sheet

Material: 60003956   HDK® H20
                         HYDROPHOBIC FUMED SILICA

Version: 1.8 (US)   Date of print: 08/06/2008   Date of last alteration: 08/05/2008

12.4 Additional information

Other harmful effects
none known

General information:
No environmental problems expected if handled and treated in accordance with standard
industrial practices and local regulations where applicable.

13 Disposal considerations

13.1 Product disposal
Recommendation:
After solidification, material can be stored together with domestic waste. Observe
local/state/federal regulations.

13.2 Packaging diposal
Recommendation:
Completely discharge containers (no tear drops, no powder rest, scraped carefully). Containers
may be recycled or re-used. Observe local/state/federal regulations.

14 Transport information

14.1 US DOT & CANADA TDG SURFACE
Valuation....................: Not regulated for transport

14.2 Transport by sea IMDG-Code
Valuation....................: Not regulated for transport

14.3 Air transport ICAO-TI/IATA-DGR
Valuation....................: Not regulated for transport

15 Regulatory information

15.1 U.S. Federal regulations

TSCA inventory status and TSCA information:
This material or its components are listed on or are in compliance with the requirements of the
TSCA Chemical Substance Inventory.

TSCA 12(b) Export Notification:
This material does not contain any TSCA 12(b) regulated chemicals.

CERCLA Regulated Chemicals:
This material does not contain any CERCLA regulated chemicals.

SARA 302 EHS Chemicals:
This material does not contain any SARA extremely hazardous substances.

SARA 311/312 Hazard Class:
This product does not present any SARA 311/312 hazards.

HAPS (Hazardous Air Pollutants):
This material does not contain any hazardous air pollutants.

15.2 U.S. State regulations

California Proposition 65 Carcinogens:
This material does not contain any chemicals known to the state of California to cause cancer.

California Proposition 65 Reproductive Toxins:
This material does not contain any chemicals known to the state of California to cause
reproductive effects.

Massachusetts Substance List:
This material contains no listed components.

New Jersey Right-to-Know Hazardous Substance List:
This material contains no listed components.

Material Safety Data Sheet

Material: 60003956   HDK® H20
                                 HYDROPHOBIC FUMED SILICA

Version: 1.8 (US)   Date of print: 08/06/2008   Date of last alteration: 08/05/2008

Pennsylvania Right-to-Know Hazardous Substance List:
This material contains no listed components.

15.3 Canadian regulations

This product has been classified in accordance with the Hazard criteria of the CPR and the MSDS contains all the information required by the CPR.

WHMIS Hazard Classes:
None.

DSL Status:
This material or its components are listed on the Canadian Domestic Substances List.

Non-DSL Chemicals:
This material does not contain any non-DSL chemicals.

Canadian Ingredient Disclosure List:
This material contains no listed components.

15.4 Other international regulations

EU Risk Phrases:

R-Phrase	Description
R-	-

EU Safety Phrases:

S-Phrase	Description
S-	-

Details of international registration status
Listed on or in accordance with the following inventories:
ENCS   - Japan
IECSC - China
PICCS - Philippines
ECL   - Korea
DSL   - Canada
TSCA   - USA
EINECS - Europe
AICS   - Australia
HSNO   - New Zealand

---

16   Other information

16.1 Additional information:

This Material Safety Data Sheet (MSDS) meets the requirements of the Federal OSHA Hazard Communication Standard (29 CFR 1910.1200). This product has been classified according to the hazard criteria of the Controlled Products Regulations (CPR) and the MSDS contains all of the information required by the CPR. This information relates to the specific material designated and may not be valid for such material used in combination with any other materials or in any process. Such information is to the best of our knowledge and belief accurate and reliable as of the date compiled. However, no representation, warranty or guarantee expressed or implied, is made as to its accuracy, reliability or completeness. It is the user's responsibility to satisfy himself as to the suitability and completeness of such information for his own particular use. We do not accept liability for any loss or damage that may occur from the use of this information. Nothing herein shall be construed as a recommendation for uses which infringe valid patents or as extending a license under valid patents. This MSDS provides selected regulatory information on this product, including its components. This is not intended to include all regulations. It is the responsibility of the user to know and comply with all applicable rules, regulations and laws relating to the product being used.

Vertical lines in the left-hand margin indicate changes compared with the previous version.

Material Safety Data Sheet

Material: 60003956   HDK® H20
                           HYDROPHOBIC FUMED SILICA

Version: 1.8 (US)   Date of print: 08/06/2008   Date of last alteration: 08/05/2008

16.2 Glossary of Terms:

ACGIH - American Conference of Governmental Industrial Hygienists	ppm - Parts per Million
DOT - Department of Transportation	SARA - Superfund Amendments and Reauthorization Act
hPa - Hectopascals	STEL - Short Term Exposure Limit
mPa*s - Milli Pascal-Seconds	TSCA - Toxic Substances Control Act
OSHA - Occupational Safety and Health Administration	TWA - Time Weighted Average
PEL - Permissible Exposure Limit	WHMIS - Canadian Workplace Hazardous Materials Identification System

Flash point determination methods	Common name
ASTM D56	Tagliabue (Tag) closed cup
ASTM D92, DIN 51376, ISO 2592	Cleveland open cup
ASTM D93, DIN 51758, ISO 2719	Pensky-Martens closed cup
ASTM D3278, DIN 55680, ISO 3679	Setaflash or Rapid closed cup
DIN 51755	Abel-Pensky closed cup

16.3 Conversion table:

Pressure: 1 hPa * 0.75 = 1 mm Hg = 1 Torr; 1 bar = 1000 hPa
Viscosity: 1 mPa*s = 1 Centipoise (Cp)

The MSDS for a 40-70% suspension of colloidal silica suspension is described on the following two pages.[62]

ALLIED HIGH TECH PRODUCTS, INC.

2376 E. Pacifica Place Rancho Dominguez, CA 90220 (800) 675-1118 www.alliedhightech.com

MATERIAL/CHEMICAL SAFETY DATA SHEET

SECTION 1: CHEMICAL PRODUCT & COMPANY IDENTIFICATION

Product Details

Product Name: 0.06μm White Colloidal Silica Suspension

Allied Item No.: 180-50000, -50005-G, -50010, -50015

Chemical Name: Colloidal Silica Dispersion

Company Identification
Allied High Tech Products, Inc.
2376 East Pacifica Place
Rancho Dominguez, CA 90220
(310) 635-2466

Contact Point
Transportation for United States
Chemtrec (800) 424-9300 * (202) 483-7616

SECTION 2: COMPOSITION/INFORMATION ON INGREDIENT

Chemical Name	CAS No.	Exposure Limits in Air ACGIH TLVorTWA	OSHA PEL	Carcin. Y/N
Colloidal Silica (amorphous) 40-70%	7631-86-9	10 mg/m3	6 mg/m3	

Ingredients are listed on the TSCA Inventory of Chemical Substances.
Those not identified are non-hazardous.

Page 1 of 2:

HMIS Ratings
Health: 1
Flammability: 0
Reactivity: 0

SECTION 3: HAZARDS IDENTIFICATION

Hazard Statement: Inhalation of mist or dust may be harmful. Avoid repeated or prolonged breathing of spray mist or dust.

SECTION 4: FIRST AID MEASURES

	Potential Health Effects	First Aid/ Medical Info.
Eye Contact:	Can cause transient irritations.	Flush with water for 15 minutes, seek medical attention.
Skin Contact:	Can cause transient irritation.	Wash with soap and water.
Inhalation:	May cause irritation to the respiratory tract and lungs if dust is inhaled.	Remove to fresh air. Treat symptoms. Seek medical attention.
Ingestion:	NAIF	Do NOT induce vomiting. Give water. Seek medical attention.

Note: Silica, prolonged exposure to dust/mist can produce pneumoco-niosis. Prolonged inhalation of dust can increase lung injury in individuals with emphysema, asthma or other lung disorders.

SECTION 5: FIRE FIGHTING MEASURES

Extinguishing Media: Not applicable.

SECTION 6: ACCIDENTAL RELEASE MEASURES

Dike to prevent further movement. Contain with absorbent material such as clay, soil or any commercially available absorbent. Shovel reclaimed liquid and absorbent into recovery or salvage drums for disposal.

---

[62] Two page document copied from http://www.alliedhightech.com/msds/ColloidalSilicaWhite.pdf (11-29-09)

SECTION 7: HANDLING & STORAGE	SECTION 12: ECOLOGICAL INFORMATION
Handling: Use in well ventilated areas. Observe good housekeeping practices. Storage: Keep container closed when not in use. Do not reuse containers.	Environmental Hazard Characterization: Potential human hazard is low.

SECTION 8: EXPOSURE CONTROL & PERSONAL PROTECTION	SECTION 13: DISPOSAL INFORMATION
Engineering Measures: General ventilation. Respiratory Protection: Respiratory protection is not normally needed since volatility and toxicity are low. If significant mists are generated, use either chemical cartridge respirator with a dust/mist prefilter or supplied air. Protective Gloves: Impervious, nitrile, if hot plastic is handled. Eye Protection: Safety glasses or chemical splash goggles. Other: Eyewash, safety shower and impervious clothing are recommended.	If this product becomes a waste, it does not meet the criteria of a hazardous waste as defined under the Resource Conservation and Recovery Act (RCRA 40 CFR 261). As a non-hazardous liquid waste, it should be solidified with stabilizing agents (such as sand, fly ash or cement) so that no free liquid remains before disposal to an industrial waste landfill. A non-hazardous liquid waste can also be deep-well injected in accordance with Federal, State and Local regulations.

SECTION 9: PHYSICAL & CHEMICAL PROPERTIES	SECTION 14: TRANSPORT INFORMATION
Appearance: White translucent liquid Odor: NA Solubility: Completely Boiling Point: 212°F (100°C) @760 mm/Hg Melting Point: NA Flash Point: NA Vapor Pressure: NA Vapor Density: 11.5-11.6 lbs/gal Evaporation Rate: NA Specific Gravity: 1.38-1.39 @ 77°F (25°C) Flammable Limits LEL: NA Flammable Limits UEL: NA	Product is not regulated by DOT or IATA.

SECTION 10: STABILITY & REACTIVITY	SECTION 15: REGULATORY INFORMATION
Stability: Conditions to Avoid/Incompatibles: Avoid contact with strong acids (e.g. sulfuric, phosphoric, nitric, hydrochloric, chromic, sulfonic) which can generate heat, splattering or boiling and the release of toxic fumes. Avoid contact with aluminum. Decomposition Products: Methacrylate Monomer and Oxides of Carbon when burned. Hazardous Polymerization: Will not occur.	OSHA Hazard Communication Rule, 29 CFR 1910.1200: This product is classified as a hazardous chemical. Silica (amorphous) =TWA 10 mg/m3 (ACGIH) 6 mg/m3 OSHA. Toxic Substance Control Act: The chemical ingredients in this product are on the 8 (b) Inventory List (40 CFR 710). CERCLA/Superfund, 40 CFR 117.302: Notification of spills of this product is not required. Canadian WHMIS: This is a controlled product under The House of Commons of Canada Bill C-71 (Class D2B)

SECTION 11: TOXICOLOGICAL INFORMATION	SECTION 16: OTHER INFORMATION
Human Hazard Characterization: Potential human hazard is low.	**Legend** NAIF: No Applicable Information Found NA: Not Available/Applicable NE: None Established **DISCLAIMER:** The above information and recommendations are believed accurate and reliable. Because it is not possible to anticipate all conditions of use, additional safety precautions may be required. ALLIED HIGH TECH PRODUCTS, INC. makes no warranty, either express or implied, as to its accuracy or completeness and none is made as to the fitness of this material for any purpose. The manufacturer/distributor shall not be liable for damages to person or property resulting from its use. Nothing herein shall be construed as a recommendation for use in violation of any patent.

| Page 2 of 2: | Form Prepared By: Allied High Tech Products, Inc.   2/1/2006 |

Silica Gel is the form of amorphous silica most widely used in laboratory settings.[63]

Fisher Scientific - MSDS   Page 1 of 5

[X] Fisher Scientific   Back to Silica Gel Desiccant (60-200 Mesh, Grade 62/Chromatographic Grade)

Material Safety Data Sheet
Silica Gel Dessiccant

ACC# 20665

Section 1 - Chemical Product and Company Identification

MSDS Name: Silica Gel Dessiccant
Catalog Numbers: S80160, S80160-1, EES684200LB, FAIRXXS679, NC9495198, NC9505828, NC9517555, S156 212, S156 25LB, S156 5LB, S156-25LB, S156-5LB, S156212, S15625LB, S1565LB, S157 212, S157-5LB, S157212, S160-200LB, S160-500, S679 212, S679 500, S679-500, S679-5LB, S679212, S679500, S684 10, S684 212, S684-25LB, S684-5LB, S68410, S684212, S692 212, S692-200LB, S692-5LB, S692212, S698-5LB, S701 212, S701-6LB, S701212, S704 10, S704 25, S704-15LB, S704-55LB, S70410, S70425, S7321, S73225, S733 1, S733-1, S7331, S734 1, S734-1, S7341, S735 1, S735-1, S7351, S736 1, S736-1, S7361, S743 1, S743-1, S7431, S744 1, S744-1, S7441, S745 1, S745-1, S7451, S746 1, S746-1, S7461
Synonyms: Silica Gel; Silica Gel Dessicant (3 mesh-646 mesh)
Company Identification:
    Fisher Scientific
    1 Reagent Lane
    Fairlawn, NJ 07410
For information, call: 201-796-7100
Emergency Number: 201-796-7100
For CHEMTREC assistance, call: 800-424-9300
For International CHEMTREC assistance, call: 703-527-3887

Section 2 - Composition, Information on Ingredients

CAS#	Chemical Name	Percent	EINECS/ELINCS
112926-00-8	Silica, amorphous, precipitated and gel	100.0	unlisted

Section 3 - Hazards Identification

EMERGENCY OVERVIEW

Appearance: colorless to white. **Caution!** Causes respiratory tract irritation. May cause skin irritation. May cause eye irritation. May cause digestive tract irritation.
Target Organs: Lungs.

Potential Health Effects

Eye: Dust may cause mechanical irritation.
Skin: Dust may cause mechanical irritation.
Ingestion: May cause irritation of the digestive tract.
Inhalation: Dust is irritating to the respiratory tract.
Chronic: Prolonged exposure to respirable crystalline quartz may cause delayed lung injury/fibrosis (silicosis).

http://www.atmos.umd.edu/~russ/MSDS/silicagel60200.html   11/29/2009

---

[63] Five pages copied verbatim from http://www.atmos.umd.edu/~russ/MSDS/silicagel60200.html (11-29-09).

Section 4 - First Aid Measures

Eyes: Flush eyes with plenty of water for at least 15 minutes, occasionally lifting the upper and lower lids. Get medical aid.
Skin: Flush skin with plenty of soap and water for at least 15 minutes while removing contaminated clothing and shoes. Get medical aid if irritation develops or persists.
Ingestion: Treat symptomatically and supportively. Get medical aid.
Inhalation: Remove from exposure to fresh air immediately. If not breathing, give artificial respiration. If breathing is difficult, give oxygen. Get medical aid.
Notes to Physician: None
Antidote: None reported

Section 5 - Firefighting Measures

General Information: Material will not burn. Use extinguishing media appropriate to the surrounding fire.
Extinguishing Media: For small fires, use dry chemical, carbon dioxide, water spray or alcohol-resistant foam.
Autoignition Temperature: Not available.
Flash Point: Not available.
NFPA Rating: Not published. Explosion Limits, Lower: Not available. Upper: Not available.

Section 6 - Accidental Release Measures

General Information: Use proper personal protective equipment as indicated in Section 8.
Spills/Leaks: Vacuum or sweep up material and place into a suitable disposal container. Avoid generating dusty conditions.

Section 7 - Handling and Storage

Handling: Use only in a well ventilated area. Minimize dust generation and accumulation. Avoid ingestion and inhalation.
Storage: Store in a tightly closed container. Store in a dry area.

Section 8 - Exposure Controls, Personal Protection

Engineering Controls: Use adequate general or local exhaust ventilation to keep airborne concentrations below the permissible exposure limits.
Exposure Limits

Chemical Name	ACGIH	NIOSH	OSHA - Final PELs
Silica, amorphous, precipitated and gel	10 mg/m3	none listed	see Table Z-3

OSHA Vacated PELs: Silica, amorphous, precipitated and gel: 6 mg/m3 TWA
Personal Protective Equipment
Eyes: Wear appropriate protective eyeglasses or chemical safety goggles as described by OSHA's eye and face protection regulations in 29 CFR 1910.133 or European Standard EN166.
Skin: Wear appropriate gloves to prevent skin exposure.
Clothing: Wear appropriate protective clothing to minimize contact with skin.
Respirators: Follow the OSHA respirator regulations found in 29CFR 1910.134 or European Standard EN 149. Always use a NIOSH or European Standard EN 149 approved respirator when necessary.

Section 9 - Physical and Chemical Properties

Physical State: Solid
Appearance: colorless to white
Odor: odorless
pH: 2.3-7.4 (aqu. susp)
Vapor Pressure: Negligible.
Vapor Density: Not available.
Evaporation Rate:
Viscosity: Not applicable.
Boiling Point: 4046 deg F
Freezing/Melting Point:3110 deg F
Decomposition Temperature: Not available.
Solubility: insoluble in water
Specific Gravity/Density:2.1
Molecular Formula:SiO_2
Molecular Weight:

Section 10 - Stability and Reactivity

Chemical Stability: Stable.
Conditions to Avoid: Incompatible materials, moisture.
Incompatibilities with Other Materials: Strong acids, hydrogen fluoride
Hazardous Decomposition Products: No data available.
Hazardous Polymerization: Not available.

Section 11 - Toxicological Information

RTECS#:
CAS# 112926-00-8: VV7315000
LD50/LC50:
Not available.

Carcinogenicity:
CAS# 112926-00-8: Not listed by ACGIH, IARC, NIOSH, NTP, or OSHA.
Epidemiology: No data available.
Teratogenicity: No data available.

Reproductive Effects: No data available.
Neurotoxicity: No data available.
Mutagenicity: No data available.
Other Studies: No data available.

Section 12 - Ecological Information

Ecotoxicity: No information reported.
Environmental Fate: No information reported.
Physical/Chemical: No information reported.
Other: None

Section 13 - Disposal Considerations

Dispose of in a manner consistent with federal, state, and local regulations.
RCRA D-Series Maximum Concentration ofContaminants: None listed.
RCRA D-Series Chronic Toxicity ReferenceLevels: None listed.
RCRA F-Series: None listed.
RCRA P-Series: None listed.
RCRA U-Series: None listed.

Section 14 - Transport Information

	US DOT	**IATA**	**RID/ADR**	**IMO**	**Canada TDG**
Shipping Name:	No information available.	No information available.	No information available.	No information available.	No information available.
Hazard Class:					
UN Number:					
Packing Group:					

Section 15 - Regulatory Information

US FEDERAL

TSCA
CAS# 112926-00-8 is not listed on the TSCA inventory. It is for research and development use only.
Health & Safety Reporting List
None of the chemicals are on the Health & Safety Reporting List.
Chemical Test Rules
None of the chemicals in this product are under a Chemical Test Rule.
Section 12b
None of the chemicals are listed under TSCA Section 12b.
TSCA Significant New Use Rule
None of the chemicals in this material have a SNUR under TSCA.

SARA

Section 302 (RQ)
None of the chemicals in this material have an RQ.
Section 302 (TPQ)
None of the chemicals in this product have a TPQ.
Section 313
No chemicals are reportable under Section 313.
Clean Air Act:
This material does not contain any hazardous air pollutants. This material does not contain any
Class 1 Ozone depletors. This material does not contain any Class 2 Ozone depletors.
Clean Water Act:
None of the chemicals in this product are listed as Hazardous Substances under the CWA. None of
the chemicals in this product are listed as Priority Pollutants under the CWA. None of the chemicals
in this product are listed as Toxic Pollutants under the CWA.
OSHA:
None of the chemicals in this product are considered highly hazardous by OSHA.
STATE
CAS# 112926-00-8 can be found on the following state right to know lists: Pennsylvania,
Minnesota, Massachusetts.
California No Significant Risk Level: None of the chemicals in this product are listed.
European/International Regulations
European Labeling in Accordance with EC Directives
Hazard Symbols:
Not available.
Risk Phrases:

Safety Phrases:

WGK (Water Danger/Protection)
CAS# 112926-00-8: 0
Canada
CAS# 112926-00-8 is listed on Canada's DSL/NDSL List.
This product has a WHMIS classification of Not controlled..
CAS# 112926-00-8 is not listed on Canada's Ingredient Disclosure List.
Exposure Limits

Section 16 - Additional Information

MSDS Creation Date: 10/24/1995
Revision #9 Date: 9/02/1997
*The information above is believed to be accurate and represents the best information currently available to us. However, we make
no warranty of merchantability or any other warranty, express or implied, with respect to such information, and we assume no
liability resulting from its use. Users should make their own investigations to determine the suitability of the information for their
particular purposes. In no way shall Fisher be liable for any claims, losses, or damages of any third party or for lost profits or any
special, indirect, incidental, consequential or exemplary damages, howsoever arising, even if Fisher has been advised of the
possibility of such damages.*

This PPG MSDS is included due to the additional information provided about pulmonary issues.[64]

```
                                                                    Page 1 of 3


PPG INDUSTRIES INC -- HI-SIL 233 -- 6850-01-022-7031

==================== Product Identification ====================

Product ID:HI-SIL 233
MSDS Date:06/24/1994
FSC:6850
NIIN:01-022-7031
MSDS Number: CGHFV
=== Responsible Party ===
Company Name:PPG INDUSTRIES INC
Address:ONE PPG PLACE
City:PITTSBURGH
State:PA
ZIP:15272
Country:US
Info Phone Num:412-434-3131
Emergency Phone Num:304-843-1300
Preparer's Name:R. KENNETH LEE
CAGE:93915
=== Contractor Identification ===
Company Name:PPG INDUSTRIES INC CHEMICAL DIVISION
Address:ONE GATEWAY CENTER
City:PITTSBURGH
State:PA
ZIP:15222-1416
Country:US
Phone:304-843-1300
CAGE:93915

============= Composition/Information on Ingredients =============

Ingred Name:SILICA GEL; (SIO2 HYDRATE) (CONTAINS NO DETECTABLE
    CRYSTALLINE SILICA - (DETECTION LIMIT <0.01% BY WEIGHT))
CAS:112945-52-5
RTECS #:VV7310000
Fraction by Wt: 87% MIN
OSHA PEL:6 MG/M3
ACGIH TLV:10 MG/M3

Ingred Name:SUPP DATA:TWO YRS. ALTHOUGH PRECIPITATED SILICA WAS
    TEMPORARILY DEPOSITED IN ANIMALS' LUNGS, MOST OF DEPOSITED (ING 3)
RTECS #:9999999ZZ

Ingred Name:ING 2:MATL WAS CLEARED SOON AFTER DUST EXPOS ENDED. RSLTS
    OF ALL STUDIES PERFORMED BY, OR KNOWN TO, PPG INDICATE (ING 4)
RTECS #:9999999ZZ

Ingred Name:ING 3:A VERY LOW ORDER OF PULMONARY ACTIVITY FOR SYNTHETIC
    PRECIPITATED SILICAS.
RTECS #:9999999ZZ

Ingred Name:OTHER PROT EQUIP:SKIN CONTACT. PERSONAL PROTECTIVE CLOTHING
    & USE OF EQUIPMENT MUST BE I/A/W 29 CFR 1910.132 & 133.
RTECS #:9999999ZZ

==================== Hazards Identification ====================

LD50 LC50 Mixture:LD50:(ORAL) >5 G/KG.


http://hazard.com/msds/f2/cgh/cghfv.html                          11/29/2009
```

---

[64] Three pages copied verbatim from http://hazard.com/msds/f2/cgh/cghfv.html (11-29-09).

Routes of Entry: Inhalation:YES Skin:YES Ingestion:YES
Reports of Carcinogenicity:NTP:NO   IARC:NO   OSHA:NO
Health Hazards Acute and Chronic:ACUTE:EXCESSIVE CONT W/POWDER CAN
    CAUSE DRYING OF MUC MEMBS OF NOSE, EYES & THROAT DUE TO ABSORPTION
    OF MOISTURE & OILS. THIS MATL CAN ALSO CAUSE NASAL IRRIT &
    NOSEBLEEDS. EYE CONT W/POWDER CAN RSLT I N MILD IRRIT. PRLNG/RPTD
    INHAL OF DUST MAY IRRIT RESP TRACT. EYE CONT MAY CAUSE IRRIT &
    PAIN. SKIN CONT(EFTS OF OVEREXP)
Explanation of Carcinogenicity:NOT RELEVANT
Effects of Overexposure:HLTH HAZ:MAY CAUSE IRRIT & DISCOMFORT.
    CHRONIC:AN EPIDEMIOLOGICAL STUDY WAS CONDUCTED WHICH INCL 165
    PRECIPITATED SILICA WORKERS WHO HAD BEEN EXPOS AN AVG TIME SPAN OF
    8.6 YRS. OF THESE 65 WORKERS, 44 HAD BEEN EXPOS FOR AVG OF 18 YRS.
    NO ADVERSE EFTS WERE NOTED IN COMPLETE MED EXAMS (INCL CHEST
    ROENTGENOGRAMS) (SUPDAT)
Medical Cond Aggravated by Exposure:PPG RECOMMENDS THAT PERSONS
    W/BREATHING PROBLEMS OR LUNG DISEASE SHOULD NOT WORK IN DUSTY AREAS
    UNLESS MD APPROVES & CERTIFIES THEIR FITNESS TO WEAR NIOSH APPROVED
    RESPIRATORY PROTECTION.

===================== First Aid Measures =======================

First Aid:INGEST:CALL MD IMMEDIATELY . INHAL:REMOVE AFFECTED PERSON TO
    FRESH AIR. IF IRRITATION OR DISCOMFORT PERSISTS, CONSULT MD.
    EYES:FLUSH W/PLENTY OF WATER FOR AT LEAST 15 MINUTES. IF IRRITATION
    OR D ISCOMFORT OCCURS, CONSULT MD. SKIN:FLUSH W/PLENTY OF WATER. IF
    IRRITATION OR DISCOMFORT OCCURS, CONSULT MD. NOTE TO MD:TREAT
    SYMPTOMATICALLY.

==================== Fire Fighting Measures =====================

Flash Point:NONE
Extinguishing Media:MEDIA SUITABLE FOR SURROUNDING FIRE .
Fire Fighting Procedures:USE NIOSH APPROVED SCBA & FULL PROTECTIVE
    EQUIPMENT .
Unusual Fire/Explosion Hazard:NONE.

================== Accidental Release Measures ==================

Spill Release Procedures:VACUUM SPILLED MATERIAL & PLACE IN CLOSED
    PLASTIC BAGS FOR DISPOSAL. SEE SPECIAL PROTECTION INFORMATION
    SECTION FOR PERSONAL PROTECTION INFORMATION.
Neutralizing Agent:NONE SPECIFIED BY MANUFACTURER.

===================== Handling and Storage =====================

Handling and Storage Precautions:STORE IN DRY AREA. AVOID PROLONGED OR
    REPEATED INHALATION OF DUST. AVOID CONTACT W/EYES. AVOID PROLONGED,
    REPEATED OR EXCESSIVE CONTACT W/SKIN.
Other Precautions:USE W/ADEQUATE VENTILATION. DO NOT EAT, DRINK OR
    SMOKE IN WORK AREA.

============= Exposure Controls/Personal Protection =============

Respiratory Protection:USE NIOSH APPROVED DUST FILTER RESPIRATOR FOR
    EXPOSURE ABOVE PELS. RESPIRATORY USE LIMITATIONS MADE BY NIOSH OR
    MFR MUST BE OBSERVED. RESPIRATORY PROTECTION PROGRAMS MUST BE I/A/W
    29 CFR 1910.134.
Ventilation:GENERAL OR LOCAL EXHAUST SUFFICIENT TO MAINTAIN EMPLOYEE
    EXPOSURE BELOW PELS. OBSERVANCE OF LOWER LIMITS IS ADVISABLE.

Protective Gloves:CLOTH, LEATHER OR RUBBER GLOVES.
Eye Protection:ANSI APPROVED CHEM WORKERS GOGGS .
Other Protective Equipment:ANSI APPRVD EYE WASH FOUNTAIN & DELUGE
    SHOWER . BOOTS, APRONS/CHEM SUITS SHOULD BE USED WHEN NEC TO PVNT
    (ING 5)
Work Hygienic Practices:WASH THOROUGHLY EVERYDAY AFTER WORK.
Supplemental Safety and Health
PH:6.5-7.3 (5% SUSPENSION). EFTS OF OVEREXP:OF THESE WORKERS. PULM FUNC
    DECREMENTS WERE CORRELATED ONLY W/SMOKING & AGE BUT NOT W/DEGREE OR
    DURATION OF DUST EXPOS. LAB STUDIES HAVE ALSO BEEN CONDUCTED IN SM
    ANIMALS VIA INHAL TO LEVELS OF PRECIPITATED SILICA DUST OF UP TO
    126 MG/M3 FOR PERIODS FROM 6 MONTHS TO (ING 2)

================== Physical/Chemical Properties ==================

Vapor Pres:NONE
pH:SUPDAT
Solubility in Water:ESSENTIALLY SOLUBLE
Appearance and Odor:WHITE POWDER; ODORLESS.

================== Stability and Reactivity Data ==================

Stability Indicator/Materials to Avoid:YES
AVOID CALCINING, WHICH MAY RESULT IN CRYSTALLINE FORMATION OR MIXING
    W/ADDITIVES MAY ALTER TOXICOLOGICAL PROPERTIES.
Stability Condition to Avoid:HIGH TEMPERTURES (>800C) TREATMENT
    (CALCINING). AVOID ALTERATION OF PRODUCT PROPERTIES BEFORE USE.
Hazardous Decomposition Products:NONE.

==================== Disposal Considerations ====================

Waste Disposal Methods:DISPOSAL MUST BE I/A/W FEDERAL, STATE & LOCAL
    REGULATIONS . WASTE FROM THIS PRODUCT MAY BE DISPOSED OF IN A
    SANITARY LANDFILL IF STATE & LOCAL REGULATIONS PERMIT. CARE SHOULD
    BE EXERCISED TO AVO ID CREATION OF DUST DURING DISPOSAL OPERATIONS.

 Disclaimer (provided with this information by the compiling agencies):
 This information is formulated for use by elements of the Department
 of Defense. The United States of America in no manner whatsoever,
 expressly or implied, warrants this information to be accurate and
 disclaims all liability for its use. Any person utilizing this
 document should seek competent professional advice to verify and
 assume responsibility for the suitability of this information to their
 particular situation.

APPENDIX C

Initial Laboratory Methodology Used at the Start of this Buried Soil Project

Appendix 1[65]

Isolation of Phytoliths from Soils

This method for phytolith preparation was condensed from *Phytolith Analysis An Archaeological and Geological Perspective* by Piperno (1988). The phytoliths are a small part of the soil, so they must be cleaned up and concentrated in order to be readily detectable. In the following procedure, the phytoliths are isolated by deflocculating the sample which is essential as most phytoliths are not free, but rather are bound to the soil particles (Dimbleby 1985). Next, the sample is subdivided into three particle size fractions; then the carbonate and organic impurities are removed by acid treatment. In the final step, heavy liquid floatation is used to isolate the phytoliths from the remainder of the soil sample residue.

    A. Deflocculation of soil samples:

        1. Add 5% solution of Calgon (sodium hexametaphosphate) [or sodium bicarbonate) to 25-50 g of soil and stir.

        2. Put the solutions on an automatic shaker and shake overnight.

---

[65] This appendix taken from Sudbury (2000:48-52).

3. Separate sand particles (soil fraction greater than 50 μm) by wet sieving through 275 mesh sieve.

4. Set sand aside for later analysis (it may contain multi-celled aggregates of phytoliths and other taxa).

5. Remove clay by gravity sedimentation (Jackson 1956).

     i. Place soil in 1000 mL beaker.

     ii. Add water to the beaker to a depth of 10 cm.

     iii. Stir vigorously.

     iv. After one hour, pour off the supernatant leaving the silt fractions behind (5-50 μm).

     v. Repeat steps ii-iv as needed.

     vi. Clay removal is complete when the supernatant is clear.

B. Further divide the remaining silt fraction into fine (5-20 μm) and coarse (20-50 μm) fractions by gravity sedimentation. [This is done so that the analyst can look at the small phytoliths as a separate sample.]

1. Place samples in 100 mL tall form beakers.

2. Add water to each beaker to a depth of 5 cm.

3. Stir vigorously.

4. Allow to settle for 3 minutes.

5. Decant the supernatant into a 1000 mL beaker.

6. Dilute remaining suspension to a height of 5 cm with water.

7. Stir vigorously.

8. Allow to settle for 140 seconds.

9. Decant supernatant into the same 1000 mL beaker.

10. Repeat steps 6-9 about 7-8 times to effect the silt fractionation.

C. Process the isolated soil fractions:

1. Further process and analyze each of the soil fractions:

     i.   Fine silt

     ii.   Coarse Silt

     iii.   Sand.

2. Place 1-1.5 grams of each fraction into a 16 x 100 mm test tube.

3. Add a 10% solution of hydrochloric acid to remove carbonates.

4. Centrifuge samples at 500 rpm for 3 minutes.

5. Decant supernatants.

6. Repeat steps 3-5 until no reaction is noticed when adding the hydrochloric acid.

7. Wash twice with distilled water.

8. Remove organic material by adding concentrated nitric acid and placing in a boiling water bath until the reaction (if present) has subsided (about 1 hour) [can also use either hydrogen peroxide (takes longer) or chromic sulfuric acid (can't heat) so have to leave overnight].

9. If the nitric acid solution in the tube is tinted red or red orange, organic compounds are still present and will inhibit future phytolith

separations.

10. If organic materials are still present (step 9 visual evaluation), add a few 0.1 g of potassium chlorate to the heated tubes of solution to eliminate the remaining organic material. Once the reddish hue is gone, the organic components have been oxidized adequately for further processing.

D. Heavy Liquid Flotation:

Specific gravity of phytoliths ranges from 1.5 to 2.3, and that of quartz is 2.65. So, a solvent with a specific gravity between 2.3 and 2.4 is needed to float the phytoliths and allow the soil to sink. Possible solvents to use include:

     i.   cadmium iodide and potassium iodide.

     ii.   tetrabromoethane and absolute ethanol

     iii.   tetrabromoethane and nitrobenzene

     iv.   bromoform and nitrobenzene

     v.   zinc bromide and water.

1. Prepare heavy liquid solution of Zinc Bromide (70%).

2. Add 10 ml solution to each of the soil samples.

3. Mix well.

4. Centrifuge at 1000 rpm for 5 minutes.

5. Remove floating phytolith fraction at the top of the tube with a Pasteur pipette and transfer to another test tube.

6. Repeat steps 2-5 several times to maximize phytolith recovery from the samples.

7. Add distilled water to the phytolith collection tube at a ratio of 2.5: 1. This lowers the specific gravity to below 1.5 and causes the phytoliths to settle to the bottom of the new tube.

8. Centrifuge the tube at 2500 rpm for 10 minutes.

9. Decant the supernatant.

10. Repeat steps 7-9 two more times to remove all of the heavy liquid from the phytoliths.

11. Wash phytoliths twice with acetone for quick drying.

12. For light microscopy, one can mount on slides with Permount which has the correct refractive index for viewing phytoliths which have a refractive index of 1.42. (One can also view phytoliths by Phase Contrast microscopy mounted in silicone oil).

13. The phytolith portion not mounted can be stored in EtOH in vials.

E. Note:

One may have to modify this method based on problems or

9.   peculiarities of the particular soil being analyzed.

Appendix 2[66]

Isolation of Phytoliths from Ash

Piperno (1988) also has a very short section regarding the preparation of phytoliths from ash samples for microscopy. This procedure is much less involved than that presented in Appendix 1 as there is not any organic material or soil matrix to contend with. Indeed, if the concentration of phytoliths is high enough in ash, it is conceivable that sample cleanup and phytolith concentration in ash may not be required at all.

1. Mix a small ash sample in a 10 % solution of hydrochloric acid to remove carbonates.

2. Centrifuge to clear up the hydrochloric acid, and decant.

3. Repeat steps 1-2 until there is no visible reaction.

4. Wash cleaned phytolith sample several times in distilled water to remove the acid residue.

5. Dry in acetone or in an oven set at low temperature.

6. Mount on double sticky tape on SEM stubs for analysis.

7. Allow to air dry on the stub.

8. Store in a desiccator.

9. Sputter coat, and visualize by SEM.

10. Phytolith sample fractions that are not being used can be stored by suspending the phytoliths in a small amount of 95% EtOH in screw cap vials.

---

[66] This appendix taken from Sudbury (2000:53).

APPENDIX D

Variations in Laboratory Methodology During the Course of this Project

The final method developed and used in this procedure is described in the

materials and methods section. That procedure is a long way from the overview

presented in the previous literature survey (Appendix C). This current appendix fills in

some of the holes and addresses potential questions that may arise regarding the rationale

for the method as developed. Several novel ideas were tested and implemented during

this project, and are appropriately recorded here.

Once the soil sample has been collected, coarse sieved, homogenized, and

deflocculated, the normal next step is to use a 270 mesh sieve to remove the sand (> 50

microns) from the sample by washing the silt and clay through the sieve. The sand

collected on the sieve can be then be retrieved, dried, weighed, and saved for later

examination (for large phytoliths, other minerals, or component differences). While

performing this step on original samples in this project, it was noted that some brands of

1 gallon plastic pails held an 8 inch sieve—and thus provided a much larger receiving

reservoir than a normal metal sieve bottom pan (Figure 114). Tilting the pail about one

inch allows improved drainage and throughput. Once the sand collects in the lower side

of the sieve, the sieve can be rotated and the sample again slowed moved across the sieve

using a fine stream of water from a squirt bottle. Once sand removal is completed, the

receiving pail which contains the less than 50 micron particle fraction can be covered and

stored if necessary. The next separation step can actually be efficiently performed in the gallon pail.

Figure 114. 270-mesh stainless steel sieve on gallon receiving bucket. Vortex Genie, Boekel slide drier (fitted with a wooden frame and 10 glass shelves so it will hold 50 slides at one time), and centrifuge in background. Working on glass bench tops has numerous advantages for cleanup and for minimizing contamination.

Due to the liquid volumes involved, these gallon buckets were also used as the settling chambers for the initial clay removal step. A paint mixing attachment on a cordless drill was used to stir and resuspend the sediment prior to the settling interval; water in a wash bottle was used to rinse off the paint mixer between samples. After the timed settling interval, the clay fraction was collected via vacuum in a side arm flask, and transferred to storage containers pending completion of the phytolith isolation and analysis. This procedure was effectively used on 250 g soil samples in the initial experiments. Later experiments used smaller soil samples, so the equipment volumes were downsized and adjusted as appropriate.

The longer sedimentation times for fine silt fraction lighter density phytolith particles (Table 4) overall increased decanted solution storage volume needs. This was the initial reason that 2 liter soda bottles were implemented as storage containers (and later as sedimentation chambers used to pre-settle silt fractions as reported in the materials and methods section)—to replace dozens of one and two liter glass beakers. Besides low cost, other benefits are that the bottles are unbreakable, easy to seal, easy to handle, easy to stack, and easy to pour from without drippage; they have no obvious disadvantages[67]. Use of these durable universally available containers actually represents a major cost savings and procedural advance (see Figures 17-25 and 28).

The Fleakers recommended to use for sediment settling are readily available in quantity in the laboratory (Figure 115). However, quart canning jars are cheaper, universally available, very durable for handling and heating, and also seal well. Also, if you scratch a quart jar via sand abrasion and have to discard the jar, the jar is 95+%

Figure 115. Part of 1500 ml Fleaker inventory.

---

[67] Obviously the plastic bottles should not be excessively heated. These two liter bottles are also not appropriate for storing strong caustic solutions.

cheaper—assuming any Fleakers can be located for purchase. This, this adaptation

resulted as a matter of logistics, economics, and improved performance—not availability.

By using quart jars for initial sample processing, one also has the advantage of

never having to transfer the sample to another container thus minimizing transfer losses

or sample mix ups or labeling problems. For example, the sieved soil sample is mixed,

and a soil aliquot placed in the preweighed quart jar (label lid and band also to avoid later

mix ups, and weigh with and without the jar). The sample in the open jar is then oven

dried, the lid replaced and jar sealed while hot, allowed to cool, and weighed. The

detergent solution is then added to the jar which is sealed and placed on an Eberbach

shaker laying down for 24 hours. Padding between the jars prevents contact and

breakage. The jar is then removed from the shaker, the upper wall rinsed, the water

column adjusted to 10 cm, and then the timed sedimentation decants occur using the

same initial sample weighing and shaking jar. After the first decant is performed, more

water is added, the lid installed, the jar shaken vigorously (shaking and swirling are both

beneficial), the jar set down, the lid removed, the lid and walls quickly rinsed with a

minimal volume of water via squirt bottle, and the lid (not band) replaced as a dust cover.

Based on the lab temperature, a timer is set to indicate when the settling interval will be

completed.

Once the clay and then later the silt fraction have been removed, the clean sand

remaining in the jar can be oven dried and weighed in the same jar. The sand can then be

quantitatively transferred to a smaller container for curation. I have used this quart jar

procedure for four years, with 0% breakage from handling, sample processing, or the heating process. Initially, I used the drill (set on low) and paint mixer to stir the samples; however, a shoulder injury led to the method modification of shaking to resuspend the sediment prior to the timed settling interval.

Initial organic removal was effective using commercial hydrogen peroxide solution added to samples in heavy plastic bottles placed in a hot water bath; this procedure, although effective, took several weeks. The next set of silt samples were transferred to 1 ounce Boston Round bottles fitted with Polyseal lined caps for organic removal. The samples were dried, nitric acid added, and the bottles sealed, mixed, and placed on a hot plate with the surface temperature adjusted to 110ºC. This successful procedure was the fastest organic removal method tested; however, due to the obvious risks involved, it was not repeated after the initial 35 samples were processed.

Nitric acid was effective at organic removal. As the overall laboratory procedure had progressed to using quart jars for sample processing, the quart jars were used for the next organic removal trial which also proved to be effective (albeit slower than the low pressure hot plate treatment described above). The setup in operation is shown in Figure 116; nitric acid was added to the silt in the bottom of the jars. The samples were gently swirled each day (not inverted) to make certain mixing was effective. If the orange acid color was not visible during morning examination, more acid was added to each vessel at that time when they were cool and depressurized. A thermometer in an empty quart jar on this tray registered 142ºF (61ºC) during this July trial. This process was allowed to

continue for a week; there was no breakage, leakage, or sample loss—and good organic

matter removal was achieved. Once the samples were completed, the jar seals were

observed to show deterioration. Lids with white enamel on the inner surface (Ball brand)

held up better than other brands. Although very effective and requiring minimal effort,

this is a seasonal limited procedure (i.e., hot sunny weather), so it was not repeated. Use

of Parafilm liners inside the normal lids to seal the jars would potentially allow this

procedure to be performed in a laboratory oven.

Figure 116. Thermal treatment of silt samples mixed with nitric acid. The white
reinforced tray is part of a cement cone slump testing apparatus.

A crisis led to the final organic removal procedure—thermal ashing—which is

described in the materials and method chapter. A helper forgot to remove the organic

matter from a series of silt samples. Once the zinc bromide solution was added, the result

was an opaque black solution (Figure 117) and thus one was unable to observe the

effectiveness of the separation in the tube. There were no more soil samples available

from this site, so the samples in progress had to be salvaged.

Figure 117. Zinc bromide solution with phytoliths (?) after decanting from denser
(> 2.35 g/cm^3) silt residue.

The samples were all diluted to lower the solution density so the phytoliths would

sink. They were then centrifuged, and the liquid phase removed via pipette; the silts were

rinsed again, centrifuged, and pipetted until the solution density was near 1 (i.e. all the

zinc bromide had been removed). The silts were then quantitatively transferred to100 ml

crucibles, and oven dried. Having ashed botanical specimens, the operating temperature

limits were know; the three step temperature increase previously described in the

materials and methods section was implemented (4 hours at 110ºC, 325ºC for 3-6 hours, and slowly to 530ºC for 6 hours). Once cooled, the clean silts were successfully processed for phytolith recovery as described in the body of this dissertation.

Figure 118. After diluting the solutions, and recovering and reconstituting the fractions that produced the issue noted in Figure 117, and thermally ashing the recovered silt/ phytolith material, the phytoliths visibly floated away from the soil matrix onto the top of the zinc bromide solution.

One of the ongoing laboratory technique problems addressed and resolved during this project was minimizing the inclusion of other silt particles with the isolated phytoliths. Although some silt particles may be present mixed with or adhering to the floating lower density biogenic silica particles after flotation with 2.35 g/cm^3 zinc bromide solution (i.e., due to incomplete defloculation after ashing), it is probable that

407

most of the silt contamination occurs when decanting the floating fraction from the tube. The source of this contamination is thought to be the silt that is present on the tube wall above the solvent line and the isolated phytoliths following mixing (Figure 119). After stirring the soil matrix/zinc bromide mixture to release and separate the biogenic silica, some particulate remains on the tube wall (Figure 119). As the silt fraction particulate is ~1 weight per cent phytoliths, the remaining ~99% of this residual material is likely to be silt; if this visible residue is transferred with the phytoliths, false high phytolith recoveries
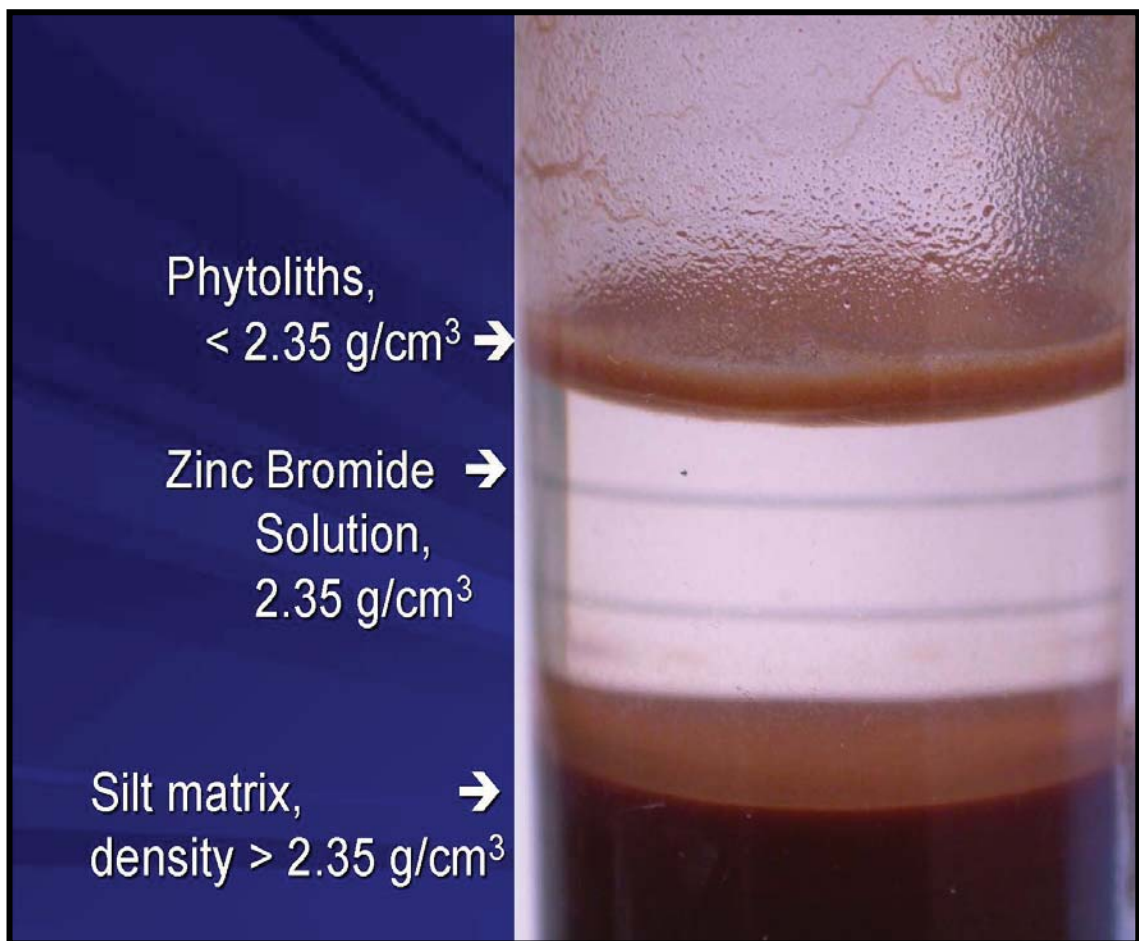

Figure 119. Phytoliths floating on zinc bromide solution. Care must be exercised to not allow the silt on the tube walls (visible in the top portion of the tube) from contaminating the final phytolith isolates. Serial centrifuging the decanted phytoliths in multiple tubes is an effective means to remove this silt contaminant. (This 50 ml centrifuge tube is about 1 inch in diameter.)

are recorded and the resulting dirty phytolith fractions are mounted on microscope slides for particle counting. By transferring the floating fraction to a new tube, reprocessing the floating decanted material (i.e., by remixing with the heavy liquid and recentrifuging in as many sequential tubes as necessary), the carried over quartz-based silt fraction (and clay if present) is all gradually transferred to the pellet and pure phytoliths can be harvested floating on the heavy density liquid.

Another problem encountered during work with this particular series of samples was concern over possible trace contamination. Although volcanic glass shards can be expected to be encountered in soil samples, some of the specimens in this sample series seemed unduly large considering the sample preparation method (c.f. Figure 4). As a volcanic ash project had recently been conducted at the school lab in use for sample preps at that time, all future sample preps were conducted at a facility and with equipment that had not had been previously used to process any volcanic ash samples. Also, volcanic ash data from these buried soil samples was not processed or reported.

Several other problems encountered during this research should be noted. First, the insoluble impurities in technical grade zinc bromide float on zinc bromide solution, and thus interfere with quantitative phytolith recovery; use of higher purity reagent grade zinc bromide is strongly recommended over technical grade.

Early in the project, while using chemical methods to remove organic material from the sample, a white floating residue was noted on a diluted zinc bromide solution

(solution density of 1.65 g/cm^3). Although some opaque phytoliths were visible in the floating residue, a dried water droplet containing this material produced a white residue; this floating material does not appear to be zinc bromide or another zinc salt. Although this material was never identified, I deduced that it could be polymer residue from the water purification cartridges. The ASTM Type A water is ionically pure (as measured by electrical conductivity), but it may potentially contain non-ionic polymeric material. The thermal ashing procedure used in later sample preparation procedures would remove any polymer residue.

APPENDIX E

Materials, Equipment, and Supplies

An inventory of the basic materials, equipment, and supplies used in this research
is document in this appendix.

Materials
   Reagents[68]

       Chemicals (reagent grade):
            Acetone
            Ammonium Perchlorate
            ASTM Type 1 Water
            Canada Balsam
            Hydrochloric Acid
          Indicator Silica Gel (for desiccator)
            Nitric Acid
            Zinc Bromide
       Chemicals (other)
          Calgon®, 5% solution, (Commercial grade Calgon®
            (sodium hexametaphosphate with calcium carbonate
             filler))
            Hydrogen Peroxide (27%)
            Sonic cleaning solution

   Supplies

       4 dram glass vials with screw lids (Kimax®)
       Beakers, Pyrex® (10ml-2000 ml assortment)
       Canada Balsam bottles
       Canning jars (quart)
       Centrifuge tubes, 15 ml plastic
       Centrifuge tubes, 50 ml plastic (Corning)
       Centrifuge tube racks
       Cover slips (assorted, 18x18 mm - 20x60 mm).
       Crucible tongs
       Engineering flags
       Filter forceps
       Filter paper (quantitative)

---

[68] Items used in this investigation; substitutions are possible for many items. Use of high-purity chemicals
is strongly recommended.

Filtration flasks, 1 liter glass (heavy walled)
Forceps (stainless surgical forceps)
Glass, tempered (8" x 8" x 1/8")
Glass and plastic funnels (stemmed and powder)
Glassware, Pyrex® - assorted (graduated cylinders, flasks, watch
     glasses, separatory funnels)
Gloves, nitrile and leather
Hose clamp
Kim Wipes
Laboratory timers
Magnetic stirring bars (assorted)
Microscope slides (Fisher)
Microscope slide storage boxes
Pasteur pipettes and 2 ml rubber pipet bulbs
Plastic bottles, 2 liter
Plastic containment basins (10-quart)
Porcelain crucibles with lids (15, 30, and 100 ml)
Pyrex® Petri dishes
Ring stands, clamps, rings, and Castalloy flask holders (plus
     framing and connectors)
Sample bottles, varied
Squirt bottles, plastic
Stainless steel spatulas and micro-spatulas
Tungsten needle
Tygon® tubing (various diameters)
Vial racks and test tube racks
Whatman ashless filter paper number 40 (55 mm, Cat No
     1440055)
Whatman ashless filter paper number 41 (70 mm, Cat No
     1441070)
ZipLoc® bags

Equipment

Brady TLS2200 Thermal Labeling System
Centrifuge, IEC Centra68R
Centrifuge, IEC HNSII
Computer (including 1TB data backup system, Microsoft Office
     Professional, Photoshop, and Adobe Professional)
Eberbach shakers
Incubator, Boekel
Laboratory ovens
Hot water bath
Mettler balances, 2-5 places
Millipore ultrafiltration assembly (mesh screen support type
     preferred)

Muffle furnace
Micrometer slide
Nikon Coolpix 4500 camera
Oakfield soil probe
Olympus BX51 petrographic microscope, with X-Y Stage
Olympus DP-11 digital camera system
Olympus SZ12 stereo zoom microscope
Rainin pipettors and disposable pipette tips (1, 5, 10 ml)
Repipettors
Stainless mesh sieves (Numbers 10, 270)
Stainless steel desiccator
Stirring hot plates
Ultrasonic bath
UV light
Vacuum oven
Vacuum pump
Vortex Genie® mixer

APPENDIX F

Soil Sample Preparation Method:

Carbonate Removal Prior to Delta 13 Analysis

Samples of a soil profile column suite are frequently submitted to an outside laboratory for carbon isotope ["Delta 13"] analysis. Historically, the procedure used at the OSU Agricultural Department to prepare samples for this analysis included carbonate removal, oven drying, and a final step that involved manually scraping dried soil residue from 400 ml beakers. A new improved laboratory protocol for this important sample preparation was developed and implemented during this phytolith study[69]. The step-wise procedure is:

1. Pulverized sieved soil samples are received for processing.

2. Mix soil sample and transfer a representative sample portion (weigh 200-500 mg) to a labeled 4 dram glass vial.

3. Dry samples in a 105°C oven.

4. Cool the hot dried samples in a desiccator.

5. Weigh the dried soil sample aliquots.

6. Add 10% hydrochloric acid to each 4 dram glass sample vial via a repipettor (set to dispense 1 ml) to react with carbonates in the soil samples.

7. Add additional acid to the vial once the effervescence subsides.

8. Cap the sample vial, and use a Vortex Genie mixer in brief pulses to help effectively mix the soil sample and acid.

---

[69] This procedure represents a marked improvement over the old method in that 100% of the mineral portion of the soil sample is included in the final sample prepped and submitted for carbon isotope testing. In the old method, a significant portion of the clay fraction was left adhering to wall of the 400 ml beaker.

9. Gently release the pressure, recap the glass vials, and centrifuge at 2000 rpm for 10 minutes.

10. Remove the clear acid layer with a glass Pasteur pipet and collect the acid for neutralization or disposal.

11. Repeat steps 6-10 as needed (~3-6 times) until two sequential acid additions do not result in effervescence.

12. Add Milli-Q water to the soil sample residue (fill ~70% of vial capacity).

13. Cap the sample vials and mix the carbonate-free soil sample and water with the Vortex Genie mixer.

14. Centrifuge the vials at 2000 rpm for 10 minutes.

15. Remove the clear water phase via Pasteur pipet.

16. Repeat steps 12-15 five more times to effective dilute and remove most of the remaining hydrochloric acid.

17. Dry the sample residues in a 105°C oven, cool in a desiccator, and cap the vials containing the dried residues.

18. A blank vial (carried through the entire analytical procedure as a control and back-ground check for possible contamination issues) is also submitted for analysis along with the sample residues.

The carbonate-free totally dry samples are then ready for shipment and Delta 13 analysis. Figure 120 shows a dried soil sample after processing for carbonate removal. In the old method, the clay coating the lower wall of the vial is the material was incompletely recovered using the scraping method to recover the dried sample. In this new procedure, 100% of the dried sample is in the sealed vial ready for analysis.

Figure 120. Soil sample after carbonate removal, centrifuging, repetitive water rinsing, and final oven drying. Even in the centrifuge, the soil sample stratifies by particle size. Three distinct zones or fractions are visible in the vial:

1) the larger particles (containing sand and silt) can be seen in the lower portion of the vial, whereas

2) some clay particles coat the vial wall above the sediment [this clay adhering to the wall remained suspended in the water as the sample was oven dried; this clay coating is the sample portion that coated the wall of a 400 ml beaker during the old processing method and would have been partially lost during recovery and transfer], and

3) the larger clay particles form a layer on top of the sample sediment (in the illustrated example, this clay layer curled when the sample was oven dried).

As clay particles contain a significant portion of the soil organic matter, it is

important that all of the clay remain with the soil sample for delta 13 analysis. Thus, this

new procedure represents a significant improvement—by miniaturizing the glassware used, and avoiding any sample transfer from the original reaction vessel/sample container. The soil sample remains intact with the carbonates completely neutralized and removed.

..

"'Land grants' could lead hunger fight

Oct 14, 2009 10:57 AM, By Forrest Laws, Farm Press Editorial Staff

Gebisa Ejeta says the world will have to increase its production of food more in the next four decades than it has since the dawn of civilization.

Accomplishing that task will require concerted efforts by governments, agribusiness and farmers, says Ejeta, the winner of this year's World Food Prize. The glue holding those parts together may be a revitalization of the land-grant university system.

With the world's population expected to grow from current estimates of 6 billion people to more than 9 billion by 2050, the world's agricultural leaders must figure out a way to double food production during the same timeframe.

'We can do this by revitalizing our agricultural sciences and recommitting to the time-tested, mission-oriented legacies of our land-grant university models and ideas,' said Gebisa, a native of Ethiopia who grew up in a one-room thatched hut with a mud floor but went on to earn a Ph.D. in plant breeding and genetics at Purdue University.

Gebisa, who is currently a distinguished professor of agronomy at Purdue, will receive the $250,000 World Food Prize during ceremonies at the Iowa State Capitol Thursday (Oct. 15). The World Food Prize was founded by Dr. Norman E. Borlaug, the universally recognized father of the Green Revolution. Borlaug, a native of Cresco, Iowa, died Sept. 12.

Ejeta, whose own work on the development of higher-yielding and weed-resistant sorghum varieties is believed to have helped feed hundreds of thousands of people in Africa, paid tribute to Borlaug during the annual Norman Borlaug Lecture at Iowa State University Monday night.

'The land-grant model legislated in 19th century helped build this great nation and made 20th Century American agriculture the envy of the world,' said Ejeta 'It has succeeded internationally, bringing about the Asian Green Revolution championed by Norm Borlaug and furthered by many others.'

Even in the face of emerging 21th Century issues like climate change and the uncertainty of global energy supplies, Ejeta said, 'the land grant model can be counted upon once again to address the challenges of doubling food and feed production.'

Over the last century, the U.S. agriculture sector has become one of the most productive in the world, and citizens of this country as well as the rest of North America and

---

[70] This article (Laws 2009) is reproduced in its entirety with permission of Forrest Laws of the *Southwest Farm Press*; the original was copied verbatim from the *Southwest Farm Press* (10-15-09). (http://southwestfarmpress.com/grains/land-grants-1014/).

Western Europe have become accustomed to a safe and relatively inexpensive supply of food.

Agricultural research and genetics, crop and animal husbandry, pest and disease control through chemical inputs and integrated pest management, post-harvest technology and value-added products have all spurred the nearly tenfold increase in commodity yields in the United States over the last 100 years.

The first agricultural revolution was brought about by the advent of corn hybrid technology which gave rise to the private seed industry and the associated complex of services and partnerships, he said, noting the role of Iowa State graduate Henry Wallace in those efforts.

'One way the success of modern agriculture is reflected is in how much we pay for food. In the 1933, according to USDA ERS, Americans spent more than 25 percent of their income on food. By 1985, that had dropped to 11.7 percent and, in 2000, below 10 percent for the first time in history.'

'In contrast, the poorest nations spend 70 percent or more of their disposable income on feeding their families.'

'The success of U.S. agriculture spurred the advent of the Asian Green Revolution, helping Borlaug and other scientists convert countries like India from "basket cases to bread baskets,' said Ejeta.

'In my view, the transformative changes brought about by modern agriculture sciences in his native Iowa inspired Norm Borlaug to dream about helping the poor in developing countries overcome hunger with the breakthrough he achieved in wheat genetics.'

Borlaug, he said, saw how the advent of hybrid corn in private sector initiatives in the seed industry and other agribusinesses spurred not only productivity increases on farms but also enhanced the livelihoods of rural Americans. 'Fresh from the economic hardship of the great depression this must have been an easy lesson for young Norm to take to heart.'

Ejeta quoted from his testimony before the U.S. Senate Committee on Foreign Relations' hearing on global food security last March.

'Norm Borlaug, the universally acknowledged father of the Green Revolution, is a hero to me and very many others. I personally admire his single-minded devotion to science and agriculture development and his unending empathy and service to the poor.'

'As I reflect on his accomplishments and leadership, however, in my view, the genius of Norm Borlaug was not in his creation of high yield potential and input responsive wheat varieties. Not even in his early grasp of the technology but to a great extent in his relentless attempts to mobilize policy support and encourage the development of the agro-industry complex, to sustain the synergistic affects of technology, education and markets.'

email: flaws@farmpress.com"

"An Urgent Appeal for Soil Stewardship
From the 2009 Bouyoucos Conference on
Soil Stewardship in an Era of Global Climate Change

Upon viewing the deforested and eroded landscape near Attica, Greece in the 4th century BC, the philosopher Plato vividly described the loss: "What now remains compared with what then existed is like the skeleton of a sick man, all the fat and soft earth having wasted away, and only the bare framework of the land being left." Plato's observation of soil degradation is no less relevant 2400 years later. If the importance of healthy soils for nutritious food and clean water has been known for millennia, why has an enduring commitment to thoughtful soil stewardship proven so elusive to so many and for so long?

Soil is a fundamental source of life. It plays a critical role in providing water, nutrients, and support for plant growth, recycling organic materials and protecting surface and ground waters from contaminants. Soil is the base of the terrestrial food chain, directly or indirectly providing over 97% of the calories that now nourish more than six billion people. This modern bounty was enabled by a providential combination of weathering processes that created fertile soils from inert rock and favorable climates suitable for growing a variety of food plants. At the start of the 21st century we express our deep-felt concern that three of the integral resources of agricultural production, soil, water and climate, are increasingly impaired by human actions with potentially serious consequences for global food security.

We are, each of us, people of the soil. Most indigenous peoples and organized religions have oral or written accounts of human origin or experiences that include a deep reverence associated with the life that springs from the soil. Our cultural traditions acknowledge the significance of soil even if our environmental practices do not. The facts about the current condition of global soil resources are sobering. Recent estimates are that one fourth of the earth's inhabitants already depend on degrading lands. Future generations may be forced to obtain ever more sustenance from decreasingly available productive land. Potential changes in rainfall and temperature patterns and their variability as the global climate changes add yet another challenge. There is a long and tragic correlation between cultures that fail to protect the health of their soil and the demise of those same cultures. Life, as we perceive it, exists only on a planet having soil, as we know it. Soil is the interface between lifeless cosmic rock and all terrestrial life. Healthy soil is itself a living community, containing up to four billion microorganisms in each teaspoon. But soil is also a fragile, finite resource requiring care. Destroying soil is the equivalent of destroying the self-renewing capacity of the Earth.

---

[71] This document (Bouyoucos 2009) copied in entirety from
http://pss.okstate.edu/home/rightsidebar/anurgentappealforsoilstewardship.pdf.

Too often we forget our shared human history and the reality of our dependence on the soil. Too often we fail to enact our historical and rightful commitment to the land, our home place. We are therefore shirking our inherent responsibility to care for the planet. The poor of the world are those most immediately and dramatically affected by both soil degradation and climate change, therefore, soil stewardship is both an environmental and a moral challenge to society.

What is the way forward? What is our task in the face of this reality, this disconnect between the importance and the condition of our soil? We recognize and affirm a cultural and physical link to soil. We assert a shared obligation to soil stewardship that is based on more than purely utilitarian concerns. We acknowledge that soil degradation is an ethical issue, that science and economics alone will not and can not determine a proper course of action. We cannot therefore ignore the mistreatment of our lands and at the same time escape moral denunciation. Encouraging a more broad and thoughtful soil stewardship ethic is not naïve, idealistic, or altruistic but rather perceptive, pragmatic, and essential to our societal response to the challenges posed by global climate change and an increasing human population.

Given that our environmental problems stretch beyond the domain of any particular discipline, genuine solutions to these problems will only be found by engaging all facets of the human mind. **We call for soil scientists to humbly and dutifully work across disciplines – including the humanities and the arts, in efforts to engage in a practice of public scholarship with the goal of building new relationships and networks that advance the soil stewardship ethic. We call for the products of such collaborations to be openly communicated to the public and to policy makers, raising awareness and urging proactive action. Finally, we call for the recognition and celebration of successful soil stewardship stories to serve as examples, to inspire, and to lead us forward."**

VITA

John Byron Sudbury

Candidate for the Degree of

Doctor of Philosophy

Dissertation: QUANTITATIVE PHYTOLITH ANALYSIS: THE KEY TO UNDERSTANDING BURIED SOILS AND TO RECONSTRUCTING PALEOENVIRONMENTS

Major Field: Soil Science

Biographical:

Education:
Graduated from Ponca City High School May, 1969. Earned a Bachelor of Science degree in Chemistry from Oklahoma Christian College in April, 1973. Earned a Bachelor of Science degree in Biology from Oklahoma Christian College in April, 1973. Earned a Master of Science degree in Forensic Science/Criminalistics from University of Central Oklahoma in December, 2001. Completed the requirements for the Doctor of Philosophy in Soil Science at Oklahoma State University, Stillwater, Oklahoma, in May, 2010.

Experience:
Distinguished career as an analytical chemist in the petroleum and petrochemical industries, with strong interest in archeology as well as in the degreed fields. Established a commercial contract analytical laboratory specializing in phytolith and soil analysis. Additional detail available at http//www.phytolithanalysis.com/CV.pdf (jschemistry@hotmail.com).

Professional Memberships:
Soil Science Society of America
Society for Phytolith Research
American Chemical Society
Oklahoma Microscopy Society
Microscopy Society of America
National Environmental Health Association
Académie Internationale de la Pipe

Registered Professional Environmental Specialist (Oklahoma)
Certified Soil Profiler (Oklahoma)

John Byron Sudbury   Date of Degree: May, 2010

Institution: Oklahoma State University   Stillwater, Oklahoma, USA

Title of Study: QUANTITATIVE PHYTOLITH ANALYSIS: THE KEY TO
                 UNDERSTANDING BURIED SOILS AND TO RECONSTRUCTING
                 PALEOENVIRONMENTS

Pages in Study: 421   Candidate for the Degree of Doctor of Philosophy

Major Field: Soil Science

Scope and Method of Study: The purpose of this study is to quantitatively recover and
        analyze the phytoliths from modern and prehistoric prairie soils, and to use the
        resulting phytolith signatures to develop a better understanding of pedogenic
        processes and to determine past climatic conditions. Improvements in analytical
        laboratory protocols will be developed as needed to meet these objectives.

Findings and Conclusions: Phytoliths were quantitatively recovered from A horizons of
        three modern prairies (Shortgrass, Mixedgrass, and Tallgrass Prairies) and from
        three sites with buried soils of known age. Phytoliths were separated from other
        soil particles based on differences in particle size and particle density. Using
        polarized light microscopy, the morphologic distribution of Poaceae short cell
        phytoliths present in the isolated soil sample fractions was ascertained. The
        phytolith distribution within buried A horizons reveals information about soil
        forming processes. The relative phytolith concentration mirrors the soil organic
        carbon content in well-developed melanized A horizons. In a normal melanized
        A horizon, the phytolith concentration decreases exponentially with depth, in a
        soil developed by cumulic growth the phytolith concentration is relatively
        constant, and in a new soil formed on an alluvial deposit the phytoliths are
        concentrated in the upper portion of the deposit. The phytolith signature of
        modem soils mirrors the environmental conditions at the time of soil formation.
        Comparison of modern prairie short cell phytolith signatures to the signature in
        buried soils permits determination of climatic conditions at the time of past stable
        environments. The various phytolith forms evaluated are indicative of C3 vs. C4
        grasses thus revealing climatic information. A higher C3 phytolith content
        indicates a cooler moister climate whereas a stronger C4 signature indicates a
        warmer climate. Phytolith seasonality groupings proved to be more reproducible
        that the individual phytolith short cell morphotypes. It was discovered that
        saddle-shaped phytoliths appear to hold great potential for understanding changes
        in botanical signature due to climate. Significant improvements to available
        published laboratory protocols for phytolith isolation were developed and
        implemented. Phytolith analysis leads to a better understanding of soil genesis
        and provides a method to ascertain past climatic changes.

ADVISER'S APPROVAL: Dr. Brian J. Carter